INTERNATIONAL DOCTORAL
SCHOOL OF THE USC

María
Cascallar Castro

PhD Thesis

In vitro and *in vivo* evaluation of lipidic nanosystems for cancer therapy

Santiago de Compostela, 2023

Doctoral Programme in Molecular Medicine

DOCTORAL THESIS

IN VITRO AND *IN VIVO* EVALUATION OF LIPIDIC NANOSYSTEMS FOR CANCER THERAPY

María Cascallar Castro

INTERNATIONAL PHD SCHOOL OF THE UNIVERSITY OF SANTIAGO DE COMPOSTELA

PHD PROGRAMME IN MOLECULAR MEDICINE

SANTIAGO DE COMPOSTELA

2023

DECLARACIÓN DE LA AUTORA DE LA TESIS

Dña. **María Cascallar Castro**

Título de la tesis**: *In vitro* and *in vivo* evaluation of lipidic nanosystems for cancer therapy**

Presento mi tesis, siguiendo el procedimiento adecuado al Reglamento y declaro que:

1) La tesis abarca los resultados de la elaboración de mi trabajo.
2) De ser el caso, en la tesis se hace referencia a las colaboraciones que tuvo este trabajo.
3) Confirmo que la tesis no incurre en ningún tipo de plagio de otros autores ni de trabajos presentados por mí para la obtención de otros títulos.
4) La tesis es la versión definitiva presentada para su defensa y coincide la versión impresa con la presentada en formato electrónico.

Y me comprometo a presentar el Compromiso Documental de Supervisión en el caso que el original no esté depositado en la Escuela.

En **Santiago de Compostela**, **17 de junio de 2022**.

AUTORIZACIÓN DE LAS DIRECTORAS DE LA TESIS

In vitro and *in vivo* evaluation of lipidic nanosystems for cancer therapy

Dra. María de la Fuente Freire
Dra. Laura Elena Sánchez Piñón

INFORMAN:

Que la presente tesis, se corresponde con el trabajo realizado por Dª. María Cascallar Castro, bajo mi dirección, y autorizo su presentación, considerando que reúne los requisitos exigidos en el Reglamento de Estudios de Doctorado de la USC, y que como director de esta no incurre en las causas de abstención establecidas en la Ley 40/2015.

De acuerdo con lo indicado en el Reglamento de Estudios de Doctorado, declara también que la presente tesis doctoral es idónea para ser defendida en base a la modalidad de **Monográfica con reproducción de publicaciones**, en los que la participación del doctorando/a fue decisiva para su elaboración y las publicaciones se ajustan al Plan de Investigación.

En Santiago de Compostela/Lugo, 17 de junio de 2023

Dra. María de la Fuente Freire Dra. Laura Elena Sánchez Piñón

AUTORIZACIÓN DE LA TUTORA DE LA TESIS

In vitro and in vivo evaluation of lipidic nanosystems for cancer therapy

Dra. Laura Elena Sánchez Piñón

INFORMA:

Que la presente tesis, se corresponde con el trabajo realizado por D/Dª. María Cascallar Castro, bajo mi tutorización, y autorizo su presentación, considerando que reúne los requisitos exigidos en el Reglamento de Estudios de Doctorado de la USC, y que como tutora de esta no incurre en las causas de abstención establecidas en la Ley 40/2015.

De acuerdo con lo indicado en el Reglamento de Estudios de Doctorado, declara también que la presente tesis doctoral es idónea para ser defendida en base a la modalidad de **Monográfica con reproducción de publicaciones**, en los que la participación del doctorando/a fue decisiva para su elaboración y las publicaciones se ajustan al Plan de Investigación.

En Lugo, 17 de junio de 2023

DECLARATION OF THE AUTHOR

I, María Cascallar Castro, author of this thesis, have no conflict of interest to declare.

Á miña familia

Science and everyday life cannot and should not be separated. Science, for me, gives a partial explanation of life. In so far as it goes, it is based on fact, experience, and experiment.

ROSALIND FRANKLIN

TABLE OF CONTENTS

TABLE OF CONTENTS

ABSTRACT

ABSTRACT

Since the FDA-approval of the first nanomedicines, the development of innovative therapeutic approaches based on nanotechnology has been continuously growing in the biomedical field. Some of the benefits that nanomedicine offer are the improvement of drugs' stability and half-life, as well as the possibility to develop targeted therapies. In the field of cancer, novel therapeutic strategies are urgently need, and nanomedicine can strongly contribute to respond to this demand. It is also necessary to improve the translation of novel nanomedicines by implementing preclinical tools that that mimics efficiently the tumor structure for a correct evaluation of the therapy and allow a better understanding of their efficacy and toxicity prior testing in advanced models of the disease.

In this line, our group has developed a novel type of nanoemulsion which is versatile, biocompatible and biodegradable, and is composed by vitamin E and sphingomyelin. These nanosystems previously demonstrated their capacity to encapsulate drugs, associate therapeutic biomolecules, and also contrast agents for diagnosis. In this thesis, their application for the development of treatments for lung cancer (targeting cancer stem cells and a specific cell subpopulation expressing a certain biomarker), and breast cancer (a gene therapy approach) will be explored. For this, static and non-static 3D *in vitro* models, and alternative *in vivo* models based on zebrafish embryo, will be developed.

In the first chapter, sphingomyelin nanoemulsions were used for the encapsulation of the drug Disulfiram for cancer stem cell treatment in non-small cell lung cancer. Spheroids were the study model proposed due to their enriched population of cancer stem cells. The results demonstrated the capacity of nanosystems to encapsulate the disulfiram and to penetrate into the inner core of 3D models producing a therapeutic effect. Moreover, spheroids proved their potential to be a platform for nanomedicine evaluation.

In the second chapter, sphingomyelin nanosystems were functionalized with a specific aptamer to target TAS1R3 positive non-small cell lung cancer cells, for targeted therapy. Organ-on-a-chip microfluidic devices were the advanced non-static 3D study model to recreate the tumor structure and the vasculature. The results proved an efficient targeting in 2D cell cultures, and the microfluidic chips demonstrated their potential to be a model to evaluate the capacity of nanosystems to cross biological barriers.

In the third chapter, sphingomyelin nanosystems were modified with a cationic lipid for the association of nucleic acids for gene therapy. Zebrafish embryos were the *in vivo* models selected to evaluate the potential of the nanosystems. The results demonstrated the versatility of the nanoemulsions to carry different types of nucleic acids, as well as the potential of zebrafish embryos as a platform to evaluate gene therapies based on nanomedicine.

Overall, this thesis proves the versatility of sphingomyelin nanosystems for being loaded different types of therapeutic molecules and decorated with specific ligands for cancer treatment, and, importantly, the critical role of 3D *in vitro* models, static and non-static, and zebrafish embryos, to evaluate the behavior and efficacy of cancer nanomedicines.

RESUMEN

RESUMEN

Desde la aprobación por la FDA de las primeras nanomedicinas, el desarrollo de innovadoras aproximaciones terapéuticas basadas en nanotecnología ha estado creciendo continuamente en el campo biomédico. Algunos de los beneficios que la nanomedicina ofrece son la mejora de la estabilidad y vida media de fármacos, así como la posibilidad para desarrollar terapias dirigidas. En el campo del cáncer, hay una urgente necesidad de nuevas estrategias terapéuticas, y la nanomedicina puede contribuir considerablemente a responder a esta demanda. Es también necesaria la mejora de la traslación de medicinas novedosas, con la implementación de herramientas preclínicas que imiten eficazmente la estructura del tumor para una correcta evaluación de la terapia y permitan entender mejor su eficacia y toxicidad antes del testado en modelos avanzados de la enfermedad.

En esta línea, nuestro grupo ha desarrollado un novedoso tipo de nanoemulsión que es versátil, biocompatible y biodegradable, y que se compone de vitamina E y esfingomielina. Estos nanosistemas han demostrado previamente su capacidad para encapsular fármacos, asociar biomoléculas terapéuticas, y también agentes de contraste para diagnosis. En esta tesis, su aplicación para el desarrollo de tratamientos para cáncer de pulmón (direccionamiento a células madre tumorales e a una subpoblación celular específica que expresa cierto biomarcador), y cáncer de mama (una aproximación de terapia génica) serán exploradas. Para ello, modelos *in vitro*,

estáticos y no estáticos, y modelos *in vivo* alternativos basados en embriones de pez cebra serán desarrollados.

En el primer capítulo, las nanoemulsiones de esfingomielina fueron usadas para la encapsulación del fármaco Disulfiram para el tratamiento de células madre tumorales en cáncer de pulmón no microcítico. Los esferoides fueron en modelo de estudio propuesto debido a su enriquecida población de células madre tumorales. Los resultados demostraron la capacidad de los nanosistemas de encapsular el disulfiram y de penetrar en el núcleo interno de los modelos 3D produciendo un efecto terapéutico. Además, los esferoides probaron su potencial para ser una plataforma para la evaluación de nanomedicinas.

En el segundo capítulo, los nanosistemas de esfingomielina fueron funcionalizados con un aptámero específico para el direccionamiento a las células de pulmón no microcíticas TAS1R3 positivas para terapia dirigida. Dispositivos de microfluídica *organ-on-a-chip* fueron los modelos avanzados 3D no estáticos de estudio para recrear la estructura tumoral y la vasculatura. Los resultados probaron un eficiente direccionamiento en cultivos celulares 2D, y los chips de microfluídica demostraron su potencial para ser un modelo para evaluar la capacidad de los nanosistemas para cruzar barreras biológicas.

En el tercer capítulo, los nanosistemas de esfingomielina fueron modificados con un lípido catiónico para la asociación de ácidos nucleicos para terapia génica. Los embriones de pez cebra son los modelos *in vivo* seleccionados para evaluar el potencial de los nanosistemas. Los resultados demostraron la versatilidad de las nanoemulsiones para transportar diferentes tipos de ácidos nucleicos, así como el potencial de los embriones de pez cebra

como plataforma para la evaluación de terapias génicas basadas en nanomedicina.

En general, esta tesis prueba la versatilidad de los nanosistemas de esfingomielina para ser cargados con diferentes tipos de moléculas terapéuticas y decorados con ligandos específicos para el tratamiento del cáncer, y de manera importante, el papel crítico de los modelos *in vitro*, estáticos y no estáticos, y de los embriones de pez cebra, para evaluar el comportamiento y la eficacia de nanomedicinas para el cáncer.

RESUMO

RESUMO

Dende a aprobación pola FDA das primeiras nanomedicinas, o desenvolvemento de innovadoras aproximacións terapéuticas baseadas en nanotecnoloxía estivo crecendo continuamente no campo biomédico. Algúns dos beneficios que a nanomedicina ofrece son a mellora da estabilidade e vida media de fármacos, así como a posibilidade para desenvolver terapias dirixidas. No campo do cancro, hai unha urxente necesidade de novas estratexias terapéuticas, e a nanomedicina pode contribuír considerablemente a responder a esta demanda. É tamén necesaria a mellora da translación de medicinas novidosas, coa implementación de ferramentas preclínicas que imiten eficazmente a estrutura do tumor para unha correcta avaliación da terapia e permitan entender mellor a súa eficacia e toxicidade antes do testado en modelos avanzados da enfermidade.

Nesta liña, o noso grupo desenvolveu un novidoso tipo de nanoemulsión que é versátil, biocompatible e biodegradable, e que se compón de vitamina E e esfingomielina. Estes nanosistemas demostraron previamente a súa capacidade para encapsular fármacos, asociar biomoléculas terapéuticas, e tamén axentes de contraste para diagnose. Nesta tese, a súa aplicación para o desenvolvemento de tratamentos para cancro de pulmón (direccionamiento a células nai tumorais e a una subpoboación celular específica que expresa certo biomarcador), e cancro de mama (unha aproximación de terapia xénica) serán exploradas. Para iso, modelos *in vitro*, estáticos e non estáticos, e *modelos in vivo* alternativos baseados en embrións de peixe cebra serán desenvolvidos.

No primeiro capítulo, as nanoemulsiones de esfingomielina foron usadas para a encapsulación do fármaco Disulfiram para o tratamento de células nai tumorais en cancro de pulmón non microcítico. Os esferoides foron o modelo de estudo proposto debido á súa enriquecida poboación de células nai tumorais. Os resultados demostraron a capacidade dos nanosistemas de encapsular o disulfiram e de penetrar no núcleo interno dos modelos 3D producindo un efecto terapéutico. Ademais, os esferoides probaron o seu potencial para ser unha plataforma para a avaliación de nanomedicinas.

No segundo capítulo, os nanosistemas de esfingomielina foron funcionalizados cun aptámero específico para o direccionamento ás células de pulmón non microcíticas TAS1R3 positivas para terapia dirixida. Dispositivos de microfluídica *organ-on-a-chip* foron os modelos avanzados 3D non estáticos de estudo para recrear a estrutura tumoral e a vasculatura. Os resultados probaron un eficiente direccionamiento en cultivos celulares 2D, e os chips de microfluídica demostraron o seu potencial para ser un modelo para avaliar a capacidade dos nanosistemas para cruzar barreiras biolóxicas.

No terceiro capítulo, os nanosistemas de esfingomielina foron modificados cun lípido catiónico para a asociación de ácidos nucleicos para terapia xénica. Os embrións de peixe cebra son os modelos *in vivo* seleccionados para avaliar o potencial dos nanosistemas. Os resultados demostraron a versatilidade das nanoemulsiones para transportar diferentes tipos de ácidos nucleicos, así como o potencial dos embrións de peixe cebra como plataforma para a avaliación de terapias xénicas baseadas en nanomedicina.

En xeral, esta tese proba a versatilidade dos nanosistemas de esfingomielina para ser cargados con diferentes tipos de moléculas terapéuticas e decorados con ligandos específicos para o tratamento do cancro, e de maneira importante, o papel crítico dos modelos *in vitro*, estáticos e non estáticos, e dos embrións de peixe cebra, para avaliar o comportamento e a eficacia de nanomedicinas para o cancro.

RESUMO *IN EXTENSO*

RESUMO *IN EXTENSO*

A nanomedicina é coñecida como a utilización da nanotecnoloxía no campo da saúde. Dende a aprobación pola FDA das primeiras nanomedicinas, o liposoma anestésico Diprivan® e o antitumoral Doxil®, o uso de tratamentos baseados na nanotecnoloxía estivo a crecer continuamente, e un claro exemplo son as recentes vacinas para a COVID-19. Os beneficios que trae a nanomedicina son, non só o tratamento de diferentes doenzas, senón que tamén a súa capacidade como axentes de contraste para diagnóstico. Modificando a súa composición e as súas propiedades fisicoquímicas, as nanopartículas poden adaptarse para transportar diferentes tipos de tratamentos, dende pequenos fármacos ata moléculas terapéuticas. Ademais, as nanopartículas poden ser decoradas con ligandos específicos para o seu direccionamento específico fronte ás células de interese. Así mesmo, teñen a capacidade de protexer a súa carga, de ser capaces de mellorar a estabilidade e vida media de moléculas terapéuticas lábiles, así como facilitar o desenvolvemento de terapias combinatorias a través de estratexias de co-encapsulación.

O cancro é responsable de millóns de mortes no mundo, chegando a case os dez millóns no ano 2020. Ademais, o número de novos casos por ano está preto dos vinte millóns, sendo o cancro de mama feminino e o cancro de pulmón os que lideran a incidencia. Estes números alertan da inmediata necesidade de novas estratexias terapéuticas para o tratamento do cancro.

Neste campo, a nanomedicina representa unha estratexia alternativa para mellorar o tratamento do cancro. Claros exemplos disto son Doxil® e Vyxeos®, que foron aprobados para o seu uso na clínica como anti-tumorais. Aínda así, tendo en conta os múltiples ensaios clínicos, ao redor de só vinte nanomedicinas para o tratamento do cancro chegaron ao mercado, o que demostra que a nanomedicina ten dificultades para chegar á clínica. Algunhas das razóns de que isto ocorra son a toxicidade e non biocompatibilidade das formulación nos ensaios clínicos, así como os problemas no escalado para a produción comercial. Nesta liña, o noso grupo desenvolveu un novo tipo de nanoemulsións versátiles, biodegradables e biocompatibles, que se compoñen de vitamina E e esfingomielina. Estes nanosistemas de esfingomielina demostraron a súa capacidade para encapsular fármacos, asociar moléculas terapéuticas, así como axentes de contraste para diagnóstico, e poden ser escalables e adaptables a procesos industriais.

A translación clínica de nanomedicinas para terapia anti-tumoral tamén se podería ver acelerada incorporando novos modelos des estudo, tanto *in vitro* coma *in vivo*, que sexan capaces de recrear eficientemente a estrutura e ambiente tumoral, ás fases de investigación preclínica. Estes modelos son chave, para estudar dunha maneira fiable o comportamento e resposta terapéutica das nanopartículas. Neste sentido destacan tres modelos de estudo, os cultivos 3D, tanto estáticos coma non estáticos, e os embrións de peixe cebra.

No caso dos modelos *in vitro* 3D estáticos, que se compoñen por esferoides e organoides, destaca a súa capacidade de reproducir a estrutura tumoral, así como as interaccións celulares, que non se representan nos modelos de cultivos en 2D. Estes modelos máis complexos permiten a

avaliación da toxicidade, internalización e efecto terapéutico, sendo estas características clave para a translación das nanomedicinas ao mercado. Outro punto a favor é o seu baixo custo en relación a modelos murinos, así como a súa capacidade para levar a cabo grandes ensaios de *screening*, o que permite executar estudos máis amplos. Ademais, os esferoides e organoides poden ser formados por células de doentes, o que permitiría un *screening* personalizado de terapias anti-tumorais.

Por outro lado, os modelos *in vitro* 3D non estáticos son plataformas baseadas en dispositivos de microfluídica *organ-on-a-chip* que permiten, ao igual que os esferoides e organoides, a recreación da estrutura e ambiente tumoral. A característica diferencial entre os modelos estáticos e os non estáticos, é que este últimos inclúen parámetros de fluxo. A presenza deste fluxo no ambiente de cultivo proporciona un acercamento maior e máis verídico do tumor. Estes dispositivos poden ser de diferente complexidade, dende a simple inclusión dun esferoide no chip, ata o desenvolvemento de canais que recreen o sistema vascular e incluso procesos tan complexos como a metástase. No ámbito da nanomedicina, estes dispositivos son extremadamente útiles para a avaliación da biodistribución e do efecto terapéutico. Ademais, ao permitir recrear barreiras biolóxicas, como a endotelial, estes dispositivos son moi interesantes para estudar a capacidade das nanopartículas de cruzar estas barreiras. No caso dos dispositivos de microfluídica, ao igual que ocorre cos modelos estáticos, é posible crear plataformas con células derivadas de doentes, que permiten o estudo personalizado das terapias anti-tumorais.

Por último, o peixe cebra (*Danio rerio*) é un modelo vertebrado de estudo *in vivo* que ofrece grandes vantaxes para a avaliación de nanopartículas para

o tratamento do cancro. Aínda que o peixe cebra é un modelo interesante en todas as súas estadías vitais, a etapa de embrión é a que destaca neste caso. As vantaxes que o definen son a súa alta homoloxía co xenoma humano, a súa alta fecundidade, o gran número de descendentes dunha posta e a fertilización externa. Os embrións, a maiores, son altamente robustos, presentan transparencia óptica e a activación tardía do seu sistema inmune adaptativo. Todo isto permite a realización de *xenografts*, xenotransplantes de células tumorais, sen que estes se vexan comprometidos polo sistema inmune, e tamén, no caso de que estas células estean marcadas fluorescentemente, a transparencia permite a súa visualización a través de técnicas de microscopía de fluorescencia ou confocal. Os modelos de peixe cebra máis relevantes para o estudo de nanomedicina son as liñas transxénicas e os xenotransplantes de células tumorais. No primeiro caso, son destacables os embrións transxénicos que teñen algún tipo de célula marcada fluorescentemente, como poden ser as células do sistema inmune ou as células do sistema vascular, que permiten avaliar a interacción dos nanosistemas nun sistema *in vivo*. No caso dos xenotransplantes, o uso da marcaxe fluorescente permite estudar a biodistribución das nanopartículas, así como a súa interacción coas células tumorais. Ademais, a capacidade terapéutica de nanomedicinas pode ser determinada ao monotorizar o crecemento ou decrecemento da masa tumoral. Os embrións *wild type* sen xenografts tamén teñen interese, sobre todo para estudos de toxicidade. En canto á medicina personalizada, o peixe cebra xoga un papel importante gracias á posibilidade de realizar *xenografts* derivados de doentes, que poden ser obxecto dun *screening* a gran escala, para dar co tratamento máis axeitado para cada caso.

Tendo en conta o previamente exposto, o principal obxectivo desta tese é a aplicación de modelos *in vitro* e *in vivo* avanzados, baseados en esferoides, dispositivos de microfluídica *organ-on-a-chip* e embrións de peixe cebra, para a avaliación preclínica de nanoemulsións de esfingomielina para o tratamento do cancro.

En primeiro lugar, encapsulouse o fármaco disulfiram nos nanosistemas de esfingomielina, como estratexia alternativa para o tratamento de células nai tumorais do cancro de pulmón non microcítico. Como modelo de estudo para avaliar o potencial desta terapia, usáronse modelos *in vitro* estáticos, concretamente esferoides (Figura 1).

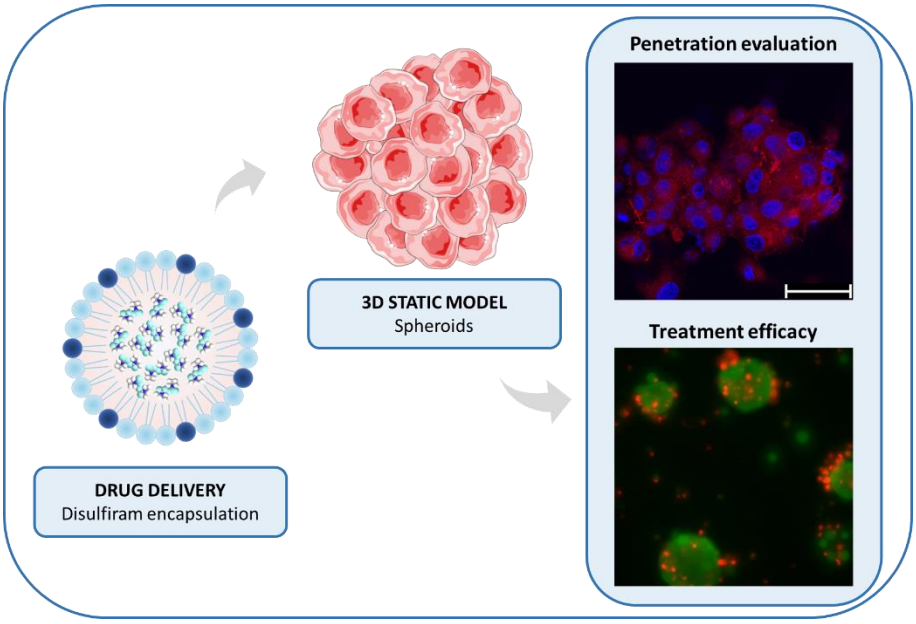

Figura 1. Resumo gráfico do Capítulo I, cuxo obxectivo foi a encapsulación do fármaco disulfiram para o tratamento de células nai tumorais de cancro de pulmón non microcítico e a súa avaliación en modelos 3D estáticos *in vitro*.

Neste caso, orientouse a estratexia terapéutica cara o cancro de pulmón, un dos máis relevantes en termos de mortalidade e prevalencia, e concretamente centrouse no estudo do cancro de pulmón non microcítico, o subtipo máis predominante. O disulfiram foi seleccionado pola súa actividade antitumoral específica nas células nai tumorais, e polos estudos previos que avalan o seu potencial como tratamento do cancro de pulmón non microcítico. Este fármaco hidrofóbico, aínda que eficaz, ten unha alta inestabilidade en circulación, así como unha baixa vida media. Para superar estes inconvenientes, propúxose a encapsulación do disulfiram nos nanosistemas lipídicos. Como modelo *in vitro* para este estudo, seleccionáronse os cultivos celulares 3D estáticos, neste caso esferoides que foron xerados a partir de células dunha liña de cancro de pulmón non microcítico (H1650). O obxectivo que se buscaba era o de recrear a estrutura tridimensional do tumor para avaliar dunha maneira máis fiable o comportamento, distribución e eficacia dos nanosistemas. Ademais, e tendo en conta que a diana terapéutica do disulfiram son as células nai tumorais, os esferoides presentan unha poboación enriquecida deste tipo de células, xerando así un modelo de estudo idóneo para a avaliación desta terapia baseada no disulfiram.

Como primeiro paso para a avaliación dos nanosistemas, realizáronse estudos de internalización en esferoides da liña celular H1650. Os nanosistemas, tanto con e sen disulfiram encapsulado, incubáronse durante diferentes tempos no medio das esferas. Previamente, os nanosistemas foron marcados fluorescentemente con esfingomielina-Cy5, o que permitiu a súa avaliación a través da microscopía confocal. Os resultados obtidos demostran unha eficiente capacidade de penetración de ambas nanoemulsións en esferoides compactos, demostrando que a encapsulación do fármaco non

afecta ás propiedades do nanosistema. Concretamente, a internalización comézase a observar aos 30 minutos de incubación, sendo despois de 1 hora, cando esta se fai claramente visible. É importante resaltar a completa penetración dos nanosistemas no interior do esferoide, demostrando que o transporte do fármaco chega correctamente a todas as células tumorais.

Como seguinte paso, estudiouse o efecto terapéutico do disulfiram, tanto encapsulado coma libre. Para iso, en primeiro lugar, avaliouse a viabilidade celular, en cultivos 2D e 3D, a través do ensaio de MTS, onde tamén se calculou a metade da concentración inhibitoria máxima (IC50). Os resultados obtidos demostraron que o disulfiram, tanto encapsulado coma libre, non ten practicamente efecto terapéutico no caso das células en monocapa, como era de esperar pola súa baixa poboación de células nai tumorais. No caso dos cultivos 3D, o resultado é completamente diferente, sendo o tratamento eficaz en ambos os dous casos. No caso do disulfiram encapsulado nos nanosistemas de esfingomielina obsérvase unha lixeira melloría na actividade do fármaco, acadando unha IC50 de 0.16, en comparación co fármaco libre con unha IC50 de 0.35. Un segundo experimento, de Calceina AM/ioduro de propidio, foi realizado para a observación das poboacións celulares vivas e mortas despois da incubación co tratamento. Os resultados obtidos neste caso mostran un patrón de células mortas semellante no caso do disulfiram libre e no encapsulado. Salientablemente, obsérvase a presenza de células mortas no interior dos esferoides, o que supón que os nanosistemas teñen a capacidade, non só de penetrar no interior do esferoide, senón que tamén teñen a capacidade de liberar eficientemente a súa carga producindo un efecto terapéutico. Con isto, pódese concluír que os nanosistemas lipídicos teñen a capacidade de transportar e de penetrar eficientemente en modelos *in vitro* 3D

estáticos. Cabe destacar o potencial demostrado polos esferoides como plataforma de avaliación para nanomedicinas para o tratamento de células nai tumorais.

En segundo lugar, os nanosistemas de esfingomielina foron funcionalizados para o desenvolvemento dunha terapia dirixida, neste caso, ao receptor TAS1R3, en células de cancro de pulmón non microcítico. Para a avaliación da terapia dirixida, desenvolvéronse modelos celulares 3D non estáticos, os dispositivos de microfluídica *organ-on-a-chip* (Figura 2).

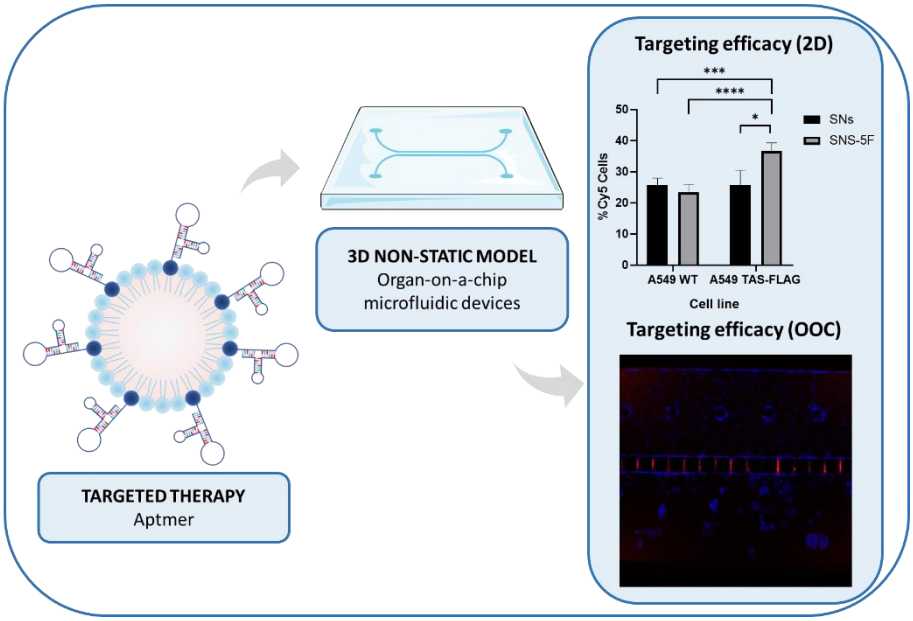

Figura 2. Resumo gráfico do Capítulo II, cuxo obxectivo foi a funcionalización dos nanosistemas de esfingomielina con aptámeros para terapia dirixida a células TAS1R3+, e a súa avaliación en modelos 3D non estáticos *in vitro*.

A metástase é a responsable da maior parte das mortes producidas polo cancro, o que demostra a necesidade urxente de tratamentos específicos contra

a poboación celular metastática. O cancro de pulmón non microcítico é un claro exemplo do efecto das metástases na supervivencia dos doentes. A nanomedicina supón unha alternativa grazas á posibilidade de decoralas para conseguir unha terapia dirixida, utilizando moléculas como os aptámeros, que teñen a capacidade de recoñecer e unirse á súa diana especificamente. Con isto, propúxose a conxugación dun aptámero específico aos nanosistemas de esfingomielina a través da reacción EDC. Concretamente, as nanoemulsións irán dirixidas ao receptor TAS1R3, que previamente foi descrito polo grupo e cuxa expresión se correlaciona co proceso metastático. A plataforma seleccionada para a avaliación desta terapia foron os dispositivos de microfluídica *organ-on-a-chip*. Este chip en concreto componse de dous canais, un que recrea o tumor en 3D e outro que imita o endotelio vascular formando unha estrutura tubular en monocapa. As células utilizadas nos experimentos son células de cancro de pulmón non microcítico, as wild type e tamén unhas transfectadas que sobre-expresan o noso receptor de interese.

Como primeiro paso avaliouse a penetración dos nanosistemas funcionalizados en modelos de esferoides. Aínda que foi utilizado un aptámero preliminar, o resultado obtido foi unha boa internalización despois de 6 horas de incubación, demostrando a súa capacidade para penetrar ata o interior dos esferoides. Este resultado onde non se observan diferenzas entre as dúas liñas celulares concorda con traballo previos onde os nanosistemas, despois de 4 horas, están case todos internalizados polas células.

O seguinte paso, e tendo en conta o resultado de internalización obtido, foi a avaliación do *targeting* específico do aptámero seleccionado facendo uso da citometría de fluxo. Neste caso a incubación dos nanosistemas marcados fluorescentemente foi de 20 minutos, para poder observar diferenzas entre os

nanosistemas con e sen aptámero e entre as dúas liñas celulares. O resultado obtido demostra un *targeting* efectivo dos nanosistemas funcionalizados cando foron utilizados nas células que sobreexpresan o receptor TAS1R3. Este resultado estatisticamente significativo demostrou un aumento do 10% na internalización nesta condición.

O último paso foron os estudos no modelo de dispositivos de microfluídica *organ-on-a-chip*, compostos por un canal con células tumorais (A549-TAS1R3+) e outro con células endoteliais (HPMEC). Como primeira aproximación antes do uso dos chips, estudouse a citotoxicidade dos nanosistemas nas células endoteliais en 2D. O resultado avaliado polo ensaio AlamarBlue demostra que tanto os nanosistemas con e sen aptámero non teñen impacto na viabilidade das células HPMEC. Este resultado é clave porque se asegura que a integridade da barreira endotelial formada non vai ser alterada polo efecto dos nanosistemas. Con isto, poderase probar a capacidade dos nanosistemas dirixidos de cruzar esta barreira biolóxica. O último paso foi unha proba de concepto para estudar o *direccionamento* específico das nanoemulsións funcionalizadas. Os nanosistemas foron incubados durante 12 horas no canal endotelial que ten perfusión por fluxo por gravidade. O resultado obtido por microscopía de fluorescencia suxire que os nanosistemas estaban a cruzar os micropilares que dividen os dous canais. Máis experimentos con maiores tempos de incubación e diferentes concentracións de nanosistemas son necesarios, para comprender completamente o comportamento das nanoemulsións funcionalizadas fronte a barreira endotelial para alcanzar as súas células diana.

Con isto, conclúese que os aptámeros foron conxugados eficientemente cos nanosistemas e que o seu *targeting* específico foi demostrado

exitosamente en modelos celulares 2D. Así mesmo, os dispositivos de microfluídica *organ-on-a-chip* demostraron o seu potencial como modelo para a avaliación da capacidade de nanomedicinas para cruzar barreiras biolóxicas. Máis experimentos neste modelo son precisos para caracterizar completamente o comportamento dos nanosistemas.

En terceiro lugar, os nanosistemas lipídicos foron modificados con un lípido catiónico, a putrescina, para o transporte de ácidos nucleicos para terapia xénica. Neste caso, os embrións de peixe cebra foron o modelo de estudo proposto para a avaliación da capacidade dos nanosistemas para liberar o seu cargo na célula, e a súa biodistribución e interacción con células tumorais nun ambiente *in vivo* (Figura 3).

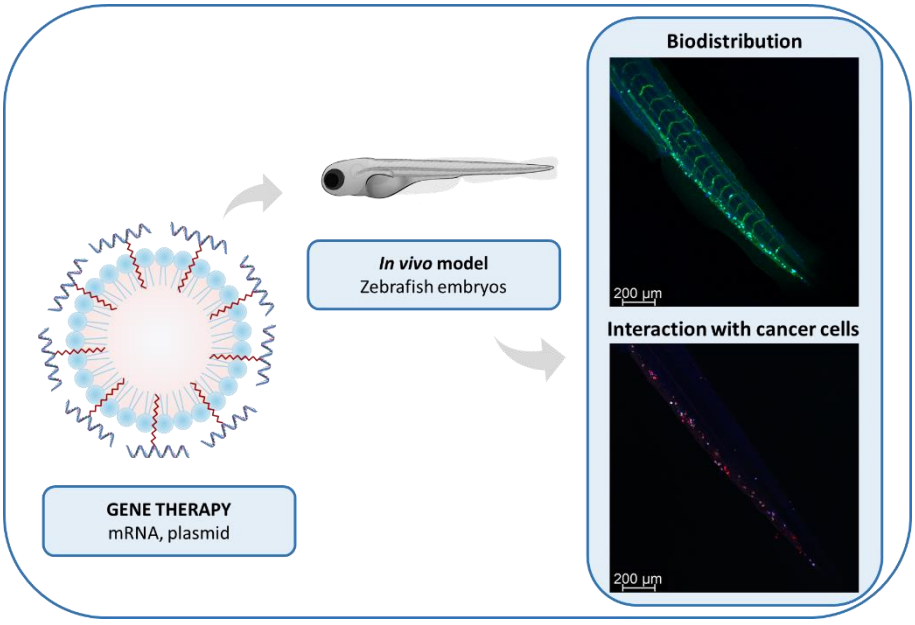

Figura 3. Resumo gráfico do Capítulo III, cuxo obxectivo foi probar a versatilidade dos nanosistemas de esfingomielina para a terapia xénica do cancro, e a súa avaliación en modelos *in vivo* de embrións de peixe cebra.

A terapia xénica estivo a crecer nos últimos anos gracias ao potencial terapéutico de microRNAs (miRs) e plásmidos, entre outros ácidos nucleicos. Aínda así, a maior limitación deste tipo de terapias é a necesidade de protexer da degradación a estas moléculas terapéuticas, así como transportalas ao interior celular. Neste sentido, a nanotecnoloxía representa unha alternativa de vectores versátiles para transportar, protexer e liberar a súa carga terapéutica nas células diana. Con este obxectivo, os nanosistemas lipídicos foron modificados catiónicamente coa adicción de putrescina para poder transportar ácidos nucleicos terapéuticos, miRs e plásmidos. Neste caso, coa finalidade de avaliar os nanosistemas en modelos preclínicos robustos que recapitulen a complexidade tumoral, así como a predición do futuro comportamento dos nanosistemas para a eficiente translación clínica, os embrións de peixe cebra foron o modelo de estudo seleccionado.

Como primeiro paso, e para determinar se os nanosistemas teñen a capacidade de liberar a molécula que transportan cando se encontran no interior celular, un miR (miR 145) con efecto na expresión de xenes de peixe cebra foi testado en embrións de 0 horas post-fecundación. Avaliouse o miR 145 libre e asociado e tamén un miR control, tanto asociado como sen asociar aos nanosistemas. Despois de microinxectar as condicións no embrión, realizouse unha RT-PCR tres días despois para analizar os xens sox9b e gata6, coñecidos por reducir a súa expresión polo efecto do miR 145. O resultado observado mostra esta baixada da expresión dos xenes só no caso dos miR 145 asociado aos nanosistemas, o que proba a súa capacidade para liberar correctamente o cargo que porta.

A continuación estudouse a penetración dos nanosistemas marcados fluorescentemente *in vivo*, incubándoos no medio dos peixes durante 72 horas.

O resultado demostrou a correcta internalización dos nanosistemas, con e sen ácidos nucleicos asociados polas células do peixe. Así mesmo, confirmouse a colocalización entre os nanosistemas e os ácidos nucleicos, probando a súa asociación no proceso de internalización.

O seguinte paso foi avaliación da biodistribución e estabilidade *in vivo* dos nanosistemas como potenciais vectores para terapia xénica. Para iso, os nanosistemas marcados fluorescentemente, con e sen ácidos nucleicos asociados (miRs e plásmidos) tamén marcados, así como este últimos libres, foron microinxectados no ducto de Cuvier e incubados 48 horas. Os resultados de microscopía confocal demostraron unha distribución ao longo do corpo do embrión no caso dos nanosistemas con e sen ácidos nucleicos, que mostran un patrón de acumulación que non aparece no caso dos ácidos nucleicos libres. Demostrouse tamén o mantemento da asociación entre nanosistemas e ácidos nucleicos *in vivo*, probando o potencial dos nanosistemas para terapia xénica.

Por último, realizáronse xenotransplantes con células de cancro de mama marcadas fluorescentemente (MDA-MB-231) para recrear un ambiente de tipo metastático. Posteriormente, as mesmas condicións do experimento anterior foron postas a proba co modelo de *xenograft*. O resultado mostrou colocalización entre os ácidos nucleicos e os nanosistemas, o que corrobora o anterior experimento; ademais de mostrar algunha colocalización entre os nanosistemas, con e sen ácidos nucleicos, e as células tumorais. Isto podería ser debido á alta absorción de poliaminas, como a putrescina, polas células tumorais. Con isto, conclúese que os embrións de peixe cebra teñen un gran potencial como plataforma *in vivo* para a avaliación de nanomedicinas para terapia xénica. Así mesmo, validouse a capacidade dos nanosistemas de asociar e transportar diferentes tipos de ácidos nucleicos.

En resumo, os nanosistemas de esfingomielina foron cargados eficientemente con diferentes tipos de moléculas e decorados con ligandos específicos, para explorar a súa aplicación no desenvolvemento de terapias innovadoras para o tratamento do cancro. Para avaliar comportamento e a eficacia de ditos nanosistemas, modelos celulares 3D estáticos e non estáticos, así como embrións de peixe cebra foron propostos e demostraron o seu potencial como modelos de estudo eficaces *in vitro* e *in vivo*, respectivamente.

INTRODUCTION

Partially adapted/extracted from Cascallar M *et al*.

Cancers, 2022, 14(9):2238

Doi: 10.3390/cancers14092238

Partially adapted/extracted from

What Zebrafish and Nanotechnology Can Offer for Cancer Treatments in the Age of Personalized Medicine

María Cascallar [1,2,3], Sandra Alijas [1], Alba Pensado-López [3,4], Abi Judit Vázquez-Ríos [1,2,5], Laura Sánchez [3,6], Roberto Piñeiro [2,7] and María de la Fuente [1,2,5,*]

[1]Nano-Oncology and Translational Therapeutics Group, Health Research Institute of Santiago de Compostela (IDIS), SERGAS, 15706 Santiago de Compostela, Spain

[2]Centro de Investigación Biomédica en Red Cáncer (CIBERONC), 28029 Madrid, Spain

[3]Department of Zoology, Genetics and Physical Anthropology, Universidade de Santiago de Compostela, Campus de Lugo, 27002 Lugo, Spain

[4]Center for Research in Molecular Medicine & Chronic Diseases (CIMUS), Campus Vida, Universidade de Santiago de Compostela, 15782 Santiago de Compostela, Spain

[5]DIVERSA Technologies S.L., 15782 Santiago de Compostela, Spain

[6]Preclinical Animal Models Group, Health Research Institute of Santiago de Compostela (IDIS), 15706 Santiago de Compostela, Spain

[7]Roche-Chus Joint Unit, Translational Medical Oncology Group, Oncomet, Health Research Institute of Santiago de Compostela, Travesía da Choupana s/n, 15706 Santiago de Compostela, Spain

*

INTRODUCTION

1. Nanotechnology-based treatments: characteristics and advantages

Nanomedicine is known as the use of nanotechnology in the health field, based on the use of nanoscale medicines [1–3]. The first nanomedicine approved by the US Food and Drug Administration (FDA) was Diprivan® in 1989; a liposomal propofol for anesthesia [4,5]. Six years later, in 1995, Doxil®, a doxorubicin liposomal formulation, was also approved for cancer treatment [6]. Since these milestones, the use of nanotechnology-based treatments in the field of medicine has been continuously growing [1]. The recent nano-based COVID-19 vaccines, Spikevax (Moderna) and Comirnaty (Pfizer-BioNTech), are the clear example of the importance of nanomedicine for the development of new therapies [7–9]. The benefits of nanomedicine are, not only the treatment of different diseases, but also their capacity to be used as contrast agents for diagnosis purposes [10–14]. By modulating the composition and physicochemical properties, nanoparticles can be tailored to carry different types of treatments, from small drugs to therapeutic biomolecules, such as nucleic acids, peptides and proteins, among others. Furthermore, nanoparticles can be surface-decorated with specific ligands, which means that they can be targeted for a more efficient interaction with the cells of interest [1,15–18]. Moreover, they protect their cargo, being able of improving the stability and half-life of labile

therapeutic molecules Due to a more precise and efficient delivery, encapsulation into nanoparticles can reduce the side-effects of drugs. An additional advantage is that nanoparticles facilitate the development of combinatorial therapies through co-encapsulation strategies. [19–22].

Nanoparticles can be subdivided in three main groups: polymeric nanoparticles, lipid-based nanoparticles and inorganic nanoparticles (Figure 1). From each general group, additional classifications depend on composition and structural disposition of the different elements, among other aspects.

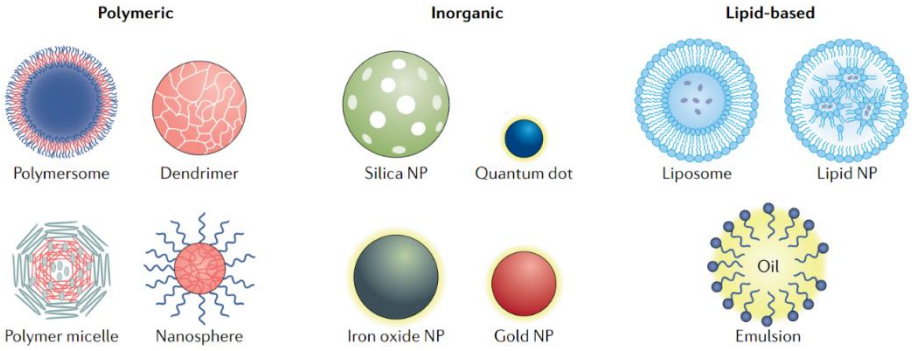

Figure 1. Types of nanosystems classified by their composition. Adapted from Mitchell M. J. *et al* 2021 with permission [23].

Polymeric nanoparticles can be formed from polymers or from monomers that can be natural or synthetic. This type of nanocarriers includes polymersomes, dendrimers, polymer micelles and nanospheres. The advantages of these nanoparticles are that they are typically biocompatibility, if the starting materials are, and that they can be tailored to transport cargos of different nature and size. As a negative point, for some types of polymers and

formulation procedures, it is necessary to use organic solvents. Several approved nanomedicines are polymeric, and a clear example is the anesthetic Diprivan® [23–25].

In the case of lipid-based nanoparticles, the main subgroups are liposomes, emulsions, and lipid nanoparticles. They are the most present among FDA-approved nanocarriers, and the main reasons of this success are their high biocompatibility, the easiness of the formulation and scalability, and the capability to modulate their physicochemical properties. The use of lipidic nanoparticles is particularly growing in the field of the nucleic acids' delivery, due to the recent Covid-19 vaccines success [23,24,26]. Nanoemulsions are a colloidal particulate system which is composed by immiscible phases which form droplets due to a surfactant. There are two different types depending on the phase forming the droplets: water-in-oil (W/O) and oil-in-water (O/W), which is the most common. Nanoemulsions have versatile characteristics which confer them the capacity to carry, for example, hydrophobic drugs to improve their administration [27–30].

Inorganic nanoparticles include quantum dots, silica nanoparticles, gold nanoparticles and iron oxide nanoparticles, among others. They are the less common of the three groups in the clinical scenario. This fact is directly related their potential toxicity. Although some uses are proposed in the therapeutic field, the most promising applications for inorganic nanoparticles fall in the diagnosis are due to their intrinsic optical properties, as for example in the case of magnetic iron oxide nanoparticles for magnetic resonance imaging [23,25,31].

2. Nanomedicine: a key strategy for cancer treatment

Cancer, as a group of diseases, is the responsible of millions of deaths in the world, reaching almost ten million of deaths in 2020. Furthermore, the number of new cases per year is nearly twenty million, and the incidence ranking is led by female breast cancer (11,7%) and lung cancer (11,4%) [32]. These numbers alert about the immediate necessity of new therapeutic strategies for cancer treatment. As explained before, nanomedicine plays an alternative strategy to improve the cancer treatment, as well as the quality of life of the patients [33]. Since the approval of Doxil®, the first nanoparticle for anti-cancer therapy, numerous cancer nanomedicines have been developed [34,35]. Some of them have reach the market, such as Vyxeos®, a liposomal that co-encapsulate cytarabine and daunorubicin for acute myeloid leukemia treatment, and Abraxane®, an albumin-bound nanoparticle of paclitaxel for breast cancer, non-small cell lung cancer and metastatic pancreatic adenocarcinoma treatment [25,36–39]. However, only around 20 anti-cancer nanomedicines were approved for clinical uses, considering the cancer field the most successful in this matter [25]. This fact, bearing in mind that there are multiple nanomedicines in clinical trials, brings to the forefront the translational difficulties of nanomedicine from the bench to the clinic [25,40]. Some of the main reasons of the slowness of this process are the toxicity and the biocompatibility of the formulations in clinical trials, as well as the implementation of a large-scale production [25,40].

In this line, our group has developed a new type of nanoemulsions, composed by sphingomyelin and vitamin E, sphingomyelin nanosystems (SNs) (Figure 2), which are biodegradable, safe-by-design and biocompatible,

due to the nature of their components [41,42]. In addition, SNs have shown capacity for the encapsulation of hydrophilic drugs and hydrophilic biomolecules, for specific applications in oncology [17,41,43,44]. Moreover, SNs can be functionalized with different biomolecules, such as peptides [17,18]. The versatility of these SNs also allows the association of nucleic acids (deoxy- and ribonucleic) for cancer gene therapy [45–48]. On top of all this, SNs have been optimized for their use as contrast agents for diagnostic purposes [11–14].

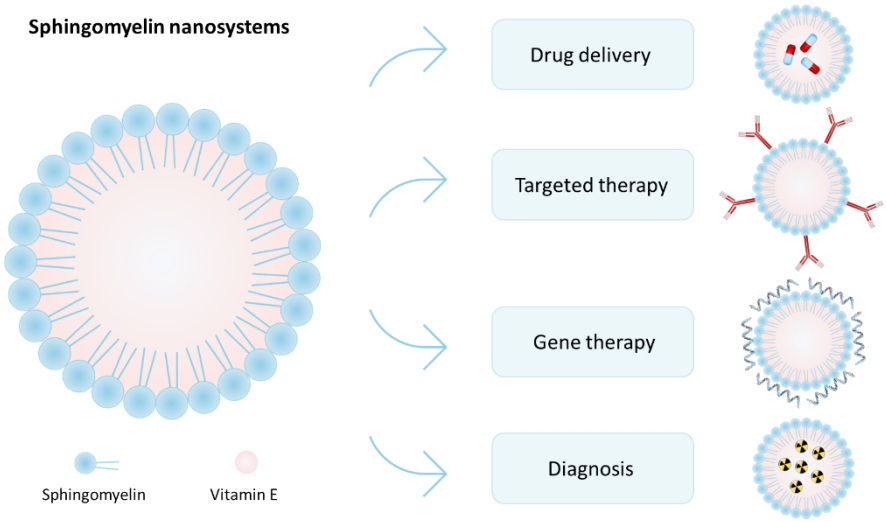

Figure 2. Structure of sphingomyelin nanosystems and their uses in cancer treatment. Adapted from Servier Medical Art.

As explained before, and despite the reached success in the field of nanomedicine, several challenges are still to be faced to reach the market [49]. For improving this low clinical translation of nanomedicines into the clinic, the development of new study models for solid evaluation is a key step to achieve this objective [50–52]. In this regard, it is necessary to have reliable study models, not only *in vitro*, but also *in vivo*, with the capacity to mimic the tumor for the study of nanomedicines [25,51,53,54]. Three-dimensional (3D) *in vitro*

models and zebrafish are suitable alternatives and complementary platforms to two-dimensional (2D) cell cultures and rodents, which are the gold-standard model of evaluation (Figure 3). Furthermore, their use can reduce the number of rodents and other animals in the next steps of the research, making use of the 3Rs for animal welfare in experimentation [55].

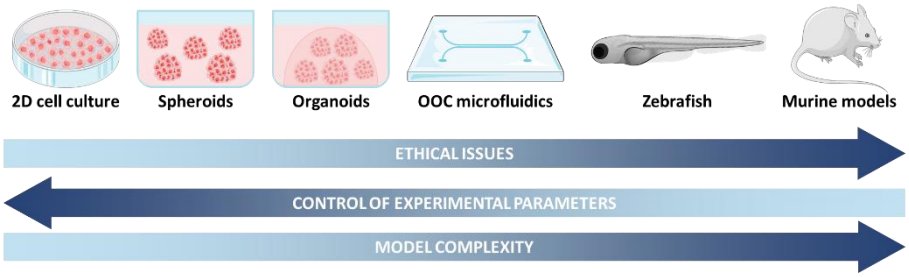

Figure 3. Advantages and disadvantages of the *in vitro* and *in vivo* cancer models. Adapted from Servier Medical Art; and from Lizzy Griffiths.

Taking into account this information, in this doctoral thesis we aim to evaluate the potential of SNs, loaded with different types of cargos (small drug and gene therapy), and surface-decorated to targeting to specific cell subpopulations, using for this purpose advanced *in vitro models* as well as zebrafish embryos.

3. Static 3D *in vitro* models

The most common *in vitro* model in the field of cancer research is the 2D cell culture. Although this is an easy and useful tool for the first research steps, it has some disadvantages. The monolayer cell culture has the lack of mimicking the tumor, not only its 3D structure, but also, the cell-cell and cell-

matrix interactions, the gases and nutrients gradients, and the tumor microenvironment [56–58]. For this reason, more complex models are needed to overcome these problems and to better evaluate the safety and efficacy of anti-cancer therapies.

3D *in vitro* models are alternatives to solve the 2D cell culture limitations and can be classified as static and non-static. Static 3D models are characterized by the lack of flow in their culture environment; on the contrary, non-static or dynamic 3D models present flow conditions in the media [58–62]. These models will be explained in the following sections.

3.1. Spheroids and organoids

The 3D static cell culture models can be divided in spheroids and organoids (Figure 4). Spheroids are spherical groups of aggregated cells which are cultured, usually, in suspension without any scaffold, and therefore, they are the simplest 3D platform [63]. In this sense, considering their value as a cancer model, it is possible to mimic the 3D disposition of the cancer cells, and to replicate the intra-cellular interactions that occur in the tumor. The formation of spheroids can be achieved following different strategies: I) hanging drop; II) ultra-low attachment (ULA) plates; III) magnetic levitation; IV) pellet culture; and V) microgravity reactors [63,64]. The selection of one or another technic depends on the aim of the study, for example, ULA plates are convenient for multicellular cultures because of the great volume of the wells, whereas microgravity reactors for high mass production [64].

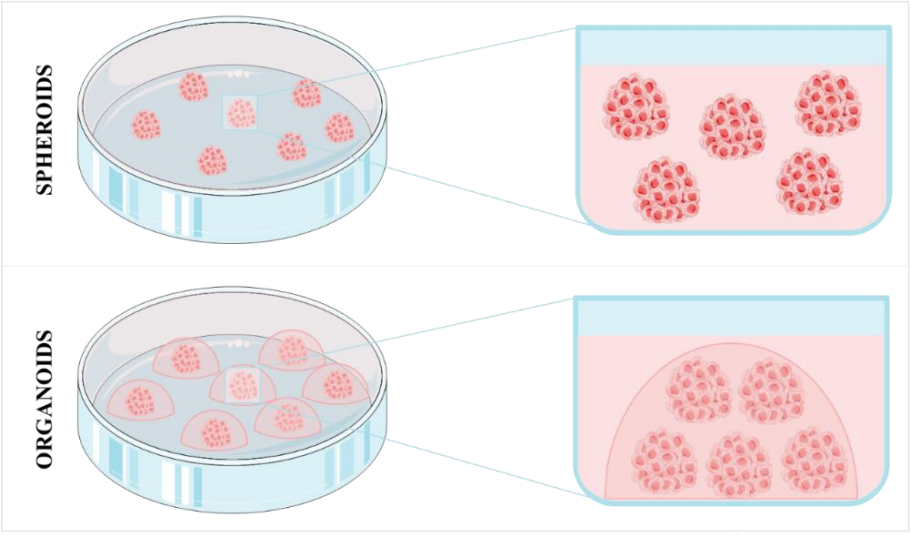

Figure 4. Types of static 3D models for cancer research: spheroids (cultured in suspension) and organoids (cultured embedded in a matrix). Adapted from Servier Medical Art.

In the same line, organoids are also 3D cells structures, but the main difference between spheroids is the presence of a scaffold which mimics the extracellular matrix of the tumor and the type of cells [64]. Moreover, organoids are developed from embryonic stem cells, adult stem cells or induced pluripotent cells, tumor cells, cell lines and tissues; and they can achieve the capacity to self-organize and differentiate, depending on the growth factors added to the media [65,66].

In this case, the complexity of the proposed platform is increased because of the intrinsic characteristics of the spheroid and the recreation of the tumor microenvironment in a more accurate way [66]. The scaffolds, which are used to growth the embedded organoids, can be composed by different natures. They can be made of natural hydrogels, such as collagen, synthetic hydrogels, hard

polymers, and proteins [58,67]. The most common matrix used to culture organoids is Matrigel® Matrix, a protein-based scaffold which mimics the composition of the basement membrane Engelbreth–Holm–Swarm tumor [58,68].

3.2. The role of 3D static models for nanomedicine evaluation

Spheroids and organoids are key models that are used as the study platform of several nanotechnology-based cancer treatments. These 3D models are fundamental to evaluate the toxic effects of anti-cancer drugs because of their better correlation with *in vivo* behavior [63,69]. Moreover, they have some advantages against *in vivo* models, such as the lower cost and their capacity to run wide screening studies [70,71].

The nanoparticles therapeutic efficacy can be studied taking advantage of these 3D models [72]. This aspect is essential for a novel nanomedicine to prove that it is capable of release its cargo in the targeted cell, and that its cargo is able to perform its effect, before carrying out *in vivo* assays, which are highly time and cost-consuming. In this sense, a recent example is the work of McCarthy *et al.*, who evaluated the photothermal ablation based on polymeric nanoparticles for the colorectal cancer treatment [73]. The use of organoids as their main study platform allows them to test not only the efficiency of the nanoparticle's treatment, but also their capacity to diffuse into the organoid's matrix, something that cannot be done in 2D cell cultures [73].

Apart from the toxicity, one of the main challenges of the nanomedicines is the efficient internalization into the cancer cells [72]. 3D models allow to evaluate if this internalization reach the inner cells of the 3D structure, meaning that the therapy will treat all the tumor cells [72,74]. In this vein, the work of Siemer *et al.* is a clear example of this use of spheroids in nanoparticles uptake study. In this case, cisplatin-loaded nanoparticles were tested in 3D models for cancer treatment, achieving good therapeutic effect [75].

3.3. Clinical output

Focusing on the translational applications of the static 3D models, there are multiple studies in which both spheroids and organoids are formed by tumor cells from the patient, better known as patient-derived spheroids (PDS) and patient-derived organoids (PDO) [76]. These *in vitro* models based on patient cells allow the screening of personalized antitumoral therapies taking into account the personal characteristics of each tumor, being an useful platform to obtain more reliable responses than the ones obtained with cellular lines [76,77].

PDS and PDO are effective platforms, evidenced by several examples which demonstrate their usefulness as study models for drug screening. Among others, Palzer *et al.* developed a magnetic fluid hyperthermia treatment based on iron oxide nanoparticles for pancreatic ductal adenocarcinoma. Using tissue from the patient to perform PDO with the aim of evaluating the therapeutic efficacy of their nanoparticles, they observed an efficient treatment of pancreatic cancer cells [78]. Another example, and in this case, based on spheroids use, is the research performed by Hofmann *et al.* In

this work patient-derived breast cancer cells were used to perform spheroids, as a platform for testing four FDA-approved drugs for cancer treatment [79].

4. Non-static 3D *in vitro* models

Although static *in vitro* platforms are highly useful for drug testing, they cannot mimic the complete interactions produced in the tumor. In this sense, microfluidic devices are a step ahead, including the fluidic parameters present in the organism, mimicking even further the tumor [80,81].

The technology of microfluidics was started in the 1980's, and since then, it was improved in different health fields of knowledge, such as cancer, osteoarthritis and amyotrophic lateral sclerosis [82–84]. Microfluidic organ-on-a-chip (OOC) devices have the capacity to partially mimic in a small-scale platform, the *in vivo* conditions of the tumor [77,80,85].

In this sense, the OOC devices allow the perfusion of the tumor mass, that is, not only more reliable, but also better for understanding the behavior of the cells and the treatments [77]. The fabrication of these chips is usually based on the polymer polydimethylsiloxane (PDMS). However, there are other alternatives, such as resins and elastomers, which are trying to overcome PDMS shortcomings, such as its limited capacity for high-throughput manufacturing [82,86]. Soft-lithography is the most common technique to reproduce device replicas with the same specific and micro-detailed channels in PDMS for OOC. In these microchannels, the culture of the cells of interest is performed, as well as the controlled flow and the biochemical stimuli [87,88].

OOC microfluidic devices allow several options for the evaluation of cancer treatments. In the case of spheroids and organoids, it is known that there is a lack of the representation of the flow in the environment of the tumor, that can be solved using microfluidics OOC. A clear example is the improvement in the study of static 3D models. To achieve that, spheroids or organoids embedded in a scaffold are grown within microfluidic device's walls with continuous perfusion, which allows the control of the nutrients, among other parameters cytokines (Figure 5A) [85,89,90].

Furthermore, there are chips with more complexity, such as the ones that can mimic the endothelial structure of the blood vessels (Figure 5B). The vascular system plays a fundamental role, not only in the development of the tumor, but also in the evaluation of the biodistribution and efficacy of novel anticancer therapies [88,91,92]. Interestingly, the metastatic cascade was replicated in microfluidic devices, allowing the evaluation of the entire process, from the intravasation to extravasation step, as well as the study of anti-cancer drugs effect [93–96].

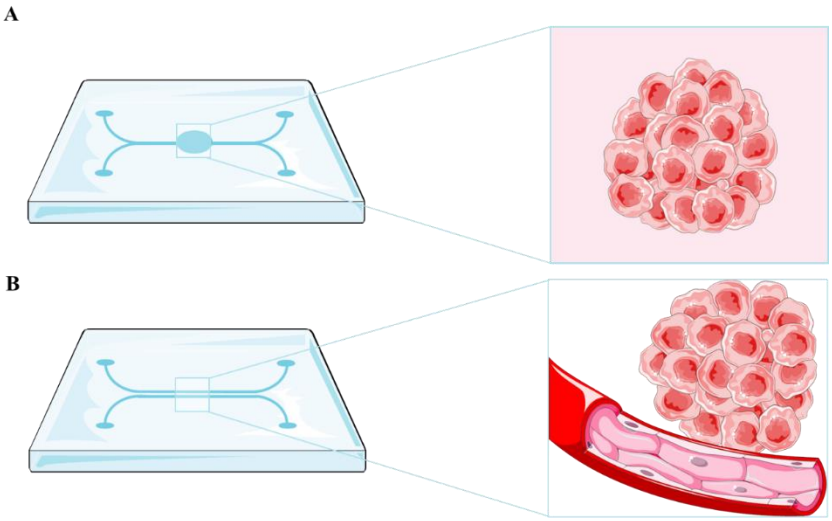

Figure 5. Example of OOC microfluidic devices: A. spheroid/organoid in a chip; B. vascularized OOC. Adapted from Servier Medical Art.

4.1. The synergy between nanomedicine and microfluidic organ-on-a-chip models

Microfluidic OOC models allow the evaluation of treatments with different bases and objectives. As mentioned before, OOC help us to mimic the complete structure, flow, extracellular matrix, and interactions of the tumors. In this line, these devices, due to their characteristics, offer the opportunity to assess, not only the biodistribution, but also the therapeutic effect of novel nanomedicines [85,97,98]. Overall, the synergy between OOC microfluidic devices and innovative therapies based on nanotechnology has a great interest for the development of novel cancer treatment.

OOC allow the recreation of vasculature, as explained in the previous section, and one of the main strategies for nano-based drugs is the evaluation of the nanosystem capacity to cross the vasculature endothelial barrier to reach the cancer cells, as well as crossing other biological barriers, such as the blood-brain barrier [99,100]. Moreover, OOC was used for evaluating the therapeutic effect of different nano-based treatments for cancer therapy. A good example is the work of Ran *et al.*, who developed a multi-well OOC, for studying the therapeutic effect of four different types of liposomes for cancer treatment. The results of uptake and treatment efficacy obtained in the OOC correlate better with the *in vivo* models than the 2D cell culture [101]. In a different perspective, Vu *et al.*, developed tumor microfluidic devices to evaluate the capacity of nanomedicines with different physiochemical characteristics to extravasate the endothelial barrier for cancer treatment. The outcomes demonstrated the importance of size and superficial chemistry for nanoparticles extravasation [102].

4.2. Microfluidic organ-on-a-chip translation to the clinic

OOC devices permit the use of patient-derived cells to create a personalized scenario for evaluating cancer treatments, though the most common chips are composed by established cellular lines [103,104]. In this sense, this possibility allows the establishment of a derived tumor-cell population in microfluidic devices, which replicate the way the tumor behaves in the real life, for anti-cancer drugs testing [98].

As an example, Haque *et al.*, performed microfluidic chips for the evaluation of patient-derived cells of pancreatic ductal adenocarcinoma. In this case, the main objective was to recapitulate the tumor microenvironment, using PDO in microfluidic devices, as well as to evaluate the efficacy of chemotherapy treatments, observing that targeting the stroma increase the therapeutic effect [105]. In a similar way, Shirure *et al.*, aimed to produce a vascularized model based on PDO to evaluate the different stages of the tumor progression. Moreover, this OOC model was used for the assessment of chemotherapeutic agents and anti-angiogenic drug's effectiveness [106].

In summary, static and non-static 3D *in vitro* models present the ability to mimic the tumor structure and to fill the gap between 2D cell cultures and *in vivo* models, which is an important advantage for nanoparticle screening. However, they cannot replace the *in vivo* models, due to their limitations. In this sense, zebrafish study models offer some advantages for the assessment of cancer nano-based therapy, which are explained in the next sections.

5. *In vivo* models: zebrafish

Zebrafish (*Danio rerio*) is a vertebrate model species traditionally used for studying developmental biology and vertebrate genetics, and more recently, to model human diseases, such as cancer, playing a key role in the discovery of new drugs for treating these illnesses [107–109]. Zebrafish characteristics define it as a model species between invertebrate and murine models because it collects the vertebrate traits and allows large experiments [107,108]. One of the features that make zebrafish an appropriate human disease

model is its homology with the human genome, around 70%, which increases to 82% in the case of human disease-related genes [110]. Furthermore, there are multiple advantages associated with the use of zebrafish, such as high fecundity and fertilization rate, producing a large offspring [111]. In addition, the external fertilization and optical transparency of embryos and larvae allow direct visualization of the overall development and enables the imaging of cells without the use of invasive techniques [112].

In terms of cancer research, aside from the robustness of zebrafish embryos to be easily manipulated, the adaptive immune system is not active until 2-4 weeks post-fertilization (wpf) and complete immunocompetence is only achieved at 4-6 wpf [113]. This feature, together with the previously mentioned transparency, enables the transplantation of fluorescent cancer cells (xenotransplantation or xenograft) and the visualization and tracking of their growth, biodistribution, metastasis and neovascularization processes, as well as the evaluation of drug responses [112,114]. The main advantages and disadvantages of zebrafish as a model for human diseases are summarized in Table 1.

Table 1. Benefits and drawbacks of using zebrafish for modeling human diseases, in comparison with other animal models [107,108].

ADVANTAGES	DISADVANTAGES
Simple anatomy	Some mammalian organs are missing
External fertilization	Optimal temperature at 28°C, compromising human cells viability
Embryo and larvae optical transparency	Lack of sexual chromosomes
Rapid development and sexual maturation	Pooling individuals prevent the observation of interindividual differences
High fertility rates	Mice genetic homology is higher
Large number of individuals and statistical power	Low amount of certain tissues for biological assays
Robust embryos	Genetic duplication
High homology in human disease-related genes	Protocols variability, limiting the comparison among studies
Late activation of the adaptive immune system	Need of mammal models for further preclinical studies
Cost-effective and easy maintenance	Low antibodies availability for molecular assays
Easy genetic manipulation	
Low number of cells for xenograft assays	
Availability of reporter lines	
Many existing zebrafish resources and repositories	

5.1. Zebrafish as a cancer study platform: models

5.1.1. Genetic models

5.1.1.1. Forward Genetics

Several carcinogens are able to induce human-like tumors in different zebrafish organs, the main ones are: N-methyl-N'-nitro-N-nitrosoguanidine (MNNG), dimethylbenzanthracene (DMBA), diethylnitrosamine (DEN), N-nitrosodimethylamine (NDMA) and ethylnitrosourea (ENU) [115]. Thus, studies have been performed allowing a better understanding of the carcinogenesis

process, main target tissues, type of tumor, signaling pathways or chemoprevention measures.

For instance, the exposure of embryos to MNNG produces the development of hepatic and mesenchymal neoplasms, such as chondroma [116]. Similarly, it has been shown that exposing zebrafish to DMBA at 3 wpf led, principally, to hepatic neoplasia in adults [116]. DEN, in the same way, was used in adult zebrafish to evaluate the role of hepatocellular proteins in hepatocarcinogenesis [117]. Conversely, the relationship between polyploidy and tumor formation has been investigated through NDMA-induced hepatocarcinogenesis [118]. The mutagen ENU has been used to generate point mutations, leading to the identification of several mutant zebrafish lines with an increased incidence of spontaneous neoplasia or higher sensitivity to chemical exposure [115].

5.1.1.2. Transgenic zebrafish lines

Several zebrafish cell and tissue-specific reporter lines have been developed over the last years to improve the comprehension and characterization of different cancer traits such as tumor cells growth, migration, invasion, angiogenesis, drug responses or interactions with immune cells. Some examples are Tg(*mpx*:GFP) and Tg(*mpeg1*:eGFP) [119,120], which fluorescently label neutrophils and macrophages, respectively, or Tg(*fli1*:eGFP) [121], which labels the vasculature. Furthermore, human or murine oncogene transgenic expression in zebrafish has also helped to understand their role in tumor development, for example, Tg(*ptf1a*:eGFP-KRASG12V) in pancreatic cancer [122] and Tg(*mitfa*:HRASG12V; *mitfa*:GFP) or Tg(*mitfa*:BRAFV600E); tp53−/− for melanoma [123,124].

5.1.1.3. Reverse genetics

Morpholinos (MO) are commonly used in zebrafish to achieve transient expression silencing without modifying the genome sequence [125] and thus, to determine certain cancer invading mechanisms, such as angiogenesis.

In order to generate stable mutant models, Targeted Induced Local Lesions in Genomes (TILLING), based on the exposure to ENU and further sequencing [126], has been extensively used. In this sense, mutations in tumor suppressor genes, such as tp53, pten and apc have been identified in ENU mutagenesis libraries, and fish were found to develop malignant peripheral nerve sheath tumors, ocular hemangiosarcomas, and intestinal adenomas, hepatomas and pancreatic adenomas, respectively [127–130]. Although TILLING has proven to be useful to correlate genotypes with phenotypes, the difficulty involved in the screening process, together with the possibility of having further mutations than the one desired, led researchers to introduce other methodologies, such as nuclease-based techniques, which include Zinc Finger Nucleases (ZFNs) and Transcription Activator-Like Effector Nucleases (TALENs). ZFNs were used to generate tet2 mutants, which developed progressive clonal myelodysplasia, culminating in myelodysplastic syndrome, with dysplasia of myeloid progenitor cells and abnormal circulating erythrocytes [131]. Nevertheless, the design of nuclease-bases systems is challenging and there is still a high rate of off-targets. Thus, the introduction of the CRISPR/Cas9 system has allowed the optimization of the genome editing protocols and the improvement of efficiency and accuracy of zebrafish lines [132].

4.1.2. Transplantation models

Transplantation in zebrafish is based on the injection of fluorescently labeled cancer cells into zebrafish embryos. The main transplantation techniques include allotransplantation and xenotransplantation, and both can be orthotopic or heterotopic depending on whether the cells are injected in an equivalent anatomical site to tumor origin or into a different anatomical site, respectively.

Allograft consists of tumor cells being transferred from one individual to another of the same species [133], while xenograft is based on the injection of labeled human, murine or patient-derived cancer cells into zebrafish, to track their survival, engraftment, growth, behavior, and interaction with the microenvironment [134]. The common sites for heterotopic transplantation are (Figure 6): a) yolk sac, to track survival and proliferation [135]; b) duct of Cuvier, to observe migration, invasion, and mesenchymal-epithelial transition [136]; c) perivitelline space, to investigate mainly neovascularization [134]; intraperitoneal cavity, when adult individuals are used.

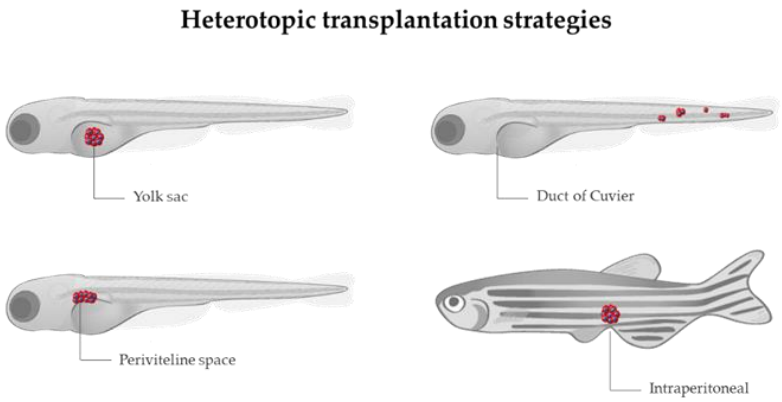

Figure 6. Sites for heterotopic transplantation of tumor cells (in red) in zebrafish. Adapted from Servier Medical Art and Lizzy Griffiths.

The majority of transplantations assays are performed at 2 days post-fertilization (dpf), taking advantage of the transparency of the embryos and the lack of adaptive immunity, although some experiments have been carried out using adults. In order to avoid immune rejection in adults, transplantations require immunosuppression with sublethal γ-irradiation or dexamethasone [137,138] or the use of immunocompromised lines, such as the Rag2, lacking mature T-cells and having a reduced number of B cells, or the compound mutant prkdc-/-, il2rga-/-, lacking T, B and natural killer cells [139,140].

The first xenograft assay was performed by injecting melanoma cells in zebrafish blastula, which showed the ability of melanoma cells to survive, proliferate and specifically migrate to the skin, highlighting the validity of the zebrafish for cancer research [141]. Since then, this technique has been improved and extended for studying several cancer features, not only survival, proliferation or migration, but also the ability to invade, form new blood vessels (angiogenesis), metastasize and their capability to respond or resist different treatments. Additionally, researchers have made efforts to mimic human tumor conditions and microenvironment as much as possible, as reviewed by Cabezas-Sáinz *et al.* [142]. For instance, the use of transgenic zebrafish lines, such as the previously mentioned ones, labeling immune cells or vasculature, has led several researchers to better understand the interaction among tumor cells and macrophages or neutrophils, and their involvement in tumor growth, vascularization, invasion and metastasis [143–146].

5.2. Zebrafish as a platform for drug screening: its role in nanomedicine

Zebrafish are used as a screening platform to adjust drug concentrations, to improve combinatorial treatments for a less toxic effect on the patient or overcome resistances, as well as a tool to study the mechanism of action of drugs in the organism and to alter the function of a biological pathway without previously knowing the components. Small molecule screening in zebrafish started in 2000 with a work by Peterson *et al.* who tested the effect of a variety of molecules in the development of vertebrate animals and to understand how these molecules can be used to determine the timing of critical developmental events [147].

In the context of cancer, zebrafish xenotransplants have been useful as *in vivo* preclinical tools for drug testing. This approach has been validated by different works, showing its complementarity with other *in vivo* models such as the mouse [148]. However, xenotransplantation of human cancer cells into the zebrafish is not without difficulties. For instance, the normal growth of human cells is at 37°C, and the temperature of development of the zebrafish is 28°C. To overcome this issue, the field has established 31-34°C as a consensus temperature for xenograft assays. However, these temperatures could cast some doubts about the efficiency of xenograft models for drug screening and the subsequent translation to the patient. In this sense, Cabezas-Sáinz *et al.* demonstrated that zebrafish larvae can live until 36°C allowing them to test drugs in a cancer model with characteristics close to humans [149]. In addition, Cornet *et al.* developed the ZeOnco Test, an optimized and standardized (regarding cell labeling, injection site, image acquisition, etc.) xenograft assay, aiming at reducing attrition rate [150,151].

Zebrafish is being a useful *in vivo* model to be a platform for screening different types of cancer treatments, such as peptide-based drugs, gene therapy, immunotherapy and nanomedicine (Figure 7).

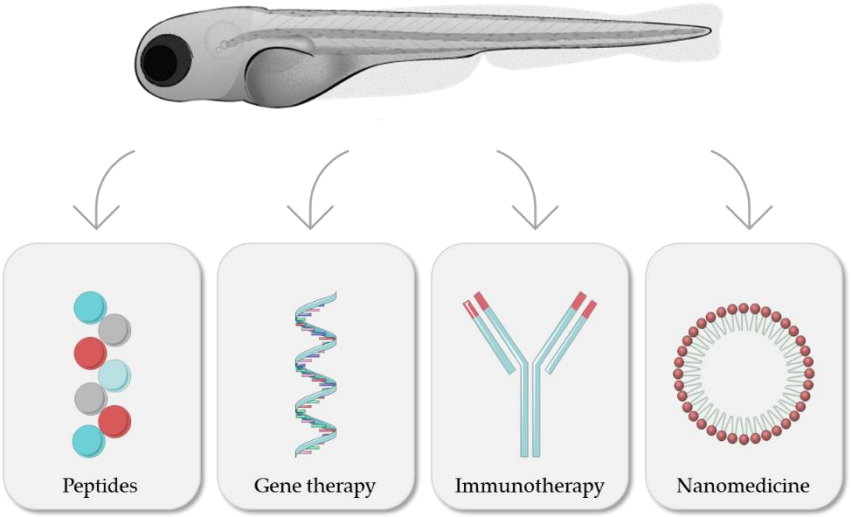

Figure 7. Zebrafish as a model for evaluation of different cancer treatments. Adapted from Servier Medical Art and Lizzy Griffiths.

Zebrafish embryos are currently used for nanomedicine toxicity testing due to their advantages such as their high fertilization rate, as explained in Section 3. The most common method to perform toxicity assays is the incubation of nanomedicines into zebrafish medium, usually with dechorionated zebrafish. As well as the incubation, microinjection of test drug into zebrafish circulation ensures the concentration absorbed by the embryos [111]. Several aspects of zebrafish embryos can be analyzed to determine the toxicity of a specific nanomedicine. The correct hatching process, malformations appearance, the response of the immune system and mortality are some of the guidelines to evaluate the toxicity effect of nanoparticles [152,153].

As a result, toxicity tests based on zebrafish have become an indispensable step to assess the effect of several therapies based on nanosystems, encompassing from metal-based nanoparticles to lipidic nanosystems [154–156].

In vivo behavior, distribution along the body and interaction with tumor cells are key qualities to develop new anticancer nanomedicines; therefore, analyzing these aspects is essential to achieve a translation to the clinic of nano-based therapies. Due to this, zebrafish embryos play an important role as a platform to evaluate these nanoparticles' properties *in vivo* [157,158]. In this sense, transgenic lines are very useful, particularly the ones with labeled vasculature and immune system cells. These lines can provide information about the behavior between nanoparticles and the blood vessels and the ability to extravasate, as well as their half-life in the organism and their uptake by macrophages [159–163].

Zebrafish has turned into an anticancer nanomedicine platform to evaluate the efficacy of this treatment, since they allow the modeling of several types of cancer and different tumor stages.

The microinjection of cancer cells allows assessing the capacity of nanoparticles to interact with xenotransplanted cells as well as their antitumoral efficacy [164–167]. In addition, metastasis modelling in zebrafish embryos can be performed as a result of spreading across the circulation of xenotransplanted tumor cells. The microinjection or incubation of different types of antitumoral drugs allow the evaluation of their capacity to inhibit these metastatic processes [168,169].

5.3. Zebrafish as a tool in personalized medicine

The zebrafish as a preclinical disease model has proven to be key to inform about human disease mechanisms and therapy. Aside from the generation of powerful cancer models for the identification of therapeutic targets, this disease model must achieve an instrumental role in the era of precision medicine in oncology, allowing the tailoring of the treatments to the individual characteristics of each patient. It is known that tumors present high interindividual heterogeneity and established cancer cell lines often differ significantly from patients' tumor cells. Thus, to preserve the patients' tumor biological and genetic profile and improve the accuracy of tumor drug-response studies, zebrafish patient-derived xenografts (zPDXs) have arisen as a potential solution [145,170]. zPDXs are established from tumor cells or masses isolated from patients during biopsy or excision which are subsequently hetero- or orthotopically implanted into zebrafish. The pioneers of this technique were Marques *et al.*, who observed cell invasion and metastasis formation after injection of colon, pancreas, and stomach primary tumors samples into the yolk sac[171]. Since then, the survival, proliferation, angiogenesis or invasion ability of different patient-derived tumor cells have been studied in zebrafish models, from pancreatic, colon, gastric, head and neck or pituitary cancer, to abdominal liposarcoma or T-cell acute lymphoblastic leukemia [172–176]. Furthermore, in order to improve patients' treatments, zPDXs have served as a platform to develop drug response/resistance assays and thus move towards personalized medicine [170,172,173,176–180].

Overall, static and non-static *in vitro* models and *in vivo* zebrafish embryos have the potential to be valuable study models to evaluate cancer nanomedicines. In the next chapters of this doctoral thesis, these models are going to be tested with different strategies based on nanotechnology for the cancer treatment.

BIBLIOGRAPHY

1. Farjadian, F. *et al.* Nanopharmaceuticals and nanomedicines currently on the market: Challenges and opportunities. *Nanomedicine* **14**, 93–126 (2019).

2. Afzal, O. *et al.* Nanoparticles in Drug Delivery: From History to Therapeutic Applications. *Nanomaterials* **12**, (2022).

3. Jia, Y. *et al.* Approved Nanomedicine against Diseases. *Pharmaceutics* **15**, 774 (2023).

4. Anselmo, A. C. & Mitragotri, S. Nanoparticles in the clinic: An update. *Bioeng Transl Med* **4**, (2019).

5. Anselmo, A. C. & Mitragotri, S. Nanoparticles in the clinic: An update post COVID-19 vaccines. *Bioeng Transl Med* **6**, (2021).

6. Makwana, V., Karanjia, J., Haselhorst, T., Anoopkumar-Dukie, S. & Rudrawar, S. Liposomal doxorubicin as targeted delivery platform: Current trends in surface functionalization. *Int J Pharm* **593**, 120117 (2021).

7. Corbett, K. S. *et al.* SARS-CoV-2 mRNA vaccine design enabled by prototype pathogen preparedness. *Nature* **586**, 567–571 (2020).

8. Polack, F. P. *et al.* Safety and Efficacy of the BNT162b2 mRNA Covid-19 Vaccine. *New England Journal of Medicine* **383**, 2603–2615 (2020).

9. Taina-González, L. & de la Fuente, M. The Potential of Nanomedicine to Unlock the Limitless Applications of mRNA. *Pharmaceutics* **14**, (2022).

10. Zhu, W., Wei, Z., Han, C. & Weng, X. Nanomaterials as Promising Theranostic Tools in Nanomedicine and Their Applications in Clinical Disease Diagnosis and Treatment. *Nanomaterials* **11**, (2021).

11. Nagachinta, S. *et al.* Radiolabelling of lipid-based nanocarriers with fluorine-18 for in vivo tracking by PET. *Colloids Surf B Biointerfaces* **188**, 110793 (2020).

12. Díez-Villares, S. *et al.* Biodistribution of 68/67Ga-Radiolabeled Sphingolipid Nanoemulsions by PET and SPECT Imaging. *Int J Nanomedicine* **16**, 5923 (2021).

13. Díez-Villares, S. *et al.* Quantitative PET tracking of intra-articularly administered 89Zr-peptide-decorated nanoemulsions. *Journal of Controlled Release* **356**, 702–713 (2023).

14. Díez-Villares, S. *et al.* Manganese Ferrite Nanoparticles Encapsulated into Vitamin E/Sphingomyelin Nanoemulsions as Contrast Agents for High-Sensitive Magnetic Resonance Imaging. *Adv Healthc Mater* **10**, 2101019 (2021).

15. Roma-rodrigues, C., Rivas-garcía, L., Baptista, P. v. & Fernandes, A. R. Gene Therapy in Cancer Treatment: Why Go Nano? *Pharmaceutics* **12**, (2020).

16. Solak, K., Mavi, A. & Yılmaz, B. Disulfiram-loaded functionalized magnetic nanoparticles combined with copper and sodium nitroprusside in breast cancer cells. *Materials Science and Engineering: C* **119**, 111452 (2021).

17. Bouzo, B. L. *et al.* Sphingomyelin nanosystems loaded with uroguanylin and etoposide for treating metastatic colorectal cancer. *Sci Rep* **11**, 17213 (2021).

18. Jatal, R. *et al.* Sphingomyelin nanosystems decorated with TSP-1 derived peptide targeting senescent cells. *Int J Pharm* **617**, 121618 (2022).

19. Pei, Z. *et al.* Current perspectives and trend of nanomedicine in cancer: A review and bibliometric analysis. *Journal of Controlled Release* **352**, 211–241 (2022).

20. Abdelkader, A., Fathi, H. A., Hamad, M. A. & Elsabahy, M. Nanomedicine: a new paradigm to overcome drug incompatibilities. *Journal of Pharmacy and Pharmacology* **72**, 1289–1305 (2020).

21. Fadeel, B. & Alexiou, C. Brave new world revisited: Focus on nanomedicine. *Biochem Biophys Res Commun* **533**, 36–49 (2020).

22. Sindhwani, S. & Chan, W. C. W. Nanotechnology for modern medicine: next step towards clinical translation. *J Intern Med* **290**, 486–498 (2021).

23. Mitchell, M. J. *et al.* Engineering precision nanoparticles for drug delivery. *Nat Rev Drug Discov* **20**, 101 (2021).

24. Zielinska, A. *et al.* Polymeric Nanoparticles: Production, Characterization, Toxicology and Ecotoxicology. *Molecules* **25**, (2020).

25. Halwani, A. A. Development of Pharmaceutical Nanomedicines: From the Bench to the Market. *Pharmaceutics* **14**, (2022).

26. Sheoran, S., Arora, S., Samsonraj, R., Govindaiah, P. & vuree, S. Lipid-based nanoparticles for treatment of cancer. *Heliyon* **8**, e09403 (2022).

27. Mazza, M., Alonso-Sande, M., Jones, M. C. & De La Fuente, M. The potential of nanoemulsions in biomedicine. in *Fundamentals of Pharmaceutical Nanoscience* 117–158 (Springer New York, 2013). doi:10.1007/978-1-4614-9164-4_6.

28. Elzayat, A., Adam-Cervera, I., Álvarez-Bermúdez, O. & Muñoz-Espí, R. Nanoemulsions for synthesis of biomedical nanocarriers. *Colloids Surf B Biointerfaces* **203**, 111764 (2021).

29. Mushtaq, A. *et al.* Recent insights into Nanoemulsions: Their preparation, properties and applications. *Food Chem X* **18**, 100684 (2023).

30. Ashaolu, T. J. Nanoemulsions for health, food, and cosmetics: a review. *Environ Chem Lett* **19**, 3381 (2021).

31. Bayda, S., Adeel, M., Tuccinardi, T., Cordani, M. & Rizzolio, F. The history of nanoscience and nanotechnology: From chemical-physical applications to nanomedicine. *Molecules* **25**, (2020).

32. Sung, H. *et al.* Global Cancer Statistics 2020: GLOBOCAN Estimates of Incidence and Mortality Worldwide for 36 Cancers in 185 Countries. *CA Cancer J Clin* **71**, 209–249 (2021).

33. The two directions of cancer nanomedicine. *Nature Nanotechnology 2019 14:12* **14**, 1083–1083 (2019).

34. Barenholz, Y. Doxil® — The first FDA-approved nano-drug: Lessons learned. *Journal of Controlled Release* **160**, 117–134 (2012).

35. Giri, P. M., Banerjee, A. & Layek, B. A Recent Review on Cancer Nanomedicine. *Cancers (Basel)* **15**, (2023).

36. Kundranda, M. N. & Niu, J. Albumin-bound paclitaxel in solid tumors: clinical development and future directions. *Drug Des Devel Ther* **9**, 3767 (2015).

37. Miele, E., Spinelli, G. P., Miele, E., Tomao, F. & Tomao, S. Albumin-bound formulation of paclitaxel (Abraxane® ABI-007) in the treatment of breast cancer. *Int J Nanomedicine* **4**, 99 (2009).

38. Krauss, A. C. *et al.* FDA approval summary: (daunorubicin and cytarabine) liposome for injection for the treatment of adults with high-risk acute myeloid leukemia. *Clinical Cancer Research* **25**, 2685–2690 (2019).

39. Lancet, J. E. *et al.* CPX-351 (cytarabine and daunorubicin) Liposome for Injection Versus Conventional Cytarabine Plus Daunorubicin in Older Patients With Newly Diagnosed Secondary Acute Myeloid Leukemia. *Journal of Clinical Oncology* **36**, 2684 (2018).

40. Nirmala, M. J. *et al.* Cancer nanomedicine: a review of nano-therapeutics and challenges ahead. *RSC Adv* **13**, 8606 (2023).

41. Bouzo, B. L., Calvelo, M., Martín-Pastor, M., García-Fandiño, R. & de La Fuente, M. In Vitro- In Silico Modeling Approach to Rationally Designed Simple and Versatile Drug Delivery Systems. *Journal of Physical Chemistry B* **124**, 5788–5800 (2020).

42. de la Fuente, M., López-López, R., Bouzo, B. L., Vázquez-Ríos, A. J. & Alonso-Nocelo, M. Nanosystems as selective vehicles, WO/2019/138139. (2019).

43. Bidan, N. *et al.* Before in vivo studies: In vitro screening of sphingomyelin nanosystems using a relevant 3D multicellular pancreatic tumor spheroid model. *Int J Pharm* **617**, (2022).

44. Saraiva, S. M. *et al.* Edelfosine nanoemulsions inhibit tumor growth of triple negative breast cancer in zebrafish xenograft model. *Sci Rep* **11**, (2021).

45. Cascallar, M. *et al.* Zebrafish as a platform to evaluate the potential of lipidic nanoemulsions for gene therapy in cancer. *Front Pharmacol* **13**, 4602 (2022).

46. Lores, S. *et al.* Effectiveness of a novel gene nanotherapy based on putrescine for cancer treatment. *Biomater Sci* **11**, 4210–4225 (2023).

47. Masoumi, F. *et al.* Modulation of Colorectal Tumor Behavior via lncRNA TP53TG1-Lipidic Nanosystem. *Pharmaceutics* **13**, (2021).

48. Nagachinta, S., Bouzo, B. L., Vazquez-Rios, A. J., Lopez, R. & de la Fuente, M. Sphingomyelin-based nanosystems (SNs) for the development of anticancer miRNA therapeutics. *Pharmaceutics* **12**, (2020).

49. Gadekar, V. *et al.* Nanomedicines accessible in the market for clinical interventions. *Journal of Controlled Release* **330**, 372–397 (2021).

50. Park, H., Otte, A. & Park, K. Evolution of Drug Delivery Systems: From 1950 to 2020 and Beyond. *J Control Release* **342**, 53 (2022).

51. Farjadian, F. *et al.* Nanopharmaceuticals and nanomedicines currently on the market: challenges and opportunities. *Nanomedicine* **14**, 93 (2019).

52. Corrò, C., Novellasdemunt, L. & Li, V. S. W. Making Cell Culture More Physiological: A brief history of organoids. *Am J Physiol Cell Physiol* **319**, C151 (2020).

53. Sieber, S. *et al.* Zebrafish as a preclinical in vivo screening model for nanomedicines. *Adv Drug Deliv Rev* **151–152**, 152–168 (2019).

54. Nascimento-Gonçalves, E., Ferreira, R., Oliveira, P. A. & Colaço, B. J. A. An Overview of Current Alternative Models for Use in the

Context of Prostate Cancer Research. *Altern Lab Anim* **48**, 58–69 (2020).

55. Lewis, D. I. Animal experimentation: Implementation and application of the 3Rs. *Emerg Top Life Sci* **3**, 675–679 (2019).

56. Duval, K. *et al.* Modeling physiological events in 2D vs. 3D cell culture. *Physiology* **32**, 266–277 (2017).

57. Ishiguro, T. *et al.* Tumor-derived spheroids: Relevance to cancer stem cells and clinical applications. *Cancer Sci* **108**, 283 (2017).

58. Habanjar, O., Diab-Assaf, M., Caldefie-Chezet, F. & Delort, L. 3D Cell Culture Systems: Tumor Application, Advantages, and Disadvantages. *Int J Mol Sci* **22**, (2021).

59. Decarli, M. C. *et al.* Cell spheroids as a versatile research platform: formation mechanisms, high throughput production, characterization and applications. *Biofabrication* **13**, (2021).

60. Giusti, S. *et al.* A novel dual-flow bioreactor simulates increased fluorescein permeability in epithelial tissue barriers. **9**, 1175–1184 (2014).

61. Carton, F. & Malatesta, M. In Vitro Models of Biological Barriers for Nanomedical Research. *Int J Mol Sci* **23**, 8910 (2022).

62. Collins, T. *et al.* Spheroid-on-chip microfluidic technology for the evaluation of the impact of continuous flow on metastatic potential in cancer models in vitro. *Biomicrofluidics* **15**, 44103 (2021).

63. Zanoni, M., Pignatta, S., Arienti, C., Bonafè, M. & Tesei, A. Anticancer drug discovery using multicellular tumor spheroid models. *Expert Opin Drug Discov* **14**, 289–301 (2019).

64. Jensen, C. & Teng, Y. Is It Time to Start Transitioning From 2D to 3D Cell Culture? *Front Mol Biosci* **7**, 33 (2020).

65. Gunti, S., Hoke, A. T. K., Vu, K. P. & London, N. R. Organoid and Spheroid Tumor Models: Techniques and Applications. *Cancers (Basel)* **13**, 1–18 (2021).

66. Gilazieva, Z., Ponomarev, A., Rutland, C., Rizvanov, A. & Solovyeva, V. Promising Applications of Tumor Spheroids and Organoids for Personalized Medicine. *Cancers (Basel)* **12**, 1–19 (2020).

67. Kaur, S., Kaur, I., Rawal, P., Tripathi, D. M. & Vasudevan, A. Non-matrigel scaffolds for organoid cultures. *Cancer Lett* **504**, 58–66 (2021).

68. Benton, G., Arnaoutova, I., George, J., Kleinman, H. K. & Koblinski, J. Matrigel: From discovery and ECM mimicry to assays and models for cancer research. *Adv Drug Deliv Rev* **79**, 3–18 (2014).

69. Lelièvre, S. A., Kwok, T. & Chittiboyina, S. Architecture in 3D cell culture: An essential feature for in vitro toxicology. *Toxicology in Vitro* **45**, 287–295 (2017).

70. Ravi, M., Paramesh, V., Kaviya, S. R., Anuradha, E. & Paul Solomon, F. D. 3D cell culture systems: Advantages and applications. *J Cell Physiol* **230**, 16–26 (2015).

71. Jensen, C. & Teng, Y. Is It Time to Start Transitioning From 2D to 3D Cell Culture? *Front Mol Biosci* **7**, 33 (2020).

72. Mó, I. *et al.* The importance of spheroids in analyzing nanomedicine efficacy. *Nanomedicine* **15**, 1513–1525 (2020).

73. McCarthy, B., Cudykier, A., Singh, R., Levi-Polyachenko, N. & Soker, S. Semiconducting polymer nanoparticles for photothermal ablation of colorectal cancer organoids. *Sci Rep* **11**, 1532 (2021).

74. Tchoryk, A. *et al.* Penetration and uptake of nanoparticles in 3D tumor spheroids. *Bioconjug Chem* **30**, 1371–1384 (2019).

75. Siemer, S. *et al.* Targeting Cancer Chemotherapy Resistance by Precision Medicine-Driven Nanoparticle-Formulated Cisplatin. *ACS Nano* **15**, 18541–18556 (2021).

76. Idrisova, K. F., Simon, H. U. & Gomzikova, M. O. Role of Patient-Derived Models of Cancer in Translational Oncology. *Cancers (Basel)* **15**, (2023).

77. Sun, W. *et al.* Organ-on-a-Chip for Cancer and Immune Organs Modeling. *Adv Healthc Mater* **8**, e1801363 (2019).

78. Palzer, J. *et al.* Magnetic Fluid Hyperthermia as Treatment Option for Pancreatic Cancer Cells and Pancreatic Cancer Organoids. *Int J Nanomedicine* **16**, 2965 (2021).

79. Hofmann, S., Cohen-Harazi, R., Maizels, Y. & Koman, I. Patient-derived tumor spheroid cultures as a promising tool to assist personalized therapeutic decisions in breast cancer. *Transl Cancer Res* **11**, 134–147 (2022).

80. Ma, C., Peng, Y., Li, H. & Chen, W. Organ-on-a-Chip: A new paradigm for drug development. *Trends Pharmacol Sci* **42**, 119 (2021).

81. Wu, Q. *et al.* Organ-on-a-chip: Recent breakthroughs and future prospects. *Biomed Eng Online* **19**, 1–19 (2020).

82. Regmi, S., Poudel, C., Adhikari, R. & Luo, K. Q. Applications of Microfluidics and Organ-on-a-Chip in Cancer Research. *Biosensors (Basel)* **12**, (2022).

83. Banh, L., Cheung, K. K., Chan, M. W. Y., Young, E. W. K. & Viswanathan, S. Advances in organ-on-a-chip systems for modelling joint tissue and osteoarthritic diseases. *Osteoarthritis Cartilage* **30**, 1050–1061 (2022).

84. Arjmand, B. *et al.* Organ on a Chip: A Novel in vitro Biomimetic Strategy in Amyotrophic Lateral Sclerosis (ALS) Modeling. *Front Neurol* **12**, 788462 (2021).

85. Leung, C. M. *et al.* A guide to the organ-on-a-chip. *Nature Reviews Methods Primers 2022 2:1* **2**, 1–29 (2022).

86. Campbell, S. B. *et al.* Beyond Polydimethylsiloxane: Alternative Materials for Fabrication of Organ-on-a-Chip Devices and Microphysiological Systems. *ACS Biomater Sci Eng* **7**, 2880–2899 (2021).

87. Ko, J., Park, D., Lee, S., Gumuscu, B. & Jeon, N. L. Engineering Organ-on-a-Chip to Accelerate Translational Research. *Micromachines (Basel)* **13**, (2022).

88. Tajeddin, A. & Mustafaoglu, N. Design and Fabrication of Organ-on-Chips: Promises and Challenges. *Micromachines (Basel)* **12**, (2021).

89. Yu, F., Hunziker, W. & Choudhury, D. Engineering microfluidic organoid-on-a-chip platforms. *Micromachines (Basel)* **10**, (2019).

90. Collins, T. *et al.* Spheroid-on-chip microfluidic technology for the evaluation of the impact of continuous flow on metastatic potential in cancer models in vitro. *Biomicrofluidics* **15**, 44103 (2021).

91. Sobrino, A. *et al.* 3D microtumors in vitro supported by perfused vascular networks. *Sci Rep* **6**, (2016).

92. Luque-González, M. A., Reis, R. L., Kundu, S. C. & Caballero, D. Human Microcirculation-on-Chip Models in Cancer Research: Key Integration of Lymphatic and Blood Vasculatures. *Adv Biosyst* **4**, (2020).

93. Aleman, J. & Skardal, A. A multi-site metastasis-on-a-chip microphysiological system for assessing metastatic preference of cancer cells. *Biotechnol Bioeng* **116**, 936–944 (2019).

94. Del Piccolo, N. *et al.* Tumor-on-chip modeling of organ-specific cancer and metastasis. *Adv Drug Deliv Rev* **175**, (2021).

95. Mollica, H., Palomba, R., Primavera, R. & Decuzzi, P. Two-Channel Compartmentalized Microfluidic Chip for Real-Time Monitoring of the Metastatic Cascade. *ACS Biomater Sci Eng* **5**, 4834–4843 (2019).

96. Sontheimer-Phelps, A., Hassell, B. A. & Ingber, D. E. Modelling cancer in microfluidic human organs-on-chips. *Nat Rev Cancer* **19**, 65–81 (2019).

97. Kang, S., Park, S. E. & Huh, D. D. Organ-on-a-chip technology for nanoparticle research. *Nano Converg* **8**, (2021).

98. Zhang, Y. S., Zhang, Y. N. & Zhang, W. Cancer-on-a-chip systems at the frontier of nanomedicine. *Drug Discov Today* **22**, 1392 (2017).

99. Peng, B. *et al.* In Situ Surface Modification of Microfluidic Blood-Brain-Barriers for Improved Screening of Small Molecules and Nanoparticles. *ACS Appl Mater Interfaces* **12**, 56753–56766 (2020).

100. Chen, X., Zhang, Y. S., Zhang, X. & Liu, C. Organ-on-a-chip platforms for accelerating the evaluation of nanomedicine. *Bioact Mater* **6**, 1012–1027 (2021).

101. Ran, R. *et al.* A Microfluidic Tumor-on-a-Chip for Assessing Multifunctional Liposomes' Tumor Targeting and Anticancer Efficacy. *Adv Healthc Mater* **8**, (2019).

102. Vu, M. N. *et al.* Rapid Assessment of Nanoparticle Extravasation in a Microfluidic Tumor Model. *ACS Appl Nano Mater* **2**, 1844–1856 (2019).

103. Zheng, F., Xiao, Y., Liu, H., Fan, Y. & Dao, M. Patient-Specific Organoid and Organ-on-a-Chip: 3D Cell-Culture Meets 3D Printing and Numerical Simulation. *Adv Biol* **5**, (2021).

104. Jodat, Y. A. *et al.* Human-Derived Organ-on-a-Chip for Personalized Drug Development. *Curr Pharm Des* **24**, 5471–5486 (2019).

105. Haque, M. R. *et al.* Patient-derived pancreatic cancer-on-a-chip recapitulates the tumor microenvironment. *Microsyst Nanoeng* **8**, (2022).

106. Shirure, V. S. *et al.* Tumor-on-a-chip platform to investigate progression and drug sensitivity in cell lines and patient-derived organoids. *Lab Chip* **18**, 3687–3702 (2018).

107. Delvecchio, C., Tiefenbach, J. & Krause, H. M. The Zebrafish: A powerful platform for in vivo, HTS drug discovery. *Assay Drug Dev Technol* **9**, 354–361 (2011).

108. Lieschke, G. J. & Currie, P. D. Animal models of human disease: Zebrafish swim into view. *Nat Rev Genet* **8**, 353–367 (2007).

109. Zon, L. I. Zebrafish: A new model for human disease. *Genome Res* **9**, 99–100 (1999).

110. Howe, K. *et al.* The zebrafish reference genome sequence and its relationship to the human genome. *Nature* **496**, 498–503 (2013).

111. Sieber, S. *et al.* Zebrafish as a preclinical in vivo screening model for nanomedicines. *Adv Drug Deliv Rev* **151–152**, 152–168 (2019).

112. Zhao, S., Huang, J. & Ye, J. A fresh look at zebrafish from the perspective of cancer research. *Journal of Experimental and Clinical Cancer Research* **34**, (2015).

113. Lam, S. H., Chua, H. L., Gong, Z., Lam, T. J. & Sin, Y. M. Development and maturation of the immune system in zebrafish, Danio rerio: A gene expression profiling, in situ hybridization and immunological study. *Dev Comp Immunol* **28**, 9–28 (2004).

114. Zon, L. I. & Peterson, R. The new age of chemical screening in Zebrafish. *Zebrafish* **7**, 1 (2010).

115. Raby, L., Völkel, P., Le Bourhis, X. & Angrand, P. O. Genetic engineering of zebrafish in cancer research. *Cancers (Basel)* **12**, 1–36 (2020).

116. Spitsbergen, J. M. *et al.* Neoplasia in zebrafish (Danio rerio) treated with 7,12-dimethylbenz[a]anthracene by two exposure routes at different developmental stages. *Toxicol Pathol* **28**, 705–715 (2000).

117. Fujisawa, K. *et al.* Evidence for a role of the transcriptional regulator Maid in tumorigenesis and aging. *PLoS One* **10**, 1–17 (2015).

118. Mizgireuv, I. V., Majorova, I. G., Gorodinskaya, V. M., Khudoley, V. V. & Revskoy, S. Y. Carcinogenic Effect of N-Nitrosodimethylamine on Diploid and Triploid Zebrafish (Danio rerio). *Toxicol Pathol* **32**, 514–518 (2016).

119. Renshaw, S. A. *et al.* A transgenic zebrafish model of neutrophilic inflammation. *Blood* **108**, 3976–3978 (2006).

120. Ellett, F., Pase, L., Hayman, J. W., Andrianopoulos, A. & Lieschke, G. J. mpeg1 promoter transgenes direct macrophage-lineage expression in zebrafish. *Blood* **117**, e49 (2011).

121. Lawson, N. D. & Weinstein, B. M. In vivo imaging of embryonic vascular development using transgenic zebrafish. *Dev Biol* **248**, 307–318 (2002).

122. Park, S. W. *et al.* Oncogenic KRAS Induces Progenitor Cell Expansion and Malignant Transformation in Zebrafish Exocrine Pancreas. *Gastroenterology* **134**, 2080–2090 (2008).

123. Michailidou, C. *et al.* Dissecting the roles of Raf- and PI3K-signalling pathways in melanoma formation and progression in a zebrafish model. *DMM Disease Models and Mechanisms* **2**, 399–411 (2009).

124. Patton, E. E. *et al.* BRAF mutations are sufficient to promote nevi formation and cooperate with p53 in the genesis of melanoma. *Current Biology* **15**, 249–254 (2005).

125. Nasevicius, A. & Ekker, S. C. Effective targeted gene 'knockdown' in zebrafish. *Nat Genet* **26**, 216–220 (2000).

126. Wienholds, E. *et al.* Efficient target-selected mutagenesis in zebrafish. *Genome Res* **13**, 2700–2707 (2003).

127. Berghmans, S. *et al.* tp53 mutant zebrafish develop malignant peripheral nerve sheath tumors. *Proc Natl Acad Sci U S A* **102**, 407 (2005).

128. Faucherre, A., Taylor, G. S., Overvoorde, J., Dixon, J. E. & Den Hertog, J. Zebrafish pten genes have overlapping and non-redundant functions in tumorigenesis and embryonic development. *Oncogene* **27**, 1079–1086 (2008).

129. Choorapoikayil, S., Kuiper, R. V., De Bruin, A. & Den Hertog, J. Haploinsufficiency of the genes encoding the tumor suppressor Pten predisposes zebrafish to hemangiosarcoma. *DMM Disease Models and Mechanisms* **5**, 241–247 (2012).

130. Haramis, A. P. G. *et al.* Adenomatous polyposis coli-deficient zebrafish are susceptible to digestive tract neoplasia. *EMBO Rep* **7**, 444–449 (2006).

131. Gjini, E. *et al.* A Zebrafish Model of Myelodysplastic Syndrome Produced through tet2 Genomic Editing . *Mol Cell Biol* **35**, 789–804 (2015).

132. Oppel, F. *et al.* Loss of atrx cooperates with p53-deficiency to promote the development of sarcomas and other malignancies. *PLoS Genet* **15**, (2019).

133. Moore, J. C. & Langenau, D. M. Allograft cancer cell transplantation in zebrafish. in *Advances in Experimental Medicine and Biology* vol. 916 265–287 (Springer, Cham, 2016).

134. Nicoli, S. & Presta, M. The zebrafish/tumor xenograft angiogenesis assay. *Nat Protoc* **2**, 2918–2923 (2007).

135. Veinotte, C. J., Dellaire, G. & Berman, J. N. Hooking the big one: The potential of zebrafish xenotransplantation to reform cancer drug screening in the genomic era. *DMM Disease Models and Mechanisms* **7**, 745–754 (2014).

136. Mercatali, L. *et al.* Development of a patient-derived xenograft (PDX) of breast cancer bone metastasis in a Zebrafish model. *Int J Mol Sci* **17**, (2016).

137. Khan, N., Mahajan, N. K., Sinha, P. & Jayandharan, G. R. An efficient method to generate xenograft tumor models of acute myeloid leukemia and hepatocellular carcinoma in adult zebrafish. *Blood Cells Mol Dis* **75**, 48–55 (2019).

138. Gómez-Abenza, E. *et al.* Zebrafish modeling reveals that SPINT1 regulates the aggressiveness of skin cutaneous melanoma and its crosstalk with tumor immune microenvironment. *J Exp Clin Cancer Res* **38**, 405 (2019).

139. Tang, Q. *et al.* Optimized cell transplantation using adult rag2 mutant zebrafsh. *Nat Methods* **11**, 821–824 (2014).

140. Yan, C. *et al.* Visualizing Engrafted Human Cancer and Therapy Responses in Immunodeficient Zebrafish. *Cell* **177**, 1903-1914.e14 (2019).

141. Lee, L. M. J., Seftor, E. A., Bonde, G., Cornell, R. A. & Hendrix, M. J. C. The fate of human malignant melanoma cells transplanted into zebrafish embryos: Assessment of migration and cell division in the absence of tumor formation. *Developmental Dynamics* **233**, 1560–1570 (2005).

142. Cabezas-Sáinz, P., Pensado-López, A., Sáinz, B. & Sánchez, L. Modeling Cancer Using Zebrafish Xenografts: Drawbacks for Mimicking the Human Microenvironment. *Cells* **9**, (2020).

143. He, S. *et al.* Neutrophil-mediated experimental metastasis is enhanced by VEGFR inhibition in a zebrafish xenograft model. *Journal of Pathology* **227**, 431–445 (2012).

144. Roh-Johnson, M. *et al.* Macrophage-Dependent Cytoplasmic Transfer during Melanoma Invasion In Vivo. *Dev Cell* **43**, 549-562.e6 (2017).

145. Hill, D., Chen, L., Snaar-Jagalska, E. & Chaudhry, B. Embryonic zebrafish xenograft assay of human cancer metastasis. *F1000Res* **7**, (2018).

146. Britto, D. D. *et al.* Macrophages enhance Vegfa-driven angiogenesis in an embryonic zebrafish tumour xenograft model. *DMM Disease Models and Mechanisms* **11**, (2018).

147. Peterson, R., Link, B., Dowling, J. & Schreiber, S. Small molecule developmental screens reveal the logic and timing of vertebrate development. *Proceedings of the national academy of sciences* **97**, 12965–12969 (2000).

148. Gianoncelli, A. *et al.* Adrenocortical Carcinoma Xenograft in Zebrafish Embryos as a Model To Study the In Vivo Cytotoxicity of Abiraterone Acetate. *Endocrinology* **160**, 2620–2629 (2019).

149. Cabezas-Sainz, P. *et al.* Improving zebrafish embryo xenotransplantation conditions by increasing incubation temperature and establishing a proliferation index with ZFtool. *BMC Cancer* **18**, 3 (2018).

150. Cornet, C., Dyballa, S., Terriente, J. & Di Giacomo, V. ZeOncoTest: Refining and Automating the Zebrafish Xenograft Model for Drug Discovery in Cancer. *Pharmaceuticals* **13**, 1 (2019).

151. ZeClinics. Powering discovery with Zebrafish. https://www.zeclinics.com/ (2020).

152. Haque, E. & Ward, A. C. Zebrafish as a model to evaluate nanoparticle toxicity. *Nanomaterials* **8**, 1–18 (2018).

153. Chakraborty, C., Sharma, A. R., Sharma, G. & Lee, S. S. Zebrafish: A complete animal model to enumerate the nanoparticle toxicity. *J Nanobiotechnology* **14**, 1–13 (2016).

154. Ramachandran, R. *et al.* Anticancer activity of biologically synthesized silver and gold nanoparticles on mouse myoblast cancer cells and their toxicity against embryonic zebrafish. *Materials Science and Engineering C* **73**, 674–683 (2017).

155. Calienni, M. N. *et al.* Zebrafish (Danio rerio) model as an early stage screening tool to study the biodistribution and toxicity profile of doxorubicin-loaded mixed micelles. *Toxicol Appl Pharmacol* **357**, 106–114 (2018).

156. Wu, Y. *et al.* Cancer-targeted and intracellular delivery of Bcl-2-converting peptide with functional macroporous silica nanoparticles for biosafe treatment. *Materials Science and Engineering C* **108**, 110386 (2020).

157. Gundersen, E. T. *et al.* Repurposing chlorpromazine for anti-leukaemic therapy by nanoparticle encapsulation. *Int J Pharm* **612**, 121296 (2022).

158. Chang, H. *et al.* Predicting the in vivo accumulation of nanoparticles in tumor based on in vitro macrophage uptake and circulation in zebrafish. *Journal of Controlled Release* **244**, 205–213 (2016).

159. Askes, S. H. C. *et al.* Dynamics of dual-fluorescent polymersomes with durable integrity in living cancer cells and zebrafish embryos. *Biomaterials* **168**, 54–63 (2018).

160. Gong, C. *et al.* Improving antiangiogenesis and anti-tumor activity of curcumin by biodegradable polymeric micelles. *Biomaterials* **34**, 1413–1432 (2013).

161. Wang, Q. *et al.* Preparation and properties of biocompatible PS-PEG/calcium phosphate nanospheres. *Nanotoxicology* **9**, 190–200 (2015).

162. Crecente-Campo, J. *et al.* The size and composition of polymeric nanocapsules dictate their interaction with macrophages and biodistribution in zebrafish. *Journal of Controlled Release* **308**, 98–108 (2019).

163. Evensen, L. *et al.* Zebrafish as a model system for characterization of nanoparticles against cancer. *Nanoscale* **8**, 862–877 (2016).

164. Mimeault, M. & Batra, S. K. Emergence of zebrafish models in oncology for validating novel anticancer drug targets and nanomaterials. *Drug Discov Today* **18**, 128–140 (2013).

165. Liu, H. na *et al.* Delivery of mitochondriotropic doxorubicin derivatives using self-assembling hyaluronic acid nanocarriers in doxorubicin-resistant breast cancer. *Acta Pharmacol Sin* **39**, 1681–1692 (2018).

166. Gao, X. *et al.* Improving the anti-ovarian cancer activity of docetaxel with biodegradable self-assembly micelles through various evaluations. *Biomaterials* **53**, 646–658 (2015).

167. Xie, Z. *et al.* Targeting tumor hypoxia with stimulus-responsive nanocarriers in overcoming drug resistance and monitoring anticancer efficacy. *Acta Biomater* **71**, 351–362 (2018).

168. Deng, S. *et al.* Biodegradable polymeric micelle-encapsulated doxorubicin suppresses tumor metastasis by killing circulating tumor cells. *Nanoscale* **7**, 5270–5280 (2015).

169. Zhou, Q. *et al.* Co-delivery nanoparticle to overcome metastasis promoted by insufficient chemotherapy. *Journal of Controlled Release* **275**, 67–77 (2018).

170. Fior, R. *et al.* Single-cell functional and chemosensitive profiling of combinatorial colorectal therapy in zebrafish xenografts. *Proc Natl Acad Sci U S A* **114**, E8234–E8243 (2017).

171. Marques, I. J. *et al.* Metastatic behaviour of primary human tumours in a zebrafish xenotransplantation model. *BMC Cancer* **9**, 128 (2009).

172. Al-Samadi, A. *et al.* PCR-based zebrafish model for personalised medicine in head and neck cancer. *J Transl Med* **17**, 1–6 (2019).

173. Bentley, V. L. *et al.* Focused chemical genomics using zebrafish xenotransplantation as a pre-clinical therapeutic platform for T-cell acute lymphoblastic leukemia. *Haematologica* **100**, 70–76 (2015).

174. Liverani, C. *et al.* Innovative approaches to establish and characterize primary cultures: An ex vivo 3D system and the zebrafish model. *Biol Open* **6**, 133–140 (2017).

175. Peverelli, E. *et al.* Dopamine receptor type 2 (DRD2) and somatostatin receptor type 2 (SSTR2) agonists are effective in inhibiting proliferation of progenitor/stem-like cells isolated from nonfunctioning pituitary tumors. *Int J Cancer* **140**, 1870–1880 (2017).

176. Usai, A. *et al.* A model of a zebrafish avatar for co-clinical trials. *Cancers (Basel)* **12**, (2020).

177. Wu, J. Q. *et al.* Patient-derived xenograft in zebrafish embryos: A new platform for translational research in gastric cancer. *Journal of Experimental and Clinical Cancer Research* **36**, 160 (2017).

178. Xu, Z. *et al.* Apatinib enhances chemosensitivity of gastric cancer to paclitaxel and 5-fluorouracil. *Cancer Manag Res* **11**, 4905–4915 (2019).

179. Costa, B. *et al.* Developments in zebrafish avatars as radiotherapy sensitivity reporters — towards personalized medicine. *EBioMedicine* **51**, 1–12 (2020).

180. di Franco, G. *et al.* Use of zebrafish embryos as avatar of patients with pancreatic cancer: A new xenotransplantation model towards personalized medicine. *World J Gastroenterol* **26**, 2792–2809 (2020).

HYPOTHESIS

HYPOTHESIS

The principal hypothesis of this doctoral thesis is that "the clinical translation of lipid nanomedicines can be improved by implementing static and non-static 3D *in vitro* platforms, as well as alternative *in vivo* models such as zebrafish embryos, for a more comprehensive *in vitro* and *in vivo* evaluation".

This main hypothesis can be divided in the subsequent partial hypothesis (H):

H1. 3D spheroids can be a reliable study model to evaluate the behavior and therapeutic effect of nanomedicines for cancer treatment.

H2. Non-static organ-on-a-chip microfluidic devices can be potential platforms for assessing the behavior of functionalized sphingomyelin nanosystems targeted to specific cancer cell subpopulations.

H3. Zebrafish embryos can be useful for the *in vivo* evaluation of innovative cancer gene nanotherapies.

OBJECTIVES

OBJECTIVES

Based on the described hypothesis, the main objective of this thesis is the application of advanced *in vitro* and alternative *in vivo* models, based on 3D spheroids, organ-on-a-chip microfluidic devices and zebrafish embryos, for the preclinical evaluation of sphingomyelin nanoemulsions for cancer treatment.

This main objective can be divided in these partial objectives (O):

CHAPTER I

O1. To efficiently encapsulate the hydrophobic drug disulfiram, into sphingomyelin nanoemulsions, and demonstrate the potential of the formulation for non-small cell lung cancer stem cells treatment.

O2. To prove the value of static 3D *in vitro* models to evaluate the internalization and treatment efficacy of the developed nanoformulations.

CHAPTER II

O3. To surface-decorate sphingomyelin nanosystems with specific aptamers, for targeted cancer therapy to TAS1R3 positive lung cancer cells.

O4. To develop non-static microfluidic organ-on-a-chip models for *in vitro* assessment of the ability of the surface-decorated nanoformulations to reach and interact with the targeted cells.

CHAPTER III

O5. To prove the versatility of sphingomyelin nanosystems for cancer gene therapy.

O6. To assess the stability, behavior, and interactions of the developed gene nanomedicines *in vivo*.

O7. To prove the key role of zebrafish embryos as an alternative *in vivo* model to evaluate the potential of gene therapies based on nanomedicine.

CHAPTER I

Evaluation of sphingomyelin-based nanosystems loaded with DSF in 3D cell culture models of non-small cell lung cancer

Evaluation of sphingomyelin-based nanosystems loaded with DSF in 3D cell culture models of non-small cell lung cancer

ABSTRACT

Cancer is an emergency worldwide and, specifically, lung cancer is one of the most relevant, in terms of mortality and prevalence. Non-small cell lung cancer (NSCLC) is the predominant among the lung cancer subtypes, reaching the 85%. Its treatment is still a challenge, and new specific therapies are needed. In this work, we propose the use of sphingomyelin nanosystems (SNs), loaded with disulfiram (DSF), as a potential new treatment for NSCLC. For assessment of the potential of the proposed therapy, DSF-loaded SNs (SNs-DSF) were assessed in 3D models that better represent the characteristics of the tumor. In addition, spheroids have a cancer stem cells (CSCs) like phenotype, and previous studies indicate that DSF is specifically active for treating CSCs.

SNs-DSF were developed and fully characterized for their physicochemical properties. Results proved the capacity of SNs to penetrate into the spheroids, reaching their inner nucleus, a key factor for the correct treatment of the whole tumor mass, and to efficiently deliver the encapsulated drug. Indeed, a decrease in the 50% inhibitory concentration (IC50) of DSF was observed when delivered in SNs.

In conclusion, the obtained results demonstrated the potential of DSF-loaded SNs as a new treatment in NSCLC.

1. INTRODUCTION

Cancer is an actual health emergency worldwide, reaching in 2020 more than 19 million of new cases and being the cause of 10 million deaths. Leading the mortality with a 18.0% among cancer-related deaths, lung cancer is also positioned as the second cancer type in overall incidence, with a 11.4% of the new cases [1]. Lung cancer is divided in two main types, non-small cell lung cancer (NSCLC) and small cell lung cancer (SCLC), representing the 85% and 15% cases, respectively [2]. In the case of NSCLC, it is formed by three subtypes: adenocarcinoma, squamous cell carcinoma and large cell carcinoma [3–5].

NSCLC is commonly detected in advanced stages, which normally complicates the treatment and prognosis [5]. In addition, actual therapies for NSCLC are based on radiotherapy, chemotherapy, immunotherapy, and surgery, depending on the typology and the stage of each case [6]. Even though the upgrading of the treatments, such as the personalized medicine, it is still necessary the development of novel therapies able to decrease the mortality and to improve the patients' life quality. An interesting alternative is drug repositioning, based on evaluating the potential of approved drugs for the application in other illnesses that are not the principal target [7,8]. This alternative has the advantage of reducing the time needed to develop new treatments [9]. In this sense, a good example of repurposed drug for cancer therapy is disulfiram (DSF).

DSF, commercially known as Antabuse®, has been used for alcoholism treatment since 1951, when US Food and Drug Administration (FDA) approved it [10–12]. However, its therapeutic effect as an anti-cancer treatment

was observed in 1977, when Dr. Lewison described the first case of cancer remission due to the use of DSF [11,13]. Afterwards, its potential for cancer therapy was observed in numerous types of cancers, such as non-small cell lung cancer (NSCLC) [14–16], breast cancer [17–19] or pancreatic [20,21]; among others [22–26]. Furthermore, and very importantly, the work developed by Amado Labrador *et al.* demonstrated, after a screening of two commercial chemical libraries (Myria and Prestwick) with more than 10.000 compounds, the cytotoxic potential of DSF for NSCLC cancer stem cells (CSCs) treatment [27]. This is particularly relevant as CSCs are related to tumor progression, drug resistance, metastasis and recurrence, thus it is important to develop specific treatments for them [28–30].

The mechanism of action is not well understood yet. However, several hypotheses have been described such as stress generation via ROS, inhibition of superoxide dismutase enzyme or activation of specific protein kinase pathways [31]. DSF is known for inhibiting P-glycoprotein as well as suppressing the activation of NF-kB, therefore contributing to reverse some resistance to anti-cancer drugs [32].

DSF is a promising alternative to improve NSCLC treatment, however, it presents the disadvantage of being unstable in circulation, and having a small half-life [31]. In this sense, nanomedicine plays a key role due to the fact that nanosystems can transport and protect drugs and biomolecules in the organism until they reach their target cell [33]. In the case of DSF, several studies have been reported, including polymeric nanoparticles [34,35], micelles [28,36], nanocrystals [37] and lipid-based nanoparticles [38,39]. For instance, Banarjee *et al.* reported the encapsulation of DSF in two subtypes of lipid-based formulations: i) the basic formulation composed of glycerides (Precirol ATO5,

soy lecithin) and oily (Labrafac Lipophile WL1349) excipients, along with Tween80, and ii) the basic formulation modified with Vitamin E-TPGS. Results showed lower 50% inhibitory concentration (IC50) values, enhance cellular uptake in MCF7 and 4T1 cell lines as well as improved *in vivo* anti-tumor 4T1 murine xenograft model mice for both formulations as compared to free DSF solution; with improved *in vitro* and i*n vivo* activity for the Vitamin E-TPGS modified formulation [39].

In our laboratory, we have previously developed innovative lipid nanosystems for cancer treatment, composed by sphingomyelin (SM) and vitamin E (VE), which make them biocompatible and biodegradable [40]. These versatile sphingomyelin nanosystems (SNs) allow the association of different biomolecules, such as miRNA, plasmids, and lncRNA[41–44], and radioisotopes and contrast agents for imaging applications [42,45–47]. Furthermore, hydrophobic drug encapsulation is allowed by the SNs oily core, which improves the treatment efficiency compared to the free drug [48,49]. In this respect, previous studies have demonstrated not only the efficient encapsulation of different anti-cancer drugs, but also an effective treatment [49–51]. Due to these precedents, SNs are an innovative alternative to carry DSF and improve its stability and half-life.

In order to evaluate these novel nanomedicines, it is necessary the use of proper *in vitro* models to efficiently replicate the tumor structure and environment. The traditional 2D cell cultures are widely used in cancer research, however, tumor environment and cellular interactions are not well represented in this model [52,53]. A suitable *in vitro* alternative is the spheroid, which mimics better not only the 3D structure of the tumor, but also the interactions, as well as, the drug sensitivity [52,54]. Taking into account this

information and aiming to evaluate the behavior and tumor interactions of our nanosystems, we chose spheroids as the *in vitro* model of this work.

A key point in the cancer evolution is the presence of CSCs. CSCs are a specific cell type which belong to the bulk tumor and present stem characteristics, such as the capacity of differentiation, self-renewal and plasticity [55–57]. CSCs were found in several cancer types, such as brain and pancreas, and have the ability to enter in a quiescent mode which is related with tumor resistance [58]. This fact makes CSCs an interesting target for NSCLC treatment [59]. CSCs population is enriched in 3D *in vitro* models, such as spheroids, which make of them a potential platform to evaluate anti-cancer treatments targeted to CSCs, such as DSF [60]. In this sense, spheroids are the ideal model to evaluate the DSF effect, due to its targeted effect in CSCs. In the previous work of Amado Labrador *et al.* about DSF as a potential NSCLC CSCs treatment, the main study model used was the spheroid, because of its potential to be a CSCs enriched model [27,58].

Taking all this into account, we propose here the development of SNs to carry the hydrophobic drug DSF and deliver it 3D NSCLC spheroids, as a strategy to evaluate a potential new therapy for NSCLC CSCs treatment.

2. MATERIALS AND METHODS

2.1 Materials

N-palmitoyl sphingomyelin-N-(Cyanine 5) (SM-Cy5) and 1,2-distearoyl-sn-glycero-3-phosphoethanolamine-N-[carboxy(polyethylene glycol)-2000] (sodium salt) DSPE-PEG(2000) Carboxylic Acid (PEG) were

provided by Avanti Polar Lipids (Birmingham, Alabama, USA). Non-essential amino acids (NEAA), Human fibroblast growth factor basic (bFGF), Human Epidermal growth factor (EGF), Penicillin-Streptomycin (P/S), dimethyl sulfoxide (DMSO, 99.7%), Roswell Park Memorial Institute (RPMI) 1640 Medium, Fetal Bovine Serum (FBS) and Dulbecco's Phosphate Buffered Saline (PBS), were purchased by Thermo Fisher Scientific (Whalham, Massachusetts, USA). Bovine Serum Albumin (BSA) was kindly provided by Biowest (Nuaillé, France). Ethanol (EtOH) analytical weight was purchased from VWR (Llinars del Vallés, Spain). Paraformaldehyde was obtained from IESMAT (Madrid, Spain). Disulfiram was provided by Labnet Biotécnica (Madrid, Spain). ITS + Premix Universal Culture Supplement was kindly provided by Cultek S. L. (Madrid, Spain). Sphingomyelin (SM) (Lipoid E SM) was obtained from Lipoid GmbH (Ludwigshafen, Germany). Vitamin E (VE) (DL-α-Tocopherol) were purchased from Merck Group (Darmstadt, Germany). Calcein AM and Propidium Iodide were acquired from Abcam (Cambridge, United Kingdom).

2.2 Cell culture

NCI-H1650 (CRL-5883™) non-small cell lung cancer cell line was purchased from the American Type Culture Collection (ATCC). Cells were cultured in RPMI 1640 medium supplemented with 10% FBS and 1% penicillin/streptomycin; and they were maintained at 37ºC with CO_2 5% and 95% relative humidity.

2.3 3D cell culture establishment

H1650 adherent cells were detached with Trypsin 1X for 7-8 minutes at 37 °C, previously washed with PBS. The cellular suspension was centrifuged at 1200 rpm for 5 minutes, the supernatant was discarded, and spheroids medium was added to the pellet, with the aim of eliminate FBS from the suspension. The sphere medium is composed by: RPMI 1640 medium, P/S (2%), NEAA (1/1000), BSA (0,4%), bFGF (20ng/µl), EGF (50ng/µl) and ITS (1/1000).

Ultra-low attachment (ULA) plates were used to seed cells in low density to form the spheroids.

3D static culture models of this thesis were performed in collaboration with the Molecular Oncology Laboratory of Fundación de Investigación del Hospital General Universitario de Valencia and the TRIAL Mixed Unit, Centro de Investigación Príncipe Felipe-Fundación para la Investigación del Hospital General Universitario de Valencia (Valencia, Spain).

2.4 Formulation and characterization of sphingomyelin nanosystems

SNs were prepared following the one-step ethanol injection method. Briefly, VE (5 mg), SM (0.5 mg), PEG (0.05 mg) and, in the case of the loaded SNs (SNs-DSF) also DSF (0.5 mg) (20 mg/mL EtOH stock), were dissolved in a total volume of one hundred microliters EtOH in the adequate ratio (%w/w) 1:0.1:0.01. This organic phase was injected to nine hundred microliters of ultrapure water, obtaining a 10% drug loading, with respect to

the amount of VE. Physicochemical characterization of size and homogeneity, Polydispersity Index (PDI), were performed using dynamic light scattering (DLS) measuring the samples previously diluted 1:10 in MilliQ water, using disposable microcuvettes (ZEN0040, Malvern Instruments). The surface charge, zeta potential (ZP) was measured by Laser Doppler anemometry (LDA), using a 1:40 diluted sample in MilliQ water and folded capillary cells cuvettes (DTS 1070, Malvern Instruments). This characterization was performed using a Zetasizer NanoZS® (Malvern Instrument Worcestershire, UK).

The stability of these formulations in cell culture media (RPMI; 10% FBS, 1% PenStrep RPMI; RPMI Spheroids; 30% Plasma in sodium chloride (NaCl)) was also evaluated by measuring particle size and polydispersity index (PdI) after 1, 4 and 24 h, in a 1:10 dilution.

2.5 Drug loading quantification of Sphingomyelin nanosystems

Disulfiram quantification was performed using High Performance Liquid Chromatography (HPLC) using a Reverse Phase C18 5 µm 100Å Luna Column and acetonitrile (ACN) and 0,01% Trifluoroacetic (TFA) MiliQ H2O gradient as mobile phase. The method is based on a 10-minute run at 1 mL/min with a solvent gradient detailed in the table below (Table 1):

Table 1. HPLC method followed for disulfiram quantification.

Time (minutes)	Phase A (ACN)	Phase B (0,01% TFA MilliQ)
1 - 3	50	50
3 - 5	80	20
5 - 7	90	10
7 - 8	80	20
8 - 10	50	50

SNs quantification was performed at two time points, 0 and 24h. For both time points, SNs were broken with methanol (MeOH) (1/20 dilution) to quantify the total amount of DSF present. For 24h samples, SNs were stored at 4ºC after formulation and the sample was retrieved from the upper part of the vial, so as to avoid taking any solid particles that might have precipitated. Upon HPLC injection, a calibration curve in 50:50 MilliQ:ACN was prepared, using 0,05 µg/mL and 0,5 µg/mL as Limit of Detection (LOD) and Limit of Quantification (LOQ) and additional points at 1, 10, 100 and 120 µg/mL. All points were prepared from the same DSF DMSO Stock at 1 mg/mL. Additionally, a different 100 ug/mL sample was prepared from a different 1 mg/mL DMSO Stock, so as to confirm the precise weighing. To calculate the encapsulation efficiency, the following equation was used: (Weight Encapsulated DSF / Weight Added DSF) * 100.

2.6 3D cellular uptake assay

Uptake assays were performed with the aim of evaluating the nanoemulsions internalization by the H1650 cells. Cells were seeded in ultra-low attachment 6-well plates with a final volume of 2 mL of medium and a

concentration of 10.000 cells/mL. After four days of incubation, Cy5-labelled nanosystems, with and without DSF (6,95 µg/mL) were added and incubated for different times, between 30 minutes and 6 hours. Making use of Cytospin™ 4 (Thermo Fisher Scientific, Massachusetts, USA), spheroids were attached to a slide before being fixed with 4% paraformaldehyde (PFA). Cell nuclei were stained with Hoechst 33342. Results were evaluated by confocal microscopy (Confocal microscope SP8, Leica, Wetzlar, Germany).

2.7 Efficacy of DSF-loaded SNs in CSCs

Cells were both 2D and 3D cultured in a final volume of 200 µL, in treated 96-well plates (5000 cell/well), in the first case, and in ultra-low attachment (7000 cell/well), in the second case. After 24 hours, different concentrations of DSF-loading SNs and free disulfiram were added, and their toxicity was evaluated 48 hours later.

An MTS (3-(4,5-dimethylthiazol-2-yl)-5-(3-carboxymethoxyphenyl)-2-(4-sulfophenyl)-2H-tetrazolium, inner salt) assay was carried out in both cell cultures to determine the differences in the cytotoxicity effect of DSF encapsulated and non-encapsulated in SNs. The results were analyzed with the Victor 3 plate reader (Perkin Elmer, Massachusetts, USA). The IC50 was calculated to determine the work concentration.

2.8 Viability and mortality assay

Calcein acetoxymethyl (Calcein AM) is widely used to label live cells, in the same way that propidium iodide (PI) is used to detect apoptotic cells [61,62]. For this reason, were the selected strategy to evaluate the cytotoxicity effect of the DSF, SNs and SNs-DSF.

H1650 cells were seeded in a 96-well plate with transparent flat bottom in a concentration of 7000 cell/well in a total volume of 200 µL. Spheroids were treated with 0.3 µM of DSF, encapsulated and non-encapsulated for 48 hours. After that, Calcein AM (2 µM) and PI (4 µM) were added to the spheres medium and were incubated for 30 minutes. Results were evaluated by confocal microscopy (Confocal microscope SP8, Leica, Wetzlar, Germany)

.

3. RESULTS AND DISCUSSION

3.1 Characterization of Sphingomyelin nanoemulsions

Despite the findings on anticancer activity, DSF is highly unstable in the acidic environment and systemic circulation [31,63]. Therefore, when the free drug, without a delivery vehicle, is administered the anticancer activity seems to be lost. For this reason, it is undeniable the need of designing new strategies to retain DSF's activity by protecting its integrity upon administration, as well as enhancing its tumor tissue uptake [64]. In this sense and as an example, Miao *et al.* proved *in vivo* the increasing in the half-life of DSF when it was encapsulated in micelles, confirming the potential of nanocarriers in the DSF-based treatment [65]. As earlier said, previous work in our lab has shown the potential of SNs to encapsulate small molecules [40,48–50].

Taking this into account, in this study, we propose the formulation of biodegradable and biocompatible SNs composed of VE, SM and PEG, loaded with the drug of interest, DSF at 10% of loading. These formulations were prepared following the ethanol injection method, consisting of a one-step and simple procedure based on the formation of nanoparticles upon injection of ethanolic phase to ultrapure water.

Results showed an average size below 150nm, which is similar to other DSF-encapsulated lipidic nanosystems, such as the lipidic emulsions developed by Chen *et al.*, among others [66,67]; and a great polydispersity index, around 0.2, at both 0 and 24 h measurement (Figure 1A). There were no relevant differences with respect to blank SNs. With respect to the zeta potential (ZP), SNs-DSF have a negative superficial charge around -20 mV, due to the presence of carboxylic acid groups of PEG (Figure 1B). When performing the HPLC analysis, the calibration curve was found to be y = 73,58x - 0,862; with an R^2 value of 0.999. By applying the formula described in the methodology section, we obtained an average for three different formulations (n=3) of 100% encapsulation efficiency at both 0 and 24 h storage. Our results are in line with those reported by Farooq *et al.* with DSF-encapsulated into globular protein stabilized nanoparticles [68], and encapsulation efficiencies were superior to the values reported for lactoferrin nanoparticles and PEG-PLGA/PCL nanoparticles [34,69–71].

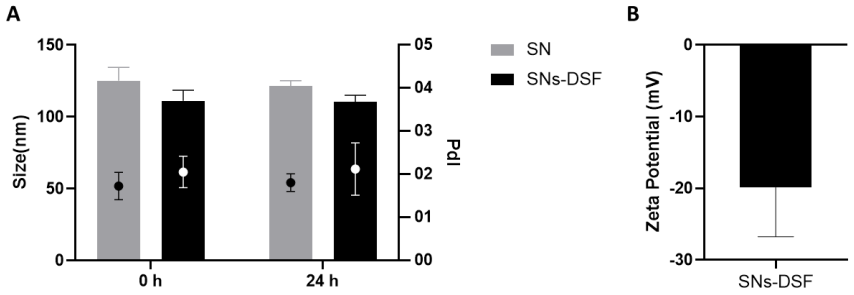

Figure 1. Physicochemical characterization of nanoemulsions with and without disulfiram. **A.** Size (nm) and Polydispersity index (PdI) at 0 and 24 hours; **B.** Zeta potential at 0 hours. All the results were measured by Zetasizer NanoZS®. Values are expressed as mean ± standard deviation, n = 3.

The stability of nanocarriers in culture media and plasma, was also explored, as it is key to explore the interaction and internalization of nanosystems into cells and for future *in vivo* assessment [72]. Stability studies were performed in supplemented RPMI (10% FBS, 1% P/S), and spheroids medium (2% P/S, 1/1000 NEAA, 0,4% BSA, 20 ng/µl bFGF, 50ng/µl EGF and 1/1000 ITS) as well as, in plasma (30% in NaCl (v/v)). As shown in figure 2A, SNs and DSF-loaded SNs were stable in cell culture medium for 4h; this is well-aligned with previous results of the group [48,49]. In the case of DSF-loaded SNs in sphere medium, an increase in size was observed after 24h incubation in spheroids medium (Figure 2B). These differences could be attributed to the creation of the protein corona due to the differential components of this medium [73]. Relevantly, next experiments (Section 3.2, Figure 3) were aimed to study the interaction of SNs-DSF with 3D spheroids, and we observed that, in less than 1 hour, nanoparticles had already penetrated the spheroids. Therefore, the compromise stability in cell spheroid cell culture medium at 24h is not affecting their interaction with the targeted cells. Of

relevance, both SNs and SNs-DSF had great stability in plasma (Figure 2C), a fact that demonstrated the potential of the formulations to carry the specific treatment to the cells via intravenous injection. The presence of the polymer PEG could be one of the factors responsible of this improving in the stability of nanosystems, because it is known for increasing not only the SNs half-life, but also their stability [48,49,74–76]. This improvement in the stability was previously reported in the work of Bouzo *et al.*, where SNs were loaded with uroguanylin and etoposide for metastatic colorectal cancer treatment. In this context, the SNs stability in relevant media was significantly enhanced after PEGylation [49].

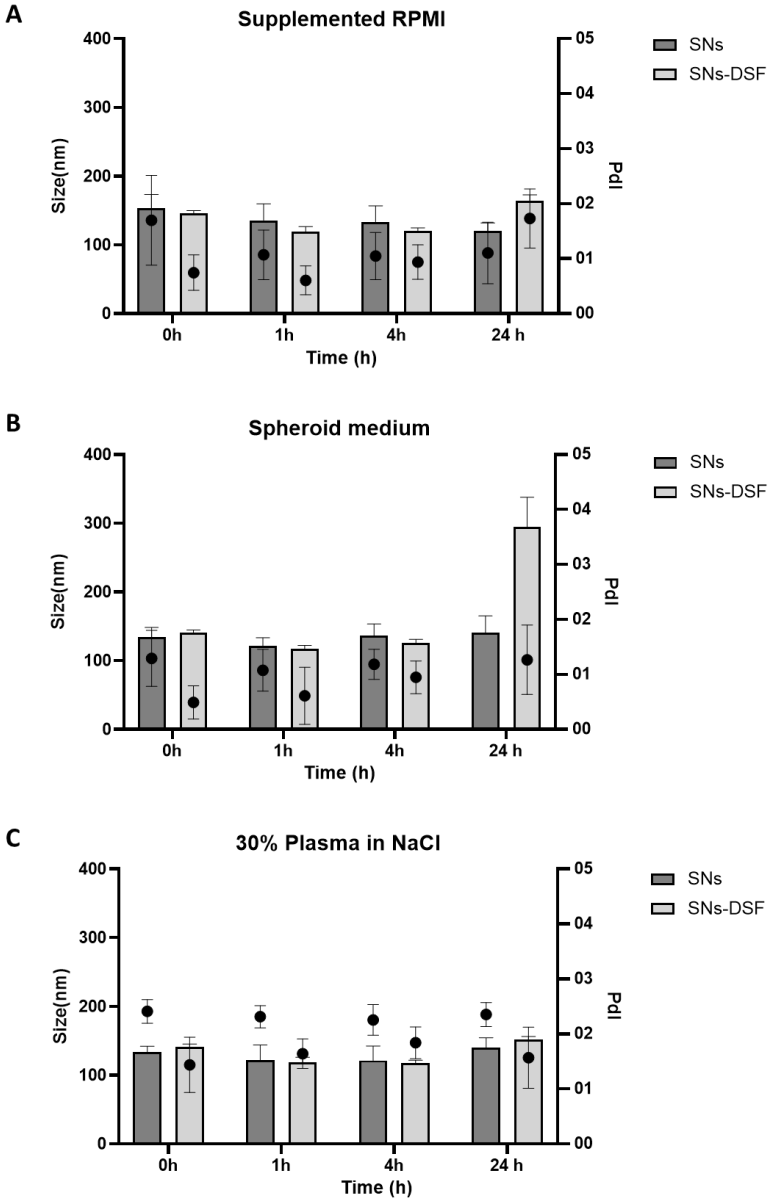

Figure 2. Nanosystems', both plain SNs and SNs-DSF, stability in different cell culture media: **A.** supplemented RPMI; **B.** spheroids medium; **C.** 30% plasma in NaCl. Values are expressed as mean ± standard deviation, n = 3.

3.2 Internalization studies

As explained before, spheroids were selected in this work to achieve an *in vitro* model which better mimics the structure, microenvironment and cell interactions of the tumor, and also as a representative model of CSCs [58,77]. This 3D model will allow to deeply understand the behavior and interactions of SNs and the efficacy of SNs-DSF proposed treatment in a model of NSCLC CSC [78–80]. SNs and SNs-DSF were labelled with Cy5 (Cy5-SM, at a concentration of 1.8 µg/mL). The labeling of SNs and SNs-DSF did not produce relevant changes in their physicochemical properties. H1650 spheroids were incubated with the Cy5-labelled nanosystems, and samples were analyzed under the confocal microscope at different time-points. Contrary to other cell lines, H1650 cells produce highly compact spheroids, providing a study model whose interior is difficult to be reached [81]. They also were proved as a 3D *in vitro* model of enriched CSCs population [82]. Even the spheroids were compact, plain nanosystems, SNs, demonstrated their capacity to penetrate and even reach the inner core (Figure 3A). Furthermore, the results show a fast internalization which can be slightly observed in the first 30 minutes, becoming clearly visible at 1 hour. SNs-DSF uptake showed a similar behavior demonstrating that the encapsulation of the drug does not alter their properties and that the drug could be efficiently delivered to the inner parts of the spheroid at short times of incubation (Figure 3A, 3B).

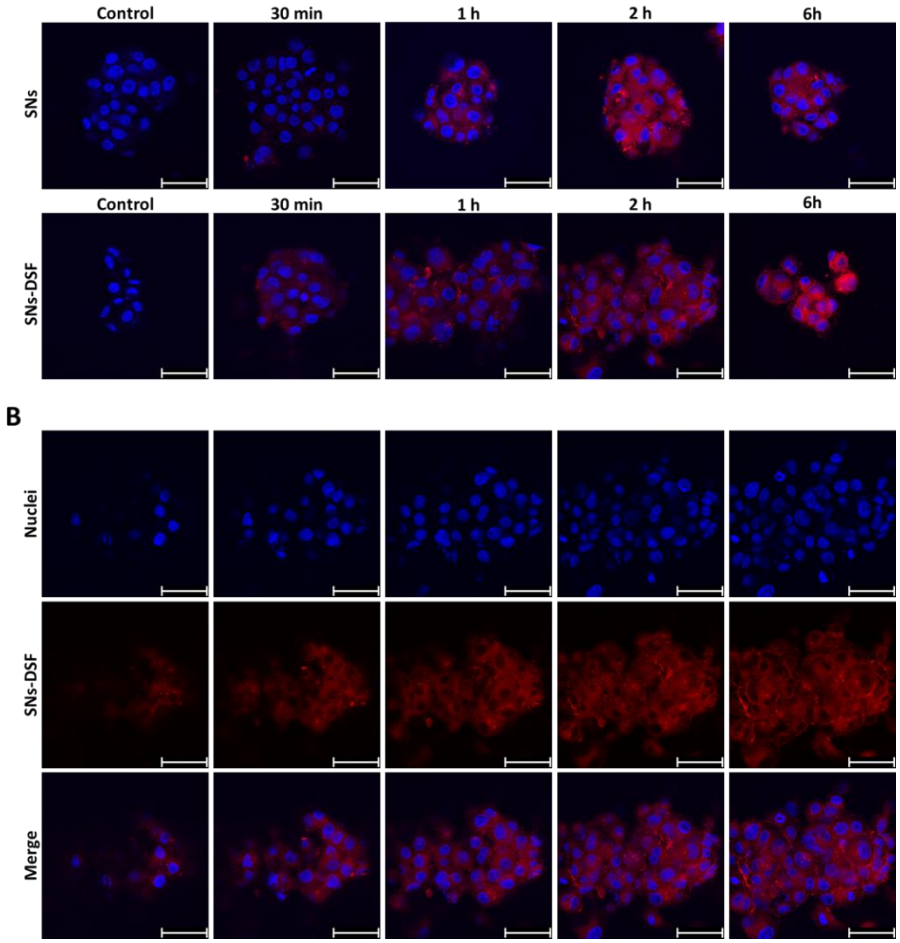

Figure 3. Confocal images (63x) of nanosystems internalization. SNs are labelled with Cy5 (in red), and nuclei are stained with Hoechst 33342 (in blue). **A.** SNs and SNs-DSF internalization in H1650 spheroids at different time points. Images are middle sections of a Z stack. Scale bar: 50 µm. **B.** SNs-DSF internalization in H1650 spheroids after 2 hours of incubation. Images of sections taken with a step of 2.5 µm. Scale bar: 50 µm.

Results are in accordance with the work of Bidan *et al.*, where SNs encapsulate gemcitabine for pancreatic cancer treatment [48]. They described the successfully penetration of Top-Fluor labeled SNs into multicellular spheroids composed by cancer-associated-fibroblasts (CAFs) and pancreatic cancer cells (PANC-1 cell line), which are more complex spheroids due to the addition of immune cells of the tumor microenvironment. In this study, the authors employed a lower dose of plain SNs labeled with a different fluorophore, TopFluor, and observed a complete internalization after 24 hours [48]. Similar studies, performed by Swetha *et al.*, evaluated the internalization efficacy of DSF and Docetaxel-encapsulated pH-responsive nanoparticles, based on PLGA. The results also demonstrated, after 24 hours of treatment, an efficient penetration of these nanoparticles into the inner of spheroids [83].

3.3 Cellular viability studies

With the aim of evaluating the activity of SNs-DSF *in vitro*, a cellular viability assay was carried out in H1650 adherent and spheroid cells after a 48-treatment (MTS assay). DSF dissolved in DMSO was used as a positive control, based on previous results [27].

As observed (Figure 4), adherent cell cultures were not affected by DSF treatment. This is an expected outcome, since CSCs are the main target of DSF, and their population is enriched in 3D cultures, not in 2D, as demonstrated by Herreros-Pomares *et al.* [58]. On the contrary, in the case of 3D cultures, the percentage of viable cells significantly decreased after incubation with SNs-DSF and the control unencapsulated drug. These results demonstrate the potential of DSF to become an efficient treatment for NSCLC. The IC50s

were calculated, and the results showed a slight decrease in the SNs-DSF IC50 value (0.16), in comparison with the free DSF (0.35). This fact indicates that the encapsulation of DSF into the SNs is not affecting the drug activity, and could also improve the penetration into spheroids, and drug stability.

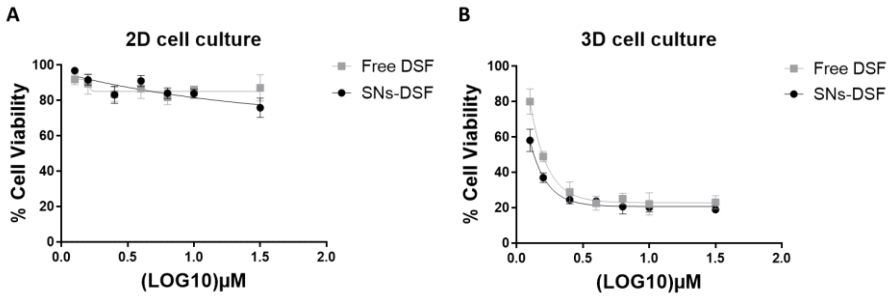

Figure 4. MTS viability assay of Free DSF and SNs-DSF in H1650 cell line. A: viability of H1650, in adherent conditions, after 48 hours of incubation. B: viability of H1650, in spheroid conditions, after 48 hours of incubation.

A second experiment was performed using Calcein AM and PI to observe, respectively, the live and dead populations in the spheroid cells after 48-hour incubation with the free DSF at a concentration of 0.30 µM (~IC50, positive control), and SNs-DSF. This evaluation based on Calcein AM and PI was previously performed to study DSF-encapsulated nanocarriers in spheroid study models [84,85].

The first step was the incubation with Calcein AM and PI, for 30 minutes, with the aim of detecting live and apoptotic cells in spheroids. The obtained results were evaluated by confocal microscopy (AX R Confocal, NIKON, Tokyo, Japan). Images show a similar pattern of apoptotic cells after both treatments (free DSF and encapsulated SNs-DSF), disposed in the inner core of the spheroid (Figure 5). This result means that SNs are able, not only to

completely penetrate in the interior of the sphere, but also to efficiently release their cargo in the targeted cells, producing an apoptotic effect in them [86–88], without interfering with the effect of the encapsulating drug, and with the potential to be used in further *in vivo* experiments, to overcome biopharmaceutical problems such as low solubility in aqueous media and low stability [11,66]. An example of this is the work of Li *et al.* who evaluated the effect of DSF (free and encapsulated in nanosuspensions) *in vivo*, and not finding therapeutic effect in the case of free DSF due to its rapid degradation [89].

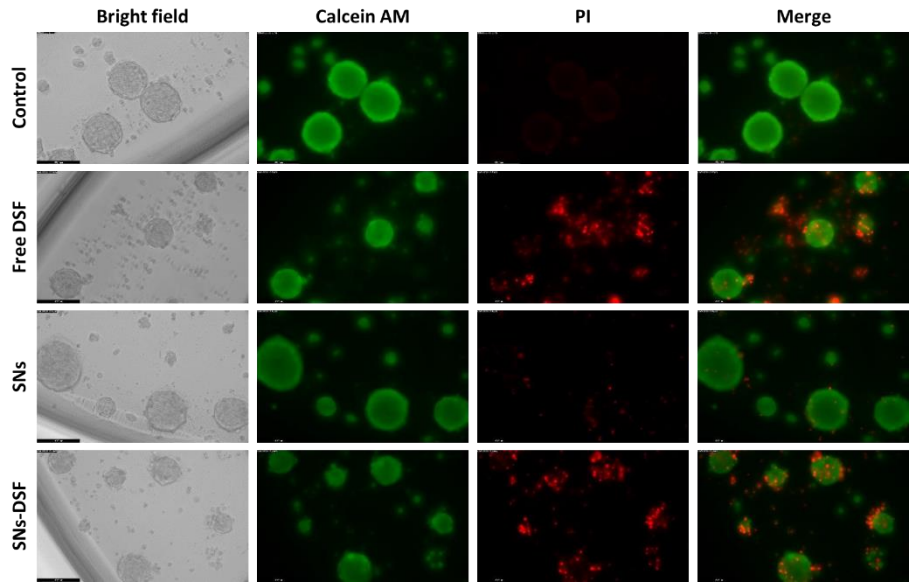

Figure 5. Viability assay of H1650 spheroids after disulfiram treatment (0.30 µM), encapsulated and non-encapsulated in SNs, for 48 hours. After treatment, spheroids were incubated with Calcein AM 2 µM and PI 4 µM for 30 minutes. In the images, Calcein AM is in green, and PI in red.

Considering the SNs efficient encapsulation of DSF, their efficient penetration into 3D complex *in vitro* models, and the effective treatment in CSCs-enriched models, the SNs functionalization can be an alternative to increase the treatment efficacy. Further experiments with functionalized SNs-DSF are going to be performed to improve nano-based NSCLC CSCs therapy.

4. CONCLUSIONS

In conclusion, we have successfully demonstrated the efficient encapsulation of the hydrophobic drug DSF into the SNs. The experimental outcomes reflect the capacity of SNs-DSF to transport the DSF to the target cells and penetrate efficiently into the inner core of 3D static *in vitro* models. Furthermore, SNs maintain the therapeutic potential of DSF, which corroborates their value as a nanocarrier for lipophilic drugs.

Relevantly, spheroids were selected as the study *in vitro* platform of this work, proving their potential to be a gold standard to evaluate the efficacy of anti-CSCs nanomedicines.

BIBLIOGRAPHY

1. Sung, H. *et al.* Global Cancer Statistics 2020: GLOBOCAN Estimates of Incidence and Mortality Worldwide for 36 Cancers in 185 Countries. *CA Cancer J Clin* **71**, 209–249 (2021).

2. Thai, A. A., Solomon, B. J., Sequist, L. V., Gainor, J. F. & Heist, R. S. Lung cancer. *The Lancet* **398**, 535–554 (2021).

3. Kim, Y. H., Nishimura, Y. & Funada, Y. How should we manage non-small-cell lung cancer "not-otherwise-specified"? *Medical Oncology 2021 38:7* **38**, 1–2 (2021).

4. Tai, Q., Zhang, L. & Hu, X. Clinical characteristics and treatments of large cell lung carcinoma: a retrospective study using SEER data. *Transl Cancer Res* **9**, 1455 (2020).

5. Nooreldeen, R. & Bach, H. Current and Future Development in Lung Cancer Diagnosis. *Int J Mol Sci* **22**, (2021).

6. Alexander, M., Kim, S. Y. & Cheng, H. Update 2020: Management of Non-Small Cell Lung Cancer. *Lung* **198**, 897 (2020).

7. Pushpakom, S. *et al.* Drug repurposing: progress, challenges and recommendations. *Nature Reviews Drug Discovery 2018 18:1* **18**, 41–58 (2018).

8. Wieder, R. & Adam, N. Drug repositioning for cancer in the era of AI, big omics, and real-world data. *Crit Rev Oncol Hematol* **175**, (2022).

9. Hua, Y. *et al.* Drug repositioning: Progress and challenges in drug discovery for various diseases. *Eur J Med Chem* **234**, 114239 (2022).

10. Li, H. *et al.* The combination of disulfiram and copper for cancer treatment. *Drug Discov Today* **25**, 1099–1108 (2020).

11. Lu, C., Li, X., Ren, Y. & Zhang, X. Disulfiram: a novel repurposed drug for cancer therapy. *Cancer Chemother Pharmacol* **87**, 159–172 (2021).

12. Suh, J. J., Pettinati, H. M., Kampman, K. M. & O'Brien, C. P. The status of disulfiram: A half of a century later. *J Clin Psychopharmacol* **26**, 290–302 (2006).

13. EF Lewison. Spontaneous regression of breast cancer. *Natl Cancer Inst Monogr* **44**, 26–26 (1976).

14. Butcher, K. *et al.* Investigation of the key chemical structures involved in the anticancer activity of disulfiram in A549 non-small cell lung cancer cell line. *BMC Cancer* **18**, (2018).

15. Wu, X. *et al.* Suppressing autophagy enhances disulfiram/copper-induced apoptosis in non-small cell lung cancer. *Eur J Pharmacol* **827**, 1–12 (2018).

16. Kryczka, J. *et al.* Isothiocyanates (ITCs) 1-(Isothiocyanatomethyl)-4-phenylbenzene and 1-Isothiocyanato-3,5-bis(trifluoromethyl)benzene—Aldehyde Dehydrogenase (ALDH) Inhibitors, Decreases Cisplatin Tolerance and Migratory Ability of NSCLC. *Int J Mol Sci* **23**, (2022).

17. Solak, K., Mavi, A. & Yılmaz, B. Disulfiram-loaded functionalized magnetic nanoparticles combined with copper and sodium nitroprusside in breast cancer cells. *Materials Science and Engineering: C* **119**, 111452 (2021).

18. Solovieva, M. *et al.* Disulfiram oxy-derivatives induce entosis or paraptosis-like death in breast cancer MCF-7 cells depending on the duration of treatment. *Biochim Biophys Acta Gen Subj* **1866**, (2022).

19. Chu, M. *et al.* Combination of the 6-thioguanine and disulfiram/Cu synergistically inhibits proliferation of triple-negative breast cancer cells by enhancing DNA damage and disrupting DNA damage checkpoint. *Biochim Biophys Acta Mol Cell Res* **1869**, (2022).

20. Li, Z. *et al.* Disulfiram Synergizes with SRC Inhibitors to Suppress the Growth of Pancreatic Ductal Adenocarcinoma Cells in Vitro and in Vivo. *Biol. Pharm. Bull* **44**, 1323–1331 (2021).

21. Xu, Y. *et al.* Disulfiram Alone Functions as a Radiosensitizer for Pancreatic Cancer Both In Vitro and In Vivo. *Front Oncol* **11**, (2021).

22. Jiapaer, Z. *et al.* Disulfiram-loaded hollow copper sulfide nanoparticles show anti-tumor effects in preclinical models of colorectal cancer. *Biochem Biophys Res Commun* **635**, 291–298 (2022).

23. Ren, X. *et al.* Overcoming the compensatory elevation of NRF2 renders hepatocellular carcinoma cells more vulnerable to disulfiram/copper-induced ferroptosis. *Redox Biol* **46**, 102122 (2021).

24. Meraz-Torres, F., Plöger, S., Garbe, C., Niessner, H. & Sinnberg, T. Disulfiram as a Therapeutic Agent for Metastatic Malignant Melanoma—Old Myth or New Logos? *Cancers (Basel)* **12**, 1–20 (2020).

25. Zirjacks, L. *et al.* Repurposing Disulfiram for Targeting of Glioblastoma Stem Cells: An In Vitro Study. *Biomolecules* **11**, (2021).

26. Lei, W. *et al.* Disulfiram-copper activates chloride currents and induces apoptosis with tyrosine kinase in prostate cancer cells. *Asia Pac J Clin Oncol* **18**, e46 (2022).

27. Amado Labrador, H. A. Tumoresferas como plataformas de cribado farmacológico in vitro/in vivo para la búsqueda de nuevas terapias contra el cáncer de pulmón no microcítico. (Universitat de València, 2019).

28. Duan, H., Liu, Y., Gao, Z. & Huang, W. Recent advances in drug delivery systems for targeting cancer stem cells. *Acta Pharm Sin B* **11**, 55 (2021).

29. Atashzar, M. R. *et al.* Cancer stem cells: A review from origin to therapeutic implications. *J Cell Physiol* **235**, 790–803 (2020).

30. Herreros-Pomares, A. Identification, Culture and Targeting of Cancer Stem Cells. *Life* **12**, (2022).

31. Farooq, M. A. *et al.* Recent advances in the delivery of disulfiram: a critical analysis of promising approaches to improve its pharmacokinetic profile and anticancer efficacy. *DARU, Journal of Pharmaceutical Sciences* **27**, 853–862 (2019).

32. Ekinci, E., Rohondia, S., Khan, R. & Dou, Q. P. Repurposing Disulfiram as An Anti-Cancer Agent: Updated Review on Literature and Patents. *Recent Pat Anticancer Drug Discov* **14**, 113–132 (2019).

33. Gonzalez-Valdivieso, J., Girotti, A., Schneider, J. & Arias, F. J. Advanced nanomedicine and cancer: Challenges and opportunities in clinical translation. *Int J Pharm* **599**, 120438 (2021).

34. Song, W. *et al.* Stable loading and delivery of disulfiram with mPEG-PLGA/PCL mixed nanoparticles for tumor therapy. *Nanomedicine* **12**, 377–386 (2016).

35. Zhuo, X. *et al.* Disulfiram-loaded mixed nanoparticles with high drug-loading and plasma stability by reducing the core crystallinity for intravenous delivery. *J Colloid Interface Sci* **529**, 34–43 (2018).

36. Huo, Q. *et al.* pH-triggered surface charge-switchable polymer micelles for the co-delivery of paclitaxel/disulfiram and overcoming multidrug resistance in cancer. *Int J Nanomedicine* **12**, 8631–8647 (2017).

37. Mohammad, I. S., He, W. & Yin, L. A Smart Paclitaxel-Disulfiram Nanococrystals for Efficient MDR Reversal and Enhanced Apoptosis. *Pharm Res* **35**, 1–18 (2018).

38. Zhang, L. *et al.* A Copper-Mediated Disulfiram-Loaded pH-Triggered PEG-Shedding TAT Peptide-Modified Lipid Nanocapsules for Use in Tumor Therapy. *ACS Appl Mater Interfaces* **7**, 25147–25161 (2015).

39. Banerjee, P. *et al.* Integrating the drug, disulfiram into the vitamin E-TPGS-modified PEGylated nanostructured lipid carriers to synergize its repurposing for anti-cancer therapy of solid tumors. *Int J Pharm* **557**, 374–389 (2019).

40. Bouzo, B. L., Calvelo, M., Martín-Pastor, M., García-Fandiño, R. & de La Fuente, M. In Vitro- In Silico Modeling Approach to Rationally Designed Simple and Versatile Drug Delivery Systems. *Journal of Physical Chemistry B* **124**, 5788–5800 (2020).

41. Cascallar, M. *et al.* Zebrafish as a platform to evaluate the potential of lipidic nanoemulsions for gene therapy in cancer. *Front Pharmacol* **13**, 4602 (2022).

42. Nagachinta, S., Bouzo, B. L., Vazquez-Rios, A. J., Lopez, R. & de la Fuente, M. Sphingomyelin-based nanosystems (SNs) for the development of anticancer miRNA therapeutics. *Pharmaceutics* **12**, (2020).

43. Masoumi, F. *et al.* Modulation of Colorectal Tumor Behavior via lncRNA TP53TG1-Lipidic Nanosystem. *Pharmaceutics* **13**, (2021).

44. Lores, S. *et al.* Effectiveness of a novel gene nanotherapy based on putrescine for cancer treatment. *Biomater Sci* **11**, 4210–4225 (2023).

45. Díez-Villares, S. *et al.* Biodistribution of 68/67Ga-Radiolabeled Sphingolipid Nanoemulsions by PET and SPECT Imaging. *Int J Nanomedicine* **16**, 5923 (2021).

46. Díez-Villares, S. *et al.* Manganese Ferrite Nanoparticles Encapsulated into Vitamin E/Sphingomyelin Nanoemulsions as Contrast Agents for High-Sensitive Magnetic Resonance Imaging. *Adv Healthc Mater* **10**, 2101019 (2021).

47. Nagachinta, S. *et al.* Radiolabelling of lipid-based nanocarriers with fluorine-18 for in vivo tracking by PET. *Colloids Surf B Biointerfaces* **188**, 110793 (2020).

48. Bidan, N. *et al.* Before in vivo studies: In vitro screening of sphingomyelin nanosystems using a relevant 3D multicellular pancreatic tumor spheroid model. *Int J Pharm* **617**, (2022).

49. Bouzo, B. L. *et al.* Sphingomyelin nanosystems loaded with uroguanylin and etoposide for treating metastatic colorectal cancer. *Sci Rep* **11**, 17213 (2021).

50. Saraiva, S. M. *et al.* Edelfosine nanoemulsions inhibit tumor growth of triple negative breast cancer in zebrafish xenograft model. *Sci Rep* **11**, (2021).

51. Jatal, R. *et al.* Sphingomyelin nanosystems decorated with TSP-1 derived peptide targeting senescent cells. *Int J Pharm* **617**, 121618 (2022).

52. Habanjar, O., Diab-Assaf, M., Caldefie-Chezet, F. & Delort, L. 3D Cell Culture Systems: Tumor Application, Advantages, and Disadvantages. *Int J Mol Sci* **22**, (2021).

53. Atat, O. el *et al.* 3D modeling in cancer studies. *Hum Cell* **35**, 23–36 (2022).

54. Hamilton, G. & Rath, B. Applicability of tumor spheroids for in vitro chemosensitivity assays. *Expert Opin Drug Metab Toxicol* **15**, 15–23 (2019).

55. MacDonagh, L. *et al.* Lung cancer stem cells: The root of resistance. *Cancer Lett* **372**, 147–156 (2016).

56. Maiuthed, A., Chantarawong, W. & Chanvorachote, P. Lung cancer stem cells and cancer stem cell-targeting natural compounds. *Anticancer Res* **38**, 3797–3810 (2018).

57. Raniszewska, A., Kwiecień, I., Rutkowska, E., Rzepecki, P. & Domagała-Kulawik, J. Lung Cancer Stem Cells—Origin, Diagnostic Techniques and Perspective for Therapies. *Cancers (Basel)* **13**, (2021).

58. Herreros-Pomares, A. *et al.* Lung tumorspheres reveal cancer stem cell-like properties and a score with prognostic impact in resected non-small-cell lung cancer. *Cell Death Dis* **10**, (2019).

59. Leon, G., MacDonagh, L., Finn, S. P., Cuffe, S. & Barr, M. P. Cancer stem cells in drug resistant lung cancer: Targeting cell surface markers and signaling pathways. *Pharmacol Ther* **158**, 71–90 (2016).

60. Yang, M., Liu, P. & Huang, P. Cancer stem cells, metabolism, and therapeutic significance. *Tumor Biology* **37**, 5735–5742 (2016).

61. Tawakoli, P. N., Al-Ahmad, A., Hoth-Hannig, W., Hannig, M. & Hannig, C. Comparison of different live/dead stainings for detection

and quantification of adherent microorganisms in the initial oral biofilm. *Clin Oral Investig* **17**, 841–850 (2013).

62. Riccardi, C. & Nicoletti, I. Analysis of apoptosis by propidium iodide staining and flow cytometry. *Nature Protocols 2006 1:3* **1**, 1458–1461 (2006).

63. Liu, P. *et al.* Cytotoxic effect of disulfiram/copper on human glioblastoma cell lines and ALDH-positive cancer-stem-like cells. *British Journal of Cancer 2012 107:9* **107**, 1488–1497 (2012).

64. Wang, L., Yu, Y., Zhou, C., Wan, R. & Li, Y. Anticancer effects of disulfiram: a systematic review of in vitro, animal, and human studies. *Syst Rev* **11**, 109 (2022).

65. Miao, L. *et al.* MPEG 5k - b -PLGA 2k /PCL 3.4k /MCT Mixed Micelles as Carriers of Disulfiram for Improving Plasma Stability and Antitumor Effect in Vivo. *Mol Pharm* **15**, 1556–1564 (2018).

66. Chen, X. *et al.* Formulation and preparation of a stable intravenous disulfiram-loaded lipid emulsion. *European Journal of Lipid Science and Technology* **117**, 869–878 (2015).

67. Sun, Y. *et al.* Degradable FeCuS-Lipid Nanoparticles Confer Ultrasound-Activated CO Release and O2-Independent Radical Production for Synergistic Therapy. *ACS Nano* **15**, 16298–16313 (2021).

68. Farooq, M. A., Li, L., Parveen, A. & Wang, B. Globular protein stabilized nanoparticles for delivery of disulfiram: fabrication, characterization, in vitro toxicity, and cellular uptake. *RSC Adv* **10**, 133 (2019).

69. Ou, A. te *et al.* Disulfiram-loaded lactoferrin nanoparticles for treating inflammatory diseases. *Acta Pharmacol Sin* **42**, 1913 (2021).

70. Luo, Q. *et al.* Tumor microenvironment-responsive shell/core composite nanoparticles for enhanced stability and antitumor efficiency based on a ph-triggered charge-reversal mechanism. *Pharmaceutics* **13**, (2021).

71. Fasehee, H., Ghavamzadeh, A., Alimoghaddam, K., Ghaffari, S. H. & Faghihi, S. A Comparative Cytotoxic Evaluation of Disulfiram Encapsulated PLGA Nanoparticles on MCF-7 Cells. *Int J Hematol Oncol Stem Cell Res* **11**, 102 (2017).

72. Moore, T. L. *et al.* Nanoparticle colloidal stability in cell culture media and impact on cellular interactions. *Chem Soc Rev* **44**, 6287–6305 (2015).

73. Falahati, M. *et al.* A health concern regarding the protein corona, aggregation and disaggregation. *Biochim Biophys Acta Gen Subj* **1863**, 971 (2019).

74. D'souza, A. A. & Shegokar, R. Polyethylene glycol (PEG): a versatile polymer for pharmaceutical applications. *Expert Opin Drug Deliv* **13**, 1257–1275 (2016).

75. Ibrahim, M. *et al.* Polyethylene glycol (PEG): The nature, immunogenicity, and role in the hypersensitivity of PEGylated products. *Journal of Controlled Release* **351**, 215–230 (2022).

76. Liu, M. *et al.* Branched PEG-modification: A new strategy for nanocarriers to evade of the accelerated blood clearance phenomenon and enhance anti-tumor efficacy. *Biomaterials* **283**, 121415 (2022).

77. Herreros-Pomares, A. *et al.* 3D printing novel in vitro cancer cell culture model systems for lung cancer stem cell study. *Materials Science and Engineering: C* **122**, 111914 (2021).

78. Tchoryk, A. *et al.* Penetration and Uptake of Nanoparticles in 3D Tumor Spheroids. (2019) doi:10.1021/acs.bioconjchem.9b00136.

79. Niora, M. *et al.* Head-to-Head Comparison of the Penetration Efficiency of Lipid-Based Nanoparticles into Tumor Spheroids. *ACS Omega* **5**, 21162–21171 (2020).

80. Zanoni, M. *et al.* Modeling neoplastic disease with spheroids and organoids. *J Hematol Oncol* **13**, (2020).

81. Sakuma, Y. *et al.* Lung adenocarcinoma cells floating in lymphatic vessels resist anoikis by expressing phosphorylated Src. *J Pathol* **220**, 574–585 (2010).

82. Yu, F. *et al.* Tumor suppressive microRNA-124a inhibits stemness and enhances gefitinib sensitivity of non-small cell lung cancer cells by targeting ubiquitin-specific protease 14. *Cancer Lett* **427**, 74–84 (2018).

83. Swetha, K. L. *et al.* Overcoming drug resistance with a docetaxel and disulfiram loaded pH-sensitive nanoparticle. *Journal of Controlled Release* **356**, 93–114 (2023).

84. Hartwig, F., Köll-Weber, M. & Süss, R. Preclinical In Vitro Studies with 3D Spheroids to Evaluate Cu(DDC)2 Containing Liposomes for the Treatment of Neuroblastoma. *Pharmaceutics* **13**, (2021).

85. Chang, Y. *et al.* Biomimetic metal-organic nanoparticles prepared with a 3D-printed microfluidic device as a novel formulation for disulfiram-based therapy against breast cancer. *Appl Mater Today* **18**, (2020).

86. Nie, D., Chen, C., Li, Y. & Zeng, C. Disulfiram, an aldehyde dehydrogenase inhibitor, works as a potent drug against sepsis and cancer via NETosis, pyroptosis, apoptosis, ferroptosis, and cuproptosis. *Blood Science* **4**, 152–154 (2022).

87. Xu, Y. *et al.* Disulfiram/copper markedly induced myeloma cell apoptosis through activation of JNK and intrinsic and extrinsic apoptosis pathways. *Biomedicine and Pharmacotherapy* **126**, (2020).

88. O'Brien, P. S. *et al.* Disulfiram (Antabuse) activates ROS-dependent ER stress and apoptosis in oral cavity squamous cell carcinoma. *J Clin Med* **8**, (2019).

89. Li, H. *et al.* Soybean lecithin stabilizes disulfiram nanosuspensions with a high drug-loading content: remarkably improved antitumor efficacy. *J Nanobiotechnology* **18**, 4 (2020).

CHAPTER II

Evaluation of TAS1R3-targeted sphingomyelin-nanosystems in cell culture models and advanced organ-on-a-chip microfluidic devices

Evaluation of TAS1R3-targeted sphingomyelin-nanosystems in cell culture models and advanced organ-on-a-chip microfluidic devices

ABSTRACT

The metastatic process is a key point for the tumoral progression. Non-small cell lung cancer (NSCLC) is a clear example of the drastic reduction of survival rates due to metastasis. In this sense, new specific therapies that target these metastatic cells are needed to improve the patients' quality of life.

Nanotechnology-based therapies can be an alternative strategy for targeting NSCLC metastasis. We have previously described SNs as a promising alternative for drug delivery to NSCLC cancer stem cells (CSCs) (Chapter I). In this chapter, we aimed to add a targeting ligand to the surface of SNs to develop targeted nanosystems able to interact more efficiently with CSCs, and specifically with the TAS1R3 receptor, recently described by our group. Aptamers able to bind TAS1R3 were selected for this specific purpose, and SNs successfully decorated.

The ability of aptamer-functionalized SNs (SNs-5F) to specifically interact with TAS1R3 was assessed in transfected A549 NSCLC TAS1R3+ cells (A549-TAS1R3+), overexpressing the targeted receptor, first in 2D cell cultures, and second in advanced organ-on-a-chip (OOC) microfluidic devices that mimic the tumor structure and vasculature. The evaluation of the specific targeting was efficiently proved in A549-TAS1R3+ cells by flow cytometry. Preliminary experiments in the developed OOC also suggest a specific targeting of the SNs-5F.

In conclusion, these results prove the capacity of the SNs to be functionalized with specific ligands for targeted therapy to improve their specificity for selected cell subpopulations (TAS1R3 positive cells). In addition, OOC microfluidic devices demonstrate their value to advance in the development of novel targeted nanomedicines.

1. INTRODUCTION

The metastatic cascade, derived from the primary tumor, is the responsible of the majority of cancer deaths [1,2]. In this sense, lung cancer stands out for being the cancer type with highest mortality rate, and, specifically, non-small cell lung cancer (NSCLC) represents 85% of the lung cancers [3,4]. Remarkably, 40% of NSCLC patients present distant metastasis at the time of diagnosis, and in these advanced stages, the 5-year survival can decrease less than 1% in [5–7]. NSCLC is a clear example of the urgent necessity of specific treatments against metastatic cells to reduce this specific population, achieving an improvement of the overall survival. For this purpose, targeted therapy is a valuable alternative to produce an accurate effect of the treatment without harmful side effects [2].

In this sense, nanomedicine can play a key role in the development of targeted therapies, due to its capacity to be functionalized and to carry therapeutic molecules. There are different strategies to functionalize nanosystems for an active targeting, such as surface-decoration with antibodies, peptides, vitamins, and aptamers, among others [8].

Particularly, aptamers are ribonucleic acid (RNA) or single-stranded deoxyribonucleic acid (DNA) oligonucleotides which have specific three-dimensional (3D) conformations, which allow them to recognize and bind to specific target molecules [9–11]. Since 2004, when Farokhzad *et al.* developed the first nanoparticle conjugated with aptamers for targeting prostate cancer cells, the aptamers became a promising methodology for the development of functionalized nanomedicines [8,12].

In relation to that, our group has previously developed lipidic nanosystems based on Vitamin E (VE) and sphingomyelin (SM) [13]. This SM-based nanosystems (SNs) have the versatility to carry hydrophobic drugs and biomolecules and, as well as be functionalized with different ligands to developed targeted therapies that can interact with specific receptors [14–21]. In this work, we aim to achieve an efficient conjugation with aptamers selected against the Taste Receptor type 1 member 3 (TAS1R3) as a strategy to target specific cell subpopulations of NSCLC.

As previously explained, the development of novel therapies for metastatic NSCLC is critical. Previous studies in our group identified the TAS1R3 receptor in non-small cell lung cancer cells and correlated its expression with the metastatic process [22]. Thus, we aimed to select aptamers against this receptor, to develop surface-decorated SNs. Secondly, studies were directed to assess their efficacy *in vitro*. For this, we used a transformed cell line overexpressing TAS1R3, and also work on the development of advanced organ-on-a-chip (OOC) microfluidic models that allow the recreation of the 3D structure and microenvironment of the tumor *in vitro* [23]. This 3D model has the same advantages as spheroids and organoids, such as the three-dimensional structure of the tumoral mass, mimicking the tumor microenvironment, as well as the different interactions produced between cells and other components of the microenvironment [24,25]. However, the main advantage of the OOC models compared to the other 3D models is the fact that they are dynamic platforms, which improves the simulation of the real scenario of cancer [26,27].

2. MATERIALS AND METHODS

2.1. Materials

SYLGARD™ 184 Silicone Elastomer Kit was provided by Dow Corning (Midland, Michigan, United States). Paraformaldehyde (PFA) was obtained from IESMAT (Madrid, Spain). Heparin sodium salt and Ethanol of analytical grade were purchased from VWR (Barcelona, Spain). Agar sLB and sLB Broth (Buffered) were provided from Condalab (Madrid, Spain). Sphingomyelin (Lipoid E SM) was obtained from Lipoid GmbH (Ludwigshafen, Germany). Penicillin-Streptomycin (P/S), fetal bovine serum (FBS), Accutase™ Cell Detachment Solution, Pierce™ Sulfo-SANPAH (sulfosuccinimidyl-6-[4′-azido-2′-nitrophenylamino]hexanoate), Trypsin, alamarBlue™ Cell Viability Reagent, Human fibroblast growth factor basic (bFGF), Human Epidermal growth factor (EGF), Wheat Germ Agglutinin (WGA) Alexa Fluor™ 488, Non-essential amino acids (NEAA), Roswell Park Memorial Institute (RPMI) 1640 Medium and Hoechst 33342 were acquired from Thermo Fisher Scientific (Whalham, Massachusetts, USA). C11 TopFluor Sphingomyelin (N-[11-(dipyrrometheneboron difluoride)undecanoyl]-D-erythro-sphingosylphosphorylcholine and 1,2-distearoyl-sn-glycero-3-phosphoethanolamine-N-[carboxy(polyethylene glycol)-2000] (sodium salt) DSPE-PEG(2000) Carboxylic Acid were provided by Avanti Polar Lipids (Alabama, USA). Bovine Serum Albumin (BSA) was provided by Biowest (Nuaillé, France). Dubbelco's Modified Eagle's Medium High Glucose (DMEM), Medium 199 (M199), ECM Gel from Engelbreth-Holm-Swarm murine sarcoma, Dulbecco′s Phosphate Buffered Saline (DPBS), Endothelial Cell Growth Supplement (ECGS), Puromycin dihydrochloride, Phalloidin–Tetramethylrhodamine B

isothiocyanate (TRICT), Ampicillin sodium salt and Vitamin E (DL-α-Tocopherol) were purchased from Merck Group (Darmstadt, Germany). ITS + Premix Universal Culture Supplement was kindly provided by Cultek S. L. (Madrid, Spain).

2.2. Cell culture

A549 (CRM-CCL-185™) non-small cell lung cancer cell line and HEK293 (CRL-1573™) embryonic kidney cells were purchased from the American Type Culture Collection (ATCC). Cells were cultured in RPMI 1640 medium supplemented with 10% FBS and 1% penicillin/streptomycin.

The human pulmonary microvascular endothelial cells (HPMEC) were kindly obtained from Instituto de Investigação e Inovação em Saúde da Universidade do Porto (i3S) (Porto, Portugal). These cells were cultured in Medium 199, supplemented with, 20% FBS, 1% penicillin/streptomycin, 25µg/ml heparin sodium salt and 25µg/ml ECGS.

All cell lines were maintained at 37 °C with 5% CO_2 and at humid atmosphere (95%).

2.3. Bacterial culture for plasmid purification

Escherichia coli (*E. coli*), strain Stbl3, were prepared to be competent following the protocol of Inoue *et al.* and DNA Repair and Genome Integrity Lab of the Center for Research in Molecular Medicine and Chronic Diseases (CiMUS) (Santiago de Compostela, Spain) led by Miguel González Blanco [28].

The next step was the bacterial transformation with our specific plasmid. Defrosted competent *E. coli* Stbl3 cells (50 µL) were mixed with 200 ng of the plasmid and incubated for 20 minutes in ice. After that, a thermal shock was performed at 42ºC for 45 seconds, followed by an incubation in ice for 5 minutes. LB broth buffered was added (800 µL) and the mix was incubated at 37 °C for 30 minutes at 500 rpm. Next, the suspension was centrifuged for 1 minute at 10000 xg. Discard 750 µL of the supernatant and resuspend the remained pellet. The bacterial lawn method was followed to culture the *E. coli* in a LB agar plate with Ampicillin (100 µg/ml), overnight at 37 °C. After that, an isolated colony was collected and diluted in LB broth buffered with ampicillin (100 µg/ml) overnight at 37 °C, for the next step.

For plasmid purification, the Plasmid DNA Maxiprep Kit (Norgen Biotek, Thorold, Canada) was used and the kit protocol was followed. The resultant plasmid concentration was measured with the NanoDrop™ One (Thermo Scientific, Massachusetts, United States).

2.4. Cell line transfection

With the aim of increasing the presence of our target receptor, A549 NSCLC line was transfected to overexpress TAS1R3 (Figure 1). The TAS1R3-FLAG plasmid was developed by the DNA Repair and Genome Integrity Lab of CiMUS led by Miguel González Blanco (Santiago de Compostela, Spain); and it was transfected into the cells using lentiviral particles.

HEK 293T cells were seeded in a 100 plate with a concentration of 4x106 cells/plate. Twenty-four hours after, cells were transfected with the specific plasmid (pTAS1R3) and the plasmid that codifies for the lentivirus (pLp1,

pLp2 and pLVSVG) with Polyethylenimine (PEI). The mix of plasmid (6.5 µg) and the PEI mix (65 µg) were diluted in a final volume of 250 µL of RPMI 1460 medium each. Both reagents were mixed, in a ratio 1:10, and were incubated for 10 minutes. After that, the plasmid:PEI mix was added to the HEK 293T cell, drop by drop. Subsequently, the medium was replaced for fresh medium after 8 hours of incubation. The next day the transfection efficiency was evaluated by fluorescent detection of the enhanced green fluorescent protein (eGFP), and the A549 WT cells were seeded in a 100 plate. The HEK 293T cell media was collected and filtered with a 0.45 µm filter, mixed with polybrene (8µg/ml) and added to the A549 cell culture. The HEK 293T were added more media, and two more rounds of transfection were applied to the A549 cells. If after the third round the A549 cells expressed the eGFP, a puromycin kill curve was performed to select the work concentration, in this case, 1.2 µg/ml. The Zeiss™ Axio Vert.A1 FL-LED Inverted Microscope (Oberkochen, Germany) was the microscope selected to evaluate the correct expression of the eGFP fluorescent protein in the transfected cells.

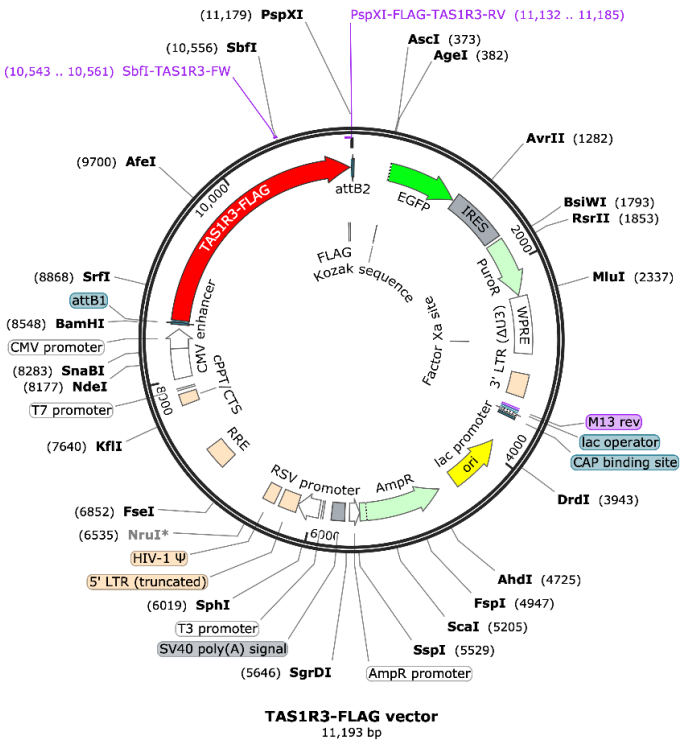

Figure 1. Scheme of the TAS1R3-FLAG plasmid.

2.5. RT-PCR

To evaluate the TAS1R3 gene expression by Real Time Polymerase Chain Reaction (RT-PCR), 3 to 5 million A549 cells were detached from a culture plate using Trypsin and pelleted.

The RNA extraction of the collected pellet was performed following the protocol of the GeneJET RNA Purification Kit (Thermo scientific). The resultant RNA was measured with the NanoDrop™ One (Thermo Scientific, Massachusetts, United States). A DNase I (Thermo Scientific, Massachusetts,

United States) treatment was applied for avoiding the presence of residual DNA. The commercial protocol was followed.

In the next step, RNA was turned into complementary DNA (cDNA) by making use of the High Capacity cDNA Reverse Transcription Kit (Thermo Scientific, Massachusetts, United States). The kit protocol was followed.

For the RT-PCR, the samples were mixed with the Master Mix (Thermo Scientific, Massachusetts, United States) and the probes for: TAS1R3; and for GAPDH, used as housekeeping (Thermo Scientific, Massachusetts, United States). The RT-PCR was performed in the StepOnePlus™ Real-Time PCR System Mix (Thermo Scientific, Massachusetts, United States), and was analyzed by the $2^{-\Delta\Delta Ct}$ Method.

2.6. Aptamers

The selection of the aptamer was developed by Aptus Biotech (Madrid, Spain). The aptamer selection strategy was Cell-Systematic Evolution of Ligands by EXponential Enrichment (SELEX). The Cell-SELEX technique is based on the pull of random DNA library which is incubated with the targeted cells. The aptamer-target complexes are isolated of the non-binding oligonucleotides of the library, and the selected aptamers are amplified and evaluated by different techniques. This procedure is repeated 8 to 16 times for selecting the aptamer (Figure 2) [8,29].

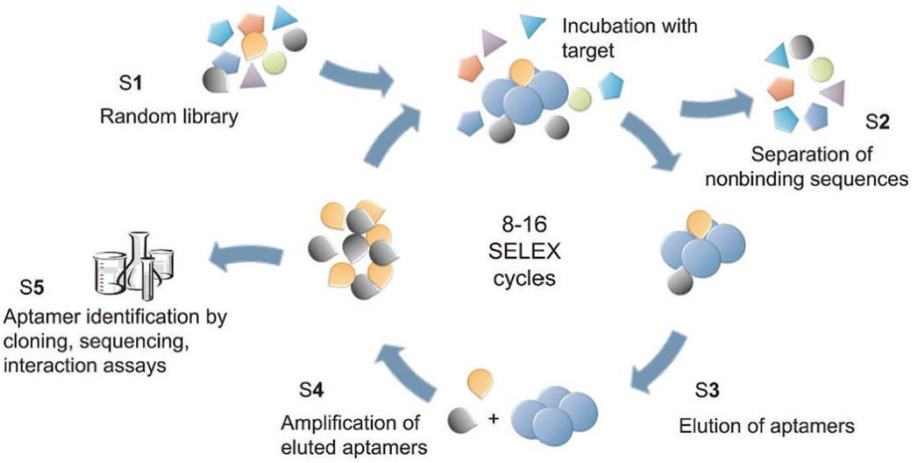

Figure 2. Scheme of the SELEX process. Adapted from Blind & Blank 2015 [29].

After the cell-SELEX process, the selected specific aptamer for the TAS1R3 receptor was: a preliminary one, the 49F, which sequence is: GCGGATGAAGACTGGTGTGCCAATAAACCATATCGCCGCGTTAGCATGTACTCGGTTGGCCCTAAATACGAGCAAC ; and the final one, the 5F, which sequence is: 5'-NH2-AGACAAGTGCTGGGAGATGGATTGGTTGTTGGTTGGGGTGGGTCTGGTTGGGGGCTTCACTTTCCCATTCCGCATT-3'. The aptamers were acquired from biomers.net (Ulm, Germany).

2.7. Nanosystems formulation and physicochemical and morphological characterization

Nanosystems were formulated and functionalized with the aptamer sequence (5'-NH2-TAS5F or 5'-NH2-TAS49F) following 1-ethyl-3-(-3-dimethylaminopropyl) carbodiimide hydrochloride (EDC) reaction. Briefly, DSPE-PEG-COOH solution (1 µg/µL) was suspended in water and incubated

with EDC (1 µg/µL, dissolved in water) with an excess of 100:1 EDC:aptamer, for 15 minutes under stirring (360 rpm) in order to activate the COO-terminal. Then, reaction was followed by adding 5'-NH_2-aptamer TAS5F (10 µM), previously denatured at 95 °C and allowed to assume binding conformation during snap-cooling on ice. The reaction took place during 2 hours at room temperature (RT), under continuous and vigorous stirring leading to formation of covalent carbodiimide binding. EDC works as a catalyzer and needs to be removed after conjugation to prevent the reversibility of the reaction. Thus, ultrafiltration by using Amicon filters 10 kDa (10,000 g, 5 minutes, 15 °C, washed with ultrapure water) was followed. Once the conjugated PEG-aptamer was purified, nanosystem were prepared following the ethanol injection method. Briefly, VE and sphingomyelin were dissolved in ethanol at concentrations of 200 mg/mL and 40 mg/mL, respectively, and added to the aptamer conjugate so the resulting formulation ratio was 1:0.1:0.01 (VE:SM:PEG). This ethanol solution was injected to aqueous phase (containing the PEG-aptamer conjugate) into a ratio 1:10 (organic phase:aqueous phase) resulting into a white emulsion immediately. After softly up and down pipetting, nanosystems were spontaneously formed. The functionalized (SNs-5F, SNs-49F) and non-functionalized SNs physicochemical characterization was performed using the Zetasizer NanoZS® (Malvern Instruments, Worcestershire, UK). Samples were diluted 1:10 in MilliQ water and analyzed in disposable microcuvettes (ZEN0040, Malvern Instruments) by dynamic light scattering (DLS) for size and Polydispersity Index (PDI) measures. For Zeta Potential measurements, samples were diluted 1:40 and analyzed by Laser Doppler anemometry (LDA) using folded capillary cells cuvettes (DTS 1070, Malvern Instruments).

Morphological examination was performed by Scanning Transmission Electron Microscopy (STEM) and images were obtained using a JEOL JEM-2010 High-Resolution Microscope (Peabody, MA, USA), operating between 120 – 200 kV accelerating voltage and configure with high brightness LaB6 filament. Preparation of STEM samples was performed as follows: nanoemulsions were firstly diluted 1:10 in filtered MilliQ water, mixed with 2% (w/v) phosphotungstic acid for staining and 10 µL were placed on a copper grid for 2 minutes. After drying overnight under vacuum, samples were washed with 0.2 mL of filtered water and dried under vacuum until analysis.

2.8. Uptake evaluation in spheroids

A549 WT and TAS1R3+ adherent cells were washed with PBS and detached with Trypsin 1X for 7-8 minutes at 37 °C. The cellular suspension was centrifugated at 1200 rpm for 5 minutes, the supernatant was discarded, and spheroids medium was added to the pellet. The spheroid medium is composed by: RPMI 1640 medium, P/S (2%), NEAA (1/1000), BSA (0,4%), bFGF (20ng/µl), EGF (50ng/µl) and ITS (1/1000). Cells were seeded in 6-well ultra-low attachment plates at a concentration of 10.000 cells/mL. After 4 days of culture, Cy5-labelled SNs-49F were added to the spheroids at a concentration of 0.2 µg/mL of Cy5 and 312 nM of aptamer. After 6 hours of incubation, spheroids were attached to a slide using the Cytospin™ 4 (Thermo Fisher Scientific, Massachusetts, USA). After that, cells were fixed with 4% paraformaldehyde (PFA), nuclei were stained with DAPI and cell membranes with WGA Alexa Fluor™ 488. Results were evaluated by confocal microscopy (Confocal microscope SP8, Leica, Wetzlar, Germany).

2.9. Flow cytometry assays

A549 cells, both WT and TAS1R3+, were cultured in 6-well plates for 24 hours, with a concentration of 300.000 cells/well. After 24 hours, they were treated with SNs and SNs-5F (50 nM) for 20 minutes. After wash the cells twice with PBS, Accutase® was added, for 10 minutes at RT, to detach them. The cellular suspension resultant was centrifuged at 200 xg for 5 minutes. The supernatant was discarded, and the pellet was washed and resuspended with PBS. The next step was a centrifugation, at 200 xg for 5 minutes, followed by the elimination of the supernatant. The resultant pellet was resuspended in 500 µL of fresh PBS and transferred to a FACS tube. To perform this evaluation, in each experiment (n=2) conditions there were between 2 and 3 replicas.

Obtained samples were assessed by the flow cytometer fACS Aria IIu, (BD Biosciences, NJ, USA); and the results were analyzed by the Software FACS Diva 6.02 (BD Biosciences, NJ, USA).

The statistical analysis was performed with the GraphPad Prism® software (version 8.0.2) (San Diego, United States). Due to the normal distribution of the data set, Two-tailed Student's t-test with Welch's correction was used to compare significant differences between two groups. P values considered significant are *($p \leq 0.05$), **($p \leq 0.01$), ***($p \leq 0.001$) and ***($p \leq 0.0001$); $\alpha = 0.05$.

2.10. Microfluidic devices design, fabrication, and cell culture

The design, fabrication, and characterization of the OOC microfluidic devices were performed by the Medical Devices group of the International

Iberian Nanotechnology Laboratory (INL) (Braga, Portugal) led by Lorena Diéguez [30].

The microfluidic devices were designed making use of CleWin4 from WieWeb Software (Hengelo, The Netherlands). The chips are composed by two 68 mm long and 600 µm wide microchannels, connected by an array of 100 µm micropillars with 5 µm gaps are in between. With the aim of avoiding the collapse of the microchannels, circular pillars are disposed along them. At the end of the microchannels, marks were included for the perforation of reservoirs (Figure 3).

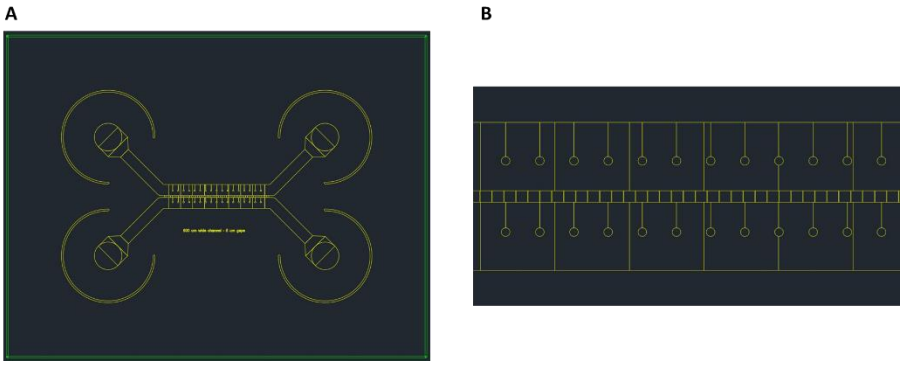

Figure 3. Design of the devices. **A.** the complete chip; **B.** details of the micropillars.

The silicon mold was produced by photolithography (Figure 4A); and replicas were fabricated by soft in polydimethylsiloxane (PDMS). The PDMS polymer was prepared following the protocol of the SYLGARD™ 184 Silicone Elastomer Kit (Dow, Michigan, United States) in a 10:1 ratio (elastomer:curing agent). After mixing the two components, the PDMS was degassed and placed onto the wafer mold at 65 °C overnight, to cure the polymer. The PDMS devices were removed from the mold and 5 mm diameter reservoirs were made using a biopsy punch (Kai Medical, Seki, Japan).

A thin layer of PDMS (1 mm height) was also prepared in a 150 mm dish, following the same protocol. The flat PDMS and the replica were irreversibly bonded after a high power 30-second treatment with oxygen plasma using the Plasma Cleaner PDC-002-CE (Harrick Plasma, Ithaca, United States) (Figure 4B).

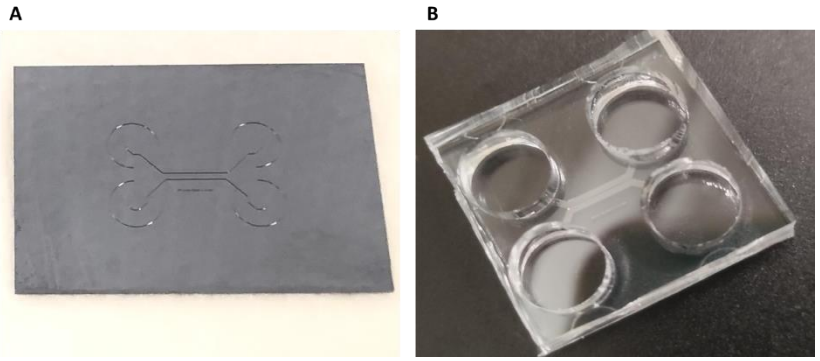

Figure 4. **A.** Silicon wafer mold. **B.** A ready to use PDMS device, adapted from Martins *et al.* 2022 [30].

Devices were sterilized by introducing 70% ethanol in the microchannels and exposing to ultra-violet (UV) light following by washing with PBS and filtered MilliQ water. With the aim of functionalizing the surface of the devices, Sulfo-SANPAH (0.5 mg/mL) solution in filtered MilliQ water was injected into the channels and incubated for 30 minutes with UV irradiation (365 nm) at a distance of 5 cm or less. The channels were washed with filtered MilliQ water and PBS.

A solution of Fibronectin (30 µg/mL) was placed into the endothelial channel of the device. A549-TAS1R3+ eGFP cells were detached from the culture flask and a cellular suspension of 10 x10^6 cells/mL was mixed 1:1 with ECM gel (4 mg/mL) and added into the cancer channel of the device. Chips

were incubated for 1 hour at 37 °C to achieve the polymerization of the ECM gel. After this, the cancer channel, as well as the reservoirs were filled with RPMI medium.

On next day, HPMEC cells were detached from the culture flask and added to the endothelial channel with a concentration of 5 x10^6 cells/mL. The devices were incubated at 37 °C for 4 hours in a 90° angle, to encourage the formation of an endothelial monolayer against the micropillars and make the barrier between the channels. After that, the inlet reservoir of the endothelial channel was filled with media for gravity-driven perfusion. Cells were cultured inside the channels for 5 days at 37 °C to achieve optimal conditions. Media was replaced every day with fresh one.

2.11. Toxicity evaluation

With the aim of evaluating the toxicity of the nanosystems (SNs and SNs-5F) in the endothelial cells, the AlamarBlue™ Cell Viability Reagent was used, which is based on resazurin [31].

HPMEC cells were seeded in 96-well plates and after 24 hours, they were incubated with the SNs treatment (25 and50 nM of aptamer) for 30 minutes and 12 hours. Next, the AlamarBlue™ reagent was added, and the result was evaluated by the FLUOstar OPTIMA microplate reader (BMG Labtech, Ortenberg, Germany). The percentage of viability obtained was calculated subtracting the background and normalizing the data to the untreated control.

2.12. Organ-on-a-chip experiments

After 3 days of cell seeding, the microfluidic devices were evaluated by confocal microscopy to confirm the correct growth of the two different cell lines. To prepare the chips, they were washed with warm PBS before fixation with PFA 4% for 15 minutes, followed by rinsing with cold PBS. Cells were permeabilized with 0.2% Triton X-100 for 10 minutes and a following wash with PBS. Devices were incubated with Blocking Buffer (2% BSA in PBS, w/v) for 45 minutes. Cells were incubated overnight with phalloidin-TRITC (0.1 µg/mL) at 4 °C, with the aim of labeling the actin filaments of endothelial cells. The next step was rinsing the devices with PBS and incubating them with Hoechst 33342 or DAPI (1 µg/mL) for 15 minutes, to stain the nuclei. Results were evaluated by the Zeiss confocal microscopy (Oberkochen, Germany).

With the aim of evaluate the SNs-5F behavior, in 5 days post-seeding devices, the endothelial medium was replaced with a suspension of SNs-5F, in fresh 199 medium, which was placed in only one of the reservoirs. The devices were incubated for 12 hours at 37 °C and flow was induced by gravity-driven perfusion in the endothelial channel. The SNs were labeled with Cy5 (2 ug/mL) and the work concentration was 50 nM of aptamer. After incubation, chips were fixed as previously described. The results were evaluated by confocal microscopy with the Leica SP5 Confocal Microscope (Leica Microsystems, Wetzlar, Germany).

3. RESULTS AND DISCUSSION

3.1. Transfected cell line

With the aim of increase the presence of the TAS1R3 receptor, the A549 cell line was lentivirally transfected with a plasmid encoding the receptor gene. Moreover, the plasmid also encodes for the eGFP protein, as well as the FLAG™ tag. The FLAG™ tag is a fusion protein peptide developed in 1988 by Hopp *et al.*, which is composed by AspTyrLysAspAspAspAspLys [32,33]. These 8 amino acids of the FLAG™ tag allow the alternative use of the TAS1R3 protein for molecular techniques, such as western blot [32]. In addition, the plasmid contains genes for resistance to antibiotics, specifically ampicillin and puromycin, that allow bacterial and cellular selection, respectively [34,35].

After the lentiviral transfection of the TAS1R3-FLAG plasmid, the cells were selected with puromycin to ensure the only presence of transfected cells. The correct selection was evaluated by fluorescent microscopy, with the Zeiss™ Axio Vert.A1 FL-LED Inverted Microscope (Oberkochen, Germany). The result obtained show a high expression of the eGFP protein in the cells (in green), meaning an efficient plasmid transfection (Figure 5A).

Furthermore, the expression of the TAS1R3 gene was assessed by RT-PCR. The results demonstrate that the mRNA of our target gene is overexpressed in the transfected cell line, compared with the wild type (WT) cell line (Figure 5B). This verifies the correct transfection of the plasmid, as well as, the correct expression of the interest gene, TAS1R3.

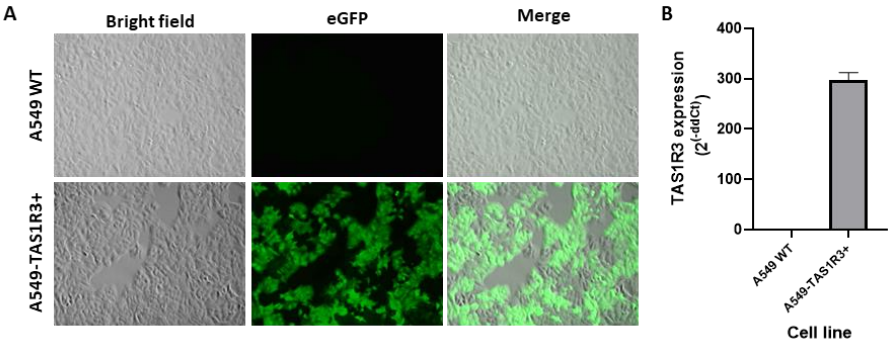

Figure 5. A. Fluorescent image of the eGFP expression in the transfected and non-transfected A549 cells; **B.** Expression of the TAS1R3 gene.

3.2. Nanosystems characterization

The SNs developed by our group [13] were modified with the addition of PEG to achieve an efficient conjugation of the aptamers. There are different strategies to conjugate aptamers to nanosystems, which can be covalent and non-covalent and direct or indirect conjugations. The most common reaction is the covalent and direct, which is based on the reaction between a functional group of the aptamer and another of the nanosystem surface [36]. We followed this last approach. The functional groups selected were the amino of the aptamer and the carboxylic acid of the PEG, and the conjugation was performed through an EDC reaction (Figure 6). After this conjugation, the formulation of the nanosystems was carried out following the ethanol injection method.

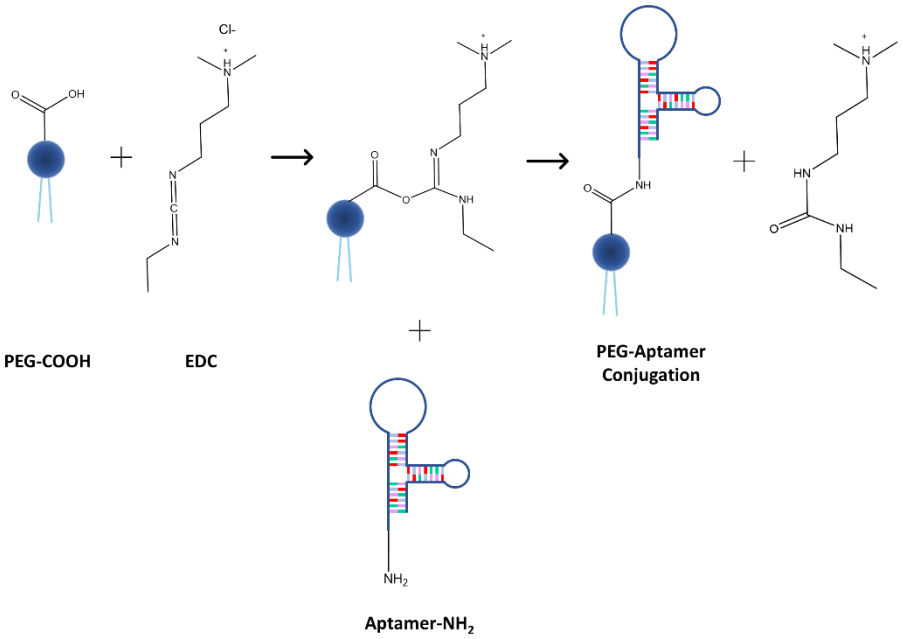

Figure 6. EDC reaction for the conjugation of the aptamer to the PEG molecule [37].

Plain SNs, PEGylated SNs and the functionalized SNs (SNs-5F and SNs-49F) were characterized making use of the Zetasizer® Nano ZS. The main effect of the addition of the PEG is the decrease in the zeta potential, going from neutral (-1.2±0.4 mV) to negative values (-25.2±0.6 mV) due to the carboxylic acid groups present in this molecule (Table 1). Similarly, the aptamer conjugation has also an impact in the superficial charge of the SNs becoming more negative (-36.6±1.6 mV). This occurs due to the negative charges of the phosphate groups present in the nucleic acids, and similar results are also observed for other aptamer-functionalized nanosystems [38]. In terms of size, there is a growth after the functionalization of the aptamer (from 138 ±1 for SNs to 195 ± 5 nm for SNs-5F). This increase could be due to the conformed structure of the aptamers disposed in the surface of the SNs, what

matches with similar works [39]. SNs-49F physicochemical results are in accordance with the ones obtained with the SNs-5F. In all cases, the SNs population demonstrated to be homogeneous in view of the low PdI, which remains under 0.1.

Table 1. Physiochemical characterization of the SNs, including the PEG and the aptamer. Values are expressed as mean ± standard deviation, n = 3.

Formulation	Size (nm)	PDI[a]	ZP[b] (mV)
SN (VE:SM)	158 ± 5	0.07	-1.2 ± 0.4
SN (VE:SM:PEG-COOH)	138 ± 1	0.04	-25.2 ± 0.6
SN:apTAS5F-NH_2	195 ± 5	0.08	-36.6 ± 1.6
SN:apTAS49F-NH_2	211 ± 7	0.05	-33 ± 0

[a]PdI, polydispersity index; [b]ZP, zeta potential.

The colloidal stability of the formulations was evaluated for up to 20 days at 4 °C. The results show the maintenance of the size, as well as the PdI, demonstrating an efficient stability (Figure 7A). These results are in agreement with previous studies in our group [13,15,17].

Furthermore, the stability was also assessed in different culture media, RMPI 1640 and DMEM, both supplemented and non-supplemented with FBS, at 37 °C up to 24 hours (Figure 7B, 7C). The outcomes show a minimum slight increase in all cases sizes, proving the efficient stability of the nanosystems in culture media conditions. Of relevance is the fact that stability is slightly improved in complete media, with FBS. This improvement in the stability could be explained by the presence of different proteins in the FBS, which can form the protein corona surrounding the SNs. It was previously reported the

capacity of the protein corona to improve the stability of lipidic nanosystems and inhibit agglomeration [40–42]. Taking into account these results, the SNs were evaluated in complete medium in the following assays.

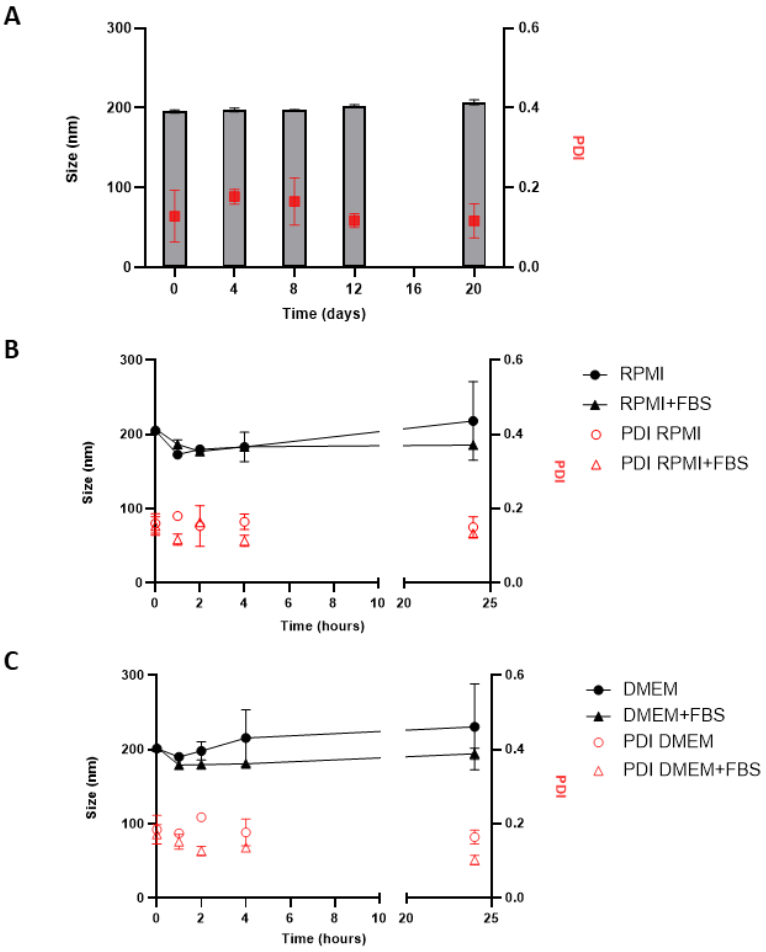

Figure 7. Stability of SNs-5F in media of interest. **A.** Colloidal stability at 4 °C up to 20 days; **B.** Stability in RPMI cell culture medium, with and without FBS, at 37 °C up to 24 hours; **C.** Stability in DMEM cell culture medium, with and without FBS, at 37 °C up to 24 hours. **Abbreviations:** PdI, polydispersity index; DMEM, Dulbecco′s Modified Eagle′s Medium; RPMI, Roswell Park Memorial Institute (RPMI) 1640

Medium; FBS, Fetal Bovine Serum. Values are expressed as mean ± standard deviation, n = 3.

In addition, STEM images demonstrated a spherical structure of both SNs with and without aptamer conjugation, as well as a homogeneous size distribution (Figure 8).

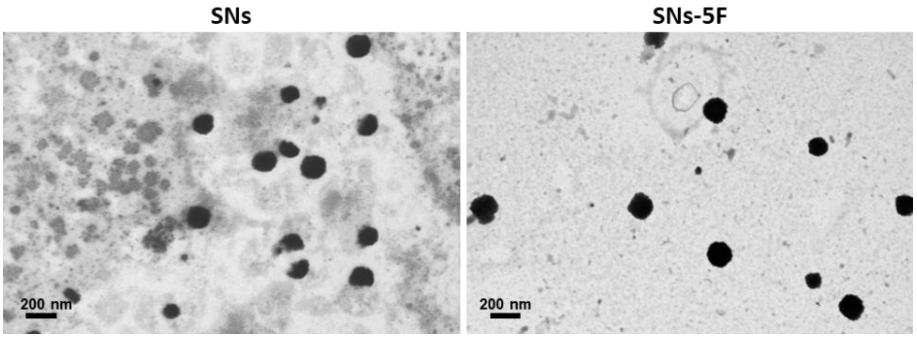

Figure 8. Scanning Transmission Electron Microscopy (STEM) images of the functionalized (SNs-5F) and non-functionalized nanosystems (SNs).

3.3. Uptake evaluation

The capacity of functionalized SNs to be internalized by NSCLC cells was evaluated by confocal microscopy in A549, WT and TAS1R3+, 3D cultures, as a proof of concept. In this case, a preliminary specific aptamer for TAS1R3 (49F) was used. After a 6-hour incubation period, the samples were evaluated by the Leica SP8 Confocal Microscope (Leica Microsystems, Wetzlar, Germany).

Results demonstrate an efficient internalization of SNs-5F, both A549 WT and TAS1R3+ spheroids, proving their capacity to penetrate into the inner parts of the spheroid (Figure 9). Visual differences between cell lines are not

perceived, probably due to the long incubation time, 6 hours. As previously works of the group described, after 4 hours, almost every SNs were internalized by cells, however, this evaluation demonstrated the internalization efficiency of the SNs [21]. Next experiments (Section 3.4), with smaller incubation times will evaluate the specific targeting of the aptamer.

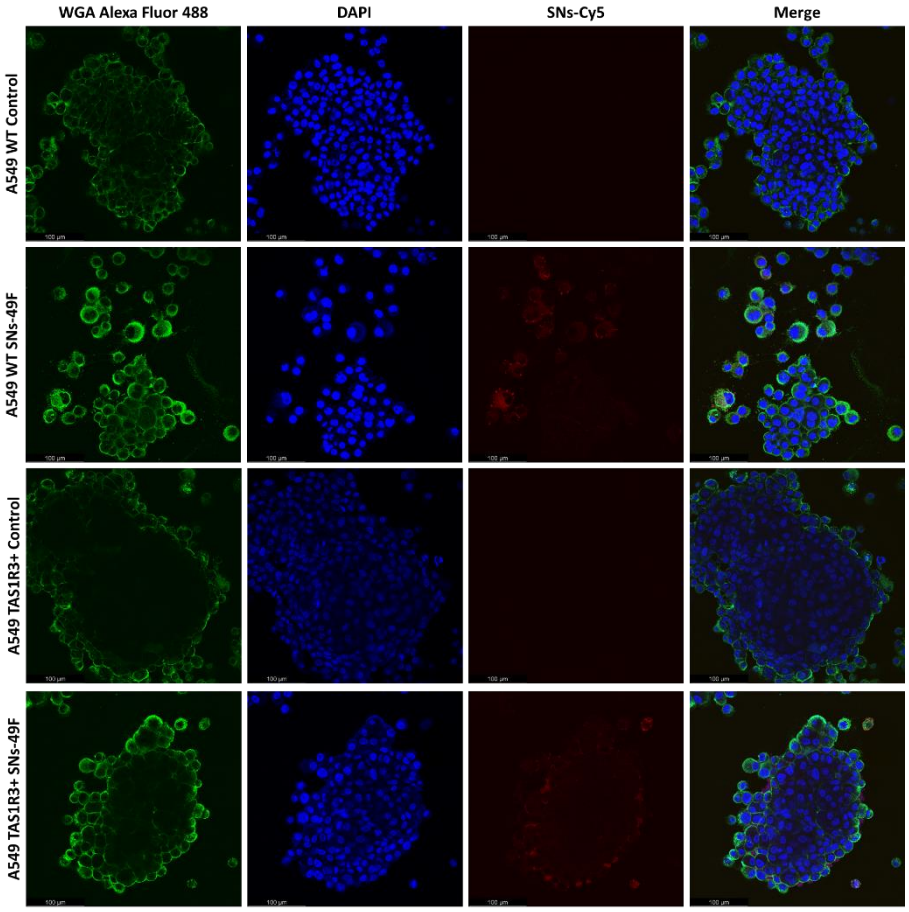

Figure 9. Confocal images of A549 WT and TAS1R3+ spheroids. Nuclei are stained with DAPI (in blue); cell membranes are stained with WGA Alexa Fluor™ 488 (in green); and SNs-49F are labelled with Cy5 (in red). Images are middle sections of a Z stack. Scale bar: 100 µm.

3.4. Flow cytometry assays

The correct and specific targeting of the aptamer with the TAS1R3 receptor was evaluated by flow cytometry, in presence of FBS. Monolayer cell cultures of A549 WT and A549-TAS1R3+ cells were treated with blank SNs and SNs-5F, both labeled with Cy5, for 20 minutes. After being detached in single cells, the analysis of fluorescent cells was performed by flow cytometry.

As shown in Figure 10, the percentage of Cy5 positive cells, correlated with the positive internalization of Cy5-labelled SNs, was about a 25% in the case of A549 WT cells, both with blank SNs and SNs-5F, and also in the A549-TAS1R3 cells incubated with the blank SNs. Importantly, targeted SNs-5F were more efficiently internalized in the transfected A549-TAS1R3+ cell line. There is an increase of about a 10% in the internalization of the SNs-5F, reaching more than a 35% after 20 minutes of incubation. These statistically significant results demonstrate a specific TAS1R3 targeting of the functionalized SNs, due to its increasing uptake in the cells which overexpressed the receptor.

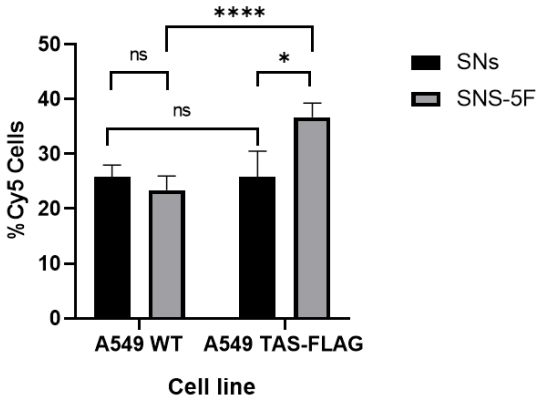

Figure 10. Cellular uptake of plain SNs and SNs-5F in A549 WT and TAS1R3+ evaluated by flow cytometry. Values are expressed as mean ± standard deviation, n = 2. Statistical analysis was performed using Two-tailed Student's t-test was used to compare significant differences between two groups. *($p \leq 0.05$), **($p \leq 0.01$), ***($p \leq 0.001$) and ****($p \leq 0.0001$).

This increased internalization result of the aptamer-functionalized SNs-5F is in line with other nanosystems that also use aptamers to target specific cell subpopulations. A recent example is the work of Wei *et al.*, which explain the development of multifunctional nanoprobes, fluorescent and magnetic, for cancer cells detection, making use aptamers to target specific liver cancer cells. They achieved an increased internalization of aptamer-functionalized nanoparticles of Fe_3O_4 core with fluorescent SiO_2 shell into these specific cells [43]. Another example was performed by Agnello *et al.*, who developed polymeric nanovectors for targeting triple negative breast cancer cells. The use of specific aptamers to target EGFR cells demonstrate a specific internalization of the nanovectors in these cells [44]. These outcomes, among others, prove the value of aptamers to be efficient ligands for, not only targeted therapy, but also for cancer diagnosis. Our results confirm that SNs can be

targeted to cells overexpressing TAS1R3 following a surface-decoration strategy with ligands specifically designed for this purpose. Next steps aimed to explore the behavior of the targeted nanosystems in a more complex model that better mimics the structure and microenvironment of the real tumor.

3.5. OOC experiments

With the aim of developing an *in vitro* proof of concept of the behavior of the functionalized SNs, an OOC microfluidic device was developed. This chip has two microchannels, one with A549-TAS1R3+ NSCLC cells, and the with other pulmonary microvascular endothelial cells, HPMEC. The cancer channel was designed to mimic the tumor, while the endothelial channel recreates the blood vessels and represents the biological barrier that the nanosystems have to cross to reach their targeted cells [45]. After 1-day post-seeding, endothelial and cancer cells started to grow in the microchannels (Figure 11), while only a small presence of dead cells was found, which is normal, as it also happens in 2D cell culture. As a result, the cells are able to proliferate successfully and achieve the correct structure.

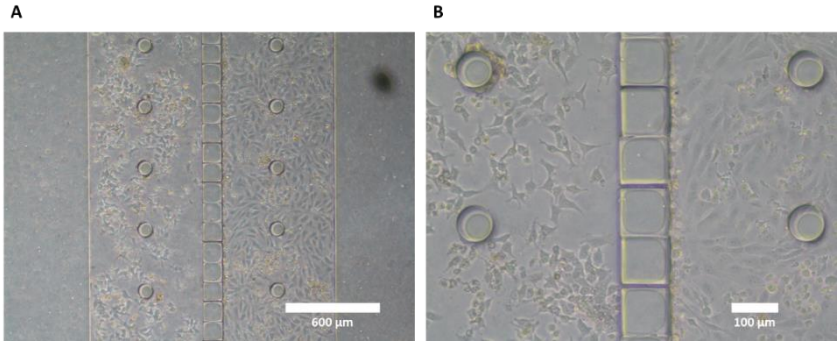

Figure 11. Bright field image of a 1-day post-seeding chip. At the left, the ECM gel-embedded cancer cells (A549-TAS1r3+); and at the right, the monolayer of endothelial cells (HPMEC). **A.** 4x; **B.** 10x.

Two days after, the devices were analyzed by confocal microscopy to evaluate the growth of both cell lines. The A549-TAS1R3+ cancer cells were cultured embedded in ECM gel and, as shown in the Figure 12, they proliferated efficiently in a 3D structure, mimicking the tumor architecture.

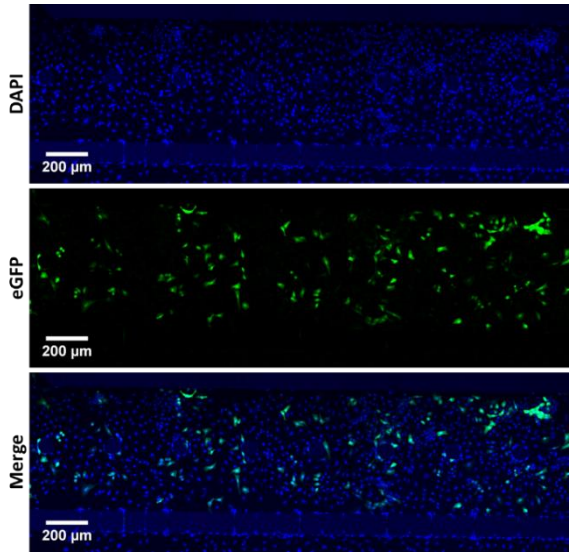

Figure 12. Confocal images of the A549-TAS1R3+ cancer cells in the microchannel after 3 days of culture. Nuclei are stained with DAPI (in blue); A549-TAS1R3+ cells are labelled with eGFP (in green). Images are maximum projection.

In the same way, HPMEC endothelial cells also show a successful proliferation in the microchannel after 3 days of culture, due to a fibronectin coating and a gravity flow perfusion (Figure 13). The cells proved to form a monolayer along the microchannel, mimicking the tubular structure of the blood vessels. Importantly, cells efficiently grew forming an endothelial barrier, which is key to evaluate the SNs behavior.

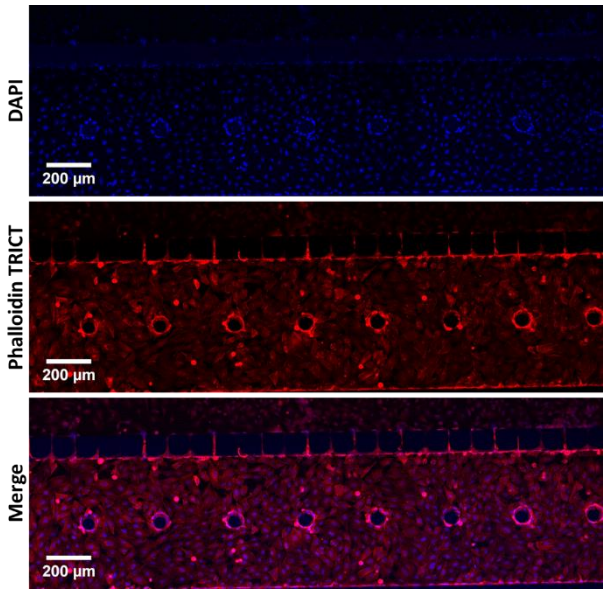

Figure 13. Confocal images of the HPMEC endothelial cells in the microchannel after 3 days of culture. Nuclei are stained with DAPI (in blue); HPMEC cells' actin filaments are stained with phalloidin TRICT (in red). Images are maximum projection.

As a preliminary step prior starting with the SNs in OOC experiments, the toxicity of SNs in HPMEC cells were evaluated. The non-toxicity in the endothelial cells is key to ensure the integrity of the barrier to correctly mimic the interactions with the SNs. AlamarBlue™ was the selected assay to assess the toxicity of cells previously treated with SNs, with and without aptamer (SNs and SNs-5F). The toxicity was evaluated at two different time points: 30 minutes and 12 hours; and at two aptamer concentrations: 25 nM and 50 nM.

The results presented in the Figure 14 proved that the formulations do not have an impact on the viability of HPMEC cells at the tested concentrations, and irrespectively of the incubation time.

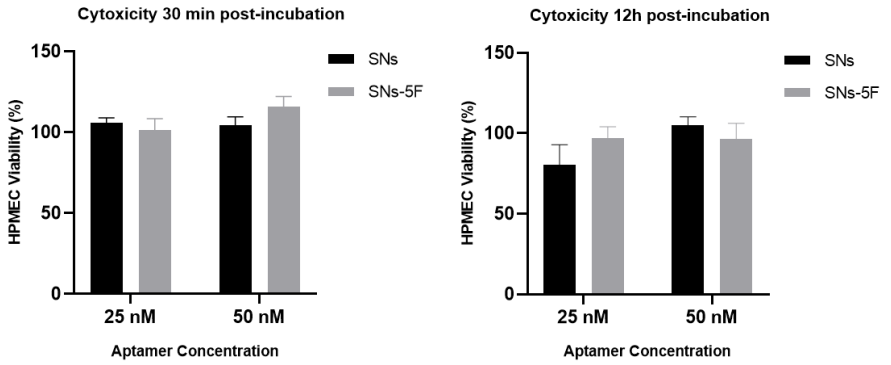

Figure 14. Cytotoxicity evaluation of the functionalized and non-functionalized SNs in HPMEC cells, ate different time points and concentrations. Values are expressed as mean ± standard deviation, n = 6.

These results were somehow expected according to previous results of SNs in colorectal cancer cells (SW480), pancreatic cancer cells (MiaPaCa2) and breast cancer cells (MCF7) [13,21]. This lack of toxicity is highly important for the correct maintenance of the endothelial barrier integrity mimicked in the device. The structural integrity of the endothelial barrier is directly associated with the permeability of the vascular vessel and, this is key for *in vivo* homeostasis [46,47]. Because our aim was to observe the capacity of SNs to cross the barrier to reach the targeted cells, the correct structure of the vasculature channel after the interaction with the SNs ensures that the following OOC experiments will demonstrate truthful results.

Next experiment was designed to assess the ability of SNs-5F to overcome the endothelial barrier and reach the targeted cells in a non-static environment. To achieve that, SNs-5F and SNs, as a control, were mixed with medium and placed in the endothelial channel for gravity flow perfusion, in a device cultured for 5 days. After a 12-hour incubation, the resultant chips were

stained with Hoechst to label the nuclei. The results were evaluated by confocal microscopy with the Leica SP5 Confocal Microscope (Leica Microsystems, Wetzlar, Germany). Figure 15 shows the presence of SNs-5F (in cyan) in the gaps that separate the micropillars. This fact suggests that the functionalized SNs were crossing the micropillars that divide the endothelial and cancer channels. Further experiments with increased incubation times and different SNs concentrations are necessary to completely understand the behavior of the SNs facing an endothelial barrier to reach their targeted cells.

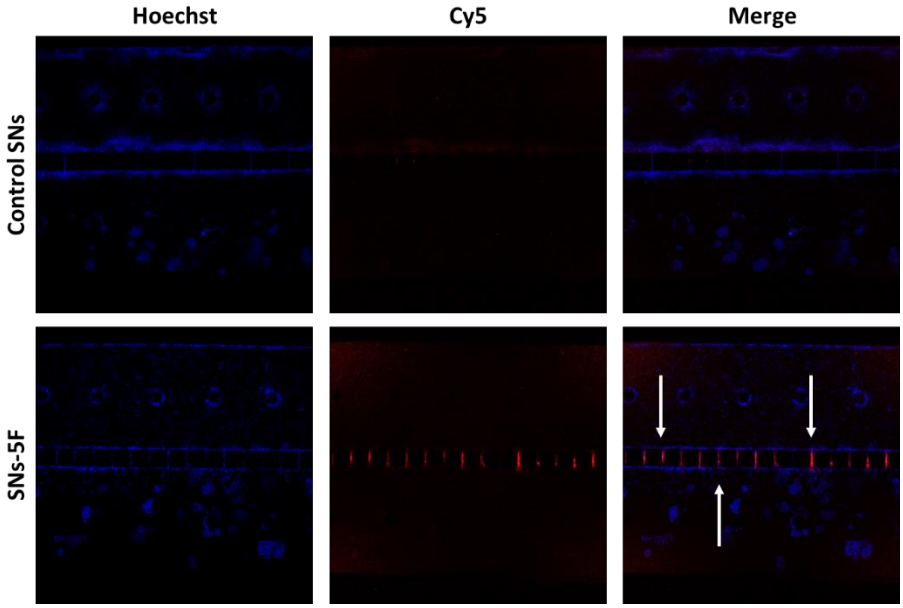

Figure 15. Confocal images of the behavior evaluation of targeted SNs-5F in OOC microfluidic devices. Nuclei are stained with Hoechst (in blue); and SNs and SNs-5F are labeled with Cy5 (in red). The upper channel is the endothelial one, and the bottom channel is the cancer one. SNs-5F are present in the gaps (white arrows).

4. CONCLUSIONS

We have successfully conjugated aptamers with SNs with the aim of targeting TAS1R3 positive NSCLC cells, as a strategy to target metastasis. The resultant nanosystems present not only a great colloidal stability, but also a maintained stability in relevant biological media. The targeting ability of surface-decorated SNs was successfully demonstrated in 2D cell culture models. OOC devices demonstrated their ability to recreate the tumor structure. Surface-decorated SNs could be tracked in the non-static OOC microfluidic platforms. OCC demonstrated to be an accurate model to evaluate the SNs capacity to cross biological barriers. Further experiments making use the OOC microfluidic technology are needed to fully characterize the SNs behavior and their efficient targeting in a more complex model.

BIBLIOGRAPHY

1. Drapela, S. & Gomes, A. P. Metabolic requirements of the metastatic cascade. *Curr Opin Syst Biol* **28**, (2021).

2. Ganesh, K. & Massagué, J. Targeting metastatic cancer. *Nat Med* **27**, 34 (2021).

3. Sung, H. *et al.* Global Cancer Statistics 2020: GLOBOCAN Estimates of Incidence and Mortality Worldwide for 36 Cancers in 185 Countries. *CA Cancer J Clin* **71**, 209–249 (2021).

4. Thai, A. A., Solomon, B. J., Sequist, L. V., Gainor, J. F. & Heist, R. S. Lung cancer. *The Lancet* **398**, 535–554 (2021).

5. Simeone, J. C., Nordstrom, B. L., Patel, K. & Klein, A. B. Treatment patterns and overall survival in metastatic non-small-cell lung cancer in a real-world, US setting. *Future Oncology* **15**, 3491–3502 (2019).

6. Min, H. Y. & Lee, H. Y. Mechanisms of resistance to chemotherapy in non-small cell lung cancer. *Archives of Pharmacal Research 2021 44:2* **44**, 146–164 (2021).

7. Waqar, S. N. *et al.* Non-small cell lung cancer with brain metastasis at presentation. *Clin Lung Cancer* **19**, e373 (2018).

8. Fu, Z. & Xiang, J. Aptamer-Functionalized Nanoparticles in Targeted Delivery and Cancer Therapy. *Int J Mol Sci* **21**, 1–39 (2020).

9. Guan, B. & Zhang, X. Aptamers as versatile ligands for biomedical and pharmaceutical applications. *Int J Nanomedicine* **15**, 1059–1071 (2020).

10. Sinitsyna, V. V. & Vetcher, A. A. Nucleic Acid Aptamers in Nanotechnology. *Biomedicines* **10**, (2022).

11. Fu, Z. & Xiang, J. Aptamers, the nucleic acid antibodies, in cancer therapy. *Int J Mol Sci* **21**, (2020).

12. Farokhzad, O. C. *et al.* Nanoparticle-Aptamer BioconjugatesA New Approach for Targeting Prostate Cancer Cells. *Cancer Res* **64**, 7668–7672 (2004).

13. Bouzo, B. L., Calvelo, M., Martín-Pastor, M., García-Fandiño, R. & de La Fuente, M. In Vitro- In Silico Modeling Approach to Rationally Designed Simple and Versatile Drug Delivery Systems. *Journal of Physical Chemistry B* **124**, 5788–5800 (2020).

14. Nagachinta, S., Bouzo, B. L., Vazquez-Rios, A. J., Lopez, R. & de la Fuente, M. Sphingomyelin-based nanosystems (SNs) for the development of anticancer miRNA therapeutics. *Pharmaceutics* **12**, (2020).

15. Bouzo, B. L. *et al.* Sphingomyelin nanosystems loaded with uroguanylin and etoposide for treating metastatic colorectal cancer. *Sci Rep* **11**, 17213 (2021).

16. Saraiva, S. M. *et al.* Edelfosine nanoemulsions inhibit tumor growth of triple negative breast cancer in zebrafish xenograft model. *Sci Rep* **11**, (2021).

17. Bidan, N. *et al.* Before in vivo studies: In vitro screening of sphingomyelin nanosystems using a relevant 3D multicellular pancreatic tumor spheroid model. *Int J Pharm* **617**, (2022).

18. Cascallar, M. *et al.* Zebrafish as a platform to evaluate the potential of lipidic nanoemulsions for gene therapy in cancer. *Front Pharmacol* **13**, 4602 (2022).

19. Díez-Villares, S. *et al.* Biodistribution of 68/67Ga-Radiolabeled Sphingolipid Nanoemulsions by PET and SPECT Imaging. *Int J Nanomedicine* **16**, 5923 (2021).

20. Díez-Villares, S. *et al.* Manganese Ferrite Nanoparticles Encapsulated into Vitamin E/Sphingomyelin Nanoemulsions as Contrast Agents for High-Sensitive Magnetic Resonance Imaging. *Adv Healthc Mater* **10**, 2101019 (2021).

21. Jatal, R. *et al.* Sphingomyelin nanosystems decorated with TSP-1 derived peptide targeting senescent cells. *Int J Pharm* **617**, 121618 (2022).

22. Vázquez Ríos, A. J. Development of targeted therapeutic strategies for metastatic lung cancer. (Universidade de Santiago de Compostela, 2020).

23. Del Piccolo, N. *et al.* Tumor-on-chip modeling of organ-specific cancer and metastasis. *Adv Drug Deliv Rev* **175**, (2021).

24. Leung, C. M. *et al.* A guide to the organ-on-a-chip. *Nature Reviews Methods Primers 2022 2:1* **2**, 1–29 (2022).

25. Regmi, S., Poudel, C., Adhikari, R. & Luo, K. Q. Applications of Microfluidics and Organ-on-a-Chip in Cancer Research. *Biosensors (Basel)* **12**, (2022).

26. Carton, F. & Malatesta, M. In Vitro Models of Biological Barriers for Nanomedical Research. *Int J Mol Sci* **23**, 8910 (2022).

27. Collins, T. *et al.* Spheroid-on-chip microfluidic technology for the evaluation of the impact of continuous flow on metastatic potential in cancer models in vitro. *Biomicrofluidics* **15**, 44103 (2021).

28. Inoue, H., Nojima, H. & Okayama, H. High efficiency transformation of Escherichia coli with plasmids. *Gene* **96**, 23–28 (1990).

29. Blind, M. & Blank, M. Aptamer Selection Technology and Recent Advances. *Mol Ther Nucleic Acids* **4**, e223 (2015).

30. Martins, A. S. O. Engineering a metastasis-on-a-chip system towards studying cell invasion and drug efficacy in lung cancer. (Universidade do Minho, 2022).

31. Longhin, E. M., El Yamani, N., Rundén-Pran, E. & Dusinska, M. The alamar blue assay in the context of safety testing of nanomaterials. *Frontiers in Toxicology* **4**, 113 (2022).

32. Einhauer, A. & Jungbauer, A. The FLAG peptide, a versatile fusion tag for the purification of recombinant proteins. *J. Biochem. Biophys. Methods* **49**, 455–465 (2001).

33. Hopp, T. *et al.* A short polypeptide marker sequence useful for recombinant protein identification and purification. *Nature* **6**, 1204–1210 (1988).

34. Aviner, R. The science of puromycin: From studies of ribosome function to applications in biotechnology. *Comput Struct Biotechnol J* **18**, 1074 (2020).

35. Feizollahzadeh, S. *et al.* The Increase in Protein and Plasmid Yields of E. coli with Optimized Concentration of Ampicillin as Selection Marker. *Iran J Biotechnol* **15**, 128 (2017).

36. Fu, Z. & Xiang, J. Aptamer-functionalized nanoparticles in targeted delivery and cancer therapy. *Int J Mol Sci* **21**, 1–39 (2020).

37. Nakajima, N. & Ikada, Y. Mechanism of Amide Formation by Carbodiimide for Bioconjugation in Aqueous Media. *Bioconjug Chem* **6**, 123–130 (1995).

38. Jianghong, L. *et al.* Aptamer and Peptide-Modified Lipid-Based Drug Delivery Systems in Application of Combined Sequential Therapy of Hepatocellular Carcinoma. *ACS Biomater Sci Eng* **7**, 2558–2568 (2021).

39. Jianghong, L. *et al.* Aptamer and Peptide-Modified Lipid-Based Drug Delivery Systems in Application of Combined Sequential Therapy of Hepatocellular Carcinoma. *ACS Biomater Sci Eng* **7**, 2558–2568 (2021).

40. Bai, X., Wang, J., Mu, Q. & Su, G. In vivo Protein Corona Formation: Characterizations, Effects on Engineered Nanoparticles' Biobehaviors, and Applications. *Front Bioeng Biotechnol* **9**, (2021).

41. Singh, N. *et al.* In vivo protein corona on nanoparticles: does the control of all material parameters orient the biological behavior? *Nanoscale Adv* **3**, 1209–1229 (2021).

42. Francia, V., Schiffelers, R. M., Cullis, P. R. & Witzigmann, D. The Biomolecular Corona of Lipid Nanoparticles for Gene Therapy. *Bioconjug Chem* **31**, 2046–2059 (2020).

43. Wei, Z. *et al.* Multifunctional nanoprobe for cancer cell targeting and simultaneous fluorescence/magnetic resonance imaging. *Anal Chim Acta* **938**, 156–164 (2016).

44. Agnello, L. *et al.* Optimizing cisplatin delivery to triple-negative breast cancer through novel EGFR aptamer-conjugated polymeric nanovectors. *J Exp Clin Cancer Res* **40**, (2021).

45. Rodrigues, R. O. *et al.* Organ-on-a-Chip: A Preclinical Microfluidic Platform for the Progress of Nanomedicine. *Small* **16**, 2003517 (2020).

46. Dejana, E., Tournier-Lasserve, E. & Weinstein, B. M. The Control of Vascular Integrity by Endothelial Cell Junctions: Molecular Basis and Pathological Implications. *Dev Cell* **16**, 209–221 (2009).

47. Alimperti, S. *et al.* Three-dimensional biomimetic vascular model reveals a RhoA, Rac1, and N-cadherin balance in mural cell–endothelial cell-regulated barrier function. *Proc Natl Acad Sci U S A* **114**, 8758–8763 (2017).

CHAPTER III

Zebrafish as a platform to evaluate the potential of lipidic nanoemulsions for gene therapy in cancer

Adapted/extracted from Cascallar M *et al.*

Frontiers in Pharmacology, 2022, 13:1007018

Doi: 10.3389/fphar.2022.1007018

Zebrafish as a platform to evaluate the potential of lipidic nanoemulsions for gene therapy in cancer

María Cascallar[1,2,3], Pablo Hurtado[2,4], Saínza Lores[1,3], Alba Pensado-López[5,6], Ana Quelle-Regaldie[5], Laura Sánchez[5,7], Roberto Piñeiro[2,4] and María de la Fuente[1,2,3,8*]

[1]Nano-Oncology and Translational Therapeutics Group, Health Research Institute of Santiago de Compostela (IDIS), SERGAS, Santiago de Compostela, Spain

[2]Centro de Investigación Biomédica en Red Cáncer (CIBERONC), Madrid, Spain

[3]Universidade de Santiago de Compostela (USC), Santiago de Compostela, Spain

[4]Roche-Chus Joint Unit, Translational Medical Oncology Group, Oncomet, Health Research Institute of Santiago de Compostela, Santiago de Compostela, Spain

[5]Department of Zoology, Genetics and Physical Anthropology, Universidade de Santiago de Compostela, Campus de Lugo, Lugo, Spain

[6]Center for Research in Molecular Medicine and Chronic Diseases (CIMUS), Campus Vida, Universidade de Santiago de Compostela, Santiago de Compostela, Spain

[7]Preclinical Animal Models Group, Health Research Institute of Santiago de Compostela (IDIS), Santiago de Compostela, Spain

[8]DIVERSA Technologies S.L, Santiago de Compostela, Spain

ABSTRACT

Gene therapy is a promising therapeutic approach that has experienced significant growth in recent decades, with gene nanomedicines reaching the clinics. However, it is still necessary to continue developing novel vectors able to carry, protect, and release the nucleic acids into the target cells, to respond to the widespread demand for new gene therapies to address current unmet clinical needs. We propose here the use of zebrafish embryos as an *in vivo* platform to evaluate the potential of newly developed nanosystems for gene therapy applications in cancer treatment. Zebrafish embryos have several advantages such as low maintenance costs, transparency, robustness, and a high homology with the human genome. In this work, a new type of putrescine-sphingomyelin nanosystems (PSN), specifically designed for cancer gene therapy applications, was successfully characterized and demonstrated its potential for delivery of plasmid DNA (pDNA) and miRNA (miR). On one hand, we were able to validate a regulatory effect of the PSN/miR on gene expression after injection in embryos of 0 hpf. Additionally, experiments proved the potential of the model to study the transport of the associated nucleic acids (pDNA and miR) upon incubation in zebrafish water. The biodistribution of PSN/pDNA and PSN/miR *in vivo* was also assessed after microinjection into the zebrafish vasculature, demonstrating that the nucleic acids remained associated with the PSN in an *in vivo* environment, and could successfully reach disseminated cancer cells in zebrafish xenografts. Altogether, these results demonstrate the potential of zebrafish as an *in vivo* model to evaluate nanotechnology-based gene therapies for cancer treatment, as well as the capacity of the developed versatile PSN formulation for gene therapy applications.

1. INTRODUCTION

Over the past decades, gene therapy has flourished. The basis of this therapy is focused on the use of exogenous therapeutic nucleic acids (NAs) that have the capacity to modify the expression of disease-related genes. NAs involved in gene therapy are micro RNAs (miRs), small interfering RNAs (siRNAs), short hairpin RNAs (shRNAs), antisense oligonucleotides (ASOs) and DNA plasmids (pDNAs) [1].

One of the main limitations in the development of novel gene therapies is the need for efficient carriers capable of protecting and transporting them to their site of action. Viral vectors are the carriers that have moved most quickly to clinical trials, due to the ability of the virus to carry and protect the genetic material to specific cells [2,3]. Despite this, viral vectors accumulate several disadvantages, such as limitation in the length of the cargo (e. g. 10 kb in lentiviral vectors), insertional mutagenesis, and immunogenicity due to the antibodies against these common viruses produced throughout life [3–6]. In this sense, non-viral vectors have been proven to successfully resolve the limitations of viral vectors [3]. A clear example is nanomedicine, which arises from the application of nanotechnology in the field of biomedicine, providing several advantages for the intracellular delivery of macromolecules, such as NAs. As proof of this, in recent years several breakthroughs have taken place. In 2018, Onpattro® became the first FDA-approved lipid nanoparticle for gene therapy [7,8]. Additionally, in 2021, mRNA-based vaccines against Covid-19 reached the market [9,10], opening a new era for the engineering and application of gene therapy.

Despite the successful advances of the past few years, translating more gene nanomedicines from bench to bedside is still a challenge. In this sense, the use of robust preclinical models that can better predict the future behavior of nanosystems is essential for their development and validation, improving the translation process [11–15]. *In vivo* models are needed to evaluate biodistribution, toxicity and efficacy, among other parameters. Rodents, the most common animal model, have multiple advantages, such as anatomical and genomic similarities to humans. Nevertheless, they entail certain disadvantages, including the high cost of maintenance and small progeny that prevents the possibility of carrying out large studies [16,17]. A valuable alternative as an *in vivo* platform to evaluate the potential of nanomedicine is the zebrafish [18–21].

The use of the zebrafish (*Danio rerio*) in developmental biology and genetics studies dates back to the 1970s [22]. Since then, applications have expanded to study multiple human pathologies, such as cancer, as well as biodistribution, toxicity and pharmacological screening of new drugs [23]. The success of zebrafish in research is based on their biological characteristics [24]. Specifically, their small size enables easy handling, and large number of individuals can be maintained in optimal experimental conditions. Due to their short life cycle, the main organs develop practically within 48 hours, sexual maturity is reached at approximately 3 months of life, and large offspring allow large-scale studies to be carried out [25]. Additionally, the zebrafish reference genome has revealed that approximately 80% of the genes have a human orthologue related to diseases [26].

Based on these features, in the field of nanomedicine this model is being proposed to assess the biocompatibility and toxicity of several nanomaterials, but also to validate their therapeutic efficacy [17,18,21,27,28]. The presence in zebrafish of organs and metabolic pathways analogous to those of humans allows toxicological and biocompatibility evaluations, and the large number of offspring enables high-throughput and multi- and transgenerational screens [29]. In addition, the response of zebrafish to several substances has been reported to be concordant with that observed in mammalian models [30]. In the context of cancer, the transparency of embryos and the availability of fluorescently labelled transgenic zebrafish lines offer the possibility to track cancer cells in xenograft assays or genetic models and thus understand their behavior, dissemination, metastasis, extravasation, or interaction with the tumor microenvironment or immune cells [31–33]. On the other hand, the transparency of zebrafish allows the determination of the toxicity of nanosystems in different anatomical sites of the fish and their tracking to establish biodistribution and interaction profiles with tumor cells without the need for invasive techniques [34]. In this sense, transgenic zebrafish models allow for real-time tracking of tumor cells without the need to immunostain cells, thus avoiding non-specific labeling and imaging issues derived. As a consequence of the abovementioned, several nanomedicines have been developed and tested in zebrafish, including gene therapies [35–37].

In our group, we have previously developed different types of nanosystems for miR-based gene therapy for cancer treatment. These nanocarriers, protamine nanocapsules and sphingomyelin-based nanosystems, demonstrated their *in vitro* potential to interfere in the cancer process [38,39]. On subsequent studies by our group, Lores *et al.* developed putrescine-

sphingomyelin nanosystems (PSN) for cancer gene therapy applications establishing for the first time the use of the natural polyamine putrescine for the development of non-viral vectors, taking advantage of the cationic nature of this compound and the greater affinity of cancer cells for this type of molecules [40–42]. In this work, a therapeutic plasmid DNA (pDNA) encoding for the Fas Ligand protein, which promotes the activation of apoptotic pathways, was associated to PSN, and the potential of the developed formulation confirmed *in vitro*, in a triple negative breast cancer cell line (MDA-MB-231), and *in vivo*, in both a zebrafish embryo xenograft model and in an orthotopic mouse model after intraperitoneal and intravenous inoculation, evidencing a high correlation in terms of efficacy. Based on this data, the present work aimed to further demonstrate the potential of zebrafish embryos as an intermediate model between *in vitro* and *in vivo* mammalian models for the evaluation of novel gene therapies, using for this purpose PSN associated with two different types of nucleic acids, miR and pDNA [42].

2. MATERIALS AND METHODS

2.1. Materials

All the miRs used in this work (Table 1) were purchased from Eurofins Genomics (Ebersberg, Germany). Penicillin-Streptomycin, Hoechst 33342, DiI (1,1'-Dioctadecyl-3,3,3',3'-Tetramethylindocarbocyanine Perchlorate), agarose and SYBR Gold were provided by Thermo Fisher (Massachusetts, USA). C11 TopFluor Sphingomyelin (N-[11-(dipyrromethene boron difluoride)undecanoyl]-D-erythro-sphingosylphosphorylcholine was

purchased from Avanti Polar Lipids (Alabama, USA). Brilliant III Ultra-Fast SYBR Green QPCR Master Mix Kit was acquired from Agilent Technologies (California, USA). Nuclease-free water was provided by Corning (New York, USA). NYzol reagent was purchased from NZYtech (Lisboa, Portugal). Dulbecco′s Modified Eagle′s Medium (DMEM), Phosphate Buffered Saline (PBS), Tricaine methanesulfonate, Vitamin E (DL-α-Tocopherol), N-Phenylthiourea (PTU), Polyvinylpyrrolidone (PVP), Trypsin-EDTA Solution and MOWIOL® 4-88 Reagent were kindly provided by Merck (Darmstadt, Germany). Ethanol of analytical grade was purchase from VWR (Barcelona, Spain). Paraformaldehyde was provided by IESMAT (Madrid, España). Sphingomyelin (Lipoid E SM) was acquired from Lipoid GmbH (Ludwigshafen, Germany). Oleamide-modified putrescine ((9Z)-N-(4-Aminobutyl)-9-octadecenamide, CAS RN: 1005454-33-0) was provided by GalChimia (A Coruña, Spain). The plasmid pcDNA4TO-mito-mCherry-10xGCN4_v4 was purchased in AddGene (Plasmid #60914; http://n2t.net/addgene:60914; RRID:Addgene_60914) (Massachusetts, USA).

Table 1. Compilation of sequences of the miR used in this work.

	Sequence
miR control	5'CAGUACUUUUGUGUAGUACAA3'
miR control-Cy5	5'Cy5-CAGUACUUUUGUGUAGUACAA3'
miR 145	5'GUCCAGUUUUCCCAGGAAUCCCU3'

2.2. Formulation of the nanosystems and nucleic acid association

As previously described [42], putrescine nanosystems were formulated by ethanol injection method. Briefly, 5 mg of vitamin E (VE), 0.5 mg of sphingomyelin (SM) and 0.25 mg of putrescine modified with oleamide (Pt) were dissolved in 100 µL of ethanol and injected under magnetic stirring at 700 RPM in 1 ml of Molecular Grade Water. The suspension was kept under stirring at room temperature for 5 min. Then, 5 µg of miR were dissolved in 100 µL of H2O nuclease-free and added over 100 µL of preformed nanocarriers, for 20 min under magnetic stirring at 500 RPM to achieve the association.

Moreover, previously to the pDNA-Cy5 association with the PSN, it was labelled with Cy5 with the Label IT® TrackerTM Intracellular Nucleic Acid Localization Kit (Mirus Bio, Madison, USA).

2.3. Physicochemical characterization

Physicochemical characterization of the nanosystems were performed using a Zetasizer® Nano ZS (Malvern Instruments, England), which provides mean size, polydispersity index (PdI) and zeta potential (ZP). Dynamic light scattering (DLS) allows to perform size and PdI measurements of samples previously diluted 1:10 in MilliQ water. Samples were analysed in disposable microcuvettes (ZEN0040, Malvern Instruments) with a detection angle of 173º at room temperature. Laser Doppler anemometry (LDA) allows to evaluate ZP using folded capillary cells cuvettes (DTS 1070, Malvern Instruments) and a 1:40 diluted sample in MilliQ water.

2.4. Association efficiency

A 3% agarose gel electrophoresis was performed to evaluate the association efficiency of the miR. A known amount of miR (2 µg) was mixed with Loading buffer, Tris-Borate-EDTA (TBE) buffer and SYBR Gold. The agarose gel was prepared in TAE buffer, composed by Tris, acetic acid and EDTA 0,5 M. Prepared samples were loaded, and the gel was run at 80 V for 40 minutes, making use of a Mini-Sub Cell GT Cell (BioRad, California, USA). The result was evaluated with the ChemiDocTM MP Imaging System (Bio-Rad, California, USA), in which the free miR appears as a band in the gel. In the case of pDNA, 0.2 µg was loaded in a 1% agarose gel, following the same protocol.

2.5. miR-145 effects in sox9b and gata6 expression- zebrafish as a feasible model for gene therapy

2.5.1. Zebrafish husbandry and microinjection

Zebrafish embryos were obtained by mating wild type adults, which were maintained in 30-litre tanks with a 14 h/10 h light/dark cycle and a temperature of 28.5°C. Embryos of 0 hour post fertilization (hpf) were collected, placed in 90x15 mm Petri dishes, and subsequently microinjected with 1-3 nL of free miR Control, free miR145, PSN alone, PSN/miR Control or PSN/miR 145 (0.25 µg/µL). Microinjected embryos as well as controls were kept at 28.5°C until 72 hpf. All the procedures described for zebrafish were performed in agreement with the Animal Care and Use Committee of the University of Santiago de Compostela and the standard protocols (Directive 2012-63-UE).

2.5.2. RT-qPCR

Real-time quantitative polymerase chain reaction (RT-qPCR) was performed with three biological replicates (10 embryos/pool) and three technical replicates for each. Total RNA was isolated from the embryos with the NYzol reagent and the purification was based on a phenol-chloroform protocol. Reverse transcription was performed with the AffinityScript Multiple Temperature cDNA Synthesis Kit (Agilent) following the manufacturer's protocol. RT-qPCR was performed using the Brilliant III Ultra-Fast SYBR Green QPCR Master Mix Kit and the Stratagene Mx3005P Thermal Cycler (Agilent Technologies, California, United States). To analyze the expression levels, the ΔΔCT method was applied, using the actb2 gen as housekeeping and statistical analyses were performed in SPSS Statistics (IBM) through a T Student test. Statistical significance was considered if $p<0,05$. The actb2 primers (Forward: ACTTCACGCCGACTCAAACT; Reverse: ATCCTGAGTCAAGCGCCAAA) were designed using Primer BLAST [43], while those for sox9b (Forward: AGCTCAGCAAAACACTCGGC; Reverse: CCGTCTGGGCTGGTATTTGT) [44] and gata6 (Forward: AAACCTCAGAAGCGCATGTC; Reverse: AGACCACAGGCGTTGCAC) [45] were obtained in the literature.

2.6. Cell Culture

MDA-MB-231 (CRM-HTB-26™) triple negative breast cancer cell line and MCF7 (HTB-22™) breast cancer cell line (supplementary material) were

obtained from the American Type Cell Culture (ATCC). Cells were cultured in Dulbecco′s Modified Eagle′s Medium (DMEM) - high glucose, supplemented with 10% Fetal bovine serum (FBS) and 1% penicillin/streptomycin (P/S). Cells were maintained in a humid atmosphere (95%), 5% of CO_2 and 37 ºC.

2.7. Cellular uptake

Internalization assays were performed on MDA-MB-231 and MCF7 cells to evaluate nanoemulsions labelled with sphingomyelin TopFluor® (4.5 µg/nanoemulsion) (Suppementary material). Cells were seeded on an 8-well chambered slide at 40.000 cell/well. After 24 hours of incubation at 37 °C, cells were washed with PBS and 200 µL of non-supplemented DMEM were added per well. Nanocarriers with and without associated miR-Cy5 were mixed in each well at a concentration of 0.2 mg/mL. Cells were incubated with the nanocarriers for 4 hours at 37 °C. After this time, cells were washed twice with PBS and fixed with 4% (w/v) paraformaldehyde for 15 minutes. Cells were again washed twice with PBS and cellular nuclei were stained with Hoechst (0.01 mg/ml in PBS) for 5 min in darkness at room temperature. After that, cells were washed 3 times for 5 min with PBS, which was aspirated after the last wash. Then, walls were removed and Mowiol® 4-88 was added for placing a coverslip; after that, samples were kept drying in darkness overnight. Uptake results were evaluated by confocal microscopy (SP8 Laser Microscope, Leica).

2.8. Zebrafish maintenance

Wildtype zebrafish embryos were maintained in E3 medium with 1-phenyl 2-thiourea (PTU) at 28.5 °C. E3 is a saline medium composed by NaCl, KCl, $CaCl_2 \cdot 2H_2O$ and $MgSO_4$ [46], traditionally used for maintaining the embryos, whereas PTU is a compound that inhibits the melanogenesis [47], maintaining the transparency of embryos for a longer time and avoiding the pigmentation, which could interfere later in confocal microscopy. PTU was only used in the assays evaluated by confocal imaging to improve the transparency of the embryos.

Zebrafish embryos were kindly provided by the aquarium (REGA code ES270280346401) located in the veterinary facility of the University of Santiago de Compostela (Lugo, Spain). All the procedures described for zebrafish embryos were performed in agreement with the current legislation (RD53/2013, Directive 2010/63/UE). In this work only zebrafish embryos of 120 hpf or less were used, which are not considered experimental animals by the European legislation, Directive 2010/63/EU, because they are not independently feeding larval forms.

2.9. *In vivo* uptake

Nanoemulsions labeled with TopFluor were incubated with the embryos in a 96-well plate with a final volume of 100 µL per well, for 72 h at 34 ºC. The lipidic concentration used in these assays was 0.5 mg/mL and the concentration of TopFluor was 20 µg/mL. Internalization was tested in three different conditions with at least 16 replicates per condition: Control (MilliQ

water), PSN, PSN/miR, and PSN/pDNA (with Cy5-labelled miR and pDNA). Permeability was evaluated by confocal microscope after embryos suppression with tricaine overdose, fixation with paraformaldehyde 4% for 30 minutes, and wash with PBS twice.

Moreover, in the case of PSN and PSN/pDNA, mortality assessment was performed to evaluate the toxicity of the nanosystems. Embryos were evaluated each 24 hours and mortality was observed.

2.10. Nanoemulsions biodistribution *in vivo*

To evaluate the biodistribution of nanoemulsions *in vivo*, 48 hpf zebrafish embryos were microinjected in the duct of Cuvier with TopFluor-labelled PSN (with and without Cy5-labelled miR/pDNA) previously concentrated 10 times by the SpeedVac Concentrator (Savant SPD111V-120, Cambridge Scientific, Massachusetts, USA). The microinjection was carried out with a binocular loupe (SMZ745, Nikon), the IM 300 Microinjector (Narishige, Tokyo, Japan), and needles made with the PC-10 Puller (Narishige, Tokyo, Japan) from glass capillaries (Harvard Apparatus, Massachusetts, United States). After 48 hours from the microinjection, embryos were processed as explained in section 2.9 and nanoemulsions biodistribution was evaluated by confocal microscopy.

2.11. Nanoemulsions behavior in xenografted zebrafish

In order to evaluate the behavior of the nanoemulsions in a metastatic-like *in vivo* environment, 48 hpf zebrafish embryos were xenografted with MDA-MB-231 cells, previously labelled with DiI. Cells were resuspended in PVP 2% and 200-300 cells were injected into the perivitelline space, as explained in section 2.9. After 24 hours, TopFluor-labelled PSN (with and without Cy5-labelled miR/pDNA), previously concentrated 10 times by the SpeedVac Concentrator, were microinjected into the Duct of Cuvier. *In vivo* behavior and interaction between developed nanocarriers and cancer cells were evaluated by confocal microscopy subsequent to following the same protocol as explained in section 2.9.

3. RESULTS

3.1. Nanoemulsions (PSN) characterization

In this work, we wanted to evaluate the potential of zebrafish to test novel gene nanotherapies, and for that purpose, we associated two different types of NAs to versatile PSN, namely miR and pDNA. To formulate the PSN, we followed the ethanol injection method, as previously described [13,42]. PSN have a mean size below 100 nm, a positive zeta potential (ZP) (around +60 mV) and a polydispersity index (PdI) around 0.2 (Table 2), as determined by Dynamic Light Scattering (DLS) and Laser Doppler Anemometry (LDA).

Table 2. Physicochemical characterization of PSN with and without different miR associated by DLS and LDA**.** Values are expressed as mean ± standard deviation, n=3.

Formulation	Length (bp[a])	Size (nm)	PdI[b]	ZP (mV)[c]
PSN	-	91±6	0,23	+58±6
PSN/miR control	21	123±2	0,17	+45±1
PSN/miR 145	23	108±3	0,20	+40±2
PSN/pDNA	6717	164±4	0,09	+44±5

[a]Bp: Base pairs, [b]PdI, polydispersity index; [c]ZP, zeta potential.

The conditions for an efficient NA association preserving the colloidal properties of the nanocarriers were conveniently adjusted. As observed in Table 2, in all tested conditions, an increase in the hydrodynamic size and a decrease in the ZP were observed after the association of the NA, due to the interaction between their phosphate groups and the primary amines from the putrescine. Particularly, the association of the miR showed an increase in the size of around 30 nm. After the incubation with the pDNA, a higher increase in size was observed, which could be due to the higher molecular weight of the NA (near 7000 bp compared to the 21-23 bp of the miRs). In both cases, the resulting changes in the physicochemical parameters suggest a successful association, as was shown in other works [39,48]. Moreover, the PdI remained below 0.2 after NAs association, demonstrating that the PSN population is homogeneous. Even though these results indicate an efficient association of the NAs, an agarose gel electrophoresis was performed to provide additional evidence. (Figure 1). As observed, miR and pDNA were successfully retained

in the well, as consequence of their interaction with PSN. Only naked NA molecules, loaded for control, freely moved in the gel.

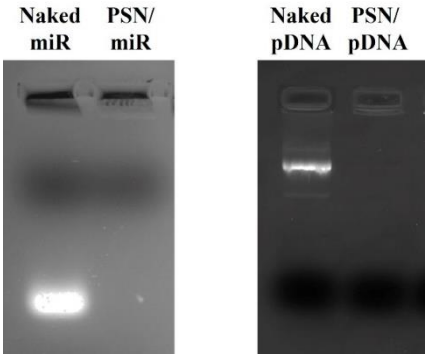

Figure 1. 1% agarose gel electrophoresis (80V, 40 minutes) to evaluate the association efficacy between PSN and nucleic acids: miR (2 µg) and pDNA (0.2 µg).

Moreover, in the previous work carried out by Lores *et al.*, PSN stability experiments were carried out. PSN stability under storage conditions, at 4 °C, was evaluated, and the results demonstrate that they are stable for up to 21 days, according to the lack of variation in size, PdI, and ZP. Furthermore, the association between the pDNA and the PSN was studied and confirmed to remain stable by agarose gel electrophoresis. The conditions evaluated were the stability upon incubation with complete cellular medium, after incubation with DNases and after 3 months of storage at 4 °C, demonstrating the high stability of the association as well as the protective role of PSN against DNases [42].

3.2. Transfection efficacy in the zebrafish embryo: *in vivo* effects of PSN/miR 145 in sox9b and gata6 expression

The characterization of PNS demonstrates the correct association of different NAs, however, for the PNS to exert the desired therapeutic effect, a key factor is the release of the cargo inside the cells. In this sense, zebrafish embryos allow us to evaluate *in vivo* the transfection capacity of the NAs. As mentioned before, zebrafish compile characteristics that make them highly appropriate to evaluate gene therapies. In this specific case, embryo robustness, their external fecundation, and the ease with which they are genetically manipulated make zebrafish the ideal model for this kind of assessment.

With the aim of studying the correct release of the associated NAs inside the cells, miR 145 was chosen due to its effect on gene expression in the zebrafish embryo. This miR is known to downregulate sox9b and gata6 genes when overexpressed in zebrafish [44,45]. Embryos of 0 hpf, one-cell stage, were microinjected with PSN associated and non-associated with miR (Control and 145), and with free miR (Control and 145). The chosen stage to start the treatment was 0 hpf to potentially modulate the genes during the first cell division and avoid possible interference in successive stages. Furthermore, microinjection was the selected method to ensure the introduction of the PSN/miR 145 into zebrafish embryos.

In order to determine if the microinjected PSN miR145 or the free miR145 were able to modify sox9b and/or gata6 expression, a RT-qPCR was performed three days later (72 hpf). In accordance with previous observations [44,45], miR145 increase led to a significant decrease in sox9b (p value 0,0347) and gata6 (p value 0,0364) expression but only when associated in PSN (Figure 2), and not when microinjected alone, in 72 hpf zebrafish embryos. Similarly, neither free miR control nor PSN alone nor PSN/miR control were able to modify their expression.

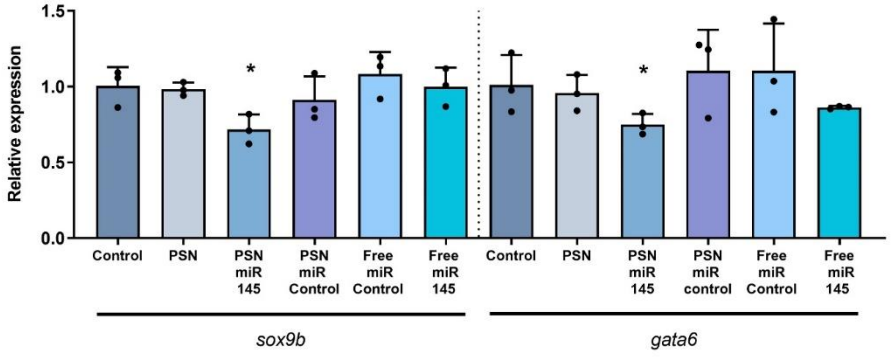

Figure 2. RT-qPCR results of the effect of miR 145 associated and non-associated with PSN in the relative expression of sox9b and gata6 genes in zebrafish embryos.

3.3. PSN/miR-pDNA *in vivo* uptake

Zebrafish is also characterized by being transparent in their first embryonic stages, and this fact allows us to evaluate fluorescent-labelled compounds as well as cells and nanoparticles [17,18]. It is relevant that nanosystem internalization experiments based on incubation are easily performed in zebrafish embryos, however, this cannot be done in rodents,

demonstrating the advantages of zebrafish as a model. Taking advance of this, an *in vivo* internalization assay was performed in 48 hpf embryos to study PSN behavior.

Cy5-labelled miR and pDNA were associated with fluorescent PSN (labelled with TopFluor®-sphingomyelin). The use of zebrafish embryos for this type of assay allows us to easily incubate NA-loaded PSN in their media, in this case, 72 hours. The results observed by confocal microscopy demonstrated a high internalization by cells of the fluorescent PSN, and most importantly, also allowed to determine the presence of the associated NAs, miR and pDNA (Figure 3). Furthermore, experiments confirmed the co-localization (in cyan) of PSN (in green) and NAs (in blue) in an *in vivo* model with a superior level of complexity (Figure 3). This colocalization proves that PSN and NAs remain associated during the uptake process, allowing the efficient transport of NAs into the cells, which is a key step for successful gene therapy.

Furthermore, these uptake studies demonstrated the low toxicity of the nanocarriers (Figure S1), producing less than 20% of mortality in the embryos.

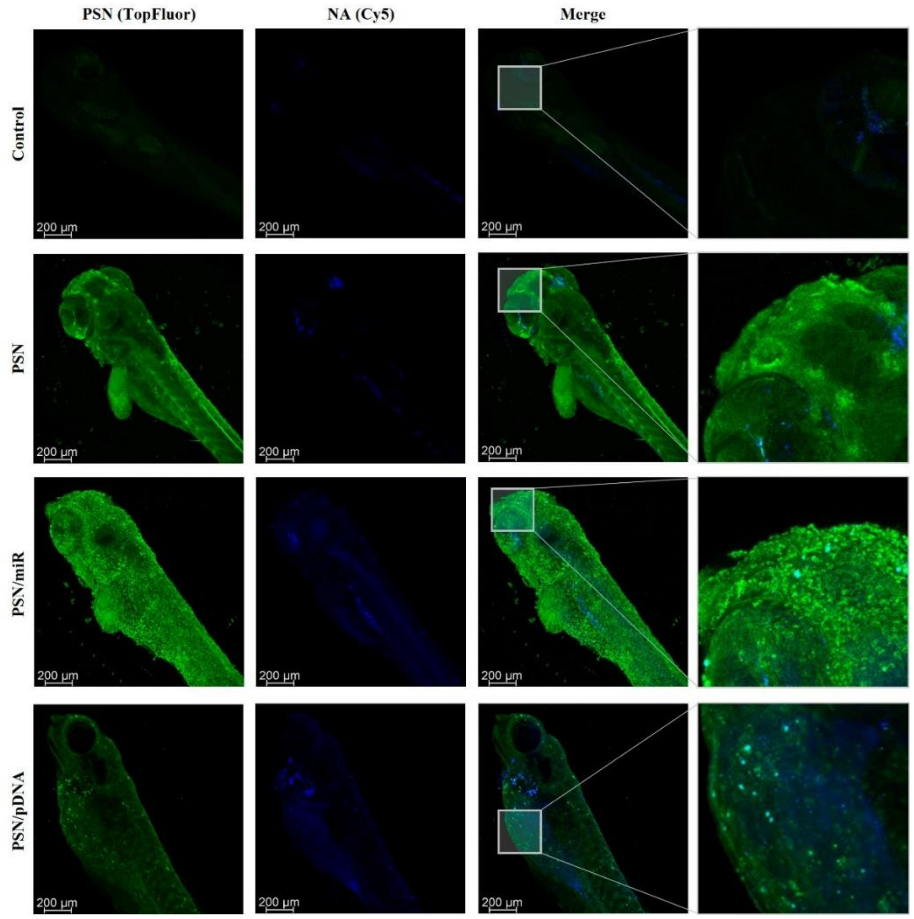

Figure 3. Confocal images of zebrafish embryos after a 72h incubation with TopFluor-PSN (in green) associated and non-associated with Cy5-labelled miR and pDNA (in blue).

3.4. PSN/miR-pDNA *in vivo* biodistribution

Following the same strategy of leveraging zebrafish embryo transparency, a PSN biodistribution assay was subsequently performed. Zebrafish transparency, which lasts until 24 hpf and can be extended with the use of PTU [47], allowed us to demonstrate the potential of PSN to be a carrier for gene therapy since we can monitor their stability and biodistribution in the circulatory system of the fish [17].

For this purpose, 48 hpf embryos were microinjected in the Duct of Cuvier with the PNS, associated and non-associated with NAs (miR and pDNA), as well as free NAs. After 48 hours of incubation, embryos were fixed and analyzed by confocal microscopy. The obtained results show the biodistribution of PSN along the zebrafish embryo body through the vasculature and their accumulation in the tail (Figure 4). In the case of PSN associated with NAs (PSN/miR and PSN/pDNA), it is observed that the association between NAs and nanocarriers after the microinjection in circulation is maintained *in vivo*. This maintenance is reflected by the cyan signal observed, which is a result of the co-localization of the green fluorescence of the nanosystems (with SM-TopFluor) and the blue fluorescence from the NAs (labelled with Cy5). Both PSN and PSN associated with NAs display an accumulation pattern that does not appear in the case of the naked miR and pDNA, which are spreading along the zebrafish body.

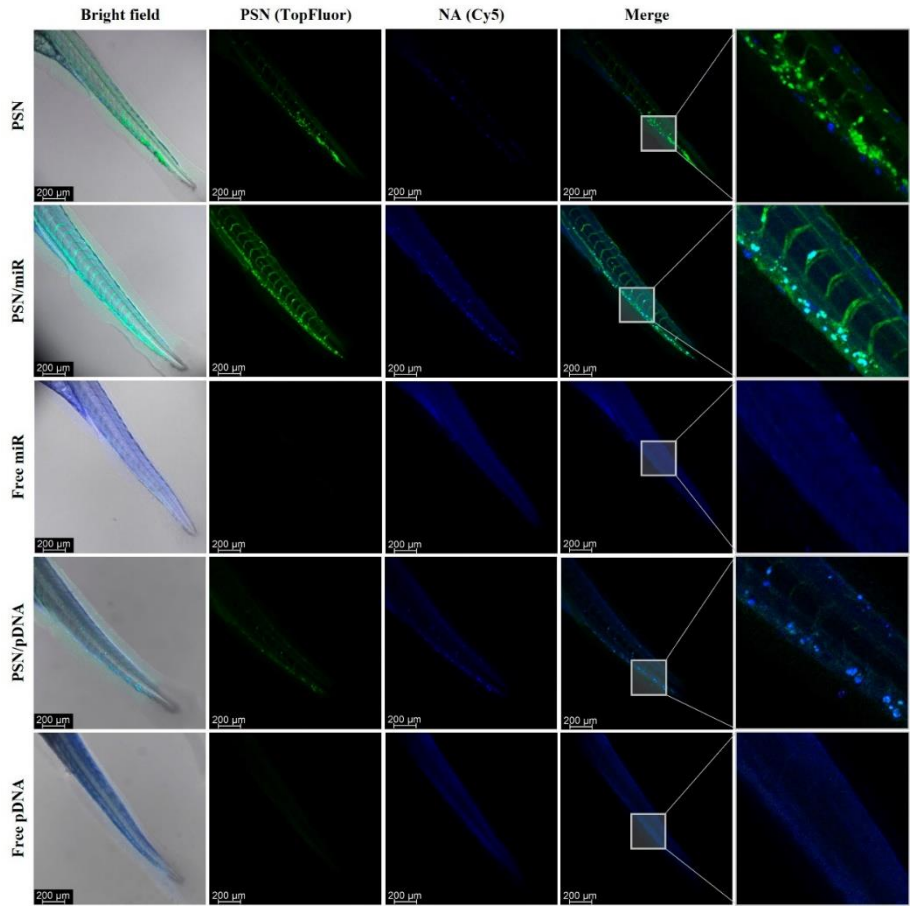

Figure 4. Confocal images of *in vivo* biodistribution of TopFluor-labelled nanoemulsions (green) with and without miR-Cy5 and pDNA (blue), after 48 hours incubation in microinjected 48 hpf zebrafish embryos.

3.5. PSN/miR-pDNA *in vivo* interaction with cancer cells

Another zebrafish embryo property that makes it suitable as an *in vivo* model for gene therapy nanomedicine is the late activation of the immune system, which is not complete until 4-6 wpf [49]. This allows us to perform xenotransplantation of cancer cells without the necessity of using genetically engineered immunodeficient *in vivo* models. Furthermore, the use of fluorescent-labelled cells, as well as fluorescent PSN and NAs, allows to evaluate how they behave in an *in vivo* tumor-like environment and how they interact with cancer cells.

Zebrafish embryos of 48 hpf were microinjected in the Duct of Cuvier with MDA-MB-231 cells, previously labelled with DiI. The result of this injection was a metastasis-like environment with cancer cells spread in the tail of the embryos, a key milieu to evaluate PSN interactions with cancer cells. Twenty-four hours after the xenograft, PSN with SM-TopFluor, associated and non-associated Cy5-NAs, were microinjected in the Duct of Cuvier. Forty-eight hours post-PSN injection, embryos were scanned by confocal microscopy. The results show that the fluorescent signal of the NAs (in blue) co-localize with the PSN (in green), corroborating the results obtained in the biodistribution assay (Figure 5). Further to this, it is observed some co-localization of the fluorescence signal of the PSN (with and without associated NAs) with the fluorescence of cancer cells; whereas free nucleic acids do not show any signal overlapping with the cancer cells. It is also important to highlight that the association between the carrier and the NA is stable for at least 48 hours after the microinjection, along the zebrafish circulation, verifying the stability of the NA-loaded PSN.

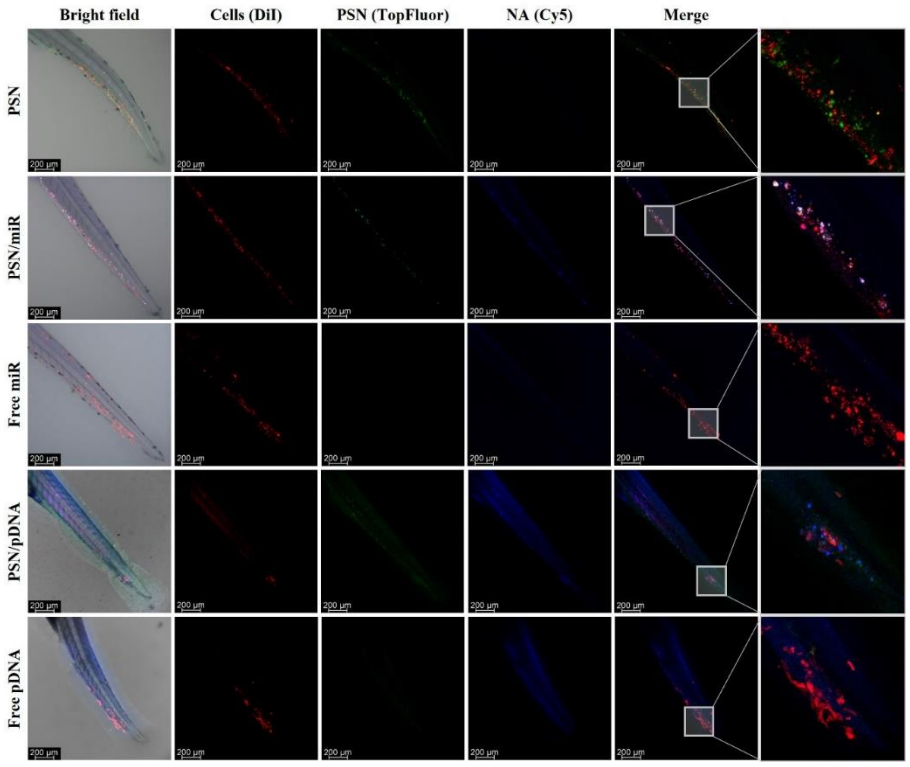

Figure 5. Images of the *in vivo* interaction between nanoemulsions, labelled with TopFluor (green), and associated and non-associated miR and pDNA Cy5-labelled (blue) with DiI-MDA-MB-231 cancer cells (red), by confocal microscopy.

4. DISCUSSION

Even though zebrafish is widely used as a model to evaluate therapies for cancer treatment [21,50], its use to develop and validate innovative gene therapy nanomedicines has not yet been fully investigated. With this aim, this work

was carried out to demonstrate the potential of zebrafish as a key model in the study of new gene therapies based on nanotechnology.

Zebrafish is an interesting *in vivo* platform that allows us to perform assays that cannot easily be performed with other *in vivo* model systems, such as rodents. Probably, the most characteristic feature of zebrafish is the transparency present in the embryonic stages [17,51]. As mentioned before, transparency allows the simple visualization of fluorescently labelled molecules, cells, and nanoparticles [17,18]. This advantage, in synergy with fluorescence/confocal microscopy, permits *in vivo* monitoring of specific structures, such as nanoparticles. As a result, we were able not only to observe how PSN behave *in vivo,* and how they interact with cancer cells, but also to confirm their stability and the maintenance of the association with NAs in an environment similar to that of patients. Our results are in line with several publications that use zebrafish as a model to evaluate nanomedicines (not for gene therapy purposes) and demonstrate how zebrafish can be used to evaluate novel cationic lipidic nanoemulsions *in vivo* with associated NAs [17,21,52,53].

Although zebrafish transparency plays a key role in carrying out this type of assays, this is not the only interesting advantage of this model system. Both embryos and adults have a small size and can be easily stored and maintained. This characteristic allows cost-effective, large-scale assays with a high number of specimens, with enough replicates to validate the experiments [16,54,55]. These types of assays are inconceivable in mice, considering the high maintenance cost and the small number of progenies [55]. In addition, zebrafish genome has a great homology with the human genome, and the body with several vertebrate structures [16,54].

Certainly, zebrafish embryo has several advantages that make it suitable as a model platform to evaluate cancer nanotechnology-based therapies, resulting in a plethora of diverse experiments that can be done to optimize and select the best treatments. However, it also has limitations in terms of similarity with humans. For instance, the lack of the physiological complexity of a non-mammalian organism implies the need to combine the zebrafish with other models, such as mice and rats, in certain types of experiments. However, in the context of animal welfare, combining the use of zebrafish embryo with more complex models may help to implement the 3R's rule: replace, reduce, and refine [56,57]. Because the zebrafish is an intermediate model between cell cultures and rodents, all experiments that can be performed in zebrafish models would inversely affect the number of mice that will be needed in subsequent experiments.

Our group has previously developed a new type of cationic nanosystems composed by VE, SM and a Putrescine derivative, PSN [42]. This formulation is an optimization of previous SM nanosystems [13,39,58], for cancer gene therapy applications, taking advantage of the intrinsic properties of putrescine. Among others, putrescine provides a cationic charge that can establish electrostatic interactions with negative-charged molecules such as NAs [59–61]. In addition, cancer cells show a higher affinity for putrescine compared to normal cells, in order to maintain their metabolic activities, in which natural polyamines are involved [40,62]. Our previous results show the potential of PSN to efficiently carry anti-cancer therapeutic pDNA, achieving a therapeutic effect in cell culture. Most importantly, the results show a tumor reduction in murine models of cancer, which correlates with the reduction previously observed in xenografted zebrafish embryos [42].

Furthermore, the experiments performed in the present work allowed us to validate the adaptability of our PSN cationic nanoemulsions [42]. PSN demonstrated to be an innovative carrier for gene therapy showing a high versatility due to their ability to carry different types of NAs, not only with a huge difference in length but also with different nature, desoxyribonucleic (pDNA) and ribonucleic acids (miR). Moreover, results obtained in 0 hpf embryos confirmed that miR145 is able to develop its regulatory role in zebrafish genes when associated with nanoemulsions; and therefore, the PSN are capable of releasing their cargo inside the cell. This fact highlights the potential of zebrafish to study the transfection efficiency of gene delivery nanosystems. It is important to emphasize that this type of experiment, with 0 hpf embryos, cannot be performed in the common models used in experimentation, such as mice and rats. These models, with higher complexity, have internal fertilization, thus this assay becomes complicated by the need to perform *in vitro* fecundation.

The accumulation of PSN observed in tumor cells could be related to the incorporation of putrescine and the fact that polyamine uptake is increased in cancer cells through Polyamine Transport Systems [63]. Importantly, we observed that PSN were stable in an *in vivo* environment, maintaining an efficient association of the NAs, which were then successfully released inside the cells. This proved the ability of putrescine to protect the NAs against *in vivo* barriers due to its capacity to condense nucleic acids achieving an improvement in the transport inside the cells [41]. In this sense, zebrafish allow us to observe/visualize the interaction of PSN with cancer cells in a more complex system than the one represented by a cell culture since different cell types from the tumor environment are present in the fish. Interaction studies

verified that PSN/miR-pDNA are able to travel along the embryos and reach the cancer cells. These results corroborate the ones observed in uptakes performed in cancer cell lines, demonstrating that the PSN interaction with cancer cells happens both *in vitro* and *in vivo* (Figure S2-S3). In other words, these results confirm that we have developed an efficient and stable nanocarrier able to transport its cargo to the cancer cells. Furthermore, the working times between cell cultures and zebrafish embryos are quite similar, obtaining more complex and reliable results.

5. CONCLUSIONS

In conclusion, our results demonstrate the huge potential that zebrafish embryos have as an *in vivo* platform to evaluate nanomedicines for gene therapy in a fast, cost-effective and reliable way in contrast with other animal models. In the same vein, the experiments presented here validated the capacity of PSN to successfully associate and transport different types of NAs into a living organism.

SUPPLEMENTARY MATERIAL

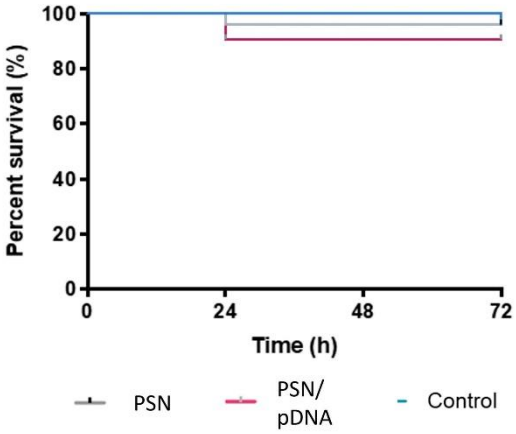

Figure S1. Toxicity assay of PSN and PSN/pDNA in zebrafish embryos after 24, 48 and 72 hours of incubation.

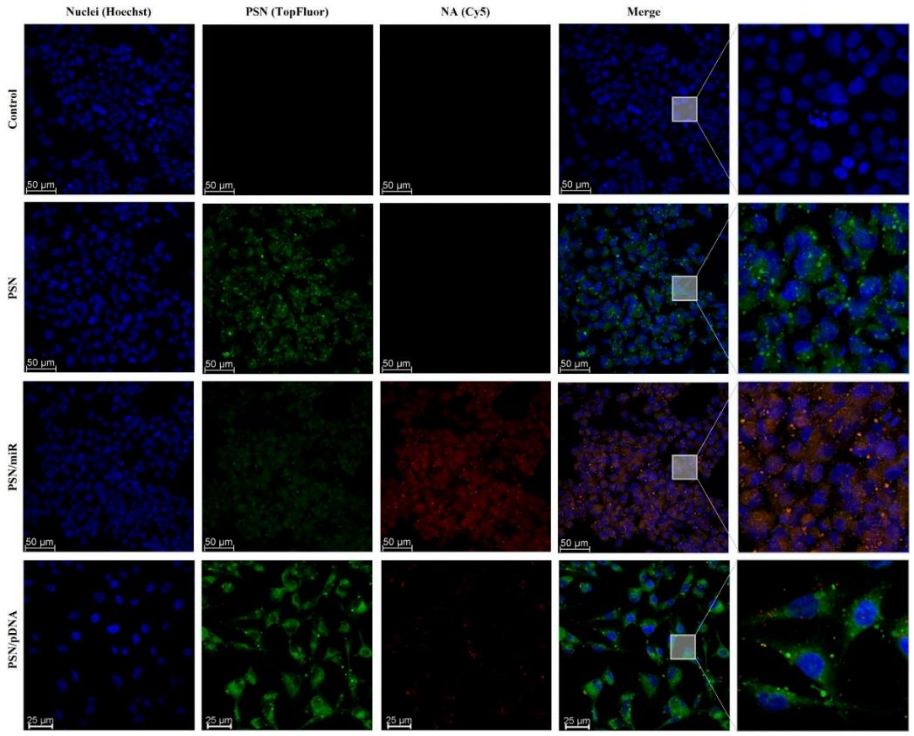

Figure S2. Confocal images of triple negative breast cancer cells (MDA-MB-231 cell line) after a 4h incubation with TopFluor-labelled nanosystems (green) associated and non-associated with miR/pDNA-Cy5 (red). Cell nuclei were stained with Hoescht (blue).

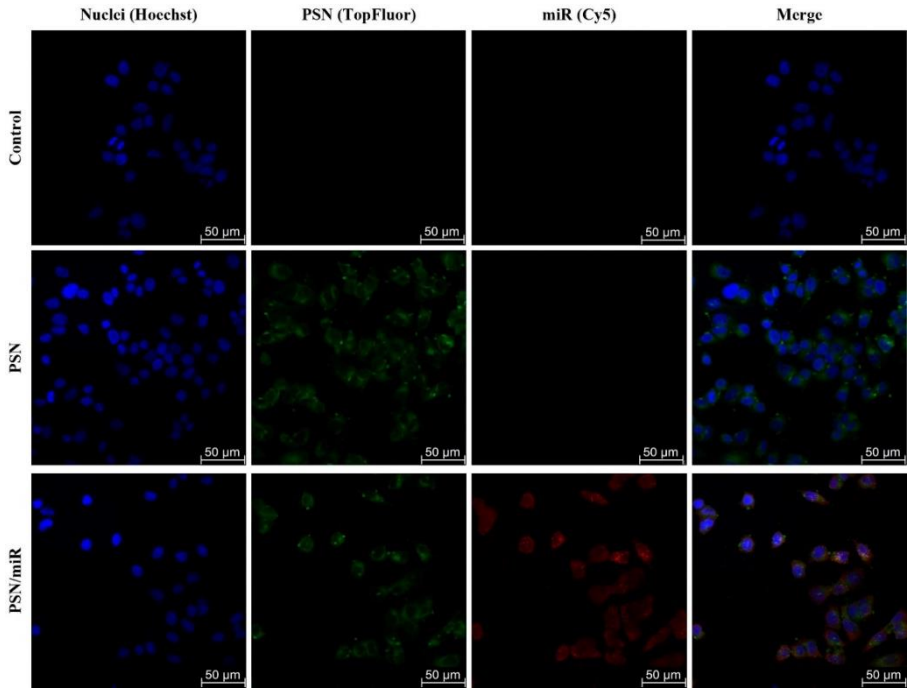

Figure S3. Confocal images of MCF7 breast cancer cells resulting after a 4h incubation with nanocarriers labelled with TopFluor (green) associated and non-associated with miR-Cy5 (red). Cell nuclei were stained with Hoescht (blue).

BIBLIOGRAPHY

1. Sayed, N. *et al.* Gene therapy: Comprehensive overview and therapeutic applications. *Life Sci* **294**, (2022).

2. Santiago-Ortiz, J. L. & Schaffer, D. V. Adeno-associated virus (AAV) vectors in cancer gene therapy. *Journal of Controlled Release* **240**, 287–301 (2016).

3. Mohammadinejad, R. *et al.* In vivo gene delivery mediated by non-viral vectors for cancer therapy. *Journal of Controlled Release* **325**, 249–275 (2020).

4. Walther, W., Drugs, U. S.- & 2000, undefined. Viral vectors for gene transfer. *Springer* **60**, 249–271 (2000).

5. Amer, M. H. Gene therapy for cancer: present status and future perspective. *Mol Cell Ther* **2**, 27 (2014).

6. Zu, H. & Gao, D. Non-viral Vectors in Gene Therapy: Recent Development, Challenges, and Prospects. *AAPS J* **23**, (2021).

7. Hoy, S. M. Patisiran: First Global Approval. *Drugs 2018 78:15* **78**, 1625–1631 (2018).

8. Akinc, A. *et al.* The Onpattro story and the clinical translation of nanomedicines containing nucleic acid-based drugs. *Nature Nanotechnology 2019 14:12* **14**, 1084–1087 (2019).

9. Corbett, K. S. *et al.* SARS-CoV-2 mRNA vaccine design enabled by prototype pathogen preparedness. *Nature* **586**, 567–571 (2020).

10. Polack, F. P. *et al.* Safety and Efficacy of the BNT162b2 mRNA Covid-19 Vaccine. *New England Journal of Medicine* **383**, 2603–2615 (2020).

11. Wick, P. *et al.* In vitro-ex vivo model systems for nanosafety assessment. *Eur J Nanomed* **7**, 169–179 (2015).

12. Sahlgren, C. *et al.* Tailored Approaches in Drug Development and Diagnostics: From Molecular Design to Biological Model Systems. *Adv Healthc Mater* **6**, (2017).

13. Bouzo, B. L., Calvelo, M., Martín-Pastor, M., García-Fandiño, R. & de La Fuente, M. In Vitro- In Silico Modeling Approach to Rationally Designed Simple and Versatile Drug Delivery Systems. *Journal of Physical Chemistry B* **124**, 5788–5800 (2020).

14. Boix-Montesinos, P., Soriano-Teruel, P. M., Armiñán, A., Orzáez, M. & Vicent, M. J. The past, present, and future of breast cancer models for nanomedicine development. *Adv Drug Deliv Rev* **173**, 306–330 (2021).

15. Sieber, S. *et al.* Zebrafish as a predictive screening model to assess macrophage clearance of liposomes in vivo. *Nanomedicine* **17**, 82–93 (2019).

16. Lieschke, G. J. & Currie, P. D. Animal models of human disease: Zebrafish swim into view. *Nat Rev Genet* **8**, 353–367 (2007).

17. Sieber, S. *et al.* Zebrafish as a preclinical in vivo screening model for nanomedicines. *Adv Drug Deliv Rev* **151–152**, 152–168 (2019).

18. Gutiérrez-Lovera, C., Vázquez-Ríos, A. J., Guerra-Varela, J., Sánchez, L. & de la Fuente, M. The potential of zebrafish as a model organism for improving the translation of genetic anticancer nanomedicines. *Genes (Basel)* **8**, 1–20 (2017).

19. Gutiérrez-Lovera, C., Vázquez-Ríos, A. J., Guerra-Varela, J., Sánchez, L. & de la Fuente, M. The potential of zebrafish as a model organism for improving the translation of genetic anticancer nanomedicines. *Genes (Basel)* **8**, 1–20 (2017).

20. Sieber, S. *et al.* Zebrafish as a preclinical in vivo screening model for nanomedicines. *Adv Drug Deliv Rev* **151–152**, 152–168 (2019).

21. Cascallar, M. *et al.* What Zebrafish and Nanotechnology Can Offer for Cancer Treatments in the Age of Personalized Medicine. *Cancers 2022, Vol. 14, Page 2238* **14**, 2238 (2022).

22. Streisinger, G., Walker, C., Dower, N., Knauber, D. & Singer, F. Production of clones of homozygous diploid zebra fish (Brachydanio rerio). *Nature 1981 291:5813* **291**, 293–296 (1981).

23. Jia, H. R., Zhu, Y. X., Duan, Q. Y., Chen, Z. & Wu, F. G. Nanomaterials meet zebrafish: Toxicity evaluation and drug delivery applications. *Journal of Controlled Release* **311–312**, 301–318 (2019).

24. Zon, L. I. Zebrafish: A New Model for Human Disease. *Genome Res* **9**, 99–100 (1999).

25. Kimmel, C. B., Ballard, W. W., Kimmel, S. R., Ullmann, B. & Schilling, T. F. Stages of embryonic development of the zebrafish. *Developmental Dynamics* **203**, 253–310 (1995).

26. Howe, K. *et al.* The zebrafish reference genome sequence and its relationship to the human genome. *Nature* **496**, 498–503 (2013).

27. Pensado-López, A. *et al.* Zebrafish Models for the Safety and Therapeutic Testing of Nanoparticles with a Focus on Macrophages. *Nanomaterials 2021, Vol. 11, Page 1784* **11**, 1784 (2021).

28. Wang, F. *et al.* Nanoparticle-mediated delivery of siRNA into zebrafish heart: a cell-level investigation on the biodistribution and gene silencing effects. *Nanoscale* **11**, 18052–18064 (2019).

29. Horzmann, K. A. & Freeman, J. L. Making Waves: New Developments in Toxicology With the Zebrafish. *Toxicological Sciences* **163**, 5 (2018).

30. Sipes, N. S., Padilla, S. & Knudsen, T. B. Zebrafish—As an integrative model for twenty-first century toxicity testing. *Birth Defects Res C Embryo Today* **93**, 256–267 (2011).

31. Lawson, N. D. & Weinstein, B. M. In Vivo Imaging of Embryonic Vascular Development Using Transgenic Zebrafish. *Dev Biol* **248**, 307–318 (2002).

32. Renshaw, S. A. *et al.* A transgenic zebrafish model of neutrophilic inflammation. *Blood* **108**, 3976–3978 (2006).

33. Ellett, F., Pase, L., Hayman, J. W., Andrianopoulos, A. & Lieschke, G. J. mpeg1 promoter transgenes direct macrophage-lineage expression in zebrafish. *Blood* **117**, e49 (2011).

34. Lee, K. Y. *et al.* Zebrafish models for functional and toxicological screening of nanoscale drug delivery systems: Promoting preclinical applications. *Biosci Rep* **37**, 1–13 (2017).

35. Wang, F. *et al.* Nanoparticle-mediated delivery of siRNA into zebrafish heart: a cell-level investigation on the biodistribution and gene silencing effects. *Nanoscale* **11**, 18052–18064 (2019).

36. Al-Thani, H. F., Shurbaji, S. & Yalcin, H. C. Zebrafish as a Model for Anticancer Nanomedicine Studies. *Pharmaceuticals 2021, Vol. 14, Page 625* **14**, 625 (2021).

37. Saraiva, S. M. *et al.* Edelfosine nanoemulsions inhibit tumor growth of triple negative breast cancer in zebrafish xenograft model. *Sci Rep* **11**, (2021).

38. Reimondez-Troitiño, S. *et al.* Versatile protamine nanocapsules to restore miR-145 levels and interfere tumor growth in colorectal cancer cells. *European Journal of Pharmaceutics and Biopharmaceutics* **142**, 449–459 (2019).

39. Nagachinta, S., Bouzo, B. L., Vazquez-Rios, A. J., Lopez, R. & de la Fuente, M. Sphingomyelin-based nanosystems (SNs) for the development of anticancer miRNA therapeutics. *Pharmaceutics* **12**, (2020).

40. Tracy, R. M. S., Woster, P. M. & Casero, R. A. Targeting polyamine metabolism for cancer therapy and prevention. *Biochem J* **473**, 2937 (2016).

41. Thomas, T. J., Tajmir-Riahi, H. A. & Thomas, T. Polyamine–DNA interactions and development of gene delivery vehicles. *Amino Acids* **48**, 2423–2431 (2016).

42. Lores, S. *et al.* Effectiveness of a novel gene nanotherapy based on putrescine for cancer treatment. *Biomater Sci* **11**, 4210–4225 (2023).

43. Altschul, S. F., Gish, W., Miller, W., Myers, E. W. & Lipman, D. J. Basic local alignment search tool. *J Mol Biol* **215**, 403–410 (1990).

44. Steeman, T. J., Rubiolo, J. A., Sánchez, L. E., Calcaterra, N. B. & Weiner, A. M. J. Conservation of zebrafish microrna-145 and its role during neural crest cell development. *Genes (Basel)* **12**, (2021).

45. Zeng, L., Carter, A. D. & Childs, S. J. miR-145 directs intestinal maturation in zebrafish. *Proc Natl Acad Sci U S A* **106**, 17793–17798 (2009).

46. Murphey, R. D. & Zon, L. I. Small molecule screening in the zebrafish. *Methods* **39**, 255–261 (2006).

47. Karlsson, J., von Hofsten, J. & Olsson, P. E. Generating transparent zebrafish: A refined method to improve detection of gene expression during embryonic development. *Marine Biotechnology* **3**, 522–527 (2001).

48. Liu, J. *et al.* MicroRNA-200c delivered by solid lipid nanoparticles enhances the effect of paclitaxel on breast cancer stem cell. *Int J Nanomedicine* **11**, 6713–6725 (2016).

49. Lam, S. H., Chua, H. L., Gong, Z., Lam, T. J. & Sin, Y. M. Development and maturation of the immune system in zebrafish, Danio rerio: A gene expression profiling, in situ hybridization and immunological study. *Dev Comp Immunol* **28**, 9–28 (2004).

50. Kwiatkowska, I. *et al.* Zebrafish—An Optimal Model in Experimental Oncology. *Molecules* **27**, 4223 (2022).

51. Lieschke, G. J. & Currie, P. D. Animal models of human disease: Zebrafish swim into view. *Nat Rev Genet* **8**, 353–367 (2007).

52. Saez Talens, V. *et al.* Stab2-Mediated Clearance of Supramolecular Polymer Nanoparticles in Zebrafish Embryos. *Biomacromolecules* **21**, 1060–1068 (2020).

53. Rességuier, J. *et al.* Biodistribution of surfactant-free poly(lactic-acid) nanoparticles and uptake by endothelial cells and phagocytes in zebrafish: Evidence for endothelium to macrophage transfer. *Journal of Controlled Release* **331**, 228–245 (2021).

54. Delvecchio, C., Tiefenbach, J. & Krause, H. M. The Zebrafish: A powerful platform for in vivo, HTS drug discovery. *Assay Drug Dev Technol* **9**, 354–361 (2011).

55. Veinotte, C. J., Dellaire, G. & Berman, J. N. Hooking the big one: The potential of zebrafish xenotransplantation to reform cancer drug screening in the genomic era. *DMM Disease Models and Mechanisms* **7**, 745–754 (2014).

56. Lewis, D. I. Animal experimentation: implementation and application of the 3Rs. *Emerg Top Life Sci* **3**, 675–679 (2019).

57. MacArthur Clark, J. The 3Rs in research: a contemporary approach to replacement, reduction and refinement. *British Journal of Nutrition* **120**, S1–S7 (2018).

58. Bidan, N. *et al.* Before in vivo studies: In vitro screening of sphingomyelin nanosystems using a relevant 3D multicellular pancreatic tumor spheroid model. *Int J Pharm* **617**, (2022).

59. Rowe, R., Sheskey, P. & Quinn, M. *Handbook of pharmaceutical excipients*. (2009).

60. Chakraborty, M. & Jiang, X. C. Sphingomyelin and its role in cellular signaling. *Adv Exp Med Biol* **991**, 1–14 (2013).

61. Agostinelli, E., Vianello, F., Magliulo, G., Thomas, T. & Thomas, T. J. Nanoparticle strategies for cancer therapeutics: Nucleic acids, polyamines, bovine serum amine oxidase and iron oxide nanoparticles. *Int J Oncol* **46**, 5–16 (2015).

62. Casero, R. A., Murray Stewart, T. & Pegg, A. E. Polyamine metabolism and cancer: treatments, challenges and opportunities. *Nat Rev Cancer* **18**, 681 (2018).

63. Novita Sari, I. *et al.* Metabolism and function of polyamines in cancer progression. *Cancer Lett* **519**, 91–104 (2021).

OVERALL DISCUSSION

OVERALL DISCUSSION

Cancer treatment is a current challenge due to the high deaths rates of this group of diseases. In addition to that, cancer situation is worsening due to an expected increase in death rates and new cases in 2040, reaching the 29.5 million and 16.4 million, respectively [1]. Cancer is a complex and heterogeneous illness, and all the different features are involved in the tumor progression [2,3]. Altered oncogenes and tumor suppressor genes, microenvironment, diversity in cell population, among other characteristic features, are key for the cancer development [4–8].

The treatments are specifically centered in the use of radiotherapy, chemotherapy, surgery, and immunotherapy, depending on the cancer type and stage [9–13]. Despite of their beneficial effects, these strategies are not enough, and it is necessary the development of novel effective therapies that can reach the cancer cell population, aiming an increase of the treatment efficacy [14]. In this sense, nanomedicine can play a key role being the basis of novel therapies.

In the recent years, nanomedicine has demonstrated its potential to be a valuable alternative to develop novel cancer treatments [1,15]. Nanocarriers have the capacity to encapsulate drugs with low solubility rates, reaching a decrease in the drug concentration needed, as well as increasing its half-life [16,17]. Moreover, nanoparticles can be developed for carrying therapeutic biomolecules, such as nucleic acids and peptides [18–20]. In relation with this,

they can also be functionalized for developing targeted therapies, which can improve the side effects of the current treatments [21–23].

Since the FDA-approval of Doxil® for ovarian cancer treatment in 1995, there were proposed multiple nanotechnology-based cancer treatments [1,24]. However, few cancer nanomedicines reached the market, being less than 20 EMA/FDA approvals [17]. This delay in the translation to the market can be overcame with the implementation of reliable *in vitro* and *in vivo* models, which can be the basis to understand the behavior and efficacy of novel nanomedicines [15,25,26].

In this thesis, sphingomyelin nanosystems (SNs), previously developed by our group, were studied with the aim of evaluate different therapeutic strategies for cancer treatment [27]. Their simple and biocompatible composition based on vitamin E and sphingomyelin, makes them easy to produce, as well as, biocompatible and stable [27]. In previous studies, SNs have demonstrated their capacity to carry biomolecules, therapeutic compounds, and imaging and contrast agents, being an innovative alternative to cancer treatment and detection [28–36].

In the current work, different strategies based on SNs were evaluated for cancer treatment: i) a drug delivery system; ii) a targeted therapy; iii) a gene therapy. The evaluation of these different approaches was performed in alternative study platforms: i) spheroids; ii) organo-on-a-chip microfluidic devices; and iii) zebrafish embryos, respectively.

Sphingomyelin nanosystems as a versatile strategy for cancer treatment

With the purpose of developing novel cancer treatment strategies based on the previously developed SNs, they were differently modified to achieve formulations for drug delivery, targeted therapy, and gene therapy (Figure 1) [27].

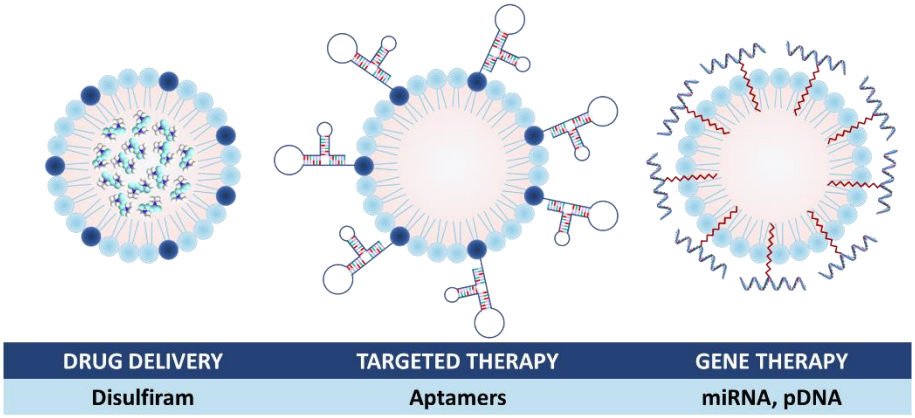

Figure 1. Summary of the therapeutical strategies based on SNs evaluated in this work.

As a first approach, 1,2-distearoyl-sn-glycero-3-phosphoethanolamine-N-[carboxy(polyethylene glycol)-2000] (DSP-PEG (2K)-COOH) was included in the SNs formulation (Figure 2A). This molecule is composed by a lipophilic core (DSPE) and a lipophobic shell (PEG), being disposed in the SNs interior and surface, respectively [37]. The PEG addition to nanoformulations is related to the increase of their stability as well as their half-life [38–40]. Previously works of our groups have implemented the use of PEG to increase stability and to develop targeted therapies [28,32,41]. Taking this into account, PEGylated SNs were used to encapsulate the hydrophobic drug disulfiram (DSF). DSF is a widely known FDA-approved drug for alcoholism

treatment, which has also demonstrated efficiency as cancer therapy [42,43]. These encapsulated SNs (SNs-DSF) were evaluated for cancer stem cell (CSCs) treatment of non-small cell lung cancer (NSCLC).

Furthermore, PEG molecule is also interesting for aptamer-based targeted therapy, due to its role as a point of attachment between aptamers and nanosystems [44–46]. As previously described, SNs are a reliable nanocarrier for targeted therapy, as well as protein-based targeting [28,41]. Thus, PEGylated SNs were also the basis for the aptamer conjugation to achieve a targeted therapy, whose target is the TAS1R3 receptor, previously described by the group [47].

A different approach was the addition of putrescine, a derivative oleamide version, for a better integration in the formulation (Figure 2B) [33]. The inclusion of this cationic molecule confers positive charges in the SNs surface, allowing the association of anionic nucleic acids. Previously studies performed by our group proved the SNs capacity to deliver gene therapies, including with the addition of putrescine to the formulation [29,30,33]. In this strategy, nucleic acids of different nature and with distinct lengths, miRNAs and plasmids, were selected to be associated with the putrescine SNs (PSN).

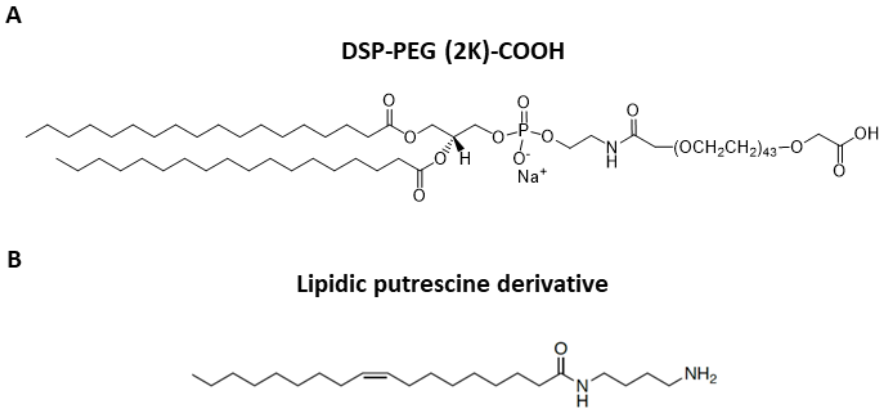

Figure 2. Chemical structure of: **A.** DSP-PEG (2K)-COOH; **B.** The lipidic putrescine derivative.

The physicochemical characterization of the SNs strategies demonstrates, in all cases, a homogeneous population due to the value of the polydispersity index, which is around 0.2. In the case of size, the values range between 91±6 and 195±5 nm, depending on the SNs category (Table 1). It is relevant the size increase observed in the case of functionalized SNs, due to the three-dimensional conformation of the aptamers. In the same way, PSN after nucleic acid association also showed an increase in size, which confirm the correct association of the miRNA or plasmid.

The surface charge varies depending on the components added to the formulation. The previously developed SNs (composed by VE and SM) had a neutral zeta potential (ZP). However, when the PEG is included, the SNs became negative, around -25 mV. This decreasing in the ZP is related to the carboxylic acid present in this molecule. This value is similar in the PEGylated SNs-DSF, and lower in the case of the functionalized SNs-5F. This decrease in the charge is produced due to the phosphate groups present in the aptamers

[48]. A completely different picture was observed in the PSN, because of the cationic character of the putrescine [33]. However, the ZP suffered a decrease when the nucleic acids were associated, due to the electrostatic interactions formed by the cationic putrescine and the anionic phosphate of the nucleic acids [33,49].

Table 1. Summary of the physicochemical characterization of the nanosystems used in this work.

Formulation	Size (nm)	PdI[a]	ZP[b] (mV)
SNs (VE:SM)	158 ± 5	0.07	-1 ± 0.4
SNs (VE:SM:PEG-COOH)	138 ± 1	0.04	-25 ± 0.1
SNs-DSF	111 ± 7	0.21	-20 ± 7
SNs-5F	195 ± 5	0.08	-37 ± 2
SNs-49F	211 ± 7	0.05	-33 ± 0
PSN	91 ± 6	0.23	+58 ± 6
PSN/miR control	123 ± 2	0.17	+45 ± 1
PSN/miR 145	108 ± 3	0.20	+40 ± 2
PSN/pDNA	164 ± 4	0.09	+44 ± 5

[a]PdI: polydispersity index; [b]ZP: zeta potential.

Effective study models for SNs evaluation

Throughout this thesis, four different study models were used for nanosystems evaluation, including *in vitro* and *in vivo* platforms: i) 2D cell cultures, ii) spheroids, iii) organ-on-a-chip (OOC) microfluidic devices, and iv) zebrafish embryos (Figure 4). The importance of using reliable models to

evaluate nanomedicines is key for the treatment fate and for a successful clinical translation [50]. With this aim, the different SNs strategies were evaluated in these models, with the objective of prove their value as study platforms for nanomedicines.

2D cell culture	Spheroids	OOC microfluidics	Zebrafish embryos
Monolayer	3D static culture	3D non-static culture	Vertebrate
Inexpensive	Structure mimicking	Controlled flow	Transparency
Simple procedure	↑ Cell interactions	Vasculature	Genome homology

Figure 4. Overview of the study platforms used in this thesis and their principal characteristics [51–55].

Even though the 2D cell culture is the basic and widely used study model for nanomedicines, more complex and reliable study platforms are needed to completely understand their behavior, internalization capacity and treatment efficacy [56,57]. Murine models are also a gold standard for the evaluation of nano-based medicines; however, they have some drawbacks. The high maintenance cost, the small offspring, and the low possibility to perform large screenings, among other characteristics, are the weaknesses of murine models [52]. Thus, the synergy of complementary *in vitro* and *in vivo* models can be an alternative to overcome the difficulties to evaluate nanomedicines for their clinical translation [58].

Taking this into account, spheroids were the static 3D *in vitro* model selected to evaluate diuslfiram (DSF) encapsulated nanosystems (SNs-DSF). As explained before, DSF target are the cancer stem cells (CSC), and their

population is enriched in 3D cultures, therefore, spheroids were the suitable platform for their study [59,60].

With the aim of confirming the correct therapeutic effect of SNs-DSF, the viability was evaluated in H1650 spheroids, which produce compact spheroids, that increase the difficulty in SNs the penetration. The results demonstrated the capacity of SNs to carry hydrophobic drugs and to release them in the cells (Figure 5A). Morover, spheroids also are convinient models for evaluating the penetration capacity of nanosystems. In this sense, nanocarriers must be fluorescencely labelled for a following evaluation by confocal microscopy or by flow cytometry [61,62]. The internalization of SNs-DSF by spheroid cells was evaluated by confocal microscopy and the results demonstrated a good capacity to penetrate into the inner parts of the shperoid Figure 5B). In addition, Calcein AM and propidium iodide are common reagents to evaluate the cytotoxicity on spheroid models [63]. The outcomes observed demosntrate a similar pattern in terms of apoptosis in the free DSF and in the SNs-DSF, which means that the treatment efficacy is not much higher when the DSF is encapsulated. However, the benefit of the SNs encapsulation is the protection of the drug, increasing its stability and half-life.

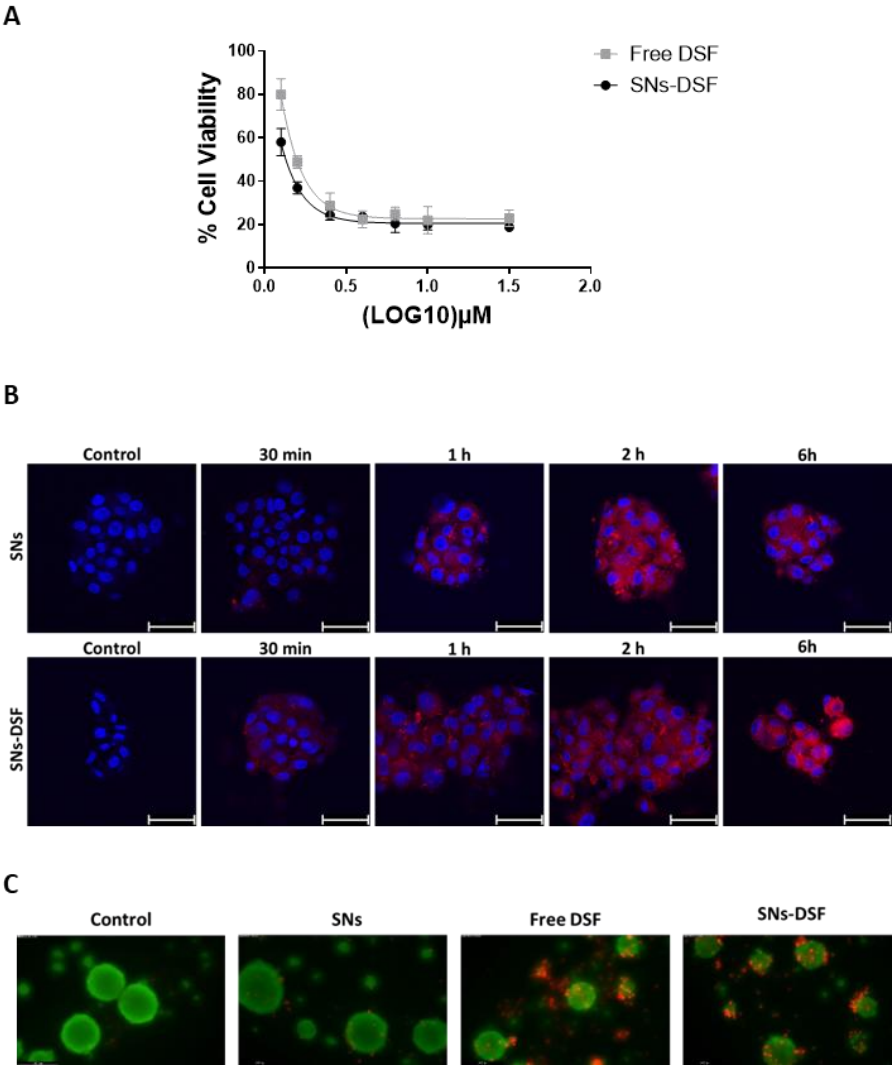

Figure 5. A. Viability evaluation after 48 hours of free DSF and SNs-DSF incubation in H1650 spheroids; **B.** Confocal images of Cy5-labeled nanoemulsions, with (SNs-DSF) and without (SNs) encapsulated disulfiram, internalized in H1650 spheroids at different time points. NEs are labelled with Cy5 (in red), and nuclei with Hoechst 33342 (in blue). **C.** Viability assay of H1650 spheroids after disulfiram treatment, encapsulated and non-encapsulated in SNs, for 48 hours. After treatment, spheroids

were incubated with Calcein AM 2µM and PI 4µM for 30 minutes. In the images, Calcein AM is in green, and PI in red.

Targeted nanomedicines need to be evaluated in terms of targeting efficacy to demonstrate their capacity to efficient discriminate between cell types [64]. In this sense, OOC microfluidic models have the ability to recreate not only the tumor structure and environment, but also the vasculature [55]. This fact makes OOC a valuable model for testing the targeting capacity of nanosystems [65]. The two-channel device used in this work mimics specifically the tumor structure and a sanguineous vessel. The tumor channel is composed by the A549 NSCLC cells that overexpress the target receptor, TAS1R3; and the endothelial one is composed by a monolayer of HPMEC cells. The gaps between the channels and the formation of the endothelial barrier mimic the biological obstacles that the functionalized SNs will find in the organism, so SNs behavior in the OOC is a good predictor of the *in vivo* results [66]. The SNs-5F preliminary results show their presence in the gaps between the micropillars, which suggests they were crossing them, but further experiments are needed to verify it (Figure 6).

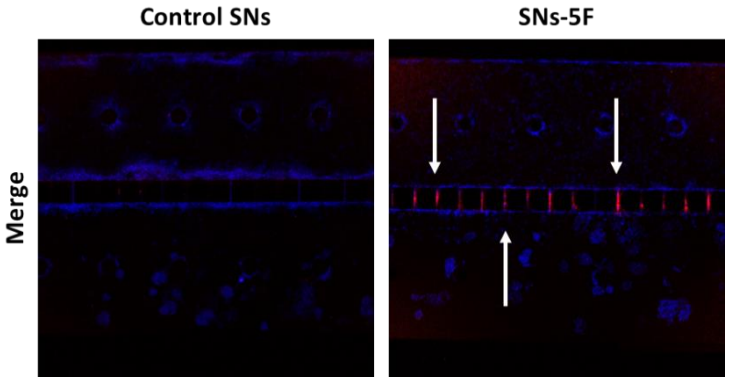

Figure 6. Confocal images of the behavior evaluation of targeted SNs-5F in OOC microfluidic devices. Nuclei are stained with Hoechst (in blue); and SNs and SNs-5F are labeled with Cy5 (in red). The upper channel is the endothelial one, and the bottom channel is the cancer one. SNs-5F are present in the gaps (white arrows).

The third strategy was the evaluation of cationic nanosystems for cancer gene therapy. PSN were evaluated with zebrafish embryos, which are able to be microinjected with fluorescent cancer cells and these can be followed by fluorescent or confocal microscopy, due to the transparence of the model. Moreover, nanosystems can be monitored in the same way, making use of fluorescent labels [58,67]. Cancer cells would not trigger the immune response in the zebrafish, due to the late activation of the adaptative immune system, thus cancer cells can proliferate correctly [68]. Considering this, PSN were labelled including TopFluor®-sphingomyelin to the formulation, and in the case of cancer cells, the selected dye was DiI.

The nanocarriers used for gene therapy need to have the capacity to carry and protect the therapeutic nucleic acids until reach the targeted cells. However, the ability to release their cargo into the cells is a key step for a

correct therapy administration and effect [69–71]. PSN demonstrated their capacity to release their cargo, in this case a miRNA. The miRNA 145 was the selected therapeutic nucleic acid, and it was tested *in vivo* in 0 hours post-fecundation (hpf) zebrafish embryos (Figure 7A). The effect in the expression of zebrafish miRNA 145-related genes, sox9b and gata6, was evaluated to verify the correct release of the nucleic acid. This advantage of the external fecundation of the zebrafish allows this in one-cell stage experiments, which cannot be performed in other *in vivo* models [67].

Moreover, 48 hpf zebrafish embryos were the study platform to evaluate the biodistribution and SNs interactions with cancer cells. As explained before, the transparency of the model permits the visualization of fluorescently labelled nanosystems and cells by fluorescent or confocal microscopy [58]. With this in mind, TopFluor-PSN demonstrated an efficient maintenance of the association between PSN and nucleic acids *in vivo*, meaning that the cargo remains protected (Figure 7B). Besides this, PSN showed *in vivo* interactions with xenografted cancer cells in the zebrafish (Figure 7C). Despite PSN are not functionalized, the affinity of the cancer cells by polyamines, such as putrescine, can be the responsible of this successful interaction [72].

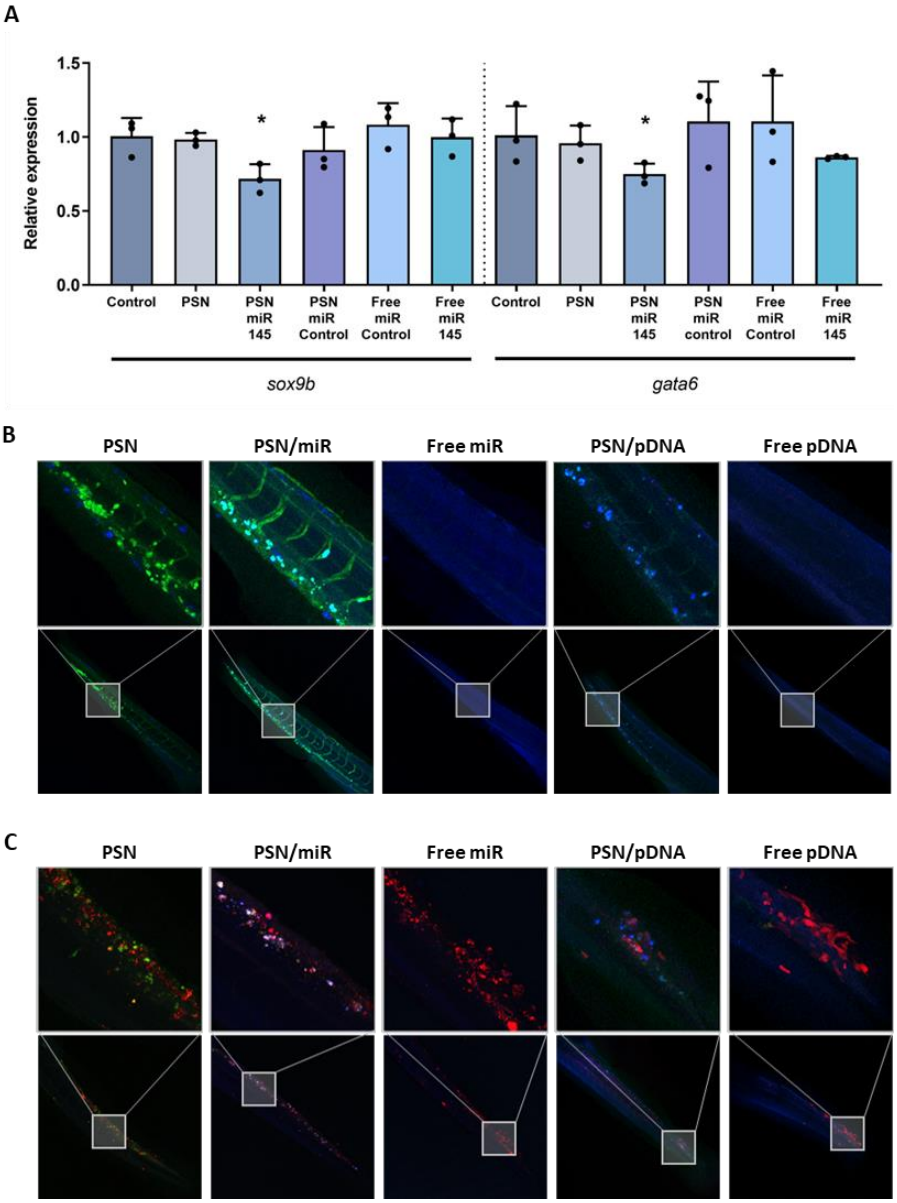

Figure 7. A. RT-qPCR results of the effect of miR 145 associated and non-associated with PSN in the relative expression of sox9b and gata6 genes in zebrafish embryos; **B.** Confocal images of *in vivo* biodistribution of TopFluor-labelled nanoemulsions

(green) with and without miR-Cy5 and pDNA (blue), after 48 hours incubation in microinjected 48 hpf zebrafish embryo; **C.** Confocal images of *in vivo* interaction between nanoemulsions, labelled with TopFluor (green), and associated and non-associated miR and pDNA Cy5-labelled (blue) with DiI-MDA-MB-231 cancer cells (red).

Overview and future perspectives

Overall, SNs have successfully demonstrated their capacity of adaptation to carry different treatment strategies: hydrophobic drugs, such as DSF; aptamers for targeted therapy; and different nucleic acids, miRNAs and plasmids, for gene therapy. Furthermore, spheroids, OOC microfluidic devices and zebrafish embryos successfully prove their capacity to be effective study platforms for the preclinical assessment of nanomedicines.

For continuation of this work, more complex 3D static models could be explored, such as organoids and 3D co-cultures, including for example cancer and immune cells [73]. Further evaluation of SNs still remains to be done in the developed OOC microfluid device. Additionally, the devices can gain value by including additional elements to mimic, for example, the metastatic cascade [74,75]. Likewise, further evaluation studies can elucidate more specific characteristics about the behavior and biodistribution of SNs in other study models. For example, transgenic ZF lines, such as the Tg(BACmpo:gfp)^{i114} and Tg(mpeg1:eGFP), which have labelled immune system cells, neutrophils and macrophages, respectively; or the Tg(fli1:eGFP) ZF transgenic line which has fluorescently labelled the endothelial cells, marking the vasculature [58,76–

[79]. These transgenic embryos will allow the evaluation of the interaction between SNs and the immune system cells.

BIBLIOGRAPHY

1. Nirmala, M. J. *et al.* Cancer nanomedicine: a review of nano-therapeutics and challenges ahead. *RSC Adv* **13**, 8606 (2023).

2. Senga, S. S. & Grose, R. P. Hallmarks of cancer—the new testament. *Open Biol* **11**, (2021).

3. Tsimberidou, A. M., Fountzilas, E., Nikanjam, M. & Kurzrock, R. Review of Precision Cancer Medicine: Evolution of the Treatment Paradigm. *Cancer Treat Rev* **86**, 102019 (2020).

4. Senga, S. S. & Grose, R. P. Hallmarks of cancer—the new testament. *Open Biol* **11**, (2021).

5. Xia, L. *et al.* The cancer metabolic reprogramming and immune response. *Mol Cancer* **20**, (2021).

6. Bruni, D., Angell, H. K. & Galon, J. The immune contexture and Immunoscore in cancer prognosis and therapeutic efficacy. *Nature Reviews Cancer 2020 20:11* **20**, 662–680 (2020).

7. Faubert, B., Solmonson, A. & DeBerardinis, R. J. Metabolic reprogramming and cancer progression. *Science* **368**, (2020).

8. Visser, K. E. de & Joyce, J. A. The evolving tumor microenvironment: From cancer initiation to metastatic outgrowth. *Cancer Cell* **41**, 374–403 (2023).

9. Liu, C., Yang, M., Zhang, D., Chen, M. & Zhu, D. Clinical cancer immunotherapy: Current progress and prospects. *Front Immunol* **13**, (2022).

10. Anwanwan, D., Singh, S. K., Singh, S., Saikam, V. & Singh, R. Challenges in liver cancer and possible treatment approaches. *Biochim Biophys Acta Rev Cancer* **1873**, 188314 (2020).

11. Burguin, A., Diorio, C. & Durocher, F. Breast Cancer Treatments: Updates and New Challenges. *Journal of Personalized Medicine 2021, Vol. 11, Page 808* **11**, 808 (2021).

12. Wood, L. D., Canto, M. I., Jaffee, E. M. & Simeone, D. M. Pancreatic Cancer: Pathogenesis, Screening, Diagnosis, and Treatment. *Gastroenterology* **163**, 386–402 (2022).

13. Chaft, J. E. *et al.* Evolution of systemic therapy for stages I–III non-metastatic non-small cell lung cancer. *Nat Rev Clin Oncol* **18**, 547 (2021).

14. Al-Zoubi, M. S. & Al-Zoubi, R. M. Nanomedicine tactics in cancer treatment: Challenge and hope. *Crit Rev Oncol Hematol* **174**, 103677 (2022).

15. Farjadian, F. *et al.* Nanopharmaceuticals and nanomedicines currently on the market: challenges and opportunities. *Nanomedicine* **14**, 93 (2019).

16. Etter, E. L., Mei, K. C. & Nguyen, J. Delivering more for less: nanosized, minimal-carrier and pharmacoactive drug delivery systems. *Adv Drug Deliv Rev* **179**, 113994 (2021).

17. Halwani, A. A. Development of Pharmaceutical Nanomedicines: From the Bench to the Market. *Pharmaceutics* **14**, (2022).

18. Chen, J. *et al.* Lipid nanoparticle-mediated lymph node–targeting delivery of mRNA cancer vaccine elicits robust CD8+ T cell response. *Proc Natl Acad Sci U S A* **119**, (2022).

19. Wang, C., Zhang, Y. & Dong, Y. Lipid Nanoparticle–mRNA Formulations for Therapeutic Applications. *Acc Chem Res* **54**, 4283 (2021).

20. Zhang, Q. *et al.* Protein-Based Nanomedicine for Therapeutic Benefits of Cancer. *ACS Nano* **15**, 8001–8038 (2021).

21. Fu, Z. & Xiang, J. Aptamer-Functionalized Nanoparticles in Targeted Delivery and Cancer Therapy. *Int J Mol Sci* **21**, 1–39 (2020).

22. Liu, M., Li, L., Jin, D. & Liu, Y. Nanobody—A versatile tool for cancer diagnosis and therapeutics. *Wiley Interdiscip Rev Nanomed Nanobiotechnol* **13**, e1697 (2021).

23. Wu, S.-Y. *et al.* Antibody-Incorporated Nanomedicines for Cancer Therapy. *Advanced Materials* **34**, 2109210 (2022).

24. Barenholz, Y. Doxil® — The first FDA-approved nano-drug: Lessons learned. *Journal of Controlled Release* **160**, 117–134 (2012).

25. Park, H., Otte, A. & Park, K. Evolution of Drug Delivery Systems: From 1950 to 2020 and Beyond. *J Control Release* **342**, 53 (2022).

26. Corrò, C., Novellasdemunt, L. & Li, V. S. W. Making Cell Culture More Physiological: A brief history of organoids. *Am J Physiol Cell Physiol* **319**, C151 (2020).

27. Bouzo, B. L., Calvelo, M., Martín-Pastor, M., García-Fandiño, R. & de La Fuente, M. In Vitro- In Silico Modeling Approach to Rationally Designed Simple and Versatile Drug Delivery Systems. *Journal of Physical Chemistry B* **124**, 5788–5800 (2020).

28. Bouzo, B. L. *et al.* Sphingomyelin nanosystems loaded with uroguanylin and etoposide for treating metastatic colorectal cancer. *Sci Rep* **11**, 17213 (2021).

29. Nagachinta, S., Bouzo, B. L., Vazquez-Rios, A. J., Lopez, R. & de la Fuente, M. Sphingomyelin-based nanosystems (SNs) for the development of anticancer miRNA therapeutics. *Pharmaceutics* **12**, (2020).

30. Masoumi, F. *et al.* Modulation of Colorectal Tumor Behavior via lncRNA TP53TG1-Lipidic Nanosystem. *Pharmaceutics* **13**, (2021).

31. Saraiva, S. M. *et al.* Edelfosine nanoemulsions inhibit tumor growth of triple negative breast cancer in zebrafish xenograft model. *Sci Rep* **11**, (2021).

32. Bidan, N. *et al.* Before in vivo studies: In vitro screening of sphingomyelin nanosystems using a relevant 3D multicellular pancreatic tumor spheroid model. *Int J Pharm* **617**, (2022).

33. Lores, S. *et al.* Effectiveness of a novel gene nanotherapy based on putrescine for cancer treatment. *Biomater Sci* **11**, 4210–4225 (2023).

34. Díez-Villares, S. *et al.* Biodistribution of 68/67Ga-Radiolabeled Sphingolipid Nanoemulsions by PET and SPECT Imaging. *Int J Nanomedicine* **16**, 5923 (2021).

35. Díez-Villares, S. *et al.* Quantitative PET tracking of intra-articularly administered 89Zr-peptide-decorated nanoemulsions. *Journal of Controlled Release* **356**, 702–713 (2023).

36. Díez-Villares, S. *et al.* Manganese Ferrite Nanoparticles Encapsulated into Vitamin E/Sphingomyelin Nanoemulsions as Contrast Agents for High-Sensitive Magnetic Resonance Imaging. *Adv Healthc Mater* **10**, 2101019 (2021).

37. Wang, R., Xiao, R., Zeng, Z., Xu, L. & Wang, J. Application of poly(ethylene glycol)–distearoylphosphatidylethanolamine (PEG-DSPE) block copolymers and their derivatives as nanomaterials in drug delivery. *Int J Nanomedicine* **7**, 4185 (2012).

38. D'souza, A. A. & Shegokar, R. Polyethylene glycol (PEG): a versatile polymer for pharmaceutical applications. *Expert Opin Drug Deliv* **13**, 1257–1275 (2016).

39. Ibrahim, M. *et al.* Polyethylene glycol (PEG): The nature, immunogenicity, and role in the hypersensitivity of PEGylated products. *Journal of Controlled Release* **351**, 215–230 (2022).

40. Liu, M. *et al.* Branched PEG-modification: A new strategy for nanocarriers to evade of the accelerated blood clearance phenomenon and enhance anti-tumor efficacy. *Biomaterials* **283**, 121415 (2022).

41. Jatal, R. *et al.* Sphingomyelin nanosystems decorated with TSP-1 derived peptide targeting senescent cells. *Int J Pharm* **617**, 121618 (2022).

42. Lu, C., Li, X., Ren, Y. & Zhang, X. Disulfiram: a novel repurposed drug for cancer therapy. *Cancer Chemother Pharmacol* **87**, 159–172 (2021).

43. He, H., Markoutsa, E., Li, J. & Xu, P. Repurposing Disulfiram for Cancer Therapy via Targeted Nanotechnology through Enhanced

Tumor Mass Penetration and Disassembly. *Acta Biomater* **68**, 113 (2018).

44. Guo, J. *et al.* Aptamer-functionalized PEG–PLGA nanoparticles for enhanced anti-glioma drug delivery. *Biomaterials* **32**, 8010–8020 (2011).

45. Powell, D. *et al.* Aptamer-functionalized hybrid nanoparticle for the treatment of breast cancer. *Eur J Pharm Biopharm* **114**, 108 (2017).

46. Shahrad, S., Rajabi, M., Javadi, H., Karimi Zarchi, A. A. & Darvishi, M. H. Targeting lung cancer cells with MUC1 aptamer-functionalized PLA-PEG nanocarriers. *Sci Rep* **12**, (2022).

47. Vázquez Ríos, A. J. Development of targeted therapeutic strategies for metastatic lung cancer. (Universidade de Santiago de Compostela, 2020).

48. Jianghong, L. *et al.* Aptamer and Peptide-Modified Lipid-Based Drug Delivery Systems in Application of Combined Sequential Therapy of Hepatocellular Carcinoma. *ACS Biomater Sci Eng* **7**, 2558–2568 (2021).

49. Agostinelli, E., Vianello, F., Magliulo, G., Thomas, T. & Thomas, T. J. Nanoparticle strategies for cancer therapeutics: Nucleic acids, polyamines, bovine serum amine oxidase and iron oxide nanoparticles. *Int J Oncol* **46**, 5–16 (2015).

50. Pozzi, S. *et al.* Meet me halfway: Are in vitro 3D cancer models on the way to replace in vivo models for nanomedicine development? *Adv Drug Deliv Rev* **175**, 113760 (2021).

51. Delvecchio, C., Tiefenbach, J. & Krause, H. M. The Zebrafish: A powerful platform for in vivo, HTS drug discovery. *Assay Drug Dev Technol* **9**, 354–361 (2011).

52. Lieschke, G. J. & Currie, P. D. Animal models of human disease: Zebrafish swim into view. *Nat Rev Genet* **8**, 353–367 (2007).

53. Jensen, C. & Teng, Y. Is It Time to Start Transitioning From 2D to 3D Cell Culture? *Front Mol Biosci* **7**, 33 (2020).

54. Liu, X. *et al.* Recent Advances of Organ-on-a-Chip in Cancer Modeling Research. *Biosensors (Basel)* **12**, (2022).

55. Sontheimer-Phelps, A., Hassell, B. A. & Ingber, D. E. Modelling cancer in microfluidic human organs-on-chips. *Nat Rev Cancer* **19**, 65–81 (2019).

56. Habanjar, O., Diab-Assaf, M., Caldefie-Chezet, F. & Delort, L. 3D Cell Culture Systems: Tumor Application, Advantages, and Disadvantages. *Int J Mol Sci* **22**, (2021).

57. Pozzi, S. *et al.* Meet me halfway: Are in vitro 3D cancer models on the way to replace in vivo models for nanomedicine development? *Adv Drug Deliv Rev* **175**, 113760 (2021).

58. Sieber, S. *et al.* Zebrafish as a preclinical in vivo screening model for nanomedicines. *Adv Drug Deliv Rev* **151–152**, 152–168 (2019).

59. Guo, X. *et al.* Enrichment of cancer stem cells by agarose multi-well dishes and 3D spheroid culture. *Cell Tissue Res* **375**, 397–408 (2019).

60. Zhang, C. *et al.* 3D culture technologies of cancer stem cells: promising ex vivo tumor models. *J Tissue Eng* **11**, (2020).

61. Niora, M. *et al.* Head-to-Head Comparison of the Penetration Efficiency of Lipid-Based Nanoparticles into Tumor Spheroids. *ACS Omega* **5**, 21162–21171 (2020).

62. Tchoryk, A. *et al.* Penetration and uptake of nanoparticles in 3D tumor spheroids. *Bioconjug Chem* **30**, 1371–1384 (2019).

63. Arora, N., Shome, R. & Ghosh, S. S. Deciphering therapeutic potential of PEGylated recombinant PTEN-silver nanoclusters ensemble on 3D spheroids. *Mol Biol Rep* **46**, 5103–5112 (2019).

64. Veiga, N., Diesendruck, Y. & Peer, D. Targeted nanomedicine: Lessons learned and future directions. *Journal of Controlled Release* **355**, 446–457 (2023).

65. Kang, S., Park, S. E. & Huh, D. D. Organ-on-a-chip technology for nanoparticle research. *Nano Converg* **8**, (2021).

66. Mastrangeli, M., Millet, S. & van den Eijnden-Van Raaij, J. Organ-on-chip in development: Towards a roadmap for organs-on-chip. *ALTEX - Alternatives to animal experimentation* **36**, 650–668 (2019).

67. Gutiérrez-Lovera, C., Vázquez-Ríos, A. J., Guerra-Varela, J., Sánchez, L. & de la Fuente, M. The potential of zebrafish as a model organism for improving the translation of genetic anticancer nanomedicines. *Genes (Basel)* **8**, 1–20 (2017).

68. Gutiérrez-Lovera, C., Vázquez-Ríos, A. J., Guerra-Varela, J., Sánchez, L. & de la Fuente, M. The potential of zebrafish as a model organism for improving the translation of genetic anticancer nanomedicines. *Genes (Basel)* **8**, 1–20 (2017).

69. Fihurka, O., Sanchez-Ramos, J. & Sava, V. Optimizing Nanoparticle Design for Gene Therapy: Protection of Oligonucleotides from Degradation Without Impeding Release of Cargo. *Nanomed Nanosci Res* **2**, (2018).

70. Vaughan, H. J., Green, J. J. & Tzeng, S. Y. Cancer-Targeting Nanoparticles for Combinatorial Nucleic Acid Delivery. *Adv Mater* **32**, e1901081 (2020).

71. Male, D. & Gromnicova, R. Nanocarriers for Delivery of Oligonucleotides to the CNS. *Int J Mol Sci* **23**, (2022).

72. Novita Sari, I. *et al.* Metabolism and function of polyamines in cancer progression. *Cancer Lett* **519**, 91–104 (2021).

73. El Harane, S. *et al.* Cancer Spheroids and Organoids as Novel Tools for Research and Therapy: State of the Art and Challenges to Guide Precision Medicine. *Cells* **12**, (2023).

74. Imparato, G., Urciuolo, F. & Netti, P. A. Organ on Chip Technology to Model Cancer Growth and Metastasis. *Bioengineering* **9**, (2022).

75. Del Piccolo, N. *et al.* Tumor-on-chip modeling of organ-specific cancer and metastasis. *Adv Drug Deliv Rev* **175**, 113798 (2021).

76. Ellett, F., Pase, L., Hayman, J. W., Andrianopoulos, A. & Lieschke, G. J. mpeg1 promoter transgenes direct macrophage-lineage expression in zebrafish. *Blood* **117**, e49 (2011).

77. Renshaw, S. A. *et al.* A transgenic zebrafish model of neutrophilic inflammation. *Blood* **108**, 3976–3978 (2006).

78. Gillies, S. *et al.* Transgenic zebrafish larvae as a non-rodent alternative model to assess pro-inflammatory (neutrophil) responses to nanomaterials. *Nanotoxicology* **16**, 333–354 (2022).

79. Lawson, N. D. & Weinstein, B. M. In Vivo Imaging of Embryonic Vascular Development Using Transgenic Zebrafish. *Dev Biol* **248**, 307–318 (2002).

CONCLUSIONS

CONCLUSIONS

In the work developed in the framework of this thesis, sphingomyelin nanosystems were loaded with different types of molecules, and decorated with specific ligands, to explore their application in the development of innovative anticancer treatments. To assess their behavior and efficacy, the use of static and non-static models, as well as zebrafish embryos, was proposed for *in vitro* and *in vivo* evaluation. The data extracted from the experimental results led us to withdraw the following conclusions:

1. Sphingomyelin nanosystems have demonstrated their capacity to efficiently encapsulate hydrophobic drugs, such as disulfiram, as well as nucleic acids, and can also be surface-decorated with ligands for specific cell targeting.
2. Disulfiram-loaded sphingomyelin nanosystems can efficiently penetrate into non-small cell lung cancer spheroids, achieving the inner core of the structure, and inducing a therapeutic effect.
3. An effective targeting of the surface-decorated nanosystems was evidenced in TAS1R3-overexpressed non-small cell lung cancer cells, in 2D. The tracking of the formulation was also successfully achieved in a more complex non-static microfluidic device.
4. A 3D static model, cell lung cancer spheroids, and an organ-on-a-chip non-static microfluidic device, demonstrated their potential for *in*

vitro evaluation of novel anticancer treatments based on nanomedicines.

5. The capacity of nucleic acids to remain associated to sphingomyelin nanosystems after *in vivo* administration was demonstrated in zebrafish embryos.
6. Zebrafish embryos proved their ability for being a study platform to evaluate the behavior and *in vivo* interaction of gene nanomedicines. *in vivo*.

ABBREVIATIONS

ABBREVIATIONS

2D	Two dimensional
3D	Three dimensional
ACN	Acetonitrile
ASOs	Antisense oligonucleotides
ATCC	American Type Culture Collection
bFGF	Human fibroblast growth factor basic
BSA	Bovine Serum Albumin
CAFs	Cancer-associated-fibroblasts
Calcein AM	Calcein acetoxymethyl
cDNA	Complementary DNA
Cell-SELEX	Cell-Systematic Evolution of Ligands by EXponential Enrichment
CSCs	Cancer stem cells
Cy5	Cyanine 5
DEN	Diethylnitrosamine
DiI	1,1'-Dioctadecyl-3,3,3',3'-Tetramethylindocarbocyanine Perchlorate
DLS	Dynamic light scattering
DMBA	Dimethylbenzanthracene
DMEM	Dulbecco′s Modified Eagle′s Medium

DMSO	Dimethyl sulfoxide
DNA	Desoxyribonucleic acid
dpf	Days post-fecundation
DSF	Disulfiram
ECGS	Endothelial Cell Growth Supplement
EGF	Human Epidermal growth factor
ENU	Ethylnitrosourea
EMA	European Medicines Agency
EtOH	Ethanol
FBS	Fetal bovine serum
FDA	Food and Drug Administration
hpf	Hours post-fecundation
HPLC	High Performance Liquid Chromatography
HPMEC	Human pulmonary microvascular endothelial cells
IC50	50% inhibitory concentration
LDA	Laser Doppler Anemometry
LOD	Limit of Detection
LOQ	Limit of Quantification
M199	Medium 199
MeOH	Methanol
miR	microRNA
MNNG	N-methyl-N'-nitro-N-nitrosoguanidine
MO	Morpholinos

MTS	(3-(4,5-dimethylthiazol-2-yl)-5-(3-carboxymethoxyphenyl)-2-(4-sulfophenyl)-2H-tetrazolium, inner salt)
NaCl	Sodium chloride
NAs	Nucleic acids
NDMA	N-nitrosodimethylamine
NEAA	Non-essential amino acids
NSCLC	Non-small cell lung cancer
OOC	Organ-on-a-chip
P/S	Penicillin-Streptomycin
PBS	Dulbecco's Phosphate Buffered Saline
PdI	Polydispersity index
PDMS	Polydimethylsiloxane
pDNA	DNA Plasmid
PDO	Patient-derived organoids
PDS	Patient-derived spheroids
PEG	Polyethylene glycol
PEI	Polyethylenimine
PFA	Paraformaldehyde
PI	Propidium iodide
PSN	Putrescine-sphingomyelin nanosystems
PSN/miR	Putrescine-sphingomyelin nanosystems with associated miR
PSN/pDNA	Putrescine-sphingomyelin nanosystems with associated pDNA
Pt	Putrescine

PTU	Phenylthiourea
PVP	Polyvinylpyrrolidone
RNA	Ribonucleic acid
RPMI	Roswell Park Memorial Institute Medium
SCLC	Small cell lung cancer
shRNAs	Short hairpin RNAs
siRNAs	Small interfering RNAs
SM	Sphingomyelin
SNs	Sphingomyelin nanosystems
SNs-49F	Sphingomyelin nanosystems functionalized with aptamer 49F
SNs-5F	Sphingomyelin nanosystems functionalized with aptamer 5F
SNs-DSF	Sphingomyelin nanosystems with encapsulated DSF
STEM	Scanning Transmission Electron Microscopy
Sulfo-SANPAH	sulfosuccinimidyl-6-[4′-azido-2′-nitrophenylamino]hexanoate
TALENs	Transcription Activator-Like Effector Nucleases
TAS1R3	Taste Receptor type 1 member 3
TBE	Tris-Borate-EDTA
TFA	Trifluoroacetic
TILLING	Targeted Induced Local Lesions in Genomes
ULA	Ultra-low attachment
UV	Ultra-violet
VE	Vitamin E

WGA	Wheat Germ Agglutinin
wpf	Weeks post-fertilization
ZFNs	Zinc Finger Nucleases
ZP	Zeta potential
zPDXs	Zebrafish patient-derived xenografts

AGRADECEMENTOS

AGRADECEMENTOS

Estes catro anos de tese foron, sen dúbida, unha montaña rusa de emocións. Levo comigo moita aprendizaxe, moitas experiencias, momentos bos e malos, e moitas persoas, esas que me acompañaron neste camiño e que fixeron, sen dubida, que fose inolvidable.

Primeiramente, agradecer ás miñas directoras de tese, María de la Fuente e Laura Sánchez. María, gracias por darme a oportunidade de desenvolver a miña carreira investigadora na Unidade de Nano-Oncoloxía, fuches realmente inspiradora. Estou moi agradecida pola confianza que depositaches en min durante estes anos, e por toda a axuda que me prestaches. Laura, xa na carreira, naquelas clases de xenética humana, descubríchesme o apasionante mundo dos peixes cebra, e penso que foi a clave de todo o que veu despois. Moitas gracias por estar sempre disposta a axudarme para o que necesitara e por preocuparte tanto por min.

Estou moi agradecida a todas as miñas compañeiras e compañeiros cos que tiven a fortuna de coincidir na Unidade de Nano-Oncoloxía, que fixeron que me leve un recordo inmellorable: Miguel, Raneem, Rebeca, Aurora, Sofia, Belén, Laura T, Inés, Irene M, Cris, Olaia, Abi, Gabriela, Marce, Juliane, Irene DF, Álex, Bárbara, Amelia, Javi. Neste ir e vir de xente, como é común na investigación, tiven a sorte de poder formar unha pequena gran familia, desas que se escollen, e que me brindou ás que hoxe en día podo considerar grandes amigas. Son, non só compañeiras de laboratorio, senón que tamén

compañeiras de vida, porque xuntas apoiámonos nos malos momentos, e desfrutamos dos bos. Nere, quen nos diría que, vivindo tan preto, nos reencontraríamos no Lab 20 despois de tantos anos. Foi un pracer poder compartir o meu último ano contigo. Redescubrirnos foi marabilloso e non che podo agradecer o suficiente toda a axuda que me deches. Emma, a miña macarra inconformista favorita. Chegaches dicindo que estabas chiquita, pero en pouco tempo creciches, e moito, e eu só podo ver o grande que es e serás. Foi unha chulada poder ser veciñas de poyata e de portal, por todas as risas, confidencias e merendas, e porque recorrer Av. Barcelona contigo sempre foi xenial. Sori e Lau, Pili e Mili, por moito que pasen os anos, para min sempre seredes as nanobabies. Mil gracias por ser as perfectas compis de mesa, por acollerme tantas veces na vosa habitación croma e por facerme un oco no voso fogar. Lau, non podo agradecerche o suficiente todo o que me aportaches, gracias por saber levantarme os ánimos, polas apertas curativas e por axudarme sempre en todo. Sempre nos quedará A Curra, como ese recanto do mundo onde esquecernos dos problemas, desconectar e desfrutar. Sori, dende que chegaches ao laboratorio con esa ilusión non deixaches de sorprenderme. Gracias por ser apoio básico, por axudarme en todo e por ser a miña mellor confidente e experta en skincare. Jen, nuestra postdoc favoritísima. Y como no iba a ser así, si siempre estás dispuesta a ayudar y a echar una mano cuando haga falta. Ha sido todo un privilegio poder trabajar mano a mano contigo. Gracias por mantener siempre la sonrisa, la calma, por ser tan positiva y no dejar que los ánimos decaigan nunca. Hay tres personas que necesitan una mención especial, las mismas tres que recibieron con los brazos abiertos a una estudiante de máster, allá por 2019, con muchas dudas y miedos. San, mi leonesa predilecta, que te voy a decir, gracias por ser la profe perfecta, por responder las 100 preguntas que te hacía al día, por haberme enseñado tanto,

y por disipar todos los miedos que acechaban en mi cabeza, no podría haber tenido mejor maestra. Pero, sobre todo, gracias infinitas por estar ahí siempre para todas, por los abrazos sanadores en los malos momentos y por las alegrías sinceras. San, doutora Díez, dende que cheguei, sempre estiveches aí para todo o que necesitara. Non sei como agradecerche todo o que me aportaches e axudaches nesta etapa, dende o comezo ata o final. Gracias por representar esa calma que tantas veces me fixo falta. Fuches esencial, ti e esas vibras túas tan chulas, que sempre fan que os días malos sexan menos malos e que me axudan a conservar a calma nos momentos de estrés. Sai, Dra. Lores, non sei nin por onde empezar. Dende o meu primeiro día no Lab 18, fixéchesme sentir coma na casa. Foi unha sorte poder traballar contigo codo con codo e poder aprender tantísimo de ti. Gracias por estar sempre para recollerme nos meus peores momentos, por saber como me sentía sen ter que preguntar, por escoitarme e por entenderme tan ben. Aínda estando lonxe sempre estiveches aí, nunca esquecerei aquelas conexións Valencia-París que necesitaba tanto ou os nosos audios case podcast. Gracias tamén, por ser a miña máis fiel compañeira de merendas, porque ir ao Tertulia xuntas sempre foi terapéutico.

Mil gracias a todo o equipo do acuario da Facultade de Veterinaria e ao Grupo de ZebraBioRes por toda a súa axuda. Especialmente a Ana e, sobre todo, a Alba, por axudarme tanto e tan ben nesta tese.

Quero agradecer tamén aos rapaces do Laboratorio 13, por ser os perfectos compañeiros de cultivos e por estar sempre dispostos a axudar. Ao Laboratorio 15, en especial a Laila e Pablo, por ser punto de apoio esencial e porque os cafés con vós son sempre especiais. Ao laboratorio de ONCOMET, pola inmensa axuda prestada durante estes anos.

Agradecer a todas as persoas da Unidade Mixta, sobre todo a: Inés, Nuria, José Antonio, Miriam, Celso, Cristóbal, Carmen e Sabrina. Gracias por tratarme sempre tan ben e axudarme en todo o que necesitaba. Gracias en especial a Roberto Piñeiro, por permitirme adentrarme no mundo do peixe cebra e por brindarme sempre a túa axuda. Pablo, Dr. Hurtado, no me imagino a nadie mejor con quién formar el Peixiños Team, y es que, si tengo el mejor profesor, se dice y punto. Las mañanas y tardes rodeados de peces durante horas siempre se hicieron amenas, con la buena música sonando en la radio y nuestras conversaciones frikis.

Infinitas gracias aos meus queridos compis do Club de Oncoline: Patri, Pablo, Carlos, Nico, Óscar, Ana, Carol, Aida, Aitor, Manu, Rachel, Nuria, Inés, Ramón, Cristóbal, Aroa, Mimí. Mil gracias por todo o apoio nestes anos, porque sodes ese espazo seguro onde compartir o bo e o malo da tese, onde sentirse comprendida. Sempre estivestes aí se precisaba calquera cousa. Gracias por poñerlle o punto divertido á tese, por todos os cafés, as cañas de tarde e as oncocenas, porque eses momentos son os que fan que as pilas se recarguen. Tiven sorte por poder ser partícipe deste grupo tan marabilloso, que fixo que remate esta etapa co corazón moi cheo.

Durante esta tesis he tenido la oportunidad de realizar una estancia en la soleada Valencia, que me recibió, inesperadamente, lluviosa. Agradecer a Silvia Calabuig y Eloisa Jantus el haberme abierto las puertas del laboratorio y el haberme dado la oportunidad de aprender tanto como lo hice. Mis más sinceras gracias a todo el grupo del FIHGUV y del CIPF por acogerme tan bien. Eva, muchísimas gracias por ayudarme tanto y estar al pie del cañón. Y Susana, gracias por ser mi guía en la ciudad y en el laboratorio, por estar siempre dispuesta a ayudarme.

E de Valencia, a Braga, onde tiven a sorte de aprender moitísimo no INL, da man de Lorena Diéguez e o seu grupo. Lorena, mil gracias por acollerme cos brazos abertos, non unha senón dúas veces. Moitas gracias por deixarme formar parte do grupo, pola axuda e apoio, e polas túas palabras sempre amables. Thank you very much to the whole Medical Devices group for welcoming me so well and for always helping me. Ahmed, thank you for being the best “table neighbour”, for the daily dose of "bos días" and for the unexpected chocolates. I cannot thank you enough for your kindness and all the help you have given me. Ana, amiga, não sei como começar a agradecer toda a ajuda que me deste. Desde o primeiro dia conseguiste lidar com uma galega que tentava aprender português e OOC, tudo ao mesmo tempo, e é que foste uma maravilhosa professora. Não imagino uma melhor colega para formar o OOC team. Obrigada pelas longas jornadas no CCL, que a pesares de ser longas, sempre estiveram cheias de risadas. Obrigada também pelos planos fixe, como as tostas no café do Luís, os concertos inolvidáveis, e as visitas à Galiza.

Braga também me permitiu conhecer outra pessoa que se converteu em família. Sofia, foi um desafio conseguir casa em Braga, mas foi uma sorte que a única disponível me permitisse conhecer-te. Muito obrigada por fazer que na minha estadia me sentisse na casa. Sei que sempre terei uma família em Ílhavo, e tu uma em Valga.

Gracias tamén aos meus biólogos favoritos: Ana, Carol, Miguel, JC. Fostes, sen dúbida ningunha, o mellor que me pasou na carreira, fixestes que fose inmellorable. Pero o máis importante é que, despois de tantos anos, por moi lonxe que esteamos, seguimos ben cerca. Gracias por estar sempre aí, polos ánimos constantes e esas rutas polo monte que serven de desconexión.

Iara, amiga, non puiden ter unha mellor compañeira de viaxe durante esta etapa. Poder compartir contigo os momentos bos e, o máis importante, os malos, foi terapéutico. Quen nos diría ao comezar a carreira que nos íamos acompañar non só no grao, senón tamén no mestrado e na tese. Que vivir xuntas nos faría máis fortes, e que nós sempre seremos casa.

Hai persoas que significan fogar, e eu teño a sorte de estar rodeada delas. Volver á casa sempre significa poder estar cas de sempre, as que me levan aturado tantos anos. Laura, gracias por estar sempre, por esas merendas e ceas de desconexión que tanto necesitei. Raquel, por axudarme a desconectar con esas clases de pilates tan divertidas, e os nosos post-entrenos entre confidencias. Maite, gracias por todo o teu apoio, polas tardes entre cafés e cola-caos arranxando o mundo. Iria, non podo máis que agradecerche que sempre esteas aí. Gracias por ser apoio incondicional e por confiar en min nos momentos nos que nin eu mesma confiaba.

E por último, e máis importante, non podo agradecer o suficiente o apoio da miña familia, en especial aos meus avós. Tamén ao meu irmán, Lois, o meu aventureiro e biólogo mariño favorito. A ti agradecerche todo o apoio que me deches nesta etapa e sempre, porque os quilómetros de distancia non supoñen un problema e ti sempre estás aí. E, por suposto, aos meus pais, Eva e Moncho, por confiar sempre en min, polo apoio constante todos estes anos e por ser o meu soporte esencial nos bos e malos momentos. Gracias por ser o meu exemplo de perseverancia e traballo, por axudarme a chegar ata aquí, porque sen vós nada disto sería posible.

ETHICAL ISSUES AND ANNEXES

ETHICAL ISSUES

1. IMAGES USE

Unless clarified, all the images presented in this thesis have been produced by me. In the case of images reused or adapted from other manuscripts, permission has been asked to the publishers and the mode of legal use has been clarified. In addition, some figures were drawn by using pictures from Servier Medical Art by Servier, which is licensed under a Creative Commons Attribution 3.0 Unported License (https://creativecommons.org/licenses/by/3.0/). as well as the zebrafish drawing kindly supported by Lizzy Griffiths (http://zebrafishart.blogspot.com).

2. HUMAN CELL CULTURE

All cancer lines used in this work, unless specified, were acquired from commercially available resources (American Tissue Culture Collection, ATCC) and cultured in the conditions recommended by the manufacturers and only used for the research purposes specifically described in the present thesis.

3. PATIENT'S SAMPLES

Blood samples were collected in accordance with the guidelines and protocols approved by the Institutional Ethical Committees, Galician Clinical Research Ethics Committee, SERGAS: code approval: 2017/538. All individuals signed informed consent forms and could withdraw their consent at any time. The study was performed in accordance with the Declaration of Helsinki.

4. ZEBRAFISH EMBRYOS STUDIES

All the procedures described for zebrafish embryos were performed in agreement with the current legislation (RD53/2013, Directive 2010/63/UE). In this work only zebrafish embryos of 120 hpf or less were used, which are not considered experimental animals by the European legislation, Directive 2010/63/EU, because they are not independently feeding larval forms.

ANNEXES

ANNEX 1. PUBLICATIONS PRESENTED IN THIS THESIS

Introduction: What Zebrafish and Nanotechnology Can Offer for Cancer Treatments in the Age of Personalized Medicine

María Cascallar, Sandra Alijas, Alba Pensado-López, Abi Judit Vázquez-Ríos, Laura Sánchez, Roberto Piñeiro and María de la Fuente.

Cancers, 2022, 14(9), 2238.

https://doi.org/10.3390/cancers14092238

EISSN 2072-6694

Journal impact factor (2021): 6.575

Category rank: Oncology 60/245 (Q1)

Journal Citation Indicator (JCI)

Category Rank: Oncology 76/318 (Q1)

Contribution to this work:

I, María Cascallar Castro, has been involved in the conceptualization, writing the original draft preparation and reviews.

Chapter III. Zebrafish as a platform to evaluate the potential of lipidic nanoemulsions for gene therapy in cancer

María Cascallar, Pablo Hurtado, Saínza Lores, Alba Pensado-López, Ana Quelle-Regaldie, Laura Sánchez, Roberto Piñeiro and María de la Fuente

Frontiers in Pharmacology, 2022, 13,1007018

EISSN: 1663-9812

https://doi.org/10.3389/fphar.2022.1007018

Journal impact factor (2021): 5.988

Category rank: Pharmacology & Pharmacy 50/279 (Q1)

Journal Citation Indicator (JCI)

Category Rank: Pharmacology & Pharmacy 46/361 (Q1)

Contribution to this work:

I, María Cascallar Castro, have been involved in the conceptualization, writing—original draft preparation, writing—review and writing, and experiments conduction. Particularly, I have performed the nanosystems formulation and characterization, as well as the *in vivo* experiments in collaboration with the Roche-Chus Joint Unit of the Health Research Institute of Santiago de Compostela , except for the one described in the Section 3.2.

cancers

MDPI

Review

What Zebrafish and Nanotechnology Can Offer for Cancer Treatments in the Age of Personalized Medicine

María Cascallar [1,2,3], Sandra Alijas [1], Alba Pensado-López [3,4], Abi Judit Vázquez-Ríos [1,2,5], Laura Sánchez [3,6], Roberto Piñeiro [2,7] and María de la Fuente [1,2,5,*]

1 Nano-Oncology and Translational Therapeutics Group, Health Research Institute of Santiago de Compostela (IDIS), SERGAS, 15706 Santiago de Compostela, Spain; maria.cascallarc@gmail.com (M.C.); sandraalijasperez@gmail.com (S.A.); abi.judit.vr@gmail.com (A.J.V.-R.)
2 Centro de Investigación Biomédica en Red Cáncer (CIBERONC), 28029 Madrid, Spain; roberto.pineiro.cid@sergas.es
3 Department of Zoology, Genetics and Physical Anthropology, Universidade de Santiago de Compostela, Campus de Lugo, 27002 Lugo, Spain; alba.pensado.lopez@rai.usc.es (A.P.-L.); lauraelena.sanchez@usc.es (L.S.)
4 Center for Research in Molecular Medicine & Chronic Diseases (CIMUS), Campus Vida, Universidade de Santiago de Compostela, 15782 Santiago de Compostela, Spain
5 DIVERSA Technologies S.L., 15782 Santiago de Compostela, Spain
6 Preclinical Animal Models Group, Health Research Institute of Santiago de Compostela (IDIS), 15706 Santiago de Compostela, Spain
7 Roche-Chus Joint Unit, Translational Medical Oncology Group, Oncomet, Health Research Institute of Santiago de Compostela, Travesía da Choupana s/n, 15706 Santiago de Compostela, Spain
* Correspondence: maria.de.la.fuente.freire@sergas.es; Tel.: +34-981-955-704

check for updates

Citation: Cascallar, M.; Alijas, S.; Pensado-López, A.; Vázquez-Ríos, A.J.; Sánchez, L.; Piñeiro, R.; de la Fuente, M. What Zebrafish and Nanotechnology Can Offer for Cancer Treatments in the Age of Personalized Medicine. *Cancers* **2022**, *14*, 2238. https://doi.org/10.3390/cancers14092238

Academic Editors: Eleanor Y. Chen and Myron Ignatius

Received: 26 March 2022
Accepted: 28 April 2022
Published: 30 April 2022

Publisher's Note: MDPI stays neutral with regard to jurisdictional claims in published maps and institutional affiliations.

Simple Summary: Discovering new strategies for cancer treatment is critical, considering that each year millions of deaths are caused by this disease. In this sense, therapies based on nanomedicine are an innovative approach for cancer treatment, not only because they make it possible to perform targeted therapy, but also because they can improve patients' quality of life. A key step to transfer new treatments from bench to beside is in vivo evaluation of a therapy, where zebrafish as a model organism has a fundamental role. Zebrafish has several benefits that make it ideal for studying the therapeutic capacity of novel nanotechnology-based anticancer therapies. In this review, we evaluate the potential of the nanomedicine and zebrafish synergy to achieve personalized treatments for cancer.

Abstract: Cancer causes millions of deaths each year and thus urgently requires the development of new therapeutic strategies. Nanotechnology-based anticancer therapies are a promising approach, with several formulations already approved and in clinical use. The evaluation of these therapies requires efficient in vivo models to study their behavior and interaction with cancer cells, and to optimize their properties to ensure maximum efficacy and safety. In this way, zebrafish is an important candidate due to its high homology with the human genoma, its large offspring, and the ease in developing specific cancer models. The role of zebrafish as a model for anticancer therapy studies has been highly evidenced, allowing researchers not only to perform drug screenings but also to evaluate novel therapies such as immunotherapies and nanotherapies. Beyond that, zebrafish can be used as an "avatar" model for performing patient-derived xenografts for personalized medicine. These characteristics place zebrafish in an attractive position as a role model for evaluating novel therapies for cancer treatment, such as nanomedicine.

Keywords: zebrafish; nanomedicine; cancer; personalized medicine; drug screening; xenograft

1. Emerging Cancer Therapeutics

Cancer is a major public health problem worldwide and the second-leading cause of death globally. Almost ten million people die from cancer every year, and this number is

estimated to reach over 13 million in 2030 [1]. The most common causes of cancer death are lung, liver, and stomach cancers in men, and breast, lung, and colorectal cancers in women [2].

Cancer is a complex genetic disease that is caused by specific changes to genes in one cell or group of cells. These changes include sustaining proliferative signaling, evading growth suppressors, resisting cell death, enabling replicative immortality, inducing angiogenesis, and activating invasion and metastasis [3]. Metastases are the cause of the majority of human cancer deaths [4]. In the particular case of localized-stage colorectal cancer (CRC), the 5-year survival rate is around 90%, declining to 71% and 14% for patients diagnosed with regional and distant metastatic stages, respectively (American Cancer Society, Atlanta, GA, USA, 2017); in the case of pancreatic cancer, it falls from 37% to 3% in the distal metastatic setting [5]; and in non-small-cell lung carcinoma (NSCLC), from 24% to 6% in advanced stages of the disease when metastasis occurs [6].

The process of metastasis is defined by a cascade of complex events in which malignant cells detach from the primary tumor, invade through the basement membrane, and then migrate into the circulation, either via the blood or lymphatic vessels, to finally spread to distant sites to form metastases [7]. Although most early stage tumors can be surgically removed, there is growing evidence that dissemination could indeed happen at a very early stage in the carcinogenesis process [8], a fact that could explain why, in some tumor types such as pancreatic cancer, the 5-year survival even for localized disease is so poor.

It is generally accepted that the development of metastatic cancer implies cancer cells from the primary tumor alter several distinct features in order to succeed in this very complex process. Some of these modifications are (i) a change from an epithelial to a more mesenchymal phenotype, (ii) the acquisition of stem-cell properties and phenotypic plasticity, and (iii) a change in their metabolism in a way that promotes survival and metastatic outgrowth [9–12]. Conventional anticancer treatments mainly target the bulk tumor and often fail to eliminate the highly tumorigenic and chemo-resistant cell subpopulations.

NSCLC is a clear example of the results of these prevalent tumor treatments. Curative surgery is the standard of care for early-stage patients with good performance status; however, 35–50% of the resected patients relapse after an apparently successful surgical treatment [13]. For a long time, platinum-based doublets have been the standard first-line treatment option for unresectable advanced NSCLC [14]. Despite the survival improvement achieved with first-line chemotherapy, about 30% of patients do not obtain a tumor response. Moreover, patients who are initially sensitive to treatment acquire resistance and develop tumor progression after a median of about 5 months [15]. The current treatment strategy considers factors such as histology, clinical stage, age, performance status, comorbidities, the patient's preferences, the molecular study, and an increasingly important focus on the immunological status. During the last years, a growing number of targetable major pathways have been identified, such as EGFR, PI3K/AKT/mTOR, RAS–MAPK, and NTRK/ROS1, leading to a new era of precision medicine [16].

Targeted therapy is the cornerstone of precision medicine, which seeks a molecular understanding of the disease to prevent, diagnose, and treat it. It can also be called personalized medicine, given that every patient receives the treatment that better fits their particular alterations in genes and proteins, providing them with significant responses and lesser toxicities compared with broad-spectrum cytotoxic therapy. The development of targeted therapies has resulted in substantial benefits in terms of survival and quality of life for cancer patients. Over the last twenty years, different drugs have been approved by the Food and Drug Administration (FDA) and the European Medicines Agency (EMA) for several tumor types, for example imatinib (gastrointestinal stromal tumors and dermatofibrosarcoma protuberans) [17] and cetuximab (colorectal cancer and head and neck cancer) [18], among others.

On the other hand, immunotherapy has become the most revolutionary treatment in solid tumors [19]. The discovery of ligands and receptors regulating T cell activation, called immune checkpoints, has represented a major therapeutic breakthrough in the field.

Immune checkpoint inhibitors (ICIs) are a group of antibodies designed to block specific targets present on tumor cells or lymphocyte surfaces (e.g., ipilimumab [20], the first approved anti-CTL4 antibody, and nivolumab [21–24] first approved anti-PD-1 antibody), consequently boosting the immune system to attack cancer. Immune checkpoints that target the programmed cell death-1 (PD-1), programmed cell death ligand-1 (PD-L1), and cytotoxic T-lymphocyte-associated antigen-4 (CTLA-4) have received approval across a wide range of cancer types, including lung cancer, melanoma, and head and neck, among others [16].

The current scenario for cancer research is wide and offers many possibilities for the constant improvement of therapies. In recent years, research into cancer medicine has taken remarkable steps towards more effective, precise, and less invasive cancer treatments. There is a plethora of newly proposed therapeutic options for cancer that are currently under investigation at different levels of maturity of the research stage, with some of them in clinical trials, such as oncolytic viruses [25], immune check-point antagonists [26], therapeutic cancer vaccines [27], natural antioxidants [28], hormone replacement therapy [29], exosome delivery platforms [30], aptamers [31], and thermal ablation and magnetic hyperthermia [32]. These strategies aim to provide the best personalized therapies for cancer patients and highlight the importance of combining multiple disciplines to achieve innovative approaches for the best outcome.

Other novel and promising therapeutic strategies that are already a reality in cancer treatment include antibody-drug-conjugates (such as ado-trastuzumab emtansine, approved in 2013 for treating HER2-positive metastatic breast cancer [33]); gene and cell therapy (such as tisagenlecleucel, approved by the FDA in August 2017 for certain pediatric and young adult patients with a form of acute lymphoblastic leukemia whose first-line drugs have failed [34]); and nanomedicine (for example, Doxil®, the first marketed PEGylated liposome loaded with the chemotherapeutic drug doxorubicin [35]).

2. Nanomedicine and Cancer

Nanomedicine has been widely explored during the last decades. Different nanosystems composed of a variety of materials have been proposed for the management of several diseases, such as liposomes and other lipid-based and polymer-based nanoparticles, micelles, polyplexes, dendrimers, polymersomes, and drug/protein conjugates [36]. Nanotechnology offers many advantages in drug delivery, including (i) protection of drugs from premature degradation, (ii) increased solubility and stability in biological media, (iii) prevention of premature interactions of drugs with the biological environment, (iv) controlled pharmacokinetics and biodistribution, (v) improved delivery of therapeutics across biological barriers, and (vi) targeting of drugs to the diseased area [37,38]. Due to these properties and their ability to accommodate various types of drugs and biomolecules, with different physicochemical properties and activities, nanocarriers have emerged as attractive candidates for the development of personalized medicine [39,40]. Nanotechnology-based therapeutics are paving the way in the diagnosis, imaging, screening, and treatment of primary and metastatic tumors; however, translating such advances from the bench to the bedside has been severely hampered by challenges encountered in the areas of pharmacology, toxicology, immunology, large-scale manufacturing, and regulatory issues. The latest advances in nanomedicine and cancer have been extensively reviewed in recent works due to the high potential of this nano-based therapy to improve cancer patients' quality of life [41–43]. A clear example is the work of Park et al., who reviewed how drug delivery systems progress over time, including cancer treatments such as Mylotarg® and Doxil® [44].

3. The Potential of Zebrafish for Preclinical Evaluation of Novel Cancer Therapeutics

Zebrafish (*Danio rerio*) is a vertebrate model species traditionally used for studying developmental biology and vertebrate genetics, and more recently, to model human diseases such as cancer, thus playing a key role in the discovery of new drugs for treating these

illnesses [45–47]. Zebrafish characteristics define it as a model species between invertebrate models and murine models because it collects the vertebrate traits and allows large experiments [45,46]. One of the features that make zebrafish an appropriate human disease model is its homology with the human genome, around 70%, which increases to 82% in the case of human disease-related genes [48]. Furthermore, there are multiple advantages associated with the use of zebrafish, such as high fecundity and fertilization rate, producing a large offspring [49]. In addition, the external fertilization and optical transparency of embryos and larvae allow direct visualization of the overall development and enable the imaging of cells without the use of invasive techniques [50].

In terms of cancer research, aside from the robustness of zebrafish embryos to be easily manipulated, the adaptive immune system is not active until 2–4 weeks post-fertilization (wpf), and complete immunocompetence is only achieved at 4–6 wpf [51]. This feature, together with the previously mentioned transparency, enables the transplantation of fluorescent cancer cells (xenotransplantation or xenograft) and the visualization and tracking of their growth, biodistribution, metastasis, and neovascularization processes, as well as the evaluation of drug responses [50,52]. The main advantages and disadvantages of zebrafish as a model for human diseases are summarized in Table 1.

Table 1. Benefits and drawbacks of using zebrafish for modeling human diseases in comparison with other animal models.

Advantages	Disadvantages
Simple anatomy	Some mammalian organs are missing
External fertilization	Optimal temperature at 28 °C, compromising human cell viability
Embryo and larvae optical transparency	Lack of sexual chromosomes
Rapid development and sexual maturation	Pooling individuals prevent the observation of interindividual differences
High fertility rates	Mice genetic homology is higher
Large number of individuals and statistical power	Low amount of certain tissues for biological assays
Robust embryos	Genetic duplication
High homology in human disease-related genes	Protocol variability, limiting the comparison among studies
Late activation of the adaptive immune system	Need of mammal models for further preclinical studies
Cost-effective and easy maintenance	Low antibodies availability for molecular assays
Easy genetic manipulation	
Low number of cells for xenograft assays	
Availability of reporter lines	
Many existing zebrafish resources and repositories	

The set of these characteristics have allowed researchers to develop several genetic and xenotransplantation zebrafish models and thus unravel the cellular, molecular, and physiological basis of different types of cancer, as well as drug response/resistance processes. Some relevant studies are reviewed in the following sections.

3.1. Genetic Models

3.1.1. Forward Genetics

Several carcinogens are able to induce human-like tumors in different zebrafish organs (Figure 1) [53]. Thus, studies have been performed, allowing a better understanding of the carcinogenesis process, main target tissues, type of tumor, signaling pathways, and chemoprevention measures. For instance, exposure to N1-nitro-N-nitrosoguanidine (MNNG) in 86 h post-fertilization (hpf) embryos and 3 wpf fry (immersion), 72 hpf embryos (microinjection), and 6 wpf juveniles (diet) showed that embryos and fry are responsive to carcinogenic

effects, whereas juveniles are remarkably resistant to neoplasia [54]. Embryos developed mainly hepatic and mesenchymal neoplasms, including chondroma, hemangioma, hemangiosarcoma, leiomyosarcoma, and rhabdomyosarcoma. The blood vessels and testis were the main target organs in fry, developing seminoma, hemangioma, hemangiosarcoma, and various other epithelial and mesenchymal neoplasms. Similarly, it has been shown that exposing zebrafish to Dimethylbenzanthracene (DMBA) at 3 wpf led, principally, to hepatic neoplasia in adults [55], with conservation of human transcriptome profiles, highlighting the potential of zebrafish for modeling human liver cancer [56]. Maid, a protein involved in cell proliferation, is abundantly expressed in the liver hepatocytes' cytoplasm of zebrafish; its role as a regulator of hepatocarcinogenesis was explored by treating adult zebrafish with Diethylnitrosamine (DEN) for 8 weeks. After treatment, these fish presented distended abdomens, extremely swollen livers, and different types of liver tumors. However, Maid appeared to translocate from the cytoplasm to the hepatocyte nucleus, presumably to participate in growth-inhibitory signaling and display its tumor-suppressor activity [57]. It has been stated that polyploidy in lower vertebrates decreases the probability of inactivation of all alleles of tumor suppressor genes, so the incidence of tumors might be lower [58]. In this regard, the relationship between polyploidy and tumor formation has been investigated through N-nitrosodimethylamine (NDMA)-induced hepatocarcinogenesis [59]. Diploid and triploid 6 wpf zebrafish exposed to this chemical for 8 weeks developed hepatocellular adenomas and trabecular hepatocellular carcinomas after 24 weeks from the beginning of the treatment, although cholangiolar tumors were not detected in triploid fish until 36 weeks, serving as evidence that polyploidy is a protective factor in pathogenesis of this type of tumor, probably indicating a lower probability for putative tumor suppressor genes to be inactivated in polyploid cholangiolar cells.

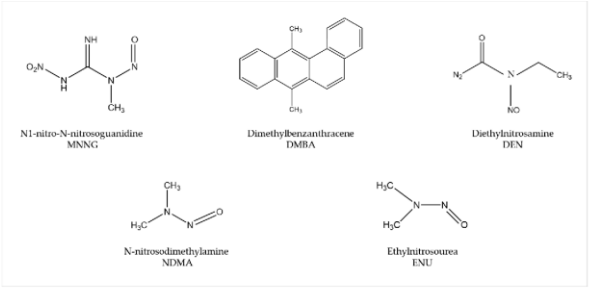

Figure 1. Most common carcinogenic substances used for tumor induction in zebrafish.

The mutagen ethylnitrosourea (ENU) has been used to generate point mutations, leading to the identification of several mutant zebrafish lines with an increased incidence of spontaneous neoplasia or higher sensitivity to chemical exposure [53]. For instance, Basten et al., in an attempt to study ciliary motility defects in the lrrc50 mutant zebrafish line, unexpectedly found development of seminomas in 2-year-old adults, with a penetrance of >90%. This observation allowed establishment of a correlation between the gen and such testicular germ cell tumors (GCTs) and proposes lrrc50 as a novel tumor suppressor [60]. Similarly, Neumann et al., while screening for cancer susceptibility genes, isolated a zebrafish mutant line with highly penetrant, heritable testicular GCTs in which testicular tumors spontaneously developed. Indeed, DMBA or MNNG exposure resulted in enhanced germ cell tumorigenesis [61].

3.1.2. Transgenic Zebrafish Lines

Several zebrafish cell and tissue-specific reporter lines have been developed over the last years to improve the comprehension and characterization of different cancer traits, such as tumor cell growth, migration, invasion, angiogenesis, drug responses, or interactions with immune cells. Some examples are Tg(mpx:GFP) and Tg(mpeg1:eGFP) [62,63], which fluorescently label neutrophils and macrophages, respectively, or Tg(fli1:eGFP) [64], which labels the vasculature. Furthermore, human or murine oncogene transgenic expression in zebrafish has also helped to understand their role in tumor development; for example, Tg(ptf1a:eGFP-KRAS^{G12V}) in pancreatic cancer [65] and Tg(mitfa:HRAS^{G12V}; mitfa:GFP) or Tg(mitfa:BRAF^{V600E}); tp53$^{-/-}$ for melanoma [66,67]. The binary transgenic system Gal4/UAS has also been extensively used. Gal4 is a transcriptional activator that, when expressed under the control specific tissue-specific promoters, binds to UAS enhancer sequences in the DNA, recruiting transcription machinery to induce gene expression, so genes under the control of UAS sites are expressed when Gal4 is present [68]. With this methodology, authors have shown, for instance, that crossing Gal4-expressing lines with Tg(UAS:HRAS^{G12V}) transgenic line resulted in the development of different types of tumors, such as leukemia, glioma, or chordoma [69–71]. As transgenic fish with overexpression of some oncogenes might not survive to adulthood, transgenic inducible lines can also be generated, for instance, TetOn system-based transgenic lines, in which the oncogene expression is induced by doxycycline. Doxycycline-inducible expression of oncogenic KRAS in brain cells under the control of the krt5 and gfap gene promoters using the TetOn system (Tg(TRE:mCherry-KRAS^{G12V}; krt5/gfap:rtTa)) led to the development of malignant tumors in the cranial cavity and parenchymal brain tumors, respectively [72].

3.1.3. Reverse Genetics

Morpholinos (MO) are commonly used in zebrafish to achieve transient expression silencing without modifying the genome sequence [73] and thus to determine certain cancer invading mechanisms, such as angiogenesis. For instance, Jacob et al. reported that Plexin-A1 (PlexA1) could be a potential prognostic marker for glioma patients' survival, as quantitative analysis correlates tumor grade and the level of PlexA1 expression in brain blood vessels [74]. They knocked down PlexA1 in Tg(kdrl:eGFP) zebrafish and observed a significant number of abnormal angiogenic sprouts in intersegmental vessels (ISVs) at 28 hpf, confirming the relevance of PlexA1 in blood vessel development. Royet et al. observed that high expression of Ephrin-B3 in human glioblastoma biopsies promotes tumor growth and angiogenesis by inhibition of EphA4-induced apoptosis [75]. They knocked down Ephrin-B3 in Tg(fli:EGFP) embryos and observed an impaired ISVs formation associated with an increase in apoptosis. Co-silencing of EphA4 resulted in the rescue of the angiogenic defects, suggesting that enhancing EphA4-induced cell death could be envisaged as a relevant strategy to slow glioblastoma (GBM) growth.

In order to generate stable mutant models, Targeted Induced Local Lesions in Genomes (TILLING), based on the exposure to ENU and further sequencing [76], has been extensively used. In this sense, mutations in tumor suppressor genes, such as tp53, pten, and apc, have been identified in ENU mutagenesis libraries, and fish were found to develop malignant peripheral nerve sheath tumors (MPNSTs), ocular hemangiosarcomas, and intestinal adenomas, hepatomas, and pancreatic adenomas, respectively [77–80]. Interestingly, ENU homozygous brca2 mutants were shown to be unable to develop ovaries during sexual differentiation, developing as infertile males that were prone to develop testicular neoplasias during adulthood [81]. By combining the use of vhl zebrafish ENU heterozygous mutants and the exposure to DMBA, Santhakumar et al. established the von Hippel-Lindau protein (pVHL) as a genuine tumor suppressor in zebrafish, due to the increase in the occurrence of hepatic and intestinal tumors in mutants [82]. Although TILLING has proven to be useful to correlate genotypes with phenotypes, the difficulty involved in the screening process, together with the possibility of having further mutations than the one desired, led researchers to introduce other methodologies, such as nuclease-based techniques, which

include Zinc Finger Nucleases (ZFNs) and Transcription Activator-Like Effector Nucleases (TALENs).

ZFNs were used to generate tet2 mutants, which developed progressive clonal myelodysplasia, culminating in myelodysplastic syndrome, with dysplasia of myeloid progenitor cells and abnormal circulating erythrocytes [83]. As it recapitulates human TET2 loss-of-function phenotypes, this model was proposed as a platform for small-molecule screenings to identify compounds with specific activity against tet2 mutant cells. The function of the neurofibromin 1 (NF1) gene in brain tumorigenesis was explored by Shin et al. through the generation of stable mutant lines for the zebrafish orthologs (nf1a and nf1b) by ENU and ZFNs [84]. nf1a+/−; nf1b−/− mutants in a p53 mutant background presented an increased penetrance of high-grade gliomas MPNSTs as well as hyperactivation of ERK and mTOR pathways, consistent with mouse and human NF1-derived MPNSTs and gliomas. Similarly, bi-allelic cdkn2a/b and rb1 mutants generated by TALENs developed MPNSTs and medulloblastoma-like primitive neuroectodermal tumors, respectively, in a p53 mutant background [85]. Nevertheless, the design of nuclease-based systems is challenging, and there is still a high rate of off-targets. Thus, the introduction of the CRISPR/Cas9 system has allowed the optimization of the genome editing protocols and the improvement of the efficiency and accuracy of zebrafish lines.

For instance, p53/nf1-deficient fish were used by Oppel et al. to knock out by CRISPR/cas9 the atrx gene, a known tumor suppressor in gliomas or sarcomas, confirming that its loss facilitates the development of various malignancies, together with the downregulation of telomerase, which causes the alternative lengthening of telomeres [86]. Loss-of-function mutations in SUZ12, a subunit of the Polycomb repressive complex 2, have been identified in a variety of tumors, including MPNSTs. The knockout of suz12a and suz12b in a p53/nf1-deficient model significantly accelerated the onset and the penetrance of MPNSTs, and additional types of tumors were detected, including leukemia with histological characteristics of lymphoid malignancies, soft tissue sarcoma, and pancreatic adenocarcinoma [87].

These are examples of studies in which researchers developed zebrafish models harboring mutations in tumor suppressor genes and novel candidate genes, among others, to investigate their roles and unravel the relationship among mutations and the tumorigenesis and progression of different types of cancer (Figure 2).

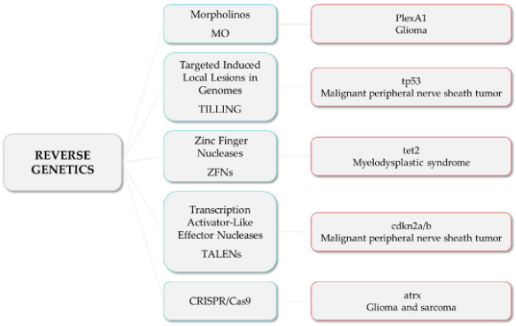

Figure 2. Reverse genetics strategies (in blue) and their respective examples of altered genes and the associated tumor types.

3.2. Transplantation Models

Transplantation in zebrafish is based on the injection of fluorescently labeled cancer cells into zebrafish embryos. The main transplantation techniques include allotransplantation and xenotransplantation, and both can be orthotopic or heterotopic, depending on whether the cells are injected in an equivalent anatomical site to tumor origin or into a different anatomical site, respectively.

Allograft consists of tumor cells being transferred from one individual to another of the same species [88], while xenograft is based on the injection of labeled human, murine, or patient-derived cancer cells into zebrafish, to track their survival, engraftment, growth, behavior, and interaction with the microenvironment [89]. The common sites for heterotopic transplantation are (Figure 3): (a) yolk sac, to track survival and proliferation [90]; (b) duct of Cuvier, to observe migration, invasion, and mesenchymal-epithelial transition (MET) [91]; (c) perivitelline space, to investigate mainly neovascularization [89]; intraperitoneal cavity, when adult individuals are used. The majority of transplantation assays are performed at 2 days post-fertilization (dpf), taking advantage of the transparency of the embryos and the lack of adaptive immunity, although several experiments have been carried out using adults. In order to avoid immune rejection in adults, transplantations require immunosuppression with sublethal γ-irradiation or dexamethasone [92,93] or the use of immunocompromised lines, such as the Rag2, lacking mature T-cells and having a reduced number of B cells, or the compound mutant prkdc−/−, il2rga−/−, lacking T, B, and natural killer (NK) cells [94,95]. In the particular case of allografts, engraftment can also be achieved without the need for immunosuppression by the transplantation from a donor fish to a genetically identical recipient (syngeneic or clonal models) [96], serving as a model for long-term engraftment and self-renewal potential [97–99]. An interesting approach combining different strategies allowed Ignatius et al. to confirm the role of tp53 in the development of a wide spectrum of tumors [100]. By using TALENs, they created tp53 mutants in which MPNSTs, angiosarcoma, germ cell tumors, and leukemia spontaneously developed during adulthood, and such tumor cells were transplantable to syngeneic fish, so engraftment of fluorescent-labeled tumors could be dynamically visualized over time. Additionally, White et al. proposed a mutant transparent recipient, known as *casper* zebrafish (roy−/−; nacre−/−), as a platform to study cancer cell engraftment, proliferation, and distant metastases in vivo [101]. Nevertheless, the prompt recovery from chemical immune ablation, the vulnerability of mutant immunocompromised fish, and the limited number of syngeneic zebrafish lines made embryo xenograft the most cost-effective technique, together with the higher number of individuals used, which increased statistical power and the reduced ethical issues in comparison with adults.

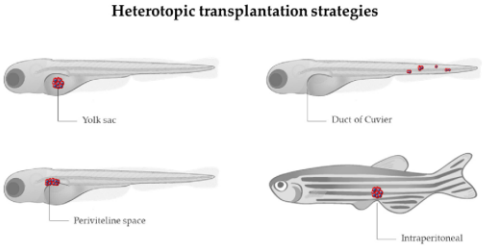

Figure 3. Sites for heterotopic transplantation of tumor cells (in red) in zebrafish. Modified from Servier Medical Art (https://smart.servier.com; accessed on 3 March 2022), licensed by a Creative Commons Attribution 3.0 Unported License, and Lizzy Griffiths.

The first xenograft assay was performed by injecting melanoma cells in zebrafish blastula, which showed the ability of melanoma cells to survive, proliferate, and specifically migrate to the skin, highlighting the validity of the zebrafish for cancer research [102]. Since then, this technique has been improved and extended for studying several cancer features, including not only survival, proliferation, or migration, but also the ability to invade, form new blood vessels (angiogenesis), metastasize, and respond or resist different treatments. Additionally, researchers have made efforts to mimic human tumor conditions and microenvironments as much as possible, as reviewed by Cabezas-Sáinz et al. [103]. For instance, the use of transgenic zebrafish lines, such as the previously mentioned ones, labeling immune cells or vasculature, has led several researchers to better understand the interaction among tumor cells and macrophages or neutrophils, and their involvement in tumor growth, vascularization, invasion, and metastasis [104–107]. In this line, Allen et al. recently presented a new model for tumor cell extravasation of both individual and multicellular circulating tumor cells, known as angiopellosis, and their ability to form tumors at distant sites [108].

With the aim of recapitulating, not only the cellular but also the non-cellular environment provided by the specific site and/or organ orthotopic xenografts have been developed, mainly with brain tumor cells. A pioneering study was performed by Lal et al., in which GBM cells behaved differently when injected into the yolk sac or in the brain. While cells in the yolk were unable to proliferate or invade, cells injected orthotopically showed the ability to invade the brain and disperse along the vessels [109]. By combining MOs, orthotopic xenograft, and 4D individual tracking technology, Gamble et al. showed that laminin subunit alpha 5, an important component of blood vessels, increases the attachment of GBM cells to blood vessels, suppressing tumor invasion but promoting tumor formation [110]. Additionally, orthotopic brain xenografts have proven to be unique models to study the ability of different drugs to penetrate the blood–brain barrier [111]. Retinoblastoma has also been studied by orthotopic xenografts. The inhibition of Nodal using short hairpin (shRNA) reduced the ability of retinoblastoma cells to disseminate outside the eye, highlighting the importance of Nodal in promoting growth, proliferation, and invasion [112].

Although the above-mentioned techniques have helped to improve the knowledge of several cancer processes, tumors present high interindividual heterogeneity. In addition, established cancer cell lines often differ significantly from patients' tumor cells. Thus, to preserve the patients' tumor biological and genetic profile and improve the accuracy of tumor drug-response studies, zebrafish patient-derived xenografts (zPDXs) have arisen as a potential solution [106]. zPDXs are established from tumor cells or masses isolated from patients during biopsy or excision, which are subsequently hetero- or orthotopically implanted into zebrafish. The pioneers of this technique were Marques et al., who observed cell invasion and metastasis formation after injection of colon, pancreas, and stomach primary tumor samples into the yolk sac [113]. Since then, the survival, proliferation, angiogenesis, or invasion ability of different patient-derived tumor cells have been studied in zebrafish models, from pancreatic, colon, gastric, head and neck, or pituitary cancer, to abdominal liposarcoma or T-cell acute lymphoblastic leukemia [114–118]. Furthermore, in order to improve patients' treatments, zPDXs have served as a platform to develop drug response/resistance assays and thus move towards personalized medicine. In this sense, several strategies are reviewed below.

4. Zebrafish as a Platform for Drug Screening

Zebrafish are used as a screening platform to adjust drug concentrations, to improve combinatorial treatments for a less toxic effect on the patient, or to overcome resistances, as well as a tool to study the mechanism of action of drugs in the organism and to alter the function of a biological pathway without previously knowing the components. Small molecule screening in zebrafish started in 2000 with a work by Peterson et al., who tested the

effect of a variety of molecules in the development of vertebrate animals to understand how these molecules can be used to determine the timing of critical developmental events [119].

In the context of cancer, zebrafish xenotransplants have been useful as in vivo preclinical tools for drug testing. This approach has been validated by different works, showing its complementarity with other in vivo models such as the mouse [120]. However, xenotransplantation of human cancer cells into the zebrafish is not without difficulties. For instance, the normal growth of human cells is at 37 °C, and the temperature of development of the zebrafish is 28 °C. To overcome this issue, the field has established 31–34 °C as a consensus temperature for xenograft assays. However, these temperatures could cast some doubts about the efficiency of xenograft models for drug screening and the subsequent translation to the patient. In this sense, Cabezas-Sáinz et al. demonstrated that zebrafish larvae can live until 36 °C, allowing them to test drugs in a cancer model with characteristics close to humans [121]. In addition, Cornet et al. developed the ZeOnco Test, an optimized and standardized (regarding cell labeling, injection site, image acquisition, etc.) xenograft assay, aiming at reducing attrition rate [122,123]. In the same way, xenografted Tg(fli1:EGFP) transgenic models with human lung cancer cell lines were used to compare the effects of different known drugs, promoting these models as a real-time drug screening platform for clinical lung cancer patients [124].

Zebrafish have been used for the development of combined treatment approaches to improve treatment efficacy. An example of this goal was the investigation of Precazzini et al., where the melanoma kita:ras transgenic zebrafish line was used to test the antifungal Clotrimazol in combination with antitumoral drugs, showing a synergistic anti-melanoma effect with limited toxicity [125]. In addition, other authors used the *casper* transgenic line to evaluate individually and in combination the antitumor activity of chemotherapy drugs used in the clinic [126].

In addition to pharmacological cancer treatments, there are other treatment options, such as radiotherapy, based on the use of ionizing radiation. An example is the work by Costa et al., who combined ionizing radiation and chemotherapy in colorectal cancer tumors xenografted into the *nacre* (*casper* and [Tg(fli1:EGFP)]) zebrafish line and observed that the responses achieved in the zebrafish matched the clinical responses of patients [127].

Transgenic Tg(fli1:EGFP) zebrafish with fluorescent vasculature has been used in a wide range of screenings in studies related to the angiogenesis process, such as new synthetic compounds [128,129], analogous molecules for drugs in use [130,131], natural compounds used in traditional medicine [132,133], and natural analogous compounds [134]. The combination between fluorescent vasculature and xenograft transplantation offers a potent cancer research tool to study the action of compounds in vivo, in which to test the potential of natural products in anticancer therapy [135,136], modification of natural compounds [137], and new chemical compound structures that are already utilized in the clinic [138]. Lin et al. combined the fluorescent vasculature of zebrafish with other genetic modifications and cancer cell xenotransplantation to screen and identify new anticancer molecules [139].

Even so, wild-type zebrafish is also used for screening of new molecules obtained from marine organisms [140–142] as well as the study of the potential of some fungicides against cancer cells [143].

Furthermore, other specific transgenic zebrafish were used in the study of different tumor drugs. For instance, the vhl^{hu2117} mutant transgenic zebrafish, which shows an excess of vascularization, was used to evaluate the antiangiogenic effect of the compound largazole [144]. In addition, a transgenic zebrafish for liver cancer overexpressing the oncogene KRAS was used to study the effects of environmental toxicants on tumor development and inflammatory response [145].

In the following sections, and as summarized in Figure 4, different therapeutic approaches for cancer treatment evaluated with the zebrafish model will be discussed.

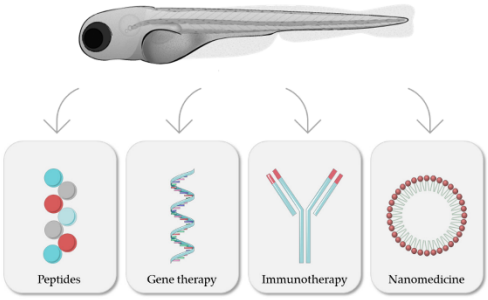

Figure 4. Zebrafish as a model for evaluation of different cancer treatments. Modified from Servier Medical Art (https://smart.servier.com; accessed on 3 March 2022), licensed by a Creative Commons Attribution 3.0 Unported License, and Lizzy Griffiths.

4.1. Peptides

Among the different types of biomolecules, zebrafish have proved their potential for evaluating the activity of novel peptide therapies. Cancer peptide-based therapy might play a role in the treatment of patients, and peptides can be obtained from different sources, such as natural organisms, peptide libraries, and de novo synthesis [146,147]. Some peptides produced by bacteria are also used to treat some types of cancer due to their antitumor effect. A shining example is the microcin E492, which is a peptide produced by the bacteria *Klebsiella pneumoniae*, which has shown antineoplasic properties in zebrafish embryos xenografted with colorectal cancer cells [148]. Another example, provided by Hsieh et al., studied the effect of TAT-NLS-BLBD-6, a synthesized peptide able to suppress breast cancer growth. This in vivo assay was carried out through a co-microinjection of peptide and labelled breast cells into the zebrafish yolk [149]. Furthermore, the evaluation of anticancer peptides in zebrafish embryos can be carried out by xenotransplantation of treated cells. An example of this assay was performed with NuBCP-9, a growth factor Nur77 derived peptide, which demonstrated apoptotic effect in paclitaxel-resistant lung tumor cells [150].

4.2. Gene Therapies

Zebrafish have also been used in the research of gene therapies based on the introduction of exogenous genomic materials on the organism to study or silence the expression of genes. A significant example is the research performed by Cordeiro et al., who used a specific ssDNA in the fli-EGFP transgenic zebrafish to measure the capacity of this material to reduce the GFP signal; the reduction of the EGFP emission indicates the downregulation of EGFP expression [151].

Transgenic zebrafish line Tg(Kdrl:eGFP)s843 has been used as an in vivo model to study the antiangiogenic effects of miRNA-based therapies. This assay was carried out with xenografts based on miRNA transfected prostate cancer cells, which allowed the evaluation of new vessel formation [152]. In the same vein, Kiener et al. studied the antitumor effect of a miRNA in the same type of cancer by microinjecting transgenic Tg(mpo:GFP)i114 zebrafish with miRNA transfected cells, proving the reduction of the tumor due to the miRNA effect [153].

4.3. Immunotherapeutics: Monoclonal Antibodies and CAR-T

Monoclonal antibodies can target cancer cells by binding to their specific surface antigens [154]. Zebrafish embryos play a meaningful role in the study of the anti-cancer

efficacy of monoclonal antibodies, their toxicity, and the comparison between different therapies.

Zebrafish were used to study cetuximab, a monoclonal antibody targeting the epidermal growth factor receptor (EGFR), for the treatment of colorectal and head and neck cancer [154]. The response of cetuximab treatment was evaluated using colorectal cancer zebrafish patient-derived xenografts (zPDX), which included the drug in the injected cell suspension, and the results showed that the zebrafish model allows the detection of differential responses to the antibody according to the *KRAS* mutational status of the tumor [155].

Furthermore, the zebrafish transgenic line Tg(fli1:EGFP) is commonly used to study the antiangiogenic capacity of drugs [156–158], such as Bevacizumab, a humanized anti-vascular endothelial growth factor (VEGF) antibody for the treatment of some solid cancers (such as breast and lung cancer). Bevacizumab was studied in this zebrafish transgenic line to define its antiangiogenic effect and antitumor capacity, in contrast to toxicity assay, which was performed in wild-type embryos [154,157,158]. Another monoclonal antibody studied in zebrafish models is ramucirumab, used to treat lung, gastric, and colorectal cancer. Its toxicity was assessed in wild-type zebrafish embryos, and the antiangiogenic and anticancer capacity was tested in the Tg(fli1:EGFP) line, in the same way as Bevacizumab [154,156].

Moreover, chimeric antigen receptor T cell (CAR-T cell) therapy has achieved clinical success in specific tumor types, such as several types of leukemia [159,160]. Recent studies by Pascoal et al., for the first time, evaluated the capacity of CAR-T cells to kill cancer cells in vivo in zebrafish. To carry out this assay, labelled Nalm-6 leukemia cells and CAR-T cells were injected into zebrafish vasculature. The results show that zebrafish embryos are a potential model for in vivo studies of the efficacy of CAR-T cell therapy against cancer [161].

4.4. Nanomedicines

4.4.1. Toxicity

Zebrafish embryos are currently used for nanomedicine toxicity testing due to advantages such as their high fertilization rate, as explained in Section 3. The most common method to perform toxicity assays is the incubation of nanomedicines into zebrafish medium, usually with dechorionated zebrafish. As well as the incubation, microinjection of test drugs into zebrafish circulation ensures that the concentration is absorbed by the embryos [49].

Table 2. Zebrafish-based toxicity studies of different nanoparticles for cancer therapies.

Nanoparticles	Conditions	Higher Mortality Rate	Morphological Effects	Ref.
AgNPs	3 hpf embryos 72 h incubation 28.5 °C	100% (3 µg/mL)	Yolk sac edema Tail malformation	[162]
AuNPs	3 hpf embryos 72 h incubation 28.5 °C	100% (300 mg/mL)	Yolk sac edema	[162]
MMDOX	4 dpf embryos 72 h incubation 28 ± 1 °C	100% (100 µg/mL)	Uninflated swim bladder Arched body Alteration of the spontaneous swimming activity	[163]
MSNs-FA	48 hpf embryos 72 h incubation 27 ± 1 °C	~30% (200 µg/mL)	Hatching rate	[164]

Several aspects of zebrafish embryos can be analyzed to determine the toxicity of a specific nanomedicine; some examples are compiled in Table 2. The correct hatching process, malformation appearance, the response of the immune system, and mortality are some of the guidelines to evaluate the toxicity effect of nanoparticles [165,166]. As a result, toxicity tests based on zebrafish have become an indispensable step to assess the effect of several therapies based on nanosystems, from metal-based nanoparticles to lipidic nanosystems. For instance, golden (AuNPs) and silver (AgNPs) nanoparticles for anticancer application were tested to evaluate their toxicity using zebrafish embryos. Mortality rate and morphological anomalies showed differences between nanoparticle types and concentration [162]. However, metal nanoparticles are not the only kind of nanomedicines evaluated by the zebrafish toxicity test. In fact, micelles loaded with doxorubicin hydrochloride (DOX-loaded mixed micelles (MMDOX)), commonly used to treat metastatic breast cancer, were tested by Calienni et al. in zebrafish embryos to rate their toxicity in vivo [163].

Another important example is the research of Wu et al., who used zebrafish embryos to evaluate the biosafety of mesoporous silica nanoparticles coated with folic acid (MSNs-FA) as carriers of therapeutic peptides, evaluating the embryo mortality and hatching [164].

Zebrafish have demonstrated their huge capacity to be a platform for testing different types of nanomaterials, not only for cancer treatment but also for other applications such as antibacterial and heart-associated disease treatment. The review of Jia et al. compiled information about different nanoparticles and their toxicity evaluation using zebrafish [167].

4.4.2. Biodistribution and Average Life in Circulation

In vivo behavior, distribution along the body, and interaction with tumor cells are key qualities to develop new anticancer nanomedicines; therefore, analyzing these aspects is essential to achieve a translation to the clinic of nano-based therapies. Due to this, zebrafish embryos play an important role as a platform to evaluate these properties in vivo.

Chang et al. performed an assay to evaluate differences in the distribution of polystyrene nanoparticles and glycol chitosan nanoparticles for cancer treatment along blood circulation. Adult wild-type zebrafish were retro-orbitally injected with nanoparticles to observe their capacity to circulate along the vasculature; this allowed the authors to predict in vivo nanoparticle behavior [168]. In the same way, Gundersen et al. also used wild-type zebrafish to evaluate the biodistribution of chlorpromazine-loaded PEGylated PLGA nanoparticles for leukemia treatment [169].

In another fashion, transgenic Tg(FLK-1: mCherry) zebrafish embryos, in which endothelial cell membranes are fluorescently labeled, were used to evaluate the distribution of nanoparticles throughout the vasculature, showing the interaction of nanoparticles with the blood vessels and the ability to extravasate [170]. Along this transgenic line, other lines with fluorescent endothelial cells have been utilized for these types of assays, such as the Tg(kdrl:GFP)^{la116tg} line, which allowed the observation of the endocytosis of nanoparticles by endothelial cells and their behavior inside them [171].

Another important trait to evaluate is the time that nanoparticles can remain in the organism. This fact depends on the composition of the nanosystem and the response of the body's immune system, such as macrophage uptake. Leveraging the zebrafish embryo transparency, microinjected fluorescent nanoparticles can be observed over time to evaluate their capacity to stay in the organism. An example that illustrates this usage is the study performed by Wang et al., involving nanosystems that can be used to carry anticancer drugs. In this study, FITC-labelled nanospheres were microinjected and evaluated during 72 h post-injection to study the biodistribution and their elimination progress of by the organism [172].

As the uptake of nanoparticles by macrophages decreases their half-life in circulation, one of the main objectives is testing the capacity of avoiding this nanoparticle uptake. To carry out this type of procedure, transgenic zebrafish reporter lines for fluorescently labelled macrophages, such as Tg(mpeg1:mCherry)^{UMSF001} and Tg(mpeg1:EGFP), have

been used [173,174]. Making use of the Tg(mpeg1:mCherry)^{UMSF001} line, Evensen et al. studied the differences of anticancer nanoparticles with and without polyethylene glycol, observing a decrease in the uptake of the former by macrophages [173].

Though the evaluation of the behavior of microinjected nanoparticles is key, it is also important to study the effect of nanoparticles that are specifically developed for external treatments. In this field, Jia et al. developed a fluorescence probe, composed of cholesterol, poly(ethylene glycol)$_{2k}$, and Cy5, for imaging zebrafish cell surfaces and demonstrated their utility for the assessment of nanoparticle toxicity in zebrafish upon observation of epidermal abnormalities related to damage [175].

4.4.3. Anticancer Drug Delivery in Targeted Medicine

Zebrafish has turned into an anticancer nanomedicine platform to evaluate the efficacy of this treatment, since it allows the modeling of several types of cancer and different tumor stages, as explained in Section 3.1.

The transgenic Tg(FLK-1:EGFP) zebrafish line, which has green fluorescent endothelial cells, is one of the most common lines used to evaluate the antiangiogenesis capacity of drugs, including nanomedicines. The antiangiogenic effect of curcumin polymeric micelles was evaluated in this transgenic line, resulting in an effective inhibition of embryonic angiogenesis as well as tumor-derived angiogenesis owing to tumor cell xenotransplantation [170].

The microinjection of cancer cells allows assessing the capacity of nanoparticles to interact with xenotransplanted cells as well as their antitumoral efficacy [176–179]. A recent example is the work of Saraiva et al., who evaluated tumor reduction in xenografted zebrafish embryos treated with nanoemulsions comprising edelfosine, as a triple negative breast cancer treatment [180]. In a similar way, Moret et al. used zebrafish embryos that were the offspring of *Casper* mutants and fli1a:EGFP transgenic zebrafish to evaluate the efficacy of biodegradable poly(ethylene glycol)-poly(ε-caprolactone) nanoparticles, loaded with docetaxel, for epithelial cancer treatment, by measuring mass tumor reduction and antiangiogenic effect [181].

In addition, metastasis modelling in zebrafish embryos can be performed as a result of spreading across the circulation of xenotransplanted tumor cells. The microinjection or incubation of different types of antitumoral drugs allows the evaluation of their capacity to inhibit these metastatic processes [182,183].

5. Zebrafish as a Tool in Personalized Medicine

Chemotherapy treatments' efficacy varies among different patients, and the results are not always successful [155]. For this reason, researchers are increasingly focusing on the development of personalized medicine strategies, such as the use of Patient Derived Xenografts (PDXs). PDXs allow the study of a particular tumor and its genome profile as well as its response to a specific treatment, owing to their capacity to maintain tumor heterogeneity. In recent years, zebrafish PDXs (zPDXs) have appeared as a new quick tool to evaluate anticancer treatments [155]. A role model was developed by Wu et al., who injected colon cancer cells from a patient into Tg(fli1:EGFP) transgenic zebrafish; the tumor–microenvironment interaction was observed, and a drug screening was carried, out allowing the selection of the most appropriate treatment for the patient based on the elimination of cancer cells [184]. This Tg(fli1:EGFP) zebrafish model, as well as the *casper* and *nacre* models, were used by Fior et al. to inject patient-derived colon cancer cells to screen different therapies. This experiment evidenced that xenografted zebrafish can be used as a fast screening platform to evaluate tumor evolution and relapse [155]. Furthermore, a *Casper* zebrafish model was used for the research of an effective treatment to inhibit leukemia cell proliferation through microinjection of patient-derived tumor cells [118] and was also used to study a chemotherapy drug combination in order to observe the reduction of tumor gastric mass [126]. In the same line of investigation, Usai et al. injected into wild-type zebrafish three different types of cancer cells from a patient, and different chemotherapy combinations were tested to determine the effective doses necessary to treat each cancer

patient [114]. Another example of the use of *casper*, *nacre*, and Tg(fli1:EGFP) models is the work of Costa et al., in which a rectal cancer zPDX was generated and then treated with chemotherapy and radiotherapy to distinguish radiosensitive from radioresistant tumors [127].

Furthermore, in other studies, after zebrafish xenotransplantation of patient-derived cancer cells, PCR analysis was performed to analyze the efficiency of several drugs instead of measuring the reduction of tumors, achieving a new method to evaluate anticancer drug screenings [115].

In the field of nanomedicine, zebrafish also play a role as a model for personalized medicine in cancer. The work of Di Franco et al. is a clear example. Pancreatic cancer patient-derived xenografts were used to evaluate different therapies and to determine the best possible treatment for each patient. In this research, albumin nanoparticles loaded with Paclitaxel (nab-Paclitaxel), co-administrated with Gemcitabine, were one of the treatments tested. Overall, this study probes the potential of zebrafish for assessment of therapies based on nanotechnology by following a personalized approach [185].

6. Clinical Output

The zebrafish as a preclinical disease model has proven to be key to inform about human disease mechanisms and therapy. Aside from the generation of powerful cancer models for the identification of therapeutic targets, this disease model plays an instrumental role in the era of precision medicine in oncology, allowing the tailoring of the treatments to the individual characteristics of each patient. Towards this end, recent efforts are being made to make use of the zebrafish as an "avatar" model for the xenotransplantation of cancer cells from individual patients (also known as zebrafish patient-derived xenografts or zPDX) and the subsequent studies of drug efficacy and response (Table 3). However, an important limitation in this regard has been the lack of criteria for the conversion of chemotherapy dosage from human to fish. This issue was recently addressed by Usai et al., who developed a formula to estimate equivalent doses (EDs) to be used on the fish [114]. The authors tested the ED for standard chemotherapy treatment in zebrafish xenotransplanted with cancer cell lines and confirmed their efficacy as determined in clinical studies [114]. Importantly, when tumor fragments derived from patients' surgical specimens were engrafted in the fish, and these were treated with the ED of chemotherapy drugs, they found a good agreement with observations registered in common clinical practice. In line with this, similar evidence has been observed in other studies, such as the ones published by Fior et al., Costa et al., Rebelo de Almeida et al., and Di Franco et al., who showed a similar response of colorectal cancer and pancreatic cancer patients and zPDX to standard chemotherapy/chemoradiotherapy or targeted therapy for the treatment of these tumors [155,185–187]. In this regard, some preliminary indications have also been observed for zPDX derived from gastric cancer samples, although this needs further validation in a larger number of patient samples [184]. In addition, this strategy has been applied for non-solid tumors, such as multiple myeloma and B-cell precursor acute lymphoblastic leukemia, showing that zebrafish xenografts show similar responses to patients [188,189]. These proof-of-concept studies suggest that avatar/zPDX models can reproduce the individual response of each patient to treatment in just a few days, representing an important step forward towards the translation of this model into clinical practice as a predictive tool for the most effective treatment for an individual patient. Indeed, expanding on the initial work by Di Franco et al., a co-clinical trial is currently evaluating if zebrafish is able to predict the therapeutic regimen with the best efficacy for patients with pancreatic, gastrointestinal, or colorectal cancer undergoing chemotherapy in an estimated cohort size of 120 patients [190]. Currently, together with this co-clinical trial, another clinical study is listed on the website of Clinical Trials Gov, in which zebrafish is used as an avatar model [191]. In this trial (NCT01395628), which was already completed, zebrafish was evaluated as a recipient for primary human leukemia samples from 10 patients, to test the anti-proliferative or toxic effects of chemotherapeutics on them. It is worth noting that one of the main limitations of

cancer models to predict patient drug responses is their limited complexity and capacity to recapitulate the intratumor heterogeneity, both genetic (clone selection) and cellular (stromal compartment). However, avatar xenotransplantation models generated from surgically resected specimens may preserve the actual complexity of the tumor, overcoming such an important limitation. Despite this, we cannot forget that these models may be limited by other factors, such as the successful engraftment in the fish of the tumor material and therefore the selection of specific tumor clones and the limited number of injected cells [192]. Therefore, despite the promising results of the zebrafish avatar/zPDX models for the prediction of patient treatment response, in order to achieve precision medicine through their use, larger clinical studies are needed to validate this strategy.

Table 3. Studies involving the use of zebrafish PDXs for drug efficacy and response.

Tumor Type	Patients (*n*)	Aim	Outcome	Ref.
Pancreatic (PC), colorectal (CRC), and gastric cancer (GC)	*n* = 24 (12 PC, 8 CRC, and 4 GC patients)	• Xenograft establishment (*n* = 6) • Response to chemotherapy options (according to the cancer type) evaluated as partial response (PR) and complete response (CR)	• Xenografted tumor tissue can engraft and survive in the zebrafish (100%). • Response to chemotherapy: ▪ PC: PR to GEM/nab-P (58.33 %), GEM (50%), GEMOX (50%), and FOLFOXIRI (33.33 %). No CR was observed. ▪ CRC: PR to FOLFOX, FOLFIRI and FOLFOXIRI (62.5%), and to 5-FU (37.5%). CR to FOLFIRI (12.5%). ▪ GC: PR to FOLFIRI (100%), FOLFOX, FLOT and ECF (25%). CR to FOLFIRI (25%).	[114]
Colorectal cancer (CRC)	*n* = 11	• Xenograft establishment (*n* = 5) • Sensitivity to standard chemotherapy and targeted therapy	• Cell engrafted in 5/5 cases (100%), with different success rates based on the percentage of fish showing engraftment (from 47 to 89%). • Zebrafish xenograft response to FOLFOX anticipated patient relapse/no relapse within 3 m to 6 m in 4/5 patients (80%). Lack of response to Cetuximab was associated with mutations highly linked to Cetuximab resistance.	[155]
Gastric cancer (GC)	*n* = 14	• Xenograft establishment • Assess the efficacy of anti-GC agents: 5-FU, docetaxel, and apatinib (*n* = 4)	• Successful transplantation in 9/14 patient samples (64.2 %). • Zebrafish xenografts subjected to 5-FU and apatinib showed different degrees of sensitivity.	[184]
Pancreatic ductal adenocarcinoma (PDAC)	*n* = 15	• Xenograft establishment • Evaluation of response to chemotherapy	• Establishment of PDAC xenografts in 15/15 cases (100%). • Significant reduction in tumor area observed in 6/15 cases (40%) for at least one chemotherapy scheme (FOLFOXIRI, GEMOX, Gem/nab-P, and GEM.	[190]

Table 3. *Cont.*

Tumor Type	Patients (*n*)	Aim	Outcome	Ref.
Breast (BC) and colorectal cancer (CRC)	*n* = 6 (3 BC and 3 CRC patients)	• Response to the anti-VEGF therapy bevacizumab • Comparison of patient's response with matching avatars (*n* = 2)	• Zebrafish avatars can reflect both pro- and anti-metastatic effects of bevacizumab. • Resistance to bevacizumab of zebrafish avatar correlation with the clinical resistance and disease progression of the matched patients.	[187]
Multiple myeloma (MM)	*n* = 6	• Xenograft establishment (perivitelline space) • Evaluate drug response in newly diagnosed (*n* = 2) and relapsed/refractory patients (*n* = 4)	• Efficiency of MM primary cell engraftment of around 80%. • Zebrafish xenograft responses to bortezomib and lenalidomide recapitulated patient responses in all 6 cases.	[189]
B-cell precursor acute lymphoblastic leukemia (BCP-ALL)	*n* = 15	• Xenograft establishment (pericardium) • Response of BCP-ALL cell lines to venetoclax (*n* = 7)	• BCP-ALL were successfully expanded in 9/15 embryos (60%). • Xenografts produced varied responses to venetoclax, mirroring in two cases the refractory response to venetoclax of the matching patients.	[188]

Abbreviations: ECF: 5-Fluorouracil + Cisplatin + Epirubicin; FOLFIRI: 5-Fluorouracil + Lederfolin + Irinotecan; FOLFOX: 5-Fluorouracil + Lederfolin + Oxaliplatin; FOLFOXIRI: 5-Fluorouracil + Folinic acid + Oxaliplatin + Irinotecan; FLOT: 5-Fluorouracil + Lederfolin + Oxaliplatin + Docetaxel; GEM: Gemcitabine; GEMOX: Gemcitabine + Oxaliplatin; GEM/nab-P: Gemcitabine + nab-Paclitaxel; 5-FU: 5-Fluorouracil.

Aside from the potential use of the zebrafish as a predictive tool of patient drug response, this model system may also represent a valuable tool for the translation of compounds derived from zebrafish screens into the clinic as part of the personalized medicine approach. Two decades ago, zebrafish was mainly used for the development of chemical phenotypic screens, meaning the screening for compounds with therapeutic properties over a specific phenotype or disease. In the last ten years or so, zebrafish models are being used following a "from bench to bedside" approach to identify the best treatment plan for an individual patient. In this sense, the screening of compounds in the zebrafish for the development of selective therapies has experienced a relative advance in recent years, with some compounds already being tested in clinical trials, or close to it, for the treatment of various diseases, including cancer [193]. This experimental approach has been pioneered by the Group of Leonard I Zon at Harvard, who has contributed to the repurposing (or reprofiling) of four compounds, two of them as anti-cancer agents and one for graft-versus-host disease in hematologic malignancies. The first example is ProHema, a derivative of prostaglandin E2 shown to increase the generation of blood stem cells, which was repurposed for its use in blood stem cell transplantation [194]. ProHema has been tested in four phase I or II clinical trials, in three of which it was evaluated for its efficacy in hematologic malignancies (NCT00890500, NCT01627314, and NCT02354417). This compound was later incorporated into a cellular immunotherapy (ProTmune; Fate Therapeutics) used for the prevention of graft-versus-host disease and is currently being evaluated in an ongoing phase II stage clinical trial in hematologic malignancies (NCT02743351). The second compound is the antirheumatic drug Leflunomide, an inhibitor of the dihydroorotate dehydrogenase, which was identified in a zebrafish screening as a drug with the potential to interfere with the growth of melanoma [195]. The drug was included in a phase I clinical trial to test its efficacy in combination with a BRAF inhibitor (NCT01611675), but it was later canceled due to adverse events. The third compound is the all-trans retinoic acid (ATRA), in this occasion identified using a pluripotent zebrafish blastomere culture system, which was shown to suppress the transcription factor c-myb, a driver of adenoid cystic carcinoma [196]. These findings led to the initiation of a phase II clinical trial (*n* = 18) evaluating the safety and effec-

tiveness of ATRA in treating adenoid cystic carcinoma, completed last year (NCT03999684), in which patient response to ATRA was not observed for the tested dose and schedule [197]. Currently, a second phase II trial ($n = 30$) is underway, testing the compound in patients with recurrent metastatic adenoid cystic carcinoma of the head and neck (NCT04433169). Another good example of this research approach is Rosuvastatin, used for the treatment of hypercholesterolemia in cardiovascular disorders and repurposed as an antiangiogenic drug after a genetic screen in zebrafish [198]. Rosuvastatin was shown to inhibit the growth of prostate cancer cells and was later included in a phase II clinical trial to evaluate the improvement in the response to its combination with standard chemotherapy in rectal cancer (NCT02569645, still recruiting an estimate of 48 patients). Moreover, zebrafish also allows for the testing of combinatory treatments. A very recently developed immune-deficient adult zebrafish model (*prkdc*$^{-/-}$, *il2rga*$^{-/-}$) by David Langenau at the Massachusetts General Hospital Research Institute has been used for the identification of a possible treatment for rhabdomyosarcoma [95]. The researchers made use of this model to prove the efficacy of the combination of a poly ADP ribose polymerase (PARP) inhibitor plus temozolomide chemotherapy, both drugs approved for use in the clinic, in eliminating engrafted rhabdomyosarcoma cells, as opposed to single drug treatment, an effect that was confirmed in a mouse xenograft model [95]. This combinatorial treatment is being investigated in a phase I study for Ewings sarcoma or Rhabdomyosarcoma in an estimated cohort of 93 patients (NCT01858168).

In addition to the above examples, some other clinically approved compounds, repurposed through zebrafish screening, have not reached the clinical testing stage. Perphenazine (PPZ), a drug approved for psychosis therapy, was found to be effective against T-cell acute lymphoblastic leukemia (T-ALL) in a combined screening for small molecules with toxic effect in MYC-overexpressing thymocytes in zebrafish and T-ALL cells [199]. More recently, a potential use of PPZ for the treatment of endometrial cancer has been suggested based on in vitro and mouse experimental data, expanding the potential use of this compound for solid tumors [200]. A zebrafish genetic model of β-catenin driven hepatocellular carcinoma (HCC) allowed the identification of two antidepressants, amitriptyline and paroxetine, as suppressors of liver growth [201]. Further experiments developed in this study have shown that paroxetine was also able to decrease tumor burden in a mouse HCC model [201]. Another successful reprofiling example was shown by Fernandez del Ama et al., who, using an oncogenic-RAS-driven zebrafish melanoma model, observed that the mTOR inhibitor rapamycin, as well as the compounds disulfiram and tanshinone, synergized with inhibitors of the MEK and PI3K/mTOR signaling pathways to inhibit melanoma development [202].

In summary, we can clearly see the huge role of zebrafish as a cancer model in the development of pre-clinical studies for the identification of compounds with antitumoral properties. However, the identification of anticancer compounds is not enough to make an impact on cancer patient care, as most do not reach the clinical testing, and more direct approaches are needed. In this sense, the field is drifting towards the development and use of zebrafish avatar models for the testing of patient drug sensitivity, since each individual patient may present a different response based on the unique genetic alterations that his/her tumor harbors. Particularly, future work should be aimed at testing the predictive value of zebrafish avatars on a reduced number of therapeutic options (targeted therapies and immunotherapies) but in larger patient cohorts, in order to achieve a truly personalized treatment. The xenograft approach is supported by multiple studies that have validated the development of zebrafish xenografts from patient-derived material [203], and, as discussed before, more studies are coming out showing the true potential of the zebrafish avatars for this purpose, predicting patient responses [115,139,155,156,184–187,189].

7. Conclusions

The zebrafish is a powerful model for studies of various cancer treatments, including new therapies, such as those based on nanomedicine. Its versatility, which allows it to

be used not only in embryonic stages but also as adult individuals, together with the enormous variety of transgenic lines available, are fundamental characteristics of this model. However, more research efforts should be directed toward the development of standardized protocols for tumor cell xenotransplantation and drug effectiveness analysis, as well as toward optimizing the routes of administration in order to translate the results to higher models and more patients. Moreover, since most of the research is performed in larvae, long-term drug exposure and the assessment of response lack translatability to patients, and for that other animal models are needed.

Furthermore, the use of zebrafish as an intermediate step between cell culture studies and higher models, such as mice and rats, reduces the number of seconds needed to perform the experiments, thus implementing the 3R (replacement, reduction, and refinement) principle of animal welfare.

Author Contributions: Conceptualization, M.C. and M.d.l.F.; writing—original draft preparation, M.C., S.A., A.P.-L., A.J.V.-R. and R.P.; writing—review and writing, M.C., A.P.-L., L.S., R.P. and M.d.l.F.; supervision, R.P. and M.d.l.F.; funding acquisition, L.S. and M.d.l.F. All authors have approved this submission. All authors have read and agreed to the published version of the manuscript.

Funding: This research was funded by the Instituto de Salud Carlos IIIISCIII and the European Regional Development Fund (FEDER) (AC18/00107, AC18/00045, PI21/01262); by the ERA-NET EURONANOMED III project METASTARG (grant number JTC2018-045) and the ERA-NET EURONANOMED III project PANIPAC (grant number JTC2018/ 041); and by Axencia Galega de Innovación (GAIN), Consellería de Economía, Emprego e Industria (IN607B2021/14). R.P. was funded by Roche-Chus Joint Unit (IN853B 2018/03) funded by Axencia Galega de Innovación (GAIN), Consellería de Economía, Emprego e Industria. A.P-L. is supported by the Xunta de Galicia Pre-doctoral Fellowship (ED481A-2018/095). L.S. acknowledges the funding given by Consellería de Educación, Universidade e Formación Profesional, Xunta de Galicia local government (ref. ED431C 2018/28).

Conflicts of Interest: M.d.l.F. is the co-founder and CEO of DIVERSA technologies. A.J.V.-R. is the co-founder and COO of DIVERSA technologies.

Abbreviations

AgNPs	Silver nanoparticles
ATRA	All-trans retinoic acid
AuNPs	Golden nanoparticles
BC	Breast cancer
BPC-ALL	B-cell precursor acute lymphoblastic leukemia
CAR-T cell	Chimeric antigen receptor T cell
CR	Complete response
CRC	Colorectal cancer
NSCLC	Non-small-cell lung cancer
CTLA-4	Cytotoxic T-lymphocyte-associated antigen-4
DEN	Diethylnitrosamine
DMBA	Dimethylbenzanthracene
Dpf	Days post-fertilization
ED	Equivalent doses
EGFR	Epidermal growth factor receptor
EMA	European Medicines Agency
ENU	Ethylnitrosourea
FDA	Food and Drug Administration
GBM	Glioblastoma
GC	Gastric cancer
GCT	Germ cell tumor

HCC	Hepatocellular carcinoma
Hpf	Hours post-fertilization
ICIs	Immune checkpoint inhibitors
ISVs	Intersegmental vessels
MET	Mesenchymal-epithelial transition
MM	Multiple myeloma
MMDOX	Doxorubicin-loaded mixed micelles
MNNG	N1-nitro-N-nitrosoguanidine
MO	Morpholinos
MPNSTs	Malignant peripheral nerve sheath tumors
MSNs-FA	Mesoporous silica nanoparticles coated with folic acid
NDMA	N-nitrosodimethylamine
NF1	Neurofibromin 1
NK	Natural killer cells
PARP	Poly ADP ribose polymerase
PC	Pancreatic cancer
PD-1	Programmed cell death-1
PDAC	Pancreatic ductal adenocarcinoma
PD-L1	Programmed cell death ligand-1
PDX	Patient Derived Xenografts
PlexA1	Plexin-A1
PPZ	Perphenazine
PR	Partial response
pVHL	Von Hippel-Lindau protein
shRNA	Short hairpin RNA
TALENs	Transcription Activator-Like Effector Nucleases
T-ALL	T-cell acute lymphoblastic leukemia
TILLING	Targeted Induced Local Lesions in Genomes
VEGF	Vascular endothelial growth factor
Wpf	Weeks post-fertilization
ZFNs	Zinc Finger Nucleases
zPDXs	zebrafish patient-derived xenografts

References

1. Siegel, R.L.; Miller, K.D.; Jemal, A. Cancer statistics, 2020. *CA Cancer J. Clin.* **2020**, *70*, 7–30. [CrossRef] [PubMed]
2. Sung, H.; Ferlay, J.; Siegel, R.L.; Laversanne, M.; Soerjomataram, I.; Jemal, A.; Bray, F. Global Cancer Statistics 2020: GLOBOCAN Estimates of Incidence and Mortality Worldwide for 36 Cancers in 185 Countries. *CA Cancer J. Clin.* **2021**, *71*, 209–249. [CrossRef]
3. Hanahan, D.; Weinberg, R.A. Hallmarks of cancer: The next generation. *Cell* **2011**, *144*, 646–674. [CrossRef] [PubMed]
4. Dillekås, H.; Rogers, M.S.; Straume, O. Are 90% of deaths from cancer caused by metastases? *Cancer Med.* **2019**, *8*, 5574–5576. [CrossRef] [PubMed]
5. Ilic, M.; Ilic, I. Epidemiology of pancreatic cancer. *World J. Gastroenterol.* **2016**, *22*, 9694–9705. [CrossRef] [PubMed]
6. Howlader, N.; Forjaz, G.; Mooradian, M.J.; Meza, R.; Kong, C.Y.; Cronin, K.A.; Mariotto, A.B.; Lowy, D.R.; Feuer, E.J. The Effect of Advances in Lung-Cancer Treatment on Population Mortality. *N. Engl. J. Med.* **2020**, *383*, 640–649. [CrossRef] [PubMed]
7. San Juan, B.P.; Garcia-Leon, M.J.; Rangel, L.; Goetz, J.G.; Chaffer, C.L. The complexities of metastasis. *Cancers* **2019**, *11*, 1575. [CrossRef]
8. Hüsemann, Y.; Geigl, J.B.; Schubert, F.; Musiani, P.; Meyer, M.; Burghart, E.; Forni, G.; Eils, R.; Fehm, T.; Riethmüller, G.; et al. Systemic Spread Is an Early Step in Breast Cancer. *Cancer Cell* **2008**, *13*, 58–68. [CrossRef]
9. Tinhofer, I.; Saki, M.; Niehr, F.; Keilholz, U.; Budach, V. Cancer stem cell characteristics of circulating tumor cells. *Int. J. Radiat. Biol.* **2014**, *90*, 622–627. [CrossRef]
10. Mason, J.A.; Hagel, K.R.; Hawk, M.A.; Schafer, Z.T. Metabolism during ECM Detachment: Achilles Heel of Cancer Cells? *Trends Cancer* **2017**, *3*, 475–481. [CrossRef]
11. De Francesco, E.M.; Sotgia, F.; Lisanti, M.P. Cancer stem cells (CSCs): Metabolic strategies for their identification and eradication. *Biochem. J.* **2018**, *475*, 1611–1634. [CrossRef] [PubMed]
12. Santamaría, P.G.; Moreno-Bueno, G.; Cano, A. Contribution of Epithelial Plasticity to Therapy Resistance. *J. Clin. Med.* **2019**, *8*, 676. [CrossRef] [PubMed]
13. Herreros-Pomares, A.; de-Maya-Girones, J.D.; Calabuig-Fariñas, S.; Lucas, R.; Martínez, A.; Pardo-Sánchez, J.M.; Alonso, S.; Blasco, A.; Guijarro, R.; Martorell, M.; et al. Lung tumorspheres reveal cancer stem cell-like properties and a score with prognostic impact in resected non-small-cell lung cancer. *Cell Death Dis.* **2019**, *10*, 660. [CrossRef] [PubMed]
14. Schiller, J.H.; Harrington, D.; Belani, C.P.; Langer, C.; Sandler, A.; Krook, J.; Zhu, J.; Johnson, D.H. Comparison of Four Chemotherapy Regimens for Advanced Non–Small-Cell Lung Cancer. *N. Engl. J. Med.* **2002**, *346*, 92–98. [CrossRef]
15. Lazzari, C.; Bulotta, A.; Ducceschi, M.; Viganò, M.G.; Brioschi, E.; Corti, F.; Gianni, L.; Gregorc, V. Historical evolution of second-line therapy in non-small cell lung cancer. *Front. Med.* **2017**, *4*, 4. [CrossRef]

16. Yuan, M.; Huang, L.L.; Chen, J.H.; Wu, J.; Xu, Q. The emerging treatment landscape of targeted therapy in non-small-cell lung cancer. *Signal Transduct. Target. Ther.* **2019**, *4*, 61. [CrossRef]
17. Committee for Medicinal Products for Human Use (CHMP). *Annex I Summary of Product Characteristics*; European Medicines Agency: Amsterdam, The Netherlands, 2006; pp. 809–822.
18. Bertino, E.M.; McMichael, E.L.; Mo, X.; Trikha, P.; Davis, M.; Paul, B.; Grever, M.; Carson, W.E.; Otterson, G.A. A phase I trial to evaluate antibody-dependent cellular cytotoxicity of cetuximab and lenalidomide in advanced colorectal and head and neck cancer. *Mol. Cancer Ther.* **2016**, *15*, 2244–2250. [CrossRef]
19. Pakkala, S.; Ramalingam, S.S. Personalized therapy for lung cancer: Striking a moving target. *JCI Insight* **2018**, *3*, e120858. [CrossRef]
20. Hodi, F.S.; O'Day, S.J.; McDermott, D.F.; Weber, R.W.; Sosman, J.A.; Haanen, J.B.; Gonzalez, R.; Robert, C.; Schadendorf, D.; Hassel, J.C.; et al. Improved Survival with Ipilimumab in Patients with Metastatic Melanoma. *N. Engl. J. Med.* **2010**, *363*, 711–723. [CrossRef]
21. Robert, C.; Long, G.V.; Brady, B.; Dutriaux, C.; Maio, M.; Mortier, L.; Hassel, J.C.; Rutkowski, P.; McNeil, C.; Kalinka-Warzocha, E.; et al. Nivolumab in Previously Untreated Melanoma without *BRAF* Mutation. *N. Engl. J. Med.* **2015**, *372*, 320–330. [CrossRef]
22. Borghaei, H.; Paz-Ares, L.; Horn, L.; Spigel, D.R.; Steins, M.; Ready, N.E.; Chow, L.Q.; Vokes, E.E.; Felip, E.; Holgado, E.; et al. Nivolumab versus Docetaxel in Advanced Nonsquamous Non–Small-Cell Lung Cancer. *N. Engl. J. Med.* **2015**, *373*, 1627–1639. [CrossRef] [PubMed]
23. Brahmer, J.; Reckamp, K.L.; Baas, P.; Crinò, L.; Eberhardt, W.E.E.; Poddubskaya, E.; Antonia, S.; Pluzanski, A.; Vokes, E.E.; Holgado, E.; et al. Nivolumab versus Docetaxel in Advanced Squamous-Cell Non–Small-Cell Lung Cancer. *N. Engl. J. Med.* **2015**, *373*, 123–135. [CrossRef] [PubMed]
24. Motzer, R.J.; Escudier, B.; McDermott, D.F.; George, S.; Hammers, H.J.; Srinivas, S.; Tykodi, S.S.; Sosman, J.A.; Procopio, G.; Plimack, E.R.; et al. Nivolumab versus Everolimus in Advanced Renal-Cell Carcinoma. *N. Engl. J. Med.* **2015**, *373*, 1803–1813. [CrossRef] [PubMed]
25. Mondal, M.; Guo, J.; He, P.; Zhou, D. Recent advances of oncolytic virus in cancer therapy. *Hum. Vaccin. Immunother.* **2020**, *16*, 2389–2402. [CrossRef]
26. Wei, S.C.; Duffy, C.R.; Allison, J.P. Fundamental Mechanisms of Immune Checkpoint Blockade Therapy. *Cancer Discov.* **2018**, *8*, 1069–1086. [CrossRef]
27. Song, Q.; Zhang, C.-D.; Wu, X.-H. Therapeutic cancer vaccines: From initial findings to prospects. *Immunol. Lett.* **2018**, *196*, 11–21. [CrossRef]
28. Dastmalchi, N.; Baradaran, B.; Latifi-Navid, S.; Safaralizadeh, R.; Khojasteh, S.M.B.; Amini, M.; Roshani, E.; Lotfinejad, P. Antioxidants with two faces toward cancer. *Life Sci.* **2020**, *258*, 118186. [CrossRef]
29. Deli, T.; Orosz, M.; Jakab, A. Hormone Replacement Therapy in Cancer Survivors–Review of the Literature. *Pathol. Oncol. Res.* **2020**, *26*, 63–78. [CrossRef]
30. Shao, J.; Zaro, J.; Shen, Y. Advances in Exosome-Based Drug Delivery and Tumor Targeting: From Tissue Distribution to Intracellular Fate. *Int. J. Nanomed.* **2020**, *15*, 9355–9371. [CrossRef]
31. Fu, Z.; Xiang, J. Aptamers, the Nucleic Acid Antibodies, in Cancer Therapy. *Int. J. Mol. Sci.* **2020**, *21*, 2793. [CrossRef]
32. Vilas-Boas, V.; Carvalho, F.; Espiña, B. Magnetic Hyperthermia for Cancer Treatment: Main Parameters Affecting the Outcome of In Vitro and In Vivo Studies. *Molecules* **2020**, *25*, 2874. [CrossRef] [PubMed]
33. Amiri-Kordestani, L.; Blumenthal, G.M.; Xu, Q.C.; Zhang, L.; Tang, S.W.; Ha, L.; Weinberg, W.C.; Chi, B.; Candau-Chacon, R.; Hughes, P.; et al. FDA approval: Ado-trastuzumab emtansine for the treatment of patients with HER2-positive metastatic breast cancer. *Clin. Cancer Res.* **2014**, *20*, 4436–4441. [CrossRef] [PubMed]
34. Medical Association, A. FDA Approval of Tisagenlecleucel Promise and Complexities of a $475 000 Cancer Drug. *JAMA* **2017**, *318*, 1861–1862. [CrossRef]
35. Barenholz, Y. Doxil®—The first FDA-approved nano-drug: Lessons learned. *J. Control. Release* **2012**, *160*, 117–134. [CrossRef]
36. Vázquez-Ríos, A.J.; Alonso-Nocelo, M.; López Bouzo, B.; Ruiz-Bañobre, J.; de la Fuente, M. Nanotheranostics and their potential in the management of metastatic cancer. In *Handbook of Nanomaterials for Cancer Theranostics*; Elsevier: Amsterdam, The Netherlands, 2018; pp. 199–244. ISBN 9780128133392.
37. Peer, D.; Karp, J.M.; Hong, S.; Farokhzad, O.C.; Margalit, R.; Langer, R. Nanocarriers as an emerging platform for cancer therapy. *Nat. Nanotechnol.* **2007**, *2*, 751–760. [CrossRef]
38. Zhang, R.X.; Li, J.; Zhang, T.; Amini, M.A.; He, C.; Lu, B.; Ahmed, T.; Lip, H.; Rauth, A.M.; Wu, X.Y. Importance of integrating nanotechnology with pharmacology and physiology for innovative drug delivery and therapy-An illustration with firsthand examples. *Acta Pharmacol. Sin.* **2018**, *39*, 825–844. [CrossRef]
39. Sanna, V.; Pala, N.; Sechi, M. Targeted therapy using nanotechnology: Focus on cancer. *Int. J. Nanomed.* **2014**, *9*, 467–483.
40. Farjadian, F.; Ghasemi, A.; Gohari, O.; Roointan, A.; Karimi, M.; Hamblin, M.R. Nanopharmaceuticals and nanomedicines currently on the market: Challenges and opportunities. *Nanomedicine* **2019**, *14*, 93–126. [CrossRef]
41. Gonzalez-Valdivieso, J.; Girotti, A.; Schneider, J.; Arias, F.J. Advanced nanomedicine and cancer: Challenges and opportunities in clinical translation. *Int. J. Pharm.* **2021**, *599*, 120438. [CrossRef]
42. de Lázaro, I.; Mooney, D.J. Obstacles and opportunities in a forward vision for cancer nanomedicine. *Nat. Mater.* **2021**, *20*, 1469–1479. [CrossRef]

43. Anselmo, A.C.; Mitragotri, S. Nanoparticles in the clinic: An update. *Bioeng. Transl. Med.* **2019**, *4*, e10143. [CrossRef] [PubMed]
44. Park, H.; Otte, A.; Park, K. Evolution of drug delivery systems: From 1950 to 2020 and beyond. *J. Control. Release* **2022**, *342*, 53–65. [CrossRef] [PubMed]
45. Delvecchio, C.; Tiefenbach, J.; Krause, H.M. The Zebrafish: A powerful platform for in vivo, HTS drug discovery. *Assay Drug Dev. Technol.* **2011**, *9*, 354–361. [CrossRef] [PubMed]
46. Lieschke, G.J.; Currie, P.D. Animal models of human disease: Zebrafish swim into view. *Nat. Rev. Genet.* **2007**, *8*, 353–367. [CrossRef]
47. Zon, L.I. Zebrafish: A new model for human disease. *Genome Res.* **1999**, *9*, 99–100. [CrossRef]
48. Howe, K.; Clark, M.D.; Torroja, C.F.; Torrance, J.; Berthelot, C.; Muffato, M.; Collins, J.E.; Humphray, S.; McLaren, K.; Matthews, L.; et al. The zebrafish reference genome sequence and its relationship to the human genome. *Nature* **2013**, *496*, 498–503. [CrossRef]
49. Sieber, S.; Grossen, P.; Bussmann, J.; Campbell, F.; Kros, A.; Witzigmann, D.; Huwyler, J. Zebrafish as a preclinical in vivo screening model for nanomedicines. *Adv. Drug Deliv. Rev.* **2019**, *151–152*, 152–168. [CrossRef]
50. Zhao, S.; Huang, J.; Ye, J. A fresh look at zebrafish from the perspective of cancer research. *J. Exp. Clin. Cancer Res.* **2015**, *34*, 80. [CrossRef]
51. Lam, S.H.; Chua, H.L.; Gong, Z.; Lam, T.J.; Sin, Y.M. Development and maturation of the immune system in zebrafish, *Danio rerio*: A gene expression profiling, in situ hybridization and immunological study. *Dev. Comp. Immunol.* **2004**, *28*, 9–28. [CrossRef]
52. Zon, L.I.; Peterson, R. The new age of chemical screening in Zebrafish. *Zebrafish* **2010**, *7*, 1.
53. Raby, L.; Völkel, P.; Le Bourhis, X.; Angrand, P.O. Genetic engineering of zebrafish in cancer research. *Cancers* **2020**, *12*, 2168. [CrossRef] [PubMed]
54. Spitsbergen, J.M.; Tsai, H.W.; Reddy, A.; Miller, T.; Arbogast, D.; Hendricks, J.D.; Bailey, G.S. Neoplasia in zebrafish (*Danio rerio*) treated with N-methyl-N′-nitro-N-nitrosoguanidine by three exposure routes at different developmental stages. *Toxicol. Pathol.* **2000**, *28*, 716–725. [CrossRef] [PubMed]
55. Spitsbergen, J.M.; Tsai, H.W.; Reddy, A.; Miller, T.; Arbogast, D.; Hendricks, J.D.; Bailey, G.S. Neoplasia in zebrafish (*Danio rerio*) treated with 7,12-dimethylbenz[a]anthracene by two exposure routes at different developmental stages. *Toxicol. Pathol.* **2000**, *28*, 705–715. [CrossRef] [PubMed]
56. Siew, H.L.; Yi, L.W.; Vega, V.B.; Miller, L.D.; Spitsbergen, J.; Tong, Y.; Zhan, H.; Govindarajan, K.R.; Lee, S.; Mathavan, S.; et al. Conservation of gene expression signatures between zebrafish and human liver tumors and tumor progression. *Nat. Biotechnol.* **2006**, *24*, 73–75. [CrossRef]
57. Fujisawa, K.; Terai, S.; Matsumoto, T.; Takami, T.; Yamamoto, N.; Nishina, H.; Furutani-Seiki, M.; Sakaida, I. Evidence for a role of the transcriptional regulator Maid in tumorigenesis and aging. *PLoS ONE* **2015**, *10*, e0129950. [CrossRef]
58. Thorgaard, G.H.; Arbogast, D.N.; Hendricks, J.D.; Pereira, C.B.; Bailey, G.S. Tumor suppression in triploid trout. *Aquat. Toxicol.* **1999**, *46*, 121–126. [CrossRef]
59. Mizgireuv, I.V.; Majorova, I.G.; Gorodinskaya, V.M.; Khudoley, V.V.; Revskoy, S.Y. Carcinogenic Effect of N-Nitrosodimethylamine on Diploid and Triploid Zebrafish (*Danio rerio*). *Toxicol. Pathol.* **2016**, *32*, 514–518. [CrossRef]
60. Basten, S.G.; Davis, E.E.; Gillis, A.J.M.; van Rooijen, E.; Stoop, H.; Babala, N.; Logister, I.; Heath, Z.G.; Jonges, T.N.; Katsanis, N.; et al. Mutations in LRRC50 Predispose Zebrafish and Humans to Seminomas. *PLoS Genet.* **2013**, *9*, e1003384. [CrossRef]
61. Neumann, J.C.; Dovey, J.S.; Chandler, G.L.; Carbajal, L.; Amatruda, J.F. Identification of a heritable model of testicular germ cell tumor in the zebrafish. *Zebrafish* **2009**, *6*, 319–327. [CrossRef]
62. Renshaw, S.A.; Loynes, C.A.; Trushell, D.M.I.; Elworthy, S.; Ingham, P.W.; Whyte, M.K.B. A transgenic zebrafish model of neutrophilic inflammation. *Blood* **2006**, *108*, 3976–3978. [CrossRef]
63. Ellett, F.; Pase, L.; Hayman, J.W.; Andrianopoulos, A.; Lieschke, G.J. mpeg1 promoter transgenes direct macrophage-lineage expression in zebrafish. *Blood* **2011**, *117*, e49. [CrossRef] [PubMed]
64. Lawson, N.D.; Weinstein, B.M. In vivo imaging of embryonic vascular development using transgenic zebrafish. *Dev. Biol.* **2002**, *248*, 307–318. [CrossRef] [PubMed]
65. Park, S.W.; Davison, J.M.; Rhee, J.; Hruban, R.H.; Maitra, A.; Leach, S.D. Oncogenic KRAS Induces Progenitor Cell Expansion and Malignant Transformation in Zebrafish Exocrine Pancreas. *Gastroenterology* **2008**, *134*, 2080–2090. [CrossRef] [PubMed]
66. Michailidou, C.; Jones, M.; Walker, P.; Kamarashev, J.; Kelly, A.; Hurlstone, A.F.L. Dissecting the roles of Raf- and PI3K-signalling pathways in melanoma formation and progression in a zebrafish model. *DMM Dis. Model. Mech.* **2009**, *2*, 399–411. [CrossRef]
67. Patton, E.E.; Widlund, H.R.; Kutok, J.L.; Kopani, K.R.; Amatruda, J.F.; Murphey, R.D.; Berghmans, S.; Mayhall, E.A.; Traver, D.; Fletcher, C.D.M.; et al. BRAF mutations are sufficient to promote nevi formation and cooperate with p53 in the genesis of melanoma. *Curr. Biol.* **2005**, *15*, 249–254. [CrossRef]
68. Busson, D.; Pret, A.-M. GAL4/UAS Targeted Gene Expression for Studying *Drosophila* Hedgehog Signaling. In *Hedgehog Signaling Protocols*; Humana Press: Totowa, NJ, USA, 2007; Volume 397, pp. 161–201. [CrossRef]
69. Alghisi, E.; Distel, M.; Malagola, M.; Anelli, V.; Santoriello, C.; Herwig, L.; Krudewig, A.; Henkel, C.V.; Russo, D.; Mione, M.C. Targeting oncogene expression to endothelial cells induces proliferation of the myelo-erythroid lineage by repressing the notch pathway. *Leukemia* **2013**, *27*, 2229–2241. [CrossRef]
70. Mayrhofer, M.; Gourain, V.; Reischl, M.; Affaticati, P.; Jenett, A.; Joly, J.S.; Benelli, M.; Demichelis, F.; Poliani, P.L.; Sieger, D.; et al. A novel brain tumour model in zebrafish reveals the role of YAP activation in MAPK- and PI3K-induced malignant growth. *DMM Dis. Model. Mech.* **2017**, *10*, 15–28. [CrossRef]

71. Burger, A.; Vasilyev, A.; Tomar, R.; Selig, M.K.; Nielsen, G.P.; Peterson, R.T.; Drummond, I.A.; Haber, D.A. A zebrafish model of chordoma initiated by notochord-driven expression of HRASV12. *DMM Dis. Model. Mech.* **2014**, *7*, 907–913. [CrossRef]
72. Ju, B.; Chen, W.; Orr, B.A.; Spitsbergen, J.M.; Jia, S.; Eden, C.J.; Henson, H.E.; Taylor, M.R. Oncogenic KRAS promotes malignant brain tumors in zebrafish. *Mol. Cancer* **2015**, *14*, 18. [CrossRef]
73. Nasevicius, A.; Ekker, S.C. Effective targeted gene "knockdown" in zebrafish. *Nat. Genet.* **2000**, *26*, 216–220. [CrossRef]
74. Jacob, L.; Sawma, P.; Garnier, N.; Meyer, L.A.T.; Fritz, J.; Hussenet, T.; Spenlé, C.; Goetz, J.; Vermot, J.; Fernandez, A.; et al. Inhibition of PlexA1-mediated brain tumor growth and tumor-associated angiogenesis using a transmembrane domain targeting peptide. *Oncotarget* **2016**, *7*, 57851–57865. [CrossRef] [PubMed]
75. Royet, A.; Broutier, L.; Coissieux, M.M.; Malleval, C.; Gadot, N.; Maillet, D.; Gratadou-Hupon, L.; Bernet, A.; Nony, P.; Treilleux, I.; et al. Ephrin-B3 supports glioblastoma growth by inhibiting apoptosis induced by the dependence receptor EphA4. *Oncotarget* **2017**, *8*, 23750–23759. [CrossRef] [PubMed]
76. Wienholds, E.; van Eeden, F.; Kosters, M.; Mudde, J.; Plasterk, R.H.A.; Cuppen, E. Efficient target-selected mutagenesis in zebrafish. *Genome Res.* **2003**, *13*, 2700–2707. [CrossRef] [PubMed]
77. Berghmans, S.; Murphey, R.D.; Wienholds, E.; Neuberg, D.; Kutok, J.L.; Fletcher, C.D.M.; Morris, J.P.; Liu, T.X.; Schulte-Merker, S.; Kanki, J.P.; et al. tp53 mutant zebrafish develop malignant peripheral nerve sheath tumors. *Proc. Natl. Acad. Sci. USA* **2005**, *102*, 407–412. [CrossRef] [PubMed]
78. Faucherre, A.; Taylor, G.S.; Overvoorde, J.; Dixon, J.E.; Den Hertog, J. Zebrafish pten genes have overlapping and non-redundant functions in tumorigenesis and embryonic development. *Oncogene* **2008**, *27*, 1079–1086. [CrossRef]
79. Choorapoikayil, S.; Kuiper, R.V.; De Bruin, A.; Den Hertog, J. Haploinsufficiency of the genes encoding the tumor suppressor Pten predisposes zebrafish to hemangiosarcoma. *DMM Dis. Model. Mech.* **2012**, *5*, 241–247. [CrossRef]
80. Haramis, A.P.G.; Hurlstone, A.; van der Velden, Y.; Begthel, H.; van den Born, M.; Offerhaus, G.J.A.; Clevers, H.C. Adenomatous polyposis coli-deficient zebrafish are susceptible to digestive tract neoplasia. *EMBO Rep.* **2006**, *7*, 444–449. [CrossRef]
81. Shive, H.R.; West, R.R.; Embree, L.J.; Azuma, M.; Sood, R.; Liu, P.; Hicksteina, D.D. Brca2 in zebrafish ovarian development, spermatogenesis, and tumorigenesis. *Proc. Natl. Acad. Sci. USA* **2010**, *107*, 19350–19355. [CrossRef]
82. Santhakumar, K.; Judson, E.C.; Elks, P.M.; McKee, S.; Elworthy, S.; Van Rooijen, E.; Walmsley, S.S.; Renshaw, S.A.; Cross, S.S.; Van Eeden, F.J.M. A zebrafish model to study and therapeutically manipulate hypoxia signaling in tumorigenesis. *Cancer Res.* **2012**, *72*, 4017–4027. [CrossRef]
83. Gjini, E.; Mansour, M.R.; Sander, J.D.; Moritz, N.; Nguyen, A.T.; Kesarsing, M.; Gans, E.; He, S.; Chen, S.; Ko, M.; et al. A Zebrafish Model of Myelodysplastic Syndrome Produced through tet2 Genomic Editing. *Mol. Cell. Biol.* **2015**, *35*, 789–804. [CrossRef]
84. Shin, J.; Padmanabhan, A.; De Groh, E.D.; Lee, J.S.; Haidar, S.; Dahlberg, S.; Guo, F.; He, S.; Wolman, M.A.; Granato, M.; et al. Zebrafish neurofibromatosis type 1 genes have redundant functions in tumorigenesis and embryonic development. *DMM Dis. Model. Mech.* **2012**, *5*, 881–894. [CrossRef] [PubMed]
85. Shim, J.; Choi, J.H.; Park, M.H.; Kim, H.; Kim, J.H.; Kim, S.Y.; Hong, D.; Kim, S.; Lee, J.E.; Kim, C.H.; et al. Development of zebrafish medulloblastoma-like PNET model by TALEN-mediated somatic gene inactivation. *Oncotarget* **2017**, *8*, 55280–55297. [CrossRef] [PubMed]
86. Oppel, F.; Tao, T.; Shi, H.; Ross, K.N.; Zimmerman, M.W.; He, S.; Tong, G.; Aster, J.C.; Thomas Look, A. Loss of atrx cooperates with p53-deficiency to promote the development of sarcomas and other malignancies. *PLoS Genet.* **2019**, *15*, e1008039. [CrossRef] [PubMed]
87. Oppel, F.; Ki, D.H.; Zimmerman, M.W.; Ross, K.N.; Tao, T.; Shi, H.; He, S.; Aster, J.C.; Look, A.T. suz12 inactivation in p53- And nf1-deficient zebrafish accelerates the onset of malignant peripheral nerve sheath tumors and expands the spectrum of tumor types. *DMM Dis. Model. Mech.* **2020**, *13*, dmm042341. [CrossRef] [PubMed]
88. Moore, J.C.; Langenau, D.M. Allograft cancer cell transplantation in zebrafish. In *Advances in Experimental Medicine and Biology*; Springer: Cham, Germany, 2016; Volume 916, pp. 265–287.
89. Nicoli, S.; Presta, M. The zebrafish/tumor xenograft angiogenesis assay. *Nat. Protoc.* **2007**, *2*, 2918–2923. [CrossRef] [PubMed]
90. Veinotte, C.J.; Dellaire, G.; Berman, J.N. Hooking the big one: The potential of zebrafish xenotransplantation to reform cancer drug screening in the genomic era. *DMM Dis. Model. Mech.* **2014**, *7*, 745–754. [CrossRef]
91. Mercatali, L.; La Manna, F.; Groenewoud, A.; Casadei, R.; Recine, F.; Miserocchi, G.; Pieri, F.; Liverani, C.; Bongiovanni, A.; Spadazzi, C.; et al. Development of a patient-derived xenograft (PDX) of breast cancer bone metastasis in a Zebrafish model. *Int. J. Mol. Sci.* **2016**, *17*, 1375. [CrossRef]
92. Khan, N.; Mahajan, N.K.; Sinha, P.; Jayandharan, G.R. An efficient method to generate xenograft tumor models of acute myeloid leukemia and hepatocellular carcinoma in adult zebrafish. *Blood Cells, Mol. Dis.* **2019**, *75*, 48–55. [CrossRef]
93. Gómez-Abenza, E.; Ibáñez-Molero, S.; García-Moreno, D.; Fuentes, I.; Zon, L.I.; Mione, M.C.; Cayuela, M.L.; Gabellini, C.; Mulero, V. Zebrafish modeling reveals that SPINT1 regulates the aggressiveness of skin cutaneous melanoma and its crosstalk with tumor immune microenvironment. *J. Exp. Clin. Cancer Res.* **2019**, *38*, 405. [CrossRef]
94. Tang, Q.; Abdelfattah, N.S.; Blackburn, J.S.; Moore, J.C.; Martinez, S.A.; Moore, F.E.; Lobbardi, R.; Tenente, I.M.; Ignatius, M.S.; Berman, J.N.; et al. Optimized cell transplantation using adult rag2 mutant zebrafish. *Nat. Methods* **2014**, *11*, 821–824. [CrossRef]
95. Yan, C.; Brunson, D.C.; Tang, Q.; Do, D.; Iftimia, N.A.; Moore, J.C.; Hayes, M.N.; Welker, A.M.; Garcia, E.G.; Dubash, T.D.; et al. Visualizing Engrafted Human Cancer and Therapy Responses in Immunodeficient Zebrafish. *Cell* **2019**, *177*, 1903–1914. [CrossRef] [PubMed]

96. Letrado, P.; De Miguel, I.; Lamberto, I.; Díez-Martínez, R.; Oyarzabal, J. Zebrafish: Speeding up the cancer drug discovery process. *Cancer Res.* **2018**, *78*, 6048–6058. [CrossRef] [PubMed]
97. Blackburn, J.S.; Liu, S.; Langenau, D.M. Quantifying the frequency of tumor-propagating cells using limiting dilution cell transplantation in syngeneic zebrafish. *J. Vis. Exp.* **2011**, *14*, e2790. [CrossRef] [PubMed]
98. Smith, A.C.H.; Raimondi, A.R.; Salthouse, C.D.; Ignatius, M.S.; Blackburn, J.S.; Mizgirev, I.V.; Storer, N.Y.; De Jong, J.L.O.; Chen, A.T.; Zhou, Y.; et al. High-throughput cell transplantation establishes that tumor-initiating cells are abundant in zebrafish T-cell acute lymphoblastic leukemia. *Blood* **2010**, *115*, 3296–3303. [CrossRef]
99. Blackburn, J.S.; Liu, S.; Wilder, J.L.; Dobrinski, K.P.; Lobbardi, R.; Moore, F.E.; Martinez, S.A.; Chen, E.A.; Lee, C.; Langenau, D.M. Clonal evolution enhances leukemia-propagating cell frequency in T cell acute lymphoblastic leukemia through Akt/mTORC1 pathway activation. *Cancer Cell* **2014**, *25*, 366–378. [CrossRef]
100. Ignatius, M.S.; Hayes, M.N.; Moore, F.E.; Tang, Q.; Garcia, S.P.; Blackburn, P.R.; Baxi, K.; Wang, L.; Jin, A.; Ramakrishnan, A.; et al. Tp53 deficiency causes a wide tumor spectrum and increases embryonal rhabdomyosarcoma metastasis in zebrafish. *eLife* **2018**, *7*, e37202. [CrossRef]
101. White, R.M.; Sessa, A.; Burke, C.; Bowman, T.; LeBlanc, J.; Ceol, C.; Bourque, C.; Dovey, M.; Goessling, W.; Burns, C.E.; et al. Transparent Adult Zebrafish as a Tool for In Vivo Transplantation Analysis. *Cell Stem Cell* **2008**, *2*, 183–189. [CrossRef]
102. Lee, L.M.J.; Seftor, E.A.; Bonde, G.; Cornell, R.A.; Hendrix, M.J.C. The fate of human malignant melanoma cells transplanted into zebrafish embryos: Assessment of migration and cell division in the absence of tumor formation. *Dev. Dyn.* **2005**, *233*, 1560–1570. [CrossRef]
103. Cabezas-Sáinz, P.; Pensado-López, A.; Sáinz, B.; Sánchez, L. Modeling Cancer Using Zebrafish Xenografts: Drawbacks for Mimicking the Human Microenvironment. *Cells* **2020**, *9*, 1978. [CrossRef]
104. He, S.; Lamers, G.E.; Beenakker, J.W.M.; Cui, C.; Ghotra, V.P.; Danen, E.H.; Meijer, A.H.; Spaink, H.P.; Snaar-Jagalska, B.E. Neutrophil-mediated experimental metastasis is enhanced by VEGFR inhibition in a zebrafish xenograft model. *J. Pathol.* **2012**, *227*, 431–445. [CrossRef]
105. Roh-Johnson, M.; Shah, A.N.; Stonick, J.A.; Poudel, K.R.; Kargl, J.; Yang, G.H.; di Martino, J.; Hernandez, R.E.; Gast, C.E.; Zarour, L.R.; et al. Macrophage-Dependent Cytoplasmic Transfer during Melanoma Invasion In Vivo. *Dev. Cell* **2017**, *43*, 549–562. [CrossRef] [PubMed]
106. Hill, D.; Chen, L.; Snaar-Jagalska, E.; Chaudhry, B. Embryonic zebrafish xenograft assay of human cancer metastasis. *F1000Research* **2018**, *7*, 1682. [CrossRef] [PubMed]
107. Britto, D.D.; Wyroba, B.; Chen, W.; Lockwood, R.A.; Tran, K.B.; Shepherd, P.R.; Hall, C.J.; Crosier, K.E.; Crosier, P.S.; Astin, J.W. Macrophages enhance Vegfa-driven angiogenesis in an embryonic zebrafish tumour xenograft model. *DMM Dis. Model. Mech.* **2018**, *11*, dmm035998. [CrossRef] [PubMed]
108. Allen, T.A.; Asad, D.; Amu, E.; Taylor Hensley, M.; Cores, J.; Vandergriff, A.; Tang, J.; Dinh, P.U.; Shen, D.; Qiao, L.; et al. Circulating tumor cells exit circulation while maintaining multicellularity, augmenting metastatic potential. *J. Cell Sci.* **2019**, *132*, jcs231563. [CrossRef]
109. Lal, S.; La Du, J.; Tanguay, R.L.; Greenwood, J.A. Calpain 2 is required for the invasion of glioblastoma cells in the zebrafish brain microenvironment. *J. Neurosci. Res.* **2012**, *90*, 769–781. [CrossRef]
110. Gamble, J.T.; Reed-Harris, Y.; Barton, C.L.; La Du, J.; Tanguay, R.; Greenwood, J.A. Quantification of glioblastoma progression in zebrafish xenografts: Adhesion to laminin alpha 5 promotes glioblastoma microtumor formation and inhibits cell invasion. *Biochem. Biophys. Res. Commun.* **2018**, *506*, 833–839. [CrossRef]
111. Zeng, A.; Ye, T.; Cao, D.; Huang, X.; Yang, Y.; Chen, X.; Xie, Y.; Yao, S.; Zhao, C. Identify a Blood-Brain Barrier Penetrating Drug-TNB using Zebrafish Orthotopic Glioblastoma Xenograft Model. *Sci. Rep.* **2017**, *7*, 14372. [CrossRef]
112. Asnaghi, L.; White, D.T.; Yoon, L.; Price, A.; Lee, G.Y.; Sahoo, A.; Mumm, J.S.; Eberhart, C.G. Downregulation of Nodal inhibits metastatic progression in retinoblastoma. *Acta Neuropathol. Commun.* **2019**, *7*, 137. [CrossRef]
113. Marques, I.J.; Weiss, F.U.; Vlecken, D.H.; Nitsche, C.; Bakkers, J.; Lagendijk, A.K.; Partecke, L.I.; Heidecke, C.D.; Lerch, M.M.; Bagowski, C.P. Metastatic behaviour of primary human tumours in a zebrafish xenotransplantation model. *BMC Cancer* **2009**, *9*, 128. [CrossRef]
114. Usai, A.; Di Franco, G.; Colucci, P.; Pollina, L.E.; Vasile, E.; Funel, N.; Palmeri, M.; Dente, L.; Falcone, A.; Morelli, L.; et al. A model of a zebrafish avatar for co-clinical trials. *Cancers* **2020**, *12*, 677. [CrossRef]
115. Al-Samadi, A.; Tuomainen, K.; Kivimäki, A.; Salem, A.; Al-Kubati, S.; Hyytiäinen, A.; Parikka, M.; Mesimäki, K.; Wilkman, T.; Mäkitie, A.; et al. PCR-based zebrafish model for personalised medicine in head and neck cancer. *J. Transl. Med.* **2019**, *17*, 235. [CrossRef] [PubMed]
116. Peverelli, E.; Giardino, E.; Treppiedi, D.; Meregalli, M.; Belicchi, M.; Vaira, V.; Corbetta, S.; Verdelli, C.; Verrua, E.; Serban, A.L.; et al. Dopamine receptor type 2 (DRD2) and somatostatin receptor type 2 (SSTR2) agonists are effective in inhibiting proliferation of progenitor/stem-like cells isolated from nonfunctioning pituitary tumors. *Int. J. Cancer* **2017**, *140*, 1870–1880. [CrossRef] [PubMed]
117. Liverani, C.; La Manna, F.; Groenewoud, A.; Mercatali, L.; Van Der Pluijm, G.; Pieri, F.; Cavaliere, D.; De Vita, A.; Spadazzi, C.; Miserocchi, G.; et al. Innovative approaches to establish and characterize primary cultures: An ex vivo 3D system and the zebrafish model. *Biol. Open* **2017**, *6*, 133–140. [CrossRef] [PubMed]

118. Bentley, V.L.; Veinotte, C.J.; Corkery, D.P.; Pinder, J.B.; Leblanc, M.A.; Bedard, K.; Weng, A.P.; Berman, J.N.; Dellaire, G. Focused chemical genomics using zebrafish xenotransplantation as a pre-clinical therapeutic platform for T-cell acute lymphoblastic leukemia. *Haematologica* **2015**, *100*, 70–76. [CrossRef]
119. Peterson, R.T.; Link, B.A.; Dowling, J.E.; Schreiber, S.L. Small molecule developmental screens reveal the logic and timing of vertebrate development. *Natl. Acad Sci.* **2020**, *97*, 12965–12969. [CrossRef]
120. Gianoncelli, A.; Guarienti, M.; Fragni, M.; Bertuzzi, M.; Rossini, E.; Abate, A.; Basnet, R.M.; Zizioli, D.; Bono, F.; Terzolo, M.; et al. Adrenocortical Carcinoma Xenograft in Zebrafish Embryos as a Model To Study the In Vivo Cytotoxicity of Abiraterone Acetate. *Endocrinology* **2019**, *160*, 2620–2629. [CrossRef]
121. Cabezas-Sainz, P.; Guerra-Varela, J.; Carreira, M.J.; Mariscal, J.; Roel, M.; Rubiolo, J.A.; Sciara, A.A.; Abal, M.; Botana, L.M.; López, R.; et al. Improving zebrafish embryo xenotransplantation conditions by increasing incubation temperature and establishing a proliferation index with ZFtool. *BMC Cancer* **2018**, *18*, 3. [CrossRef]
122. Cornet, C.; Dyballa, S.; Terriente, J.; Di Giacomo, V. ZeOncoTest: Refining and Automating the Zebrafish Xenograft Model for Drug Discovery in Cancer. *Pharmaceuticals* **2019**, *13*, 1. [CrossRef]
123. ZeClinics. Powering Discovery with Zebrafish. Available online: https://www.zeclinics.com/ (accessed on 7 May 2020).
124. Li, X.; Huang, L.; Wu, J.; He, M.; Zhu, S.; Zhan, P.; Lv, T.; Song, Y. Zebrafish Xenograft Model of Human Lung Cancer for Evaluating Osimertinib Resistance. *BioMed Res. Int.* **2019**, *2019*, 3129748. [CrossRef]
125. Precazzini, F.; Pancher, M.; Gatto, P.; Tushe, A.; Adami, V.; Anelli, V.; Mione, M.C. Automated in vivo screen in zebrafish identifies Clotrimazole as targeting a metabolic vulnerability in a melanoma model. *Dev. Biol.* **2020**, *457*, 215–225. [CrossRef]
126. Xu, Z.; Hu, C.; Chen, S.; Zhang, C.; Yu, J.; Wang, X.; Lv, H.; Cheng, X. Apatinib enhances chemosensitivity of gastric cancer to paclitaxel and 5-fluorouracil. *Cancer Manag. Res.* **2019**, *11*, 4905–4915. [CrossRef] [PubMed]
127. Costa, B.; Ferreira, S.; Póvoa, V.; Cardoso, M.J.; Vieira, S.; Stroom, J.; Fidalgo, P.; Rio-Tinto, R.; Figueiredo, N.; Parés, O.; et al. Developments in zebrafish avatars as radiotherapy sensitivity reporters—Towards personalized medicine. *EBioMedicine* **2020**, *51*, 102578. [CrossRef] [PubMed]
128. Ai, N.; Chong, C.M.; Chen, W.; Hu, Z.; Su, H.; Chen, G.; Wong, Q.W.L.; Ge, W. Ponatinib exerts anti-angiogenic effects in the zebrafish and human umbilical vein endothelial cells via blocking VEGFR signaling pathway. *Oncotarget* **2018**, *9*, 31958–31970. [CrossRef] [PubMed]
129. Reddy, V.G.; Reddy, T.S.; Jadala, C.; Reddy, M.S.; Sultana, F.; Akunuri, R.; Bhargava, S.K.; Wlodkowic, D.; Srihari, P.; Kamal, A. Pyrazolo-benzothiazole hybrids: Synthesis, anticancer properties and evaluation of antiangiogenic activity using in vitro VEGFR-2 kinase and in vivo transgenic zebrafish model. *Eur. J. Med. Chem.* **2019**, *182*, 111609. [CrossRef] [PubMed]
130. Mercurio, A.; Sharples, L.; Corbo, F.; Franchini, C.; Vacca, A.; Catalano, A.; Carocci, A.; Kamm, R.D.; Pavesi, A.; Adriani, G. Phthalimide Derivative Shows Anti-angiogenic Activity in a 3D Microfluidic Model and No Teratogenicity in Zebrafish Embryos. *Front. Pharmacol.* **2019**, *10*, 349. [CrossRef] [PubMed]
131. Beedie, S.; Rore, M.H.; Barnett, S.; Chau, H.C.; Luo, W.; Greig, N.H.; Figg, W.D.; Vargesson, N. In vivo screening and discovery of novel candidate thalidomide analogs in the zebrafish embryo and chicken embryo model systems. *Oncotarget* **2016**, *7*, 33237–33245. [CrossRef] [PubMed]
132. Yang, B.; Wang, N.; Wang, S.; Li, X.; Zheng, Y.; Li, M.; Song, J.; Zhang, F.; Mei, W.; Lin, Y.; et al. Network-pharmacology-based identification of caveolin-1 as a key target of Oldenlandia diffusa to suppress breast cancer metastasis. *Biomed. Pharmacother.* **2019**, *112*, 108607. [CrossRef]
133. Song, Z.; Zhang, Y.; Zhang, H.; Rajendran, R.S.; Wang, R.; Hsiao, C.-D.; Li, J.; Xia, Q.; Liu, K. Isoliquiritigenin triggers developmental toxicity and oxidative stress–mediated apoptosis in zebrafish embryos/larvae via Nrf2-HO1/JNK-ERK/mitochondrion pathway. *Chemosphere* **2020**, *246*, 125727. [CrossRef]
134. Wang, G.; Xiao, Q.; Wu, Y.; Wei, Y.; Jing, Y.; Cao, X.; Gong, Z. Design and synthesis of novel celastrol derivative and its antitumor activity in hepatoma cells and antiangiogenic activity in zebrafish. *J. Cell. Physiol.* **2019**, *234*, 16431–16446. [CrossRef]
135. Yang, Y.; Hao, E.; Pan, X.; Tan, D.; Du, Z.; Xie, J.; Hou, X.; Deng, J.; Wei, K. Gomisin M2 from Baizuan suppresses breast cancer stem cell proliferation in a zebrafish xenograft model. *Aging (Albany NY)* **2019**, *11*, 8347–8361. [CrossRef]
136. Liu, J.S.; Huo, C.Y.; Cao, H.H.; Fan, C.L.; Hu, J.Y.; Deng, L.J.; Lu, Z.-B.; Yang, H.Y.; Yu, L.Z.; Mo, Z.X.; et al. Aloperine induces apoptosis and G2/M cell cycle arrest in hepatocellular carcinoma cells through the PI3K/Akt signaling pathway. *Phytomedicine* **2019**, *61*, 152843. [CrossRef] [PubMed]
137. Wu, Q.; Zheng, K.; Huang, X.; Li, L.; Mei, W. Tanshinone-IIA-Based Analogues of Imidazole Alkaloid Act as Potent Inhibitors to Block Breast Cancer Invasion and Metastasis in Vivo. *J. Med. Chem.* **2018**, *61*, 10488–10501. [CrossRef] [PubMed]
138. Zhang, Y.; Hou, Q.; Li, X.; Zhu, J.; Wang, W.; Li, B.; Zhao, L.; Xia, H. Enrichment of novel quinazoline derivatives with high antitumor activity in mitochondria tracked by its self-fluorescence. *Eur. J. Med. Chem.* **2019**, *178*, 417–432. [CrossRef] [PubMed]
139. Lin, H.-S.; Huang, Y.-L.; Wang, Y.-R.S.; Hsiao, E.; Hsu, T.-A.; Shiao, H.-Y.; Jiaang, W.-T.; Sampurna, B.P.; Lin, K.-H.; Wu, M.-S.; et al. Identification of Novel Anti-Liver Cancer Small Molecules with Better Therapeutic Index Than Sorafenib via Zebrafish Drug Screening Platform. *Cancers* **2019**, *11*, 739. [CrossRef] [PubMed]
140. Costa, M.; Rosa, F.; Ribeiro, T.; Hernandez-Bautista, R.; Bonaldo, M.; Silva, N.G.; Eiríksson, F.; Thorsteinsdóttir, M.; Ussar, S.; Urbatzka, R. Identification of cyanobacterial strains with potential for the treatment of obesity-related co-morbidities by bioactivity, toxicity evaluation and metabolite profiling. *Mar. Drugs* **2019**, *17*, 280. [CrossRef]

141. Carrillo, P.; Martínez-Poveda, B.; Cheng-Sánchez, I.; Guerra, J.; Tobia, C.; López-Romero, J.M.; Sarabia, F.; Medina, M.Á.; Quesada, A.R. Exploring the Antiangiogenic Potential of Solomonamide A Bioactive Precursors: In Vitro and in Vivo Evidences of the Inhibitory Activity of Solo F-OH During Angiogenesis. *Mar. Drugs* **2019**, *17*, 228. [CrossRef]
142. Long, W.; Wang, M.; Luo, X.; Huang, G.; Chen, J. Murrangatin suppresses angiogenesis induced by tumor cell–derived media and inhibits AKT activation in zebrafish and endothelial cells. *Drug Des. Devel. Ther.* **2018**, *12*, 3107–3115. [CrossRef]
143. Jiang, J.; Wu, S.; Lv, L.; Liu, X.; Chen, L.; Zhao, X.; Wang, Q. Mitochondrial dysfunction, apoptosis and transcriptomic alterations induced by four strobilurins in zebrafish (*Danio rerio*) early life stages. *Environ. Pollut.* **2019**, *253*, 722–730. [CrossRef]
144. Bousquet, M.S.; Ma, J.J.; Ratnayake, R.; Havre, P.A.; Yao, J.; Dang, N.H.; Paul, V.J.; Carney, T.J.; Dang, L.H.; Luesch, H. Multidimensional Screening Platform for Simultaneously Targeting Oncogenic KRAS and Hypoxia-Inducible Factors Pathways in Colorectal Cancer. *ACS Chem. Biol.* **2016**, *11*, 1322–1331. [CrossRef]
145. Yang, Q.; Salim, L.; Yan, C.; Gong, Z. Rapid Analysis of Effects of Environmental Toxicants on Tumorigenesis and Inflammation Using a Transgenic Zebrafish Model for Liver Cancer. *Mar. Biotechnol.* **2019**, *21*, 396–405. [CrossRef]
146. Xiao, Y.F.; Jie, M.M.; Li, B.S.; Hu, C.J.; Xie, R.; Tang, B.; Yang, S.M. Peptide-Based Treatment: A Promising Cancer Therapy. *J. Immunol. Res.* **2015**, *2015*, 761820. [CrossRef] [PubMed]
147. Wu, D.; Gao, Y.; Qi, Y.; Chen, L.; Ma, Y.; Li, Y. Peptide-based cancer therapy: Opportunity and challenge. *Cancer Lett.* **2014**, *351*, 13–22. [CrossRef] [PubMed]
148. Varas, M.A.; Muñoz-Montecinos, C.; Kallens, V.; Simon, V.; Allende, M.L.; Marcoleta, A.E.; Lagos, R. Exploiting Zebrafish Xenografts for Testing the in vivo Antitumorigenic Activity of Microcin E492 Against Human Colorectal Cancer Cells. *Front. Microbiol.* **2020**, *11*, 405. [CrossRef] [PubMed]
149. Hsieh, T.H.; Hsu, C.Y.; Tsai, C.F.; Chiu, C.C.; Liang, S.S.; Wang, T.N.; Kuo, P.L.; Long, C.Y.; Tsai, E.M. A novel cell-penetrating peptide suppresses breast tumorigenesis by inhibiting β-catenin/LEF-1 signaling. *Sci. Rep.* **2016**, *6*, 19156. [CrossRef]
150. Pearce, M.C.; Gamble, J.T.; Kopparapu, P.R.; O'Donnell, E.F.; Mueller, M.J.; Jang, H.S.; Greenwood, J.A.; Satterthwait, A.C.; Tanguay, R.L.; Zhang, X.K.; et al. Induction of apoptosis and suppression of tumor growth by Nur77-derived Bcl-2 converting peptide in chemoresistant lung cancer cells. *Oncotarget* **2018**, *9*, 26072–26085. [CrossRef]
151. Cordeiro, M.; Carvalho, L.; Silva, J.; Saúde, L.; Fernandes, A.R.; Baptista, P.V. Gold Nanobeacons for Tracking Gene Silencing in Zebrafish. *Nanomaterials* **2017**, *7*, 10. [CrossRef]
152. Chiavacci, E.; Rizzo, M.; Pitto, L.; Patella, F.; Evangelista, M.; Mariani, L.; Rainaldi, G. The zebrafish/tumor xenograft angiogenesis assay as a tool for screening anti-angiogenic miRNAs. *Cytotechnology* **2014**, *67*, 969–975. [CrossRef]
153. Kiener, M.; Chen, L.; Krebs, M.; Grosjean, J.; Klima, I.; Kalogirou, C.; Riedmiller, H.; Kneitz, B.; Thalmann, G.N.; Snaar-Jagalska, E.; et al. MiR-221-5p regulates proliferation and migration in human prostate cancer cells and reduces tumor growth in vivo. *BMC Cancer* **2019**, *19*, 627. [CrossRef]
154. Bayer, V. An Overview of Monoclonal Antibodies. *Semin. Oncol. Nurs.* **2019**, *35*, 150927. [CrossRef]
155. Fior, R.; Póvoa, V.; Mendes, R.V.; Carvalho, T.; Gomes, A.; Figueiredo, N.; Ferreira, F.R. Single-cell functional and chemosensitive profiling of combinatorial colorectal therapy in zebrafish xenografts. *Proc. Natl. Acad. Sci. USA* **2017**, *114*, E8234–E8243. [CrossRef]
156. Wu, J.Q.; Fan, R.Y.; Zhang, S.R.; Li, C.Y.; Shen, L.Z.; Wei, P.; He, Z.H.; He, M.F. A systematical comparison of anti-angiogenesis and anti-cancer efficacy of ramucirumab, apatinib, regorafenib and cabozantinib in zebrafish model. *Life Sci.* **2020**, *247*, 117402. [CrossRef] [PubMed]
157. Jin, Y.; Wei, L.; Jiang, Q.; Song, X.; Teng, C.; Fan, C.; Lv, Y.; Liu, Y.; Shen, W.; Li, L.; et al. Comparison of efficacy and toxicity of bevacizumab, endostar and apatinib in transgenic and human lung cancer xenograftzebrafish model. *Sci. Rep.* **2018**, *8*, 15837. [CrossRef] [PubMed]
158. Zhang, J.; Gao, B.; Zhang, W.; Qian, Z.; Xiang, Y. Monitoring antiangiogenesis of bevacizumab in zebrafish. *Drug Des. Devel. Ther.* **2018**, *12*, 2423–2430. [CrossRef] [PubMed]
159. Gomes-Silva, D.; Ramos, C.A. Cancer Immunotherapy Using CAR-T Cells: From the Research Bench to the Assembly Line. *Biotechnol. J.* **2018**, *13*, 1700097. [CrossRef]
160. Wang, Z.; Wu, Z.; Liu, Y.; Han, W. New development in CAR-T cell therapy. *J. Hematol. Oncol.* **2017**, *10*, 53. [CrossRef] [PubMed]
161. Pascoal, S.; Salzer, B.; Scheuringer, E.; Wenninger-Weinzierl, A.; Sturtzel, C.; Holter, W.; Taschner-Mandl, S.; Lehner, M.; Distel, M. A preclinical embryonic zebrafish xenograft model to investigate CAR T cells in vivo. *Cancers* **2020**, *12*, 567. [CrossRef] [PubMed]
162. Ramachandran, R.; Krishnaraj, C.; Sivakumar, A.S.; Prasannakumar, P.; Abhay Kumar, V.K.; Shim, K.S.; Song, C.-G.; Yun, S.-I. Anticancer activity of biologically synthesized silver and gold nanoparticles on mouse myoblast cancer cells and their toxicity against embryonic zebrafish. *Mater. Sci. Eng. C* **2017**, *73*, 674–683. [CrossRef] [PubMed]
163. Calienni, M.N.; Cagel, M.; Montanari, J.; Moretton, M.A.; Prieto, M.J.; Chiappetta, D.A.; Alonso, S.d.V. Zebrafish (*Danio rerio*) model as an early stage screening tool to study the biodistribution and toxicity profile of doxorubicin-loaded mixed micelles. *Toxicol. Appl. Pharmacol.* **2018**, *357*, 106–114. [CrossRef]
164. Wu, Y.; Ge, P.; Xu, W.; Li, M.; Kang, Q.; Zhang, X.; Xie, J. Cancer-targeted and intracellular delivery of Bcl-2-converting peptide with functional macroporous silica nanoparticles for biosafe treatment. *Mater. Sci. Eng. C* **2020**, *108*, 110386. [CrossRef]
165. Haque, E.; Ward, A.C. Zebrafish as a model to evaluate nanoparticle toxicity. *Nanomaterials* **2018**, *8*, 561. [CrossRef]
166. Chakraborty, C.; Sharma, A.R.; Sharma, G.; Lee, S.S. Zebrafish: A complete animal model to enumerate the nanoparticle toxicity. *J. Nanobiotechnol.* **2016**, *14*, 65. [CrossRef] [PubMed]

167. Jia, H.R.; Zhu, Y.X.; Duan, Q.Y.; Chen, Z.; Wu, F.G. Nanomaterials meet zebrafish: Toxicity evaluation and drug delivery applications. *J. Control. Release* **2019**, *311–312*, 301–318. [CrossRef] [PubMed]
168. Chang, H.; Yhee, J.Y.; Jang, G.H.; You, D.G.; Ryu, J.H.; Choi, Y.; Na, J.H.; Park, J.H.; Lee, K.H.; Choi, K.; et al. Predicting the in vivo accumulation of nanoparticles in tumor based on in vitro macrophage uptake and circulation in zebrafish. *J. Control. Release* **2016**, *244*, 205–213. [CrossRef] [PubMed]
169. Gundersen, E.T.; Førde, J.L.; Tislevoll, B.S.; Leitch, C.; Barratt, G.; Gjertsen, B.T.; Herfindal, L. Repurposing chlorpromazine for anti-leukaemic therapy by nanoparticle encapsulation. *Int. J. Pharm.* **2022**, *612*, 121296. [CrossRef]
170. Gong, C.; Deng, S.; Wu, Q.; Xiang, M.; Wei, X.; Li, L.; Gao, X.; Wang, B.; Sun, L.; Chen, Y.; et al. Improving antiangiogenesis and anti-tumor activity of curcumin by biodegradable polymeric micelles. *Biomaterials* **2013**, *34*, 1413–1432. [CrossRef]
171. Askes, S.H.C.; Bossert, N.; Bussmann, J.; Talens, V.S.; Meijer, M.S.; Kieltyka, R.E.; Kros, A.; Bonnet, S.; Heinrich, D. Dynamics of dual-fluorescent polymersomes with durable integrity in living cancer cells and zebrafish embryos. *Biomaterials* **2018**, *168*, 54–63. [CrossRef]
172. Wang, Q.; Liu, P.; Sun, Y.; Gong, T.; Zhu, M.; Sun, X.; Zhang, Z.; Duan, Y. Preparation and properties of biocompatible PS-PEG/calcium phosphate nanospheres. *Nanotoxicology* **2015**, *9*, 190–200. [CrossRef]
173. Evensen, L.; Johansen, P.L.; Koster, G.; Zhu, K.; Herfindal, L.; Speth, M.; Fenaroli, F.; Hildahl, J.; Bagherifam, S.; Tulotta, C.; et al. Zebrafish as a model system for characterization of nanoparticles against cancer. *Nanoscale* **2016**, *8*, 862–877. [CrossRef]
174. Crecente-Campo, J.; Guerra-Varela, J.; Peleteiro, M.; Gutiérrez-Lovera, C.; Fernández-Mariño, I.; Diéguez-Docampo, A.; González-Fernández, Á.; Sánchez, L.; Alonso, M.J. The size and composition of polymeric nanocapsules dictate their interaction with macrophages and biodistribution in zebrafish. *J. Control. Release* **2019**, *308*, 98–108. [CrossRef]
175. Jia, H.R.; Zhu, Y.X.; Xu, K.F.; Pan, G.Y.; Liu, X.; Qiao, Y.; Wu, F.G. Efficient cell surface labelling of live zebrafish embryos: Wash-free fluorescence imaging for cellular dynamics tracking and nanotoxicity evaluation. *Chem. Sci.* **2019**, *10*, 4062–4068. [CrossRef]
176. Mimeault, M.; Batra, S.K. Emergence of zebrafish models in oncology for validating novel anticancer drug targets and nanomaterials. *Drug Discov. Today* **2013**, *18*, 128–140. [CrossRef] [PubMed]
177. Liu, H.-n.; Guo, N.-n.; Guo, W.-w.; Huang-Fu, M.-y.; Vakili, M.R.; Chen, J.-j.; Xu, W.-h.; Wei, Q.-c.; Han, M.; Lavasanifar, A.; et al. Delivery of mitochondriotropic doxorubicin derivatives using self-assembling hyaluronic acid nanocarriers in doxorubicin-resistant breast cancer. *Acta Pharmacol. Sin.* **2018**, *39*, 1681–1692. [CrossRef] [PubMed]
178. Gao, X.; Wang, S.; Wang, B.L.; Deng, S.; Liu, X.; Zhang, X.N.; Luo, L.L.; Fan, R.R.; Xiang, M.L.; You, C.; et al. Improving the anti-ovarian cancer activity of docetaxel with biodegradable self-assembly micelles through various evaluations. *Biomaterials* **2015**, *53*, 646–658. [CrossRef] [PubMed]
179. Xie, Z.; Guo, W.; Guo, N.; Huangfu, M.; Liu, H.; Lin, M.; Xu, W.H.; Chen, J.; Wang, T.T.; Wei, Q.; et al. Targeting tumor hypoxia with stimulus-responsive nanocarriers in overcoming drug resistance and monitoring anticancer efficacy. *Acta Biomater.* **2018**, *71*, 351–362. [CrossRef] [PubMed]
180. Saraiva, S.M.; Gutiérrez-Lovera, C.; Martínez-Val, J.; Lores, S.; Bouzo, B.L.; Díez-Villares, S.; Alijas, S.; Pensado-López, A.; Vázquez-Ríos, A.J.; Sánchez, L.; et al. Edelfosine nanoemulsions inhibit tumor growth of triple negative breast cancer in zebrafish xenograft model. *Sci. Rep.* **2021**, *11*, 9873. [CrossRef]
181. Moret, F.; Conte, C.; Esposito, D.; Dal Poggetto, G.; Avitabile, C.; Ungaro, F.; Tiso, N.; Romanelli, A.; Laurienzo, P.; Reddi, E.; et al. Biodegradable nanoparticles combining cancer cell targeting and anti-angiogenic activity for synergistic chemotherapy in epithelial cancer. *Drug Deliv. Transl. Res.* **2022**, 1–13. [CrossRef]
182. Deng, S.; Wu, Q.; Zhao, Y.; Zheng, X.; Wu, N.; Pang, J.; Li, X.; Bi, C.; Liu, X.; Yang, L.; et al. Biodegradable polymeric micelle-encapsulated doxorubicin suppresses tumor metastasis by killing circulating tumor cells. *Nanoscale* **2015**, *7*, 5270–5280. [CrossRef]
183. Zhou, Q.; Li, Y.; Zhu, Y.; Yu, C.; Jia, H.; Bao, B.; Hu, H.; Xiao, C.; Zhang, J.; Zeng, X.; et al. Co-delivery nanoparticle to overcome metastasis promoted by insufficient chemotherapy. *J. Control. Release* **2018**, *275*, 67–77. [CrossRef]
184. Wu, J.Q.; Zhai, J.; Li, C.Y.; Tan, A.M.; Wei, P.; Shen, L.Z.; He, M.F. Patient-derived xenograft in zebrafish embryos: A new platform for translational research in gastric cancer. *J. Exp. Clin. Cancer Res.* **2017**, *36*, 160. [CrossRef]
185. Di Franco, G.; Usai, A.; Funel, N.; Palmeri, M.; Rosamaria Montesanti, I.E.; Bianchini, M.; Gianardi, D.; Furbetta, N.; Guadagni, S.; Vasile, E.; et al. Use of zebrafish embryos as avatar of patients with pancreatic cancer: A new xenotransplantation model towards personalized medicine. *World J. Gastroenterol.* **2020**, *26*, 2792–2809. [CrossRef]
186. Costa, B.; Estrada, M.F.; Mendes, R.V.; Fior, R. Zebrafish Avatars towards Personalized Medicine—A Comparative Review between Avatar Models. *Cells* **2020**, *9*, 293. [CrossRef] [PubMed]
187. Rebelo de Almeida, C.; Mendes, R.V.; Pezzarossa, A.; Gago, J.; Carvalho, C.; Alves, A.; Nunes, V.; Brito, M.J.; Cardoso, M.J.; Ribeiro, J.; et al. Zebrafish xenografts as a fast screening platform for bevacizumab cancer therapy. *Commun. Biol.* **2020**, *3*, 299. [CrossRef] [PubMed]
188. Gauert, A.; Olk, N.; Pimentel-Gutiérrez, H.; Astrahantseff, K.; Jensen, L.D.; Cao, Y.; Eggert, A.; Eckert, C.; Hagemann, A.I.H. Fast, in vivo model for drug-response prediction in patients with b-cell precursor acute lymphoblastic leukemia. *Cancers* **2020**, *12*, 1883. [CrossRef] [PubMed]

189. Lin, J.; Zhang, W.; Zhao, J.J.; Kwart, A.H.; Yang, C.; Ma, D.; Ren, X.; Tai, Y.T.; Anderson, K.C.; Handin, R.I.; et al. A clinically relevant in vivo zebrafish model of human multiple myeloma to study preclinical therapeutic efficacy. *Blood* **2016**, *128*, 249–252. [CrossRef]
190. Usai, A.; Di Franco, G.; Piccardi, M.; Cateni, P.; Pollina, L.E.; Vivaldi, C.; Vasile, E.; Funel, N.; Palmeri, M.; Dente, L.; et al. Zebrafish patient-derived xenografts identify chemo-response in pancreatic ductal adenocarcinoma patients. *Cancers* **2021**, *13*, 4131. [CrossRef]
191. ClinicalTrials.gov. Available online: https://clinicaltrials.gov/ (accessed on 30 March 2021).
192. Fazio, M.; Ablain, J.; Chuan, Y.; Langenau, D.M.; Zon, L.I. Zebrafish patient avatars in cancer biology and precision cancer therapy. *Nat. Rev. Cancer* **2020**, *20*, 263–273. [CrossRef]
193. Cully, M. Zebrafish earn their drug discovery stripes. *Nat. Rev. Drug Discov.* **2019**, *18*, 811–813. [CrossRef]
194. North, T.E.; Goessling, W.; Walkley, C.R.; Lengerke, C.; Kopani, K.R.; Lord, A.M.; Weber, G.J.; Bowman, T.V.; Jang, I.H.; Grosser, T.; et al. Prostaglandin E2 regulates vertebrate haematopoietic stem cell homeostasis. *Nature* **2007**, *447*, 1007–1011. [CrossRef]
195. White, R.M.; Cech, J.; Ratanasirintrawoot, S.; Lin, C.Y.; Rahl, P.B.; Burke, C.J.; Langdon, E.; Tomlinson, M.L.; Mosher, J.; Kaufman, C.; et al. DHODH modulates transcriptional elongation in the neural crest and melanoma. *Nature* **2011**, *471*, 518–522. [CrossRef]
196. Mandelbaum, J.; Shestopalov, I.A.; Henderson, R.E.; Chau, N.G.; Knoechel, B.; Wick, M.J.; Zon, L.I. Zebrafish blastomere screen identifies retinoic acid suppression of MYB in adenoid cystic carcinoma. *J. Exp. Med.* **2018**, *215*, 2673–2685. [CrossRef]
197. Hanna, G.J.; ONeill, A.; Cutler, J.M.; Flynn, M.; Vijaykumar, T.; Clark, J.R.; Wirth, L.J.; Lorch, J.H.; Park, J.C.; Mito, J.K.; et al. A phase II trial of all-trans retinoic acid (ATRA) in advanced adenoid cystic carcinoma. *Oral Oncol.* **2021**, *119*, 105366. [CrossRef] [PubMed]
198. Wang, C.; Tao, W.; Wang, Y.; Bikow, J.; Lu, B.; Keating, A.; Verma, S.; Parker, T.G.; Han, R.; Wen, X.Y. Rosuvastatin, identified from a zebrafish chemical genetic screen for antiangiogenic compounds, suppresses the growth of prostate cancer. *Eur. Urol.* **2010**, *58*, 418–426. [CrossRef] [PubMed]
199. Gutierrez, A.; Pan, L.; Groen, R.W.J.; Baleydier, F.; Kentsis, A.; Marineau, J.; Grebliunaite, R.; Kozakewich, E.; Reed, C.; Pflumio, F.; et al. Phenothiazines induce PP2A-mediated apoptosis in T cell acute lymphoblastic leukemia. *J. Clin. Investig.* **2014**, *124*, 644–655. [CrossRef] [PubMed]
200. Chen, Y.; Cui, Y.; Sun, X.; Wu, H.; Ou, M.; Tang, Y.; Ni, S.; Li, X.; Zhu, J.; Mao, F.; et al. Repurposing of antipsychotics perphenazine for the treatment of endometrial cancer. *Bioorganic Med. Chem. Lett.* **2020**, *30*, 127239. [CrossRef] [PubMed]
201. Evason, K.J.; Francisco, M.T.; Juric, V.; Balakrishnan, S.; Lopez Pazmino, M.d.P.; Gordan, J.D.; Kakar, S.; Spitsbergen, J.; Goga, A.; Stainier, D.Y.R. Identification of Chemical Inhibitors of β-Catenin-Driven Liver Tumorigenesis in Zebrafish. *PLoS Genet.* **2015**, *11*, e1005305. [CrossRef] [PubMed]
202. del Ama, L.F.; Jones, M.; Walker, P.; Chapman, A.; Braun, J.A.; Mohr, J.; Hurlstone, A.F.L.; Fernandez del Ama, L.; Jones, M.; Walker, P.; et al. Reprofiling using a zebrafish melanoma model reveals drugs cooperating with targeted therapeutics. *Oncotarget* **2016**, *7*, 40348–40361. [CrossRef] [PubMed]
203. Xiao, J.; Glasgow, E.; Agarwal, S. Zebrafish Xenografts for Drug Discovery and Personalized Medicine. *Trends Cancer* **2020**, *6*, 569–579. [CrossRef]

ANNEX 2. ETHICAL COMMITTEE APPROVAL FOR THE USE OF PATIENTS' SAMPLES

XUNTA DE GALICIA
CONSELLERÍA DE SANIDADE
Secretaría Xeral Técnica

Secretaría Técnica
Comité Autonómico de Ética da Investigación de Galicia
Secretaría Xeral. Consellería de Sanidade
Edificio Administrativo San Lázaro
15703 SANTIAGO DE COMPOSTELA
Tel: 881546425. Correo-e: ceic@sergas.es

galicia

DICTAMEN DEL COMITÉ DE ÉTICA DE LA INVESTIGACIÓN DE SANTIAGO-LUGO

Guillermo José Prada Ramallal, Secretario del Comité de Ética de la Investigación de Santiago-Lugo,

CERTIFICA:

Que este Comité evaluó en su reunión del día 21 de diciembre de 2017 el estudio:

Título: Identificación de marcadores de diagnóstico, pronóstico y seguimiento mediante el análisis de Biopsia Líquida en pacientes con cáncer
Promotor: Rafael López López
Tipo de estudio: Outros
Versión: Versión 1 de 31 de Octubre de 2017
Código del Promotor:
Código de Registro: 2017/538

Y, tomando en consideración las siguientes cuestiones:

- La pertinencia del estudio, teniendo en cuenta el conocimiento disponible, así como los requisitos legales aplicables, y en particular la Ley 14/2007, de investigación biomédica, el Real Decreto 1716/2011, de 18 de noviembre, por el que se establecen los requisitos básicos de autorización y funcionamiento de los biobancos con fines de investigación biomédica y del tratamiento de las muestras biológicas de origen humana, y se regula el funcionamiento y organización del Registro Nacional de Biobancos para investigación biomédica, la ORDEN SAS/3470/2009, de 16 de diciembre, por la que se publican las Directrices sobre estudios Postautorización de Tipo Observacional para medicamentos de uso humano, y la Circular nº 07/2004, de investigaciones clínicas con productos sanitarios.
- La idoneidad del protocolo en relación con los objetivos del estudio, justificación de los riesgos y molestias previsibles para el sujeto, así como los beneficios esperados.
- Los principios éticos da Declaración de Helsinki vigente.
- Los Procedimientos Normalizados de Trabajo del Comité.

Emite un dictamen **FAVORABLE** para la realización del estudio **por el/la investigador/a del centro**:

Centros	Investigadores Principales
C.H. Universitario de Santiago	Rafael López López, Laura Muinelo Romay, Roberto Díaz Peña

En Santiago de Compostela, a 28 de diciembre 2017.

El Secretario del Comité Territorial de Ética de la Investigación de Santiago Lugo,

guillermo.jose.prada.ramallal@sergas.es
2017.12.29 13:33:30 +02'00'

Guillermo José Prada Ramallal

XUNTA DE GALICIA
CONSELLERÍA DE SANIDADE
Secretaría Xeral Técnica

Secretaría Técnica
Comité Autonómico de Ética da Investigación de Galicia
Secretaría Xeral. Consellería de Sanidade
Edificio Administrativo San Lázaro
15703 SANTIAGO DE COMPOSTELA
Tel: 881546425. Correo-e: ceic@sergas.es

galicia

Guillermo José Prada Ramallal, Secretario del Comité de Ética de la Investigación de Santiago-Lugo,

HACE CONSTAR QUE:

1.- El Comité Territorial de Ética de la Investigación de Santiago-Lugo cumple tanto en su composición como en sus PNTs los requisitos legales vigentes (RD 1090/2015 de ensayos clínicos, y la Ley 14/2007 de Investigación Biomédica).

2.- La composición actual del Comité Territorial de Ética de la Investigación de Santiago-Lugo es:

- **Juan Manuel Vázquez Lago (Presidente).** Médico especialista en Medicina Preventiva y Salud Pública. Área de Gestión Integrada de Santiago.
- **Pilar Rodríguez Ledo (Vicepresidenta).** Médico especialista en Medicina Familiar y Comunitaria. Área de Gestión Integrada de Lugo.
- **Guillermo José Prada Ramallal (Secretario).** Médico especialista en Farmacología Clínica. Área de Gestión Integrada de Santiago. Fundación Ramón Domínguez.
- **Lorenzo Armenteros del Olmo (Vicesecretario).** Médico especialista en Medicina Familiar y Comunitaria. Área de Gestión Integrada de Lugo.
- **Francisco Campos Pérez.** Biólogo. Instituto de Investigación Sanitaria de Santiago de Compostela.
- **Rosana Castelo Domínguez.** Farmacéutica de Atención Primaria. Área de Gestión Integrada de Santiago.
- **Ricardo García Martínez.** Licenciado en Derecho. Área de Gestión Integrada de Lugo.
- **Jaime Gulín Dávila**. Farmacéutico especialista en Farmacia Hospitalaria. Área de Gestión Integrada de Lugo.
- **Victor Herrán Carreira.** Paciente. ADIL-Asociación de Diabéticos Lucense.
- **María Jesús Lamas Díaz.** Farmacéutica especialista en Farmacia Hospitalaria. Área de Gestión Integrada de Santiago.
- **Carlos Rodríguez Moreno.** Médico especialista en Farmacología Clínica. Área de Gestión Integrada de Santiago.
- **Rafael Carlos Vidal Pérez.** Médico especialista en Cardiología. Área de Gestión Integrada de Lugo.
- **María Jesús Wandosell Picatoste.** Enfermera. Área de Gestión Integrada de Santiago.

Para que conste donde proceda, y a petición del promotor/investigador, en Santiago de Compostela, a 28 de diciembre de 2017.

El Secretario del Comité Territorial de Ética de la Investigación de Santiago Lugo,

guillermo.jose.prada.ramallal@sergas.es
2017.12.29 13:33:34 +02'00'

Guillermo José Prada Ramallal

ANNEX 3. IMAGES PERMISSIONS

Introduction, Figure 1:

Figure was adapted/extracted with permission from:

Mitchell, M.J., Billingsley, M.M., Haley, R.M. *et al*. Engineering precision nanoparticles for drug delivery. *Nat Rev Drug Discov* 20, 101–124 (2021). https://doi.org/10.1038/s41573-020-0090-8

Chapter II, Figure 2

Figure was adapted/extracted from:

Blind M, Blank M. Aptamer Selection Technology and Recent Advances. *Mol Ther Nucleic Acids*. 4(1):e223 (2015). https://doi.org/10.1038/mtna.2014.74

Chapter II, Figure 4B

Figure was adapted/extracted from:

Martins, A. S. O. (2022). Engineering a metastasis-on-a-chip system towards studying cell invasion and drug efficacy in lung cancer (Dissertation), Universidade do Minho. https://hdl.handle.net/1822/81245

SPRINGER NATURE LICENSE TERMS AND CONDITIONS

May 31, 2023

This Agreement between Maria Cascallar ("You") and Springer Nature ("Springer Nature") consists of your license details and the terms and conditions provided by Springer Nature and Copyright Clearance Center.

License Number	5559330128379
License date	May 31, 2023
Licensed Content Publisher	Springer Nature
Licensed Content Publication	Nature Reviews Drug Discovery
Licensed Content Title	Engineering precision nanoparticles for drug delivery
Licensed Content Author	Michael J. Mitchell et al
Licensed Content Date	Dec 4, 2020
Type of Use	Thesis/Dissertation
Requestor type	academic/university or research institute
Format	print and electronic
Portion	figures/tables/illustrations
Number of figures/tables/illustrations	1
Would you like a high resolution image with your order?	no
Will you be translating?	no
Circulation/distribution	1 - 29
Author of this Springer Nature content	no
Title	In vitro and in vivo evaluation of lipidic nanosystems for cancer therapy
Institution name	Universidade de Santiago de Compostela
Expected presentation date	Sep 2023
Order reference number	3105
Portions	Figure 2
Requestor Location	Maria Cascallar Travesia da Choupana s/n CHUS Santiago de Compostela, 15706 Spain Attn: Maria Cascallar
Total	**0.00 EUR**

Terms and Conditions

Springer Nature Customer Service Centre GmbH Terms and Conditions

The following terms and conditions ("Terms and Conditions") together with the terms specified in your [RightsLink] constitute the License ("License") between you as Licensee and Springer Nature Customer Service Centre GmbH as Licensor. By clicking 'accept' and completing the transaction for your use of the material ("Licensed Material"), you confirm your acceptance of and obligation to be bound by these Terms and Conditions.

1. Grant and Scope of License

1. 1. The Licensor grants you a personal, non-exclusive, non-transferable, non-sublicensable, revocable, world-wide License to reproduce, distribute, communicate to the public, make available, broadcast, electronically transmit or create derivative works using the Licensed Material for the purpose(s) specified in your RightsLink Licence Details

ANNEX 4. CERTIFICATE

O REITOR
DA UNIVERSIDADE DE SANTIAGO DE COMPOSTELA
(EL RECTOR DE LA UNIVERSIDAD DE SANTIAGO DE COMPOSTELA)

CONSIDERANDO QUE

dona **MARÍA CASCALLAR CASTRO** con DNI/PASAPORTE 35600589Q, superou os estudos correspondentes ao Curso de Formación de 1 ECTS, organizado pola VICERREITORÍA DE COORDINACIÓN DO CAMPUS DE LUGO, durante o ano académico 2019-2020, expide o presente

Diploma de Aproveitamento no
PROGRAMA DE FORMACIÓN DE
CAPACITACIÓN PARA A REALIZACIÓN DAS FUNCIÓNS A+B+C EN EXPERIMENTACIÓN ANIMAL: MÓDULO ESPECÍFICO PEIXES

O presente diploma, propio da Universidade de Santiago de Compostela, expídese ao abeiro do artigo 34.1 da Lei orgánica 4/2007, de 12 de abril.

*Doña **María Cascallar Castro**, con DNI/PASAPORTE 35600589Q, superó los estudios correspondientes al Curso de Formación de 1 ECTS, organizado por la VICERRECTORÍA DE COORDINACIÓN DEL CAMPUS DE LUGO, durante el año académico 2019-2020, expide el presente Diploma de Aprovechamiento en el PROGRAMA DE FORMACIÓN DE **CAPACITACIÓN PARA LA REALIZACIÓN DE LAS FUNCIONES A+B+C EN EXPERIMENTACIÓN ANIMAL: MÓDULO ESPECÍFICO PECES.***

El presente diploma, propio de la Universidad de Santiago de Compostela, se expide al amparo del artículo 34.1 de la Ley Orgánica 4/2007, de 12 de abril.

Santiago de Compostela, a 16 de noviembre de 2020

Santiago de Compostela, a 16 de novembro de 2020

O reitor,
El rector,

Antonio López Díaz

CLAVE ALFANUMÉRICA: USC-11102-FC
NÚMERO DE REXISTRO: 202011102-FC

Documento expedido en papel de seguridade reactivo ó borrado químico con filamentos luminiscentes e sélo en seco.
Documento expedido en papel de seguridad reactivo al borrado químico con filamentos luminiscentes y sello en seco.

DIDOSEG S.A.

Nanomedicines have the potential to be a key strategy for cancer treatment. To improve translation, it is necessary to include reliable *in vitro* and *in vivo* models that recreate the tumor structure in the preclinical evaluation of their behavior and therapeutic effect. In this sense, the main objective of this thesis was the use of advanced *in vitro* and alternative *in vivo* models, for the preclinical study of sphingomyelin nanoemulsions for cancer treatment. The evidence obtained demonstrated the versatility of sphingomyelin nanosystems to carry different cancer treatment strategies, and the potential of 3D, static and non-static, *in vitro* models and *in vivo* zebrafish embryos for preclinical assessment.